

This item was submitted to Loughborough University as an MPhil thesis by the author and is made available in the Institutional Repository (<https://dspace.lboro.ac.uk/>) under the following Creative Commons Licence conditions.



For the full text of this licence, please go to:
<http://creativecommons.org/licenses/by-nc-nd/2.5/>

Pilkington Library

Author/Filing Title FARAGHER, E

Accession/Copy No.

040147213

Vol. No.

Class Mark

LOAN COPY

0401472132



**STRUCTURAL PERFORMANCE OF THERMOPLASTIC
DRAINAGE PIPES**


by

EDWARD FARAGHER BEng CEng MICE

**A Master's Thesis submitted in partial fulfilment of the
requirements for the award of Master of Philosophy of
Loughborough University**

April 1997

© by Edward Faragher 1997

 through by	
Date	Sept 97
Class	
Acc No.	040147213

9960324X

CONTENTS

Abstract	i
Acknowledgements	ii
1 INTRODUCTION	1
1.1 THE DEVELOPMENT AND USE OF FLEXIBLE PIPES IN UK CIVIL ENGINEERING	1
1.2 OBJECTIVES OF THE RESEARCH WORK	3
2 LITERATURE REVIEW	6
2.1 HISTORICAL DEVELOPMENT OF DEFLECTION THEORIES FOR FLEXIBLE PIPES	6
2.1.1 Marston's Load Theory	7
2.1.2 The Iowa Deflection Theory	8
2.1.3 Summary of Main Factors Affecting Pipe Deformation	10
2.2 FACTORS AFFECTING THE DEFORMATION OF FLEXIBLE PLASTIC PIPES	11
2.2.1 Pipe Properties	11
2.2.1.1 Pipe Material	11
2.2.1.2 Pipe Geometry	12
2.2.1.3 Tests for Plastic Pipes	12
2.2.2 Soil Properties	15
2.2.2.1 Soil Type	15
2.2.2.2 Compaction	16
2.2.2.3 Water	18

2.2.2.4 Determination of Soil Stiffness Parameters	19
2.2.3 Relative Stiffness of Pipe and Surrounding Soil	20
2.2.3.1 Arching of Soil Over a Flexible Structure	20
2.2.3.2 Modes and Shapes of Deformation	21
2.2.4 Installation Environment	22
2.2.4.1 Trench	22
2.2.4.2 Embankment	23
2.2.4.3 Standard Installation Conditions	24
2.2.5 Loading	25
2.2.5.1 Static Loading	25
2.2.5.2 Dynamic Loading	26
2.2.6 Time	28
2.2.6.1 Creep of the Pipe	28
2.2.6.2 Movement of the Soil	29
2.2.6.3 Creep of the Pipe-soil System	30
2.2.7 Acceptable Limits of Pipe Deflection	31
2.3 RECENT DEVELOPMENTS OF DEFLECTION THEORIES	32
2.3.1 The USBR Equation	32
2.3.2 Greenwood and Lang's Development of the USBR Equation	33
2.3.3 Gumbel's Method	36
2.3.4 The ATV Method	38
2.3.5 Gerbault's Method	39
2.3.6 Chua and Lytton's Method	40
2.3.7 Moore's Finite Element Work on Corrugated Plastic Pipes	41
2.4 DISCUSSION	43
2.5. RESEARCH PHILOSOPHY	46
2.5.1 Realistic Long Term Plastic Pipe Performance	47
2.5.2 Development of a Laboratory Test	49
2.5.3 Better Definition of Soil Properties	49

2.5.4 Integrity of Pipe Joints	50
2.5.5 Non-Standard Surrounds	50
3 LABORATORY TESTING OF PLASTIC PIPES	51
3.1 TEST PARAMETERS AND EQUIPMENT	52
3.1.1 Testing Box	52
3.1.2 Load Application Equipment	54
3.1.3 Sizes and Types of Pipes Tested	55
3.1.4 Types and States of Pipe Surround Media	56
3.1.5 Loading Patterns	57
3.1.6 Deflection and Strain Measurement	59
3.1.6.1 Deflection Measurement	59
3.1.6.2 Wall Strain Measurement	59
3.1.6.3 Data Processing Equipment	60
3.2 TEST PROCEDURES	61
3.2.1 Preparation of the Pipe Sample	61
3.2.2 Installation of the Pipe	63
3.2.3 70kPa Static Pressure Phase	64
3.2.4 70kPa Cyclic Pressure Phase	66
3.2.4.1. Test procedures	66
3.2.4.2. Data collection	66
3.2.5 140kPa Static Pressure Phase	67
3.2.6 Removal of the Test Pipe	67
3.3 ANCILLARY TESTING	68
3.3.1 Integrity of Deflected Pipe Joints	68
3.3.2 Impact Loading of Pipes at Low Cover Depths	69
3.3.3 Frictional Effects of Test Box Walls	70
3.3.4 Experimental Repeatability	71

4 FIELD TESTING	72
4.1 TEST PARAMETERS	72
4.1.1 Test Site and Ground Conditions	72
4.1.2 Dynamic Load Application Equipment	73
4.1.3 Pipes Tested	73
4.1.4 Trench Dimensions	74
4.1.5 Pipe Surround, Trench Fill and Haul Road Materials	74
4.1.6 Pattern of Dynamic Load	75
4.1.7 Deflection and Strain Measurement	76
4.1.7.1. Deflection Measurement Equipment	76
4.1.7.2 Wall Strain Measurement Equipment	76
4.2 TEST PROCEDURES	77
4.2.1 Preparation of the Test Pipes	77
4.2.2 Installation of the Pipes	77
4.2.3 Application of Dynamic Loading	78
4.2.3.1 Test Procedures	78
4.2.3.2 Data Collection Intervals	78
4.3. MISCELLANEOUS TEST OBSERVATIONS	78
4.3.1 Flooding of the Test Site	78
4.3.2 Rutting of the Haul Road During Dynamic Loading	79
4.3.3 The Effect of One Pass of a Very High Load	79
4.3.4 Visual Observations of Pipe Deformation	79
5 RESULTS	81
5.1 RESULTS OF THE LABORATORY TESTING	81
5.1.1 Test Pipe Properties	81
5.1.2 Surround Properties	83
5.1.3 Pipe Deflections and Deformed Shapes	84
5.1.3.1 Presentation of Results	84

5.1.3.2 Overview of Results from Complete Loading Phases	86
5.1.3.3 Deformation During the Installation Phase	88
5.1.3.4 Deformation During the 70kPa Static Pressure Phase	90
5.1.3.5 Deformation During the 70kPa Cyclic Pressure Phase	92
5.1.3.6 Deformation During the 140kPa Static Pressure Phase	94
5.2 RESULTS OF THE FIELD TESTING	96
5.2.1 Presentation of Data	96
5.2.2 Pipe Deflections and Wall Strains During Installation Phase	96
5.2.2.1 Pipe Deflections	96
5.2.2.2 Pipe Wall Strains	97
5.2.3 Pipe Deflections During the Dynamic Loading Phase	98
5.2.4 Effect of One Pass of Very High Load	99
6 DISCUSSION	100
6.1 DISCUSSION OF TEST RESULTS	101
6.1.1 Other Shapes of Pipe Deformation	101
6.1.1.1 All-round Compression	101
6.1.1.2 High Tensile Strains at the Invert	102
6.1.2 The Effect of Surround Type on the Shape of Pipe Deformation	102
6.1.3 Compaction of the Surround Media by the Applied Test Pressures	103
6.1.4 Experimental Repeatability	104
6.1.5 Frictional Effects of Testing Box Walls	105
6.1.5.1 Parametric Study of Wall Friction	105
6.1.5.2 The Effect of the Less Frictional Box Wall Facing	106
6.1.6 Integrity of Deflected Joined Pipes	108
6.1.7 Application of Impact Loading to a Shallowly Buried pipe	108
6.2 CALCULATION OF SOIL STIFFNESS, DEFLECTION LAG FACTORS AND TRAFFICKING FACTORS FROM TEST DATA	109

6.2.1 Determination of Soil Stiffness and Deflection Lag Factors from Laboratory Test Data	109
6.2.1.1 Estimation of the Modulus of Soil Reaction, E'	110
6.2.1.2 Estimation of the Deflection Lag Factor, D_L	111
6.2.1.3 Estimation of Trafficking Factors	113
6.2.2 Estimation of Trafficking Factors from Field Test Data	114
6.3 COMPARISON OF LABORATORY AND FIELD RESULTS	116
6.3.1 Introduction	116
6.3.2 Installation Phases	117
6.3.3 Cyclic Loading Phases	117
6.3.4 Trafficking Factors	121
6.3.5 Concluding Discussion	122
7 CONCLUSIONS AND RECOMMENDATIONS FOR FURTHER WORK	124
7.1 CONCLUSIONS	124
7.2 RECOMMENDATIONS FOR FURTHER WORK	127
REFERENCES	130
APPENDIX A	138

ABSTRACT

An investigation of the structural response of relatively large (0.6m-1.05m diameter) thermoplastic single-wall, twin-wall corrugated and twin-wall helically-wound drainage pipes to imposed loading is presented.

Controlled laboratory testing was carried out in a steel-sided box. The pipes were installed in different types of granular surrounds and subjected to static and cyclic surface loading which simulated deep installation and the passing of traffic over shallowly-buried pipe respectively. Both deflection of the pipe wall and the strains developed therein were measured. This allowed both the deformation and the deflected shape of the pipe to be determined, which indicated the proximity of structural failure.

A full-scale field trial was executed. Pipes were buried at cover depths of approximately 1m in two common types of surround and subjected to the passage of a laden vehicle over the trench. The field trial was used to assess the validity of the laboratory testing. It also provided absolute measures of the performance of the pipes in practical installation conditions, of which there had been only limited investigation of certain types of pipes in the UK.

The trends of the field trial results correlated well with those found in laboratory tests. The magnitude of deformation varied somewhat between laboratory and field. The laboratory tests in general underestimated the deflections recorded in the field tests as a result of differences in boundary conditions, load characteristics and the degree of control achievable. The pipes did not exhibit very large deformation under the applied loads in either the laboratory or the field tests, which indicated that their design may be conservative.

Design and installation specifications for plastic pipes were critically appraised, and possible variations explored. Current design methods for flexible pipes were appraised, and their practicality assessed. The test data were used to determine soil parameters for the relevant installation conditions and the effects of time on pipe deflection, as little contemporary information on these aspects is presently available. The repeated loading of buried flexible pipes was also considered in depth using the test data, as this aspect has not previously been considered in detail.

ACKNOWLEDGEMENTS

I wish first to thank B&H (Leics) Ltd of Loughborough for providing funding for this project. I trust it is regarded as money well spent. I would like to thank the Managing Director, Mr John Berry, for his support throughout and after the research.

I wish also to thank my senior research supervisor Dr Chris Rogers for employing me in the first place (or thereabouts) and for his unfailing support and encouragement throughout this project, especially during the writing up period. His efforts as supervisor have ensured that the maximum benefit has been gained from the project and the resulting data.

Mr Paul Fleming, second supervisor, is thanked for the practical approach and the considerable expertise he brought to the project, especially in relation to the field work, and I wish him well with his writing up.

My erstwhile research colleague Mr Marvin Loeppky deserves especial thanks for sharing his considerable experience on this subject and for the assistance he was willing to give. I wish him success in his ultimate goal of completing his PhD thesis. I also wish my fellow geotechnics researchers (Robert Talby, Al-Bashir Assally, David Boardman, Matthew Frost, Brian Wakley (who will now be in Uganda) and Shaun Lander) well in their various endeavours, and to thank them and those of lesser disciplines for making my stay at Loughborough an enjoyable one.

The laboratory technicians at Loughborough, under the inestimable leadership of Brian Waterall, are thanked for their various contributions, in particular Malcolm, Mark, John and Dave. They helped to make the laboratory a happy working environment.

Finally, I would like to thank my family without whose constant encouragement, in less than perfect circumstances for most of them recently, this thesis would have been much more difficult to complete. I am ever grateful for the unwavering support they have given me during the research and everything else I have done in the past three decades.

1 INTRODUCTION

1.1 THE DEVELOPMENT AND USE OF PLASTIC PIPES IN UK CIVIL ENGINEERING

Pipes have been used since Roman times for the conveyance of fluids; the earliest types being manufactured by the hollowing of tree trunks and branches. The Industrial Revolution in the UK and elsewhere led to an increase in urban development and the use of pipes for the construction of sewers and water supplies became more widespread. These pipes were made from rigid materials. The most widely used material of construction was clay, because of its natural abundance. In the 1930s, advances in technology led to the introduction of concrete pipes. These were less brittle than clay pipes and could also be more easily manufactured in larger diameters. Previously, large diameter sewers were hand-built in brickwork, which required large amounts of skilled labour and time. Clay and concrete pipes are still in widespread use.

After the Second World War, the science of polymer technology enabled plastics to be considered for the manufacture of many types of products. A rapid increase in the production of raw plastics made the materials competitive in cost terms, and in the 1960s the pipe industry began to develop processing techniques to make plastic pipe. The first pipes were of simple, smooth wall construction and were produced by extruding molten polymer through an annular die and cooling the resultant “tube”. The most common polymer used at this time was unplasticised polyvinylchloride (PVC-U). The raw material (plastic) was melted and forced through the die by a screw in the extruder. The extrudate, which has little structural strength, is then passed through the calibrator (which causes the extrudate to maintain a circular shape) and into a cooling tank (which cools the extrudate in a controlled manner) to produce the finished pipe.

The global rise in oil prices in 1973 led to the need for a more economical use of plastics. This was more important for larger diameters of pipes whose (single) walls were of considerable thickness. The solution adopted drew on the design of culverts (large diameter pipes), which had been used in the USA since the start of the 20th century for the drainage of large arable areas. The culverts were made from corrugated segments of relatively thin steel plate. The deeper profile produced by corrugation increased the second moment of area of the sheet without increasing the weight (and hence purchase cost) of the steel. This design method was applied to plastic pipes by the inclusion of a corrugating facility in the extrusion process. The corrugator consists of a series of metal mould blocks, shaped to the desired pipe profile (see

Figure 1.1). There are two sets of “half-blocks” that form the top and bottom of the pipe. The extrudate enters the corrugator and the mould blocks surround it. A vacuum is applied via small holes in the blocks. This causes the polymer to be sucked onto the blocks and thus produce the corrugated pipe profile. The result is that a reduction in the wall thickness (and hence cost) of the pipe can be achieved without reducing the stiffness of the pipe. Conversely the pipe diameter can be increased without the need for a very thick wall, as would be required if the pipe was of smooth wall construction.

In order to produce a pipe that retained the benefits of a corrugated but also had similar hydraulic properties to a smooth-wall (rigid or flexible) pipe, the twin-wall corrugated pipe was developed in the early 1980s. The manufacturing process requires two extruders and these feed material to the die, which produces two concentric extrudates. These are not in contact with each other and enter the corrugator, where the mould blocks form the outer wall to the required profile as before. In addition, the mould blocks are so designed that they force the two walls together between the corrugation sections while they are still warm, thus producing a structural joint. The development of these types of pipes was further assisted with the introduction of polyalkane and polyalkene polymers. The most common types are high density polyethylene (HDPE) and polypropylene (PP). The pipes thus combined relatively low material costs and hydraulic properties that were at least as good as clay and concrete pipes. Single wall corrugated pipes are however still used for applications such as land drainage.

For larger sizes of pipe, the corrugator and mould blocks became very expensive. This led to the development of a completely different method of manufacture for the larger sizes of pipes, called helical winding. In this process, a small extruder is used to produce a long, hollow section which is then wound around the inside of an external former to produce a helix. The contact points between adjacent turns of the helix interlock to form a continuous pipe. There are two main advantages of this method. The first is that there is no need for a double extruder system or a corrugator, which reduces the plant costs and space requirements. The second is that the size of the finished pipe can be varied relatively easily by changing the external former. A drawback of the finished pipe is that there is a continuous “seam” between the windings which compromises the hydraulic characteristics of the pipe.

Flexible pipes are used for many applications in the civil engineering industry. The most common application is highway drainage, but other important uses are filter drainage, landfill drainage and methane venting. Plastic pipes are also used widely for ducting purposes. Ducts (for the protection of cables, for instance) are manufactured in the same way as pipes but are manufactured to different specifications.

The main concern in the civil engineering industry relates to the deflection of a flexible pipe under service conditions. Rigid pipes do not deform under loading (by definition), rather they fail under excessive loading by crushing. Traditionally, engineers have regarded the deflection of structural components such as steel beams as the early stage of structural failure. The design of structures is based on the control of deflection (the serviceability and ultimate limit states), and deflections are kept to a small scale in relation to the overall size of the structure. Plastics are not widely used for structural components in the civil engineering profession, and their behaviour under loading is quite different from those of traditional materials, especially with regard to fitness for use when deformed. In addition, the visco-elastic properties of the plastics used for pipes give rise to concerns about the behaviour of a plastic pipe that will be buried for some time and possibly subjected to external loading in addition to those caused by the soil overlying it. As well as not deforming under loading, rigid pipes have a history of use which allows their long-term behaviour to be assessed.

There is therefore a need to determine the structural performance of the types of pipes in use in the UK civil engineering industry. This covers two main areas. The first is the structural stability of a buried plastic pipe that has deformed under loading, both in absolute terms and relative to the performance limits of the pipe. The second is the way in which a buried plastic pipe behaves in the long term under loading of the magnitude and nature of application that may be expected in practice. These areas of interest therefore led to the definition of the aim of the research, that is an investigation of the structural performance of buried thermoplastic drainage pipes. The means of fulfilling the aim are now introduced below.

1.2 OBJECTIVES OF THE RESEARCH

The objectives of the research were defined to fulfil the aim of determining the structural performance of thermoplastic drainage pipes in the context of their installation to UK specifications and the way in which their performance is influenced by the external loading to which they may be subjected.

The research related to the types of pipes currently used in UK civil engineering. Testing of the pipes was carried out in a laboratory. The manner in which the pipes were tested reflected the circumstances of a pipe in "real" conditions. Installation conditions were determined from current specifications. The external loading applied to the pipe reflected both the static and dynamic cases. The static case represented the loading (manifested as a stress) that a pipe experiences by virtue of its being buried, and is caused by the soil above the pipe, whether the pipe is in a trench or an embankment. The dynamic case related to pipes buried

under highways, where the passing of vehicles over the trench gives rise to additional transient stresses on the pipe.

Both the magnitudes and trends of deformation under these loading conditions were determined. The effects of continuous static loading and repeated dynamic loading were necessary for an assessment of the longevity of the pipe to be made. The test data were analysed to allow prediction of the magnitude of pipe deflection to be estimated under prolonged static loading or sustained cyclic loading.

The testing also investigated the likely extremes of installation and loading conditions. This allowed an assessment of their limits of performance to be made, and the current installation requirements to be critically appraised. The deflection data were used to calculate soil stiffness parameters for comparison with current values.

In order to provide deformation data for realistic conditions, and to justify the laboratory tests, a full scale field trial was undertaken. This involved the installation of pipes (of the types tested in the laboratory) and the passing of a loaded vehicle over the trenches. The deformation data obtained from the field work was related to the laboratory work in order to determine whether field conditions could be replicated in the laboratory, and thus whether laboratory testing can be considered as a reliable basis for the development of design and installation specifications. The research is reported in the order now described below.

Chapter Two comprises a thorough review of the literature related to flexible pipes. The principal method of calculating the stresses on a buried pipe due to external loads is described. This was a fundamental piece of research when it was published. Partially related to this work is the first deflection theory that was developed specifically for flexible circular structures which also remains in widespread usage. From this theory, the factors affecting the deflection of circular structures are identified and discussed. Methods of quantifying these factors are appraised and previous research in these fields is discussed. The areas where further work is required are identified with specific reference to the plastic pipes in use in the UK and the criteria concerning their design and installation. The conclusions of this process define the philosophy adopted for the research work itself, and these are explained in further detail.

Chapters Three and Four describe the practical research work, which is split into laboratory testing (Chapter Three) and field testing (Chapter Four). The materials, equipment, installation practices, loading regimes and data collection procedures are all fully described and the assumptions behind them explained.

The results of the testing are then presented and discussed in Chapter Five. The properties of the test pipes are considered in relation to their methods of determination. The pipe

surrounds and their properties are also discussed in the context of their placement and compaction.

The deflection and wall strain data found in the laboratory tests are then presented. The general deflection trends for complete tests are presented first by way of an introduction to the more detailed discussion thereafter. This covers individual test phases and describes the effect of the surround type and magnitude of loading on the degree of pipe deflection.

The field test data are then presented and discussed. Most of the discussion relates to deflection trends during installation and cyclic loading because of operational problems with the strain gauges that are explained in Chapter Four.

A more detailed discussion of the test data is given in Chapter Six. The shape of the deformed pipes is considered, and the effects of the pipe surround material discussed. Compaction of the pipe surround by applied static and cyclic loading, and the effects of this on subsequent pipe deflection are explained. Experimental factors are then discussed, including repeatability and the effects of the test box walls.

The test data are then analysed in greater detail to determine soil and time-related pipe deflection parameters. The common soil stiffness parameter is determined directly from test data for each surround type and compared to commonly-used values. The increase in deflection of a buried flexible pipe under constant loading was determined in terms of the instantaneous deflection. For this work, the type of surround was considered as a variable, and multiplication factors were calculated to relate the instantaneous deflection to that after some period of burial. The increase in pipe deflection as a result of repeated loading (such as that experienced under a carriageway) was also investigated, and again the data analysis yielded multiplication factors for prediction of deflection after a large number (1 000 000) of loading cycles.

A comparison is then made of laboratory and field testing conditions and the results obtained. The differences between the two methods relate to boundary conditions, frictional properties and the effects of these on the loading experienced by the pipe.

The conclusions drawn from the work (Chapter Seven) are presented in the context of the objectives defined by the research philosophy. The conclusions also form the basis for recommendations of the ways in which the research could be carried further.

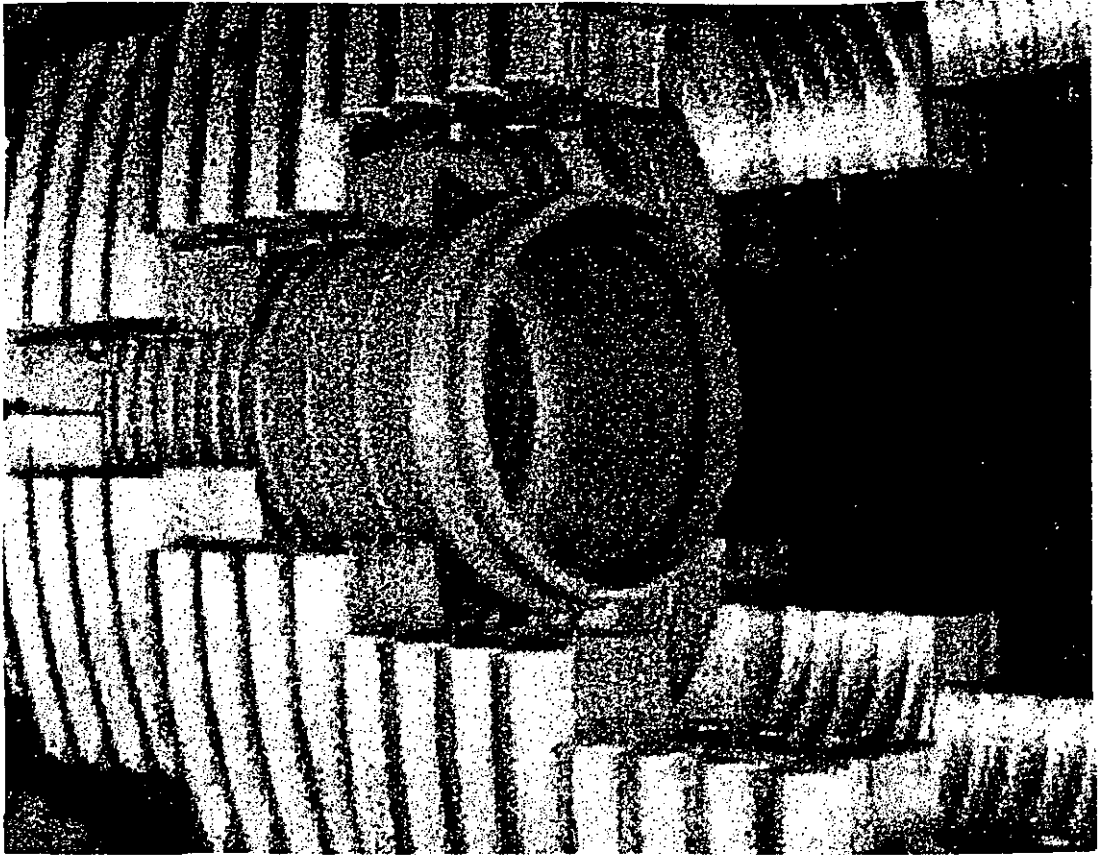


Figure 1.1. Twin-wall Pipe Corrugation Plant.

2 LITERATURE REVIEW

This chapter commences with a description of the earliest recorded experimental and theoretical investigation of flexible, buried circular structures. The work concerned both the means by which external loads acted on a buried structure, and the mechanisms of deformation of a flexible structure when subjected to such loading. The resulting deflection equation showed that the behaviour of a buried flexible structure (such as a pipe) was influenced (broadly) by the properties of the structure and its surrounding soil, and the magnitude and nature of the loading applied to it. These general subjects are investigated in further detail and the factors influencing them discussed. The discussion is developed so that it relates the initial work on large (approaching 2m) diameter steel culverts to the smaller diameter thermoplastic pipes that are the subject of this research, and to installation practices used in the UK. Plastic ducts, which have a similar form but are used to hold underground cables are not covered by this research. This is because they have different performance requirements (and therefore may have markedly different mechanical properties) and are subject to less onerous installation conditions.

The later part of this chapter comprises a review of some of the many flexible pipe deflection theories. Some of these are developed from the initial, semi-empirical work described earlier, some have a wholly theoretical basis and some use computational methods based on finite element techniques. The accuracy, scope, appropriateness and ease of use of the various theories is then discussed.

The chapter concludes with a discussion of the above and the development of the objectives of the experimental work carried out for this research.

The terminology adopted in the research work (for the description of parts of the pipe, surround regions etc.) is shown in Figure 2.1.

2.1 HISTORICAL DEVELOPMENT OF FLEXIBLE PIPE

LOAD AND DEFLECTION THEORY

The first theoretical appraisal of the manner in which a buried structure experiences loading is now described. The derivation of a deflection equation for buried flexible structures (initially intended for application to steel culverts) is then described. This arose from practical necessity and utilised the (then) relatively newly-developed load theory.

2.1.1 Marston's Load Theory

The initial work on the theory for loads on pipes was carried out in the USA during the second decade of this century (Marston, 1913). In this work, Marston made the initial distinction between rigid and flexible pipes. Three "flexibility" categories were defined, namely:

- (i) rigid: pipes whose dimensions (e.g. internal diameter) do not change by more than 0.1% under loading without causing structural damage,
- (ii) semi-rigid: pipes whose dimensions change by between 0.1% and 3.0% prior to structural damage, and
- (iii) flexible: pipes whose dimensions may change by more than 3.0% before structural damage occurs.

Two principal types of installation, which were common in the USA at that time, were defined as:

- (i) ditch installation, more commonly referred to as trench installation, and
- (ii) projecting installation, in which an embankment is built over a pipe laid on a bed on flat ground.

The trench installation is the more common of the two and is used for all standard types of drainage construction in the UK. The projecting condition is more popular in the USA, especially under deep embankments.

The load theory was based on Rankine theory and led to the following expression for the loading on a pipe in a trench:

$$W_c = C_d \gamma B_d^2 \quad \text{Eq 2.1}$$

where:

- W_c = load on pipe per unit length (Nm^{-1}),
- γ = unit weight of trench fill material (Nm^{-3}),
- B_d = trench width at top of pipe (m)
- C_d = load coefficient (dimensionless).

C_d is a function of the angle of internal friction of the backfill material, the frictional characteristics of the trench wall, the depth of cover and the trench width. The expression for the load on a pipe subject to projecting (embankment) installation is:

$$W_c = C_e \gamma B_d^2 \quad \text{Eq 2.2}$$

where C_e is a function of K_a , the pipe width and the depth of cover.

Marston also investigated the nature of transient loads on a buried pipe. He developed an expression for loads caused by imposed loading (e.g. wheel loads):

$$W_t = A^{-1} I_c C_t T \quad \text{Eq 2.3}$$

where:

W_t = load per unit length of conduit caused by imposed surface loading (Nm^{-1})

A = length of conduit (m),

I_c = impact factor, to account for moving loads (dimensionless)

C_t = load coefficient (dimensionless), and

T = magnitude of imposed load (N).

Eq 2.3 calculates the load on the conduit as the applied surface load divided by the conduit length, modified by the factors C_t and I_c . C_t , the load coefficient, is a function of the depth of installation. I_c , the impact factor, was introduced to account for the increase in applied loading that can occur when a dynamic loading source passes over a rough surface.

Values of I_c were quoted as 1.0 for static loading and between 1.5 and 2.0 for loads moving at 8.9 metres per second. These empirical values remain in current usage, although the nature of dynamic loads has been investigated in greater detail (see 2.2.5.2).

Eq 2.3 applies to concentrated imposed loads and was used to determine the average force per unit length exerted on the conduit. Marston developed the theory further so that the effect of a uniform imposed stress could be determined. The governing equation is:

$$W_{us} = C_{us} B_d U_s \quad \text{Eq 2.4}$$

where:

W_{us} = load per unit length exerted on conduit (Nm^{-1}),

C_{us} = load coefficient (dimensionless),

B_d = trench width (m), and

U_s = magnitude of imposed stress (Nm^{-2}).

Eq 2.4 is of similar form to Eq 2.1 and Eq 2.2, and is useful for applications such as increased overburden on the buried pipe after installation and uniform stresses caused by buildings placed over the pipeline.

2.1.2 Spangler's Deflection Theory

At about the same time as Marston developed his load theory, the State of Iowa was being developed intensively as an agricultural region. This required the drainage of very large areas of land so that they could be planted with cereal crops. Segmental steel prefabricated

culverts were used. As the need for more cultivable land (and hence drainage) increased, the diameters of these had exceeded five metres by end of the 1930s.

A structural appraisal of the behaviour of these large structures was put forward by one of Marston's colleagues (Spangler, 1941), who first proposed a mechanism of failure of a flexible pipe under loading. Figure 2.2 shows that an initially circular pipe deforms into an elliptical shape as the loading (caused in this case by application of overburden) increases. The vertical diameter of the pipe decreases and the horizontal diameter increases until the outward movement of the pipe springers is resisted by the soil adjacent to them. The restraint of the springers causes the top half of the pipe to bend under increasing loading so that it "snaps through" and causes a reversal of the curvature of this part of the pipe. When this has taken place, the pipe springers are pulled inwards and support is lost at these locations, causing instability of the pipe ring and initiating the collapse of the pipe.

Spangler considered the pipe itself as a thin annulus supported at the crown and invert and acted upon by a point load applied to the crown. Thin ring theory was then used to derive expressions for the change in diameter, in terms of the applied loading, pipe radius, elastic modulus and second moment of area of the pipe.

Rankine's theory was used to quantify the passive pressures generated by the outward movement of the pipe springer as the pipe deflected under loading. The passive pressure is a function of the properties of the material surrounding the culvert. Experimental work involving the burial and observation of culverts found that the horizontal pressure generated by the outward movement of the culvert wall was approximately proportional to the horizontal movement of the wall at the point of interest. The constant of proportionality was termed the modulus of passive pressure.

The distribution of stress around a circular pipe was found by a combination of theory and approximation to have the form shown in Figure 2.3. From this pressure distribution, Spangler derived the following general expression for the increase of the horizontal diameter (δx):

$$\delta x = \frac{KW_c}{EI + 0.061er^4} \quad \text{Eq 2.5}$$

where:

W_c = load per unit length applied to pipe, (Nm^{-1})

r = radius of pipe (m),

E = elastic modulus of pipe material (Nm^{-2}),

I = second moment of area of pipe wall (m^4),

e = modulus of passive pressure of soil (Nm^{-2}), and

K = bedding factor (dimensionless).

The bedding factor K is a function of the bedding angle and varies from 0.083 for a bedding angle of 90° (that is when the pipe bedding extends up to the springers) to 0.110 for a bedding angle of zero (when the pipe is placed on a flat layer of bedding). The latter condition is the more prevalent in the UK during the installation process because of the ease of providing a relatively flat bedding layer and the greater scope for pipe realignment during installation. With heavy pipes the bedding angle may increase from zero when the alignment process causes the pipe to form a depression in the bedding under it. This is less likely to occur with lighter pipes such as those used for this research.

Because of the difficulty of determining e , and its dependence on the pipe radius r , the soil stiffness parameter (e) in Eq 2.5 was replaced with a unique soil term, termed the modulus of soil reaction and abbreviated to E' (Watkins and Spangler, 1958). The effects of time on pipe deflection (discussed in more detail in 2.2.6) were accounted for using a deflection lag factor D_L , which was determined from the observation of installed pipelines over a four year period.

Rearrangement of Eq 2.5 yielded what is now commonly called the Iowa formula:

$$\delta x = \frac{KW_e D_L}{(EI/r^3) + 0.061E'} \quad \text{Eq 2.6}$$

The vertical diametral reduction (δv) is determined by assuming that the pipe deforms to an ellipse, and hence δv is simply 0.91 times δx . However, for practical purposes the two are often assumed equal due to the lack of precision in parameter definition (especially E' , see 2.2.2.4) and the possible deviation from elliptical deformation. The first term in the denominator is often substituted by $8S_{fp}$, where S_{fp} is the flexural stiffness of a pipe of diameter D (i.e. $S_{fp} = EI/D^3$) calculated according to UK standard tests (BSI, 1989, see 2.2.1.3).

2.1.3 Summary of the Main Factors Affecting Pipe Deformation

The Iowa formula (Eq 2.6) is of the general form:

Pipe deflection	\propto	$\frac{\text{Load on pipe}}{\text{Pipe stiffness} + \text{Soil stiffness}}$	Eq 2.7
		<div style="display: flex; justify-content: space-around; width: 100%;"> term term </div>	

The three broad terms on the right-hand side will determine the behaviour of a buried flexible pipe when subjected to loading. These are now discussed in relation to the pipes tested in

subsequent chapters. The influence of specific factors on the broad terms is described and related, where appropriate, to UK manufacturing standards, construction specifications and site practices.

2.2 FACTORS AFFECTING THE DEFORMATION OF FLEXIBLE PLASTIC PIPES

2.2.1 Pipe Properties

2.2.1.1 Pipe Material

The primary material parameter is the elastic modulus (E in Eq 2.6) which is determined from standard tensile tests (BSI, 1976, Method 320). There are many factors that affect the elastic modulus of plastic pipes, the most obvious being the type of polymer that is used.

It is common in the pipe extrusion industry to include “filler” compounds which are less expensive than the raw polymer. Because the filler has generally poor mechanical properties, its presence has a deleterious effect on the mechanical properties of the pipe. The quantity of filler used will depend on the performance specification to which the pipe is subject.

The rate of loading also influences the magnitude of deflection. A slowly applied stress allows the polymer chains to move in relation to each other, and results in a relatively large deformation under a given tensile stress. A rapid stress does not allow the polymer chains to untangle and this causes smaller deformation for the same stress.

A change of the ambient temperature on a plastic pipe alters its response to an applied stress. A decrease in temperature causes the matrix of polymer chains to become less flexible, leading to an increase in stiffness of the pipe. A sufficiently low temperature will cause the transition of the polymer from a ductile state to a brittle one, which increases the likelihood of fracture of the material when it is subjected to a stress. An increase in temperature increases the ductility of the polymer; an excessive increase causing the material to soften, and thereby deform excessively under an applied stress. Such temperature effects are assumed to be negligible in the case of plastic pipes used in the UK, and are further reduced by the thermal capacitance of the overlying soil which will attenuate the temperature range. However, the response of a plastic pipe to temperature change may be significant prior to its burial (e.g. during storage on site) where winter temperatures may lead to embrittlement and high summer temperatures may allow the pipe to deform excessively during its installation.

The temperature history of the pipe is influenced by the processes involved in the manufacture of the pipe. The raw polymer, together with any fillers, is heated to a molten state, extruded, possibly corrugated and cooled to an approximately ambient temperature. There are significant and rapid changes in the temperature of the plastic during this process, and their effect is to alter the degree of crystallisation within the polymer and orientation of the polymer chains. Both of these phenomena have significant effects on the mechanical properties of the polymer and both depend on the manufacturing processes adopted. Standard reference texts (e.g. Brandrup and Immergut, 1989) recognise the significant and practically indeterminable variability that may exist in mechanical properties of polymers and quotes values for the elastic modulus of polymers with ranges frequently varying within 30% of a mean value.

2.2.1.2 Pipe Geometry

The second moment of area of the pipe wall in the longitudinal direction of the pipe (I) affects the pipe stiffness term proportionally. This property depends on the shape of the pipe wall, and for a smooth wall of thickness t , the second moment of area per unit length of the pipe is given by:

$$I = \frac{t^3}{12} \quad \text{Eq 2.8}$$

and is thus proportional to the cube of the wall thickness. As the pipe diameter is increased, the wall thickness, weight and cost of the resultant pipe become prohibitive. The advent of corrugated and helically-wound twin-wall pipes permitted the adoption of new profiles that economised on material usage. It became possible to create a deep profile (see Figure 2.4) whilst maintaining low material usage by incorporating voids between the inner and outer walls. The stiffness of the “beam” can be increased by increasing the second moment of area of the beam, along the direction of the pipe length, and is achieved by increasing the profile depth.

2.2.1.3 Tests for Plastic Pipes

Standard tests for plastic pipes differ fundamentally from those for rigid pipes. Tests for rigid pipes involve loading the pipe between two parallel plates until crushing occurs, and noting the load per unit length when this occurs. Plastic pipes, when buried and subjected to surface loading, do not crush, rather the pipe crown deflects downwards and causes the springers to move outwards until an equilibrium is reached between the forces in the pipe springer and the passive resistance of the adjacent soil.

In the UK, the Department of Transport (DoT) Specification for Highway Works (DoT, 1993) stipulates the functional criteria for all types of construction materials, including

plastic pipes. The specific test referred to is the STES (Specific Tangential Extrapolated Stiffness) test (BSI, 1989), and comprises a parallel-plate loading test, in which a constant load is applied to a laterally unrestrained pipe sample. The test load must be such that the vertical deflection of the pipe crown lies between 1% and 2% of the initial pipe diameter within five minutes of application of the load. Readings of the vertical crown deflection are then taken at set times throughout the test, which lasts for 1000 hours, and a 50 year deformation value is extrapolated from the test data using a computerised non-linear optimisation technique. The STES (in Nm^{-2} or Pa) is calculated thus:

$$\text{STES} = \frac{k w}{\delta_{50}} \quad \text{Eq 2.9}$$

where:

k = constant (dimensionless),

w = load per unit length on test sample (Nm^{-1}), and

δ_{50} = predicted pipe deflection at fifty years (m)

The Department of Transport requires that the STES exceeds 1400Pa (DoT, 1990).

This test is used for “type” testing, that is for proving the stiffness of new products. It is also carried out periodically for the purposes of ensuring that the product continues to comply with its original specifications. For the purposes of routine quality control, it is evidently impractical to carry out a test lasting nearly six weeks. Therefore, a shorter test is allowed which calculates the STIS (Specific Tangential Initial Stiffness. This is defined as:

$$\text{STIS} = \frac{k w}{\delta_5} \quad \text{Eq 2.10}$$

where:

k = constant (dimensionless),

w = load per unit length on test sample (Nm^{-1}), and

δ_5 = measured pipe deflection at five minutes (m).

The load must be such that the deflection lies between 1% and 2% of the initial diameter at the end of the five-minute test, and the STIS must exceed 7000Pa. This value ensures that any pipe that passes the STIS quality control test would also pass the STES type test.

These tests are deficient in several respects when considered in the context of a buried pipe. The creep performance of the pipe is considered out of context (i.e. with the pipe not buried in a soil surround) and therefore no account is taken of the effect of the soil around the pipe.

The plate load applied for testing is based on the deflection after five minutes and not on expected loading in service. Service stresses, perhaps for extreme conditions, could be determined from tabulated data (e.g. Young et al, 1976) or from first principles (such as Marston's Load Theory or Boussinesq's Theory), and test loads defined accordingly. It is reasonable to assume that the loading experienced by a pipe is also proportional to the pipe diameter, but this notion is disregarded as well. The use of an initial deflection requirement may produce anomalous test loads, because it ensures that the test load is in fact a function of the pipe stiffness, albeit a short term value. The extrapolation of data over such a large time period is mathematically questionable because of the relatively short test duration and the magnification of measurement errors by the extrapolation process (Evans et al, 1995). This source of error is mitigated to an extent by the requirement to run the extrapolation program using a set of sample data, which must result in an extrapolated deflection that lies within a small range.

The STIS test may therefore be considered to be more reasonable in this respect but, despite the lack of extrapolation, the minimum allowable STIS for a pipe will have been set in relation to the STES and is thus just as unrepresentative.

Studies of the various testing requirements for flexible pipes of several European countries (Joekes and Elzink, 1985) used mathematical methods to determine the probable shape of the curve resulting from a parallel plate. The closest fitting curve was achieved by plotting deflection against the logarithm of time. Recent developments in flexible pipe testing requirements have accommodated some of these recommendations. The recently introduced International standard for flexibility tests for plastic pipes (International Standards Organisation (ISO), 1994) has been published. It is likely that this will supersede the British Standard which stipulates the STES test (BSI, 1989). The ISO test includes some of the features (and deficiencies) of the STES test. A sample of pipe is subject to a parallel plate test for 1008 hours (six weeks) and the deflection extrapolated to two years. The test load is proportional to the pipe diameter, subject to a lower limit of 75N, and not the short-term deflection, which is a more rational approach. The reduced extrapolation requirement goes some way towards reducing the errors that may occur in this operation. The ISO method uses a power law method as opposed to the single logarithm plot proposed by Joekes and Elzink. A statistical analysis of the test data is stipulated to ensure acceptable correlation.

Although it is a more refined and justifiable test, this method retains the fundamental weakness of the STES test (and, by implication, the STIS test), namely that the effect of the surrounding soil is ignored. These long-term tests seem only useful for initial product assessment, and once "benchmark" stiffness values have been established, they could be related to a revised short-term test or a simple load versus deflection test.

A different test philosophy has been adopted in the USA (American Society for Testing and Materials (ASTM), 1987). This consists of a simple parallel plate test which produces a graph of load versus deflection (measured as the percentage decrease in the internal vertical diameter) for the pipe under test. The test proceeds until the pipe material yields or the deflection reaches 30%. The pipe stiffness (PS, in Nm^{-2}) is defined as :

$$\text{PS} = F / \delta y \quad \text{Eq 2.11}$$

where F is the load per unit length (Nm^{-1}) measured at a deflection of δy (m).

Values of PS are normally quoted for δy corresponding to 5% and 10% of the initial internal diameter. The state of the pipe at the end of the test (in terms of rupture, yielding or collapse of the pipe) is also noted. The term PS can be adapted for use in deflection theories by conversion to a stiffness factor (SF, in Nm) which is analogous to the pipe flexural rigidity (EI) thus:

$$\text{SF} = \text{EI} = 0.149 r^3 \times (\text{PS}) \quad \text{Eq 2.12}$$

where r is the pipe radius (m).

This allows simple and direct determination of the pipe stiffness and useful information for calculation purposes. The deflection at failure of the pipe is also determined (if failure occurs), which gives an indication of the proximity of the pipe to failure when it has deflected in use. This test again does not take account of the influence of the surrounding soil, but is a deflection-controlled test and is therefore fundamentally different from the STES test. A test similar to that used in the USA has now been introduced in the UK and Europe for flexible ducts (BSI, 1994). It would therefore seem appropriate to extend this test method to pipes since the structural requirements of a pipe are the same as those for a duct. Of course, pipes do have other performance requirements (such as leakproof joints and internal pressure capacity) but these are determined by separate procedures and as long as all individual requirements are met then acceptable pipe performance would be ensured.

2.2.2 Soil Properties

2.2.2.1 Type of Soil

The soil that typically surrounds a buried flexible pipe can be defined in terms of its particle size distribution (BS1377, 1990). Granular soils are more common surround materials than cohesive soils. The type of grading of a granular surround (e.g. close, gap, uniform) has a significant effect on its modulus of passive resistance (see Eq 2.6), for reasons that are discussed in 2.2.2.2. Typical surround materials are described in 2.2.4.3.

Typical values for E' for various surround materials are given in Table 2.1 (after Howard, 1977). Variations in the type of soil can cause changes in the soil stiffness term of $\pm 40\%$. For a given type of flexible pipe, there would not be such a large variation in the pipe stiffness and the absolute values of the short-term stiffness tend to be considerably smaller than the soil stiffness term, even accounting for the 0.061 factor in Eq 2.6. The soil stiffness term may therefore exceed the pipe stiffness term by a factor of between 6 and 200 (approximately), depending on the soil type. Therefore, the soil stiffness is by far the dominant term in the denominator of Eq 2.6 and the factors affecting this are discussed further below.

2.2.2.2 Compaction

Compactive effort is applied to a soil to reduce the volume of its air voids and thereby increase its density. Since compaction is often dependent on site practice, the deformation of a buried pipe in a given type of soil will depend to a large extent on the amount of compaction applied to the pipe surround on site. The predominant mode of compaction is treading of the surround in three layers, namely the bedding, the material up to the springers and the material above that. Mechanical compaction is not permitted within 300mm of the pipe (BS5955, 1980), but is used for compaction of the backfill material that overlies the surround. It is not common for the density of pipe surrounds or trench fills to be tested on construction sites, and this results in the pipe deformation being influenced by standards of workmanship and supervision.

The influence of compaction on the modulus of soil reaction E' can be explained in terms of the passive resistance to movement of the pipe springer that E' quantifies (see also 2.2.3.1). In Figure 2.5 (developed from Craig, 1992), the solid line shows the relationship between the Rankine earth pressure coefficient and lateral strain. The passive pressure that would resist outward movement of the pipe springer is governed by the passive lateral pressure coefficient k_p (the lower case being adopted for k to avoid confusion with the bedding factor K in Eq 2.5), and the magnitude of the resistance is seen to increase as the lateral strain (i.e. springer movement, δ_L) increases. The values of k_p (and the active coefficient k_a and at-rest coefficient k_0) and the precise shape of the S-curve in Figure 2.5 depend on the type of soil and its particle size distribution. These factors therefore affect directly the extent to which passive resistance in the soil is mobilised. The action of compacting a soil is to compress it, which has the effect of translating the horizontal axis of Figure 2.5 to the right, so that the at-rest coefficient k_0 increases (as shown by the dotted line). Thus, if the pipe surround is made more dense at the time of placement, the amount of further compression (caused by movement of the

springer and now indicated by δD) required to generate the required passive resistance is smaller. This results in smaller overall pipe deflections for any given loading.

A visual study of the range of standards of workmanship in pipelaying operations (Boden et al, 1977) found that there was a large variability in the provision of the structurally important bedding layer. The study found that large variations in the level of the bedding layer occurred on a significant number of the sites inspected. The variability of level is indicative of the variability of workmanship in general, which includes both levelling and compaction of the fill.

The ease with which the surround material can be compacted will determine the selection of the type of surround in the design process and the extent to which compaction is achieved on site. Surrounds with generally uniform particle sizes can be compacted more easily than graded aggregates (Selig, 1990), and in general the larger the nominal size of these particles the less effort is required for them to arrange into a stiff matrix. Maximum density can therefore be achieved more quickly on site, and this is an important fact in terms of economy and of consistency of acceptable standards of workmanship. Satisfactory compaction of graded aggregates requires more effort because of the time taken for the smaller particles to move and fill the voids between the larger ones. However, once compacted, the resulting surround is extremely stiff.

The action of compacting the fill above a pipe causes transient forces to be applied to the pipe by the compacting plant, which cause the pipe to deflect. The amount of deflection depends on the pipe and soil properties and the power of the compactor. One field trial (Zorn and van den Berg, 1990) showed that 75% of the deflection measured during the installation of a PVC-U pipe in a granular soil was caused by compactive effort, and only 25% resulted directly from the backfill loading. In addition, the low depths of cover which are present at the start of the backfilling operation allow larger than normal forces to be exerted on the pipe (by compacting plant and site traffic) which may cause large pipe deflections during this phase. In the UK, the type of compacting plant, layer thickness and number of passes of the compactor per layer depends on the type of soil and its location (e.g. in a verge or under a road), and are specified (e.g. DoT, 1993). There is no direct reference to flexible pipes as opposed to rigid ones (except that those complying with the relevant manufacturing standards may be used) and the effect of the compaction process on the deflection of a flexible pipe is not therefore addressed. BS5955 states that compaction plant is not to be used within 300mm of a plastic pipe, but this stipulation would be over-ridden by the contract specification. There is therefore a discrepancy between the manufacturing standard for flexible pipes and the most common installation specification for highway construction.

The effect of soil density on the soil-pipe system was investigated by Neilson (1972). A small increase in density of the surrounding soil causes a significant decrease in the pipe

deformation. In studies carried out on sand, for instance, an increase in the soil density by approximately 6% caused the pipe deflection to decrease by approximately 90%. In extreme cases (such as the compaction of a very loose sand to near its maximum density) the soil density may increase by up to 30%, and the effect of this would therefore be a substantial decrease in the pipe deflection, possibly almost to zero. This would be offset by the effect of the compaction process described above. The overall result would therefore be a larger initial deflection during installation followed by a much smaller subsequent deflection due to the resistance offered by the stiffer surround. This may be preferable in some situations to larger deflections over a longer period following installation.

2.2.2.3 Water

At some time during the lifetime of a buried pipeline, it will be acted upon by external water. This will normally take the form of groundwater, and will be controlled by water table fluctuations. These are influenced by climatic changes or alterations to the drainage characteristics of the locality such as may be caused during nearby excavation works or by dewatering.

Water exerts an approximately uniform compressive pressure on a buried pipe. A flexible pipe will therefore experience a hoop stress, resulting in a hoop strain. The effect of this will be a uniform reduction in the diameter at all points on the circumference. If the hydrostatic pressure is excessive, it is possible that buckling will occur.

A physical problem that may have a deleterious effect on pipe deflection is the washing out of pipe surround material. This problem is exacerbated by the effect of the trench which will funnel any free water down its path. Some surround media (e.g. sand and smaller size gravels) would be affected more than others of larger particle size.

The water content of a fine surround such as a sand will influence its stiffness, and will therefore have an effect on the deflection of a pipe buried in it. The amount of moisture for a sand of given dry density governs the amount of suction between individual sand particles. An increase in water content from zero causes an increase in the interparticular suctions and therefore creates a stiffer material. After a peak value is reached, a further increase in water content reduces the amount of suction and causes a reduction in stiffness. Surrounds of larger particle sizes are less susceptible to this phenomenon because the inter-particular voids are too large to retain water by capillary action.

The presence of water in a soil also affects the density that can be achieved by a given amount of compaction. As the water content increases from zero, the lubricating effect allows a greater degree of particle movement and reorientation, thus leading to a greater (dry)

density. After reaching a peak (the maximum dry density), the dry density decreases with increasing water content and the soil becomes a slurry. This affects the soil stiffness for the reasons related to compaction described in 2.2.2.2, and is therefore significant.

2.2.2.4 Determination of Soil Stiffness Parameters

Investigations have been undertaken to define better the quantity E' . The most significant was that of Howard (1977), which involved the collection of deformation data from over 100 buried pipelines, and the determination of E' by back-calculation. The loads on the pipes were simply taken as being the weight of the overlying soil prism, and would therefore lead to an underestimate of E' . Deflection lag factors were not applied because they were found to vary between various construction sites and would have a significant effect on the usefulness of the calculated values of E' . Howard's values are given in Table 2.1 and are currently used for virtually all pipe deflection calculations.

An analytical study of E' aimed to prove the relationship between it and an easily measured soil property (Neilson, 1967). The triaxial test was used as a simple soil test and the constrained modulus M_s so determined was found to be similar to E' :

$$E' \sim M_s \quad \text{Eq 2.13}$$

It was implied that because the M_s increases with depth, so will E' . This was demonstrated by Hartley and Duncan (1987).

Finite element analyses have also been used to determine the stresses and strains that would pertain in a pipe-soil structure (Krizek, 1972), and E' calculated thus:

$$E' = \frac{E_s(1 - \nu_s)}{(1 + \nu_s)(1 - 2\nu_s)} \quad \text{Eq 2.14}$$

where:

E_s = secant modulus of soil, and

ν_s = Poisson's ratio of soil

A device which simulated the region of the pipe springer was designed so that laboratory tests could be performed to determine E' more easily. The Modpares (*Modulus of passive resistance*) device (ASCE, 1964), comprised a cubical cell of side length 0.15m incorporating a semicircular membrane to represent the pipe. Overburden pressures were simulated using an inflatable rubber membrane. Movement of the pipe membrane and the pressure generated by the surround on the pipe membrane were measured. Graphs of results from the Modpares

device did not yield a straight line. An iterative method was used to produce design curves in terms of dimensionless soil, loading and deflection terms.

A method of determining the “equivalent modulus of elasticity”, defined in terms of settlement of a rigid foundation *in situ* was developed by Lawrence (1977). The trench wall jack developed is in effect a horizontal equivalent of the plate-loading test described above. A circular loading plate of area 0.1m^2 and thickness 25mm is attached to a hydraulic ram via a load transducer. A displacement transducer measures the relative movement of the loading plates. The device is lowered into the trench horizontally and secured between the trench walls, which must be suitably vertical and smooth. The load is applied and readings of load and deflection taken. Results agreed closely with those of standard laboratory tests (in terms of the secant and tangent moduli) and the method produced more consistent results than the triaxial test. The major operational problem was the seating of the loading plates on the trench walls if the water content was low. This apparatus is inappropriate for single-size gravels because of the inability of such materials to preserve a vertical face in a trench.

2.2.3 Relative Stiffness of Pipe and Surrounding Soil

2.2.3.1 Arching of Soil Over a Flexible Structure

The concept of soil arching was first introduced by Terzaghi (1943) from his yielding trap-door experiments. Arching is the phenomenon of load transfer in a soil caused by the mobilisation and redistribution of shear stresses in the soil. In the case of flexible pipes, the yielding trap-door is, in theory, replaced with the top half of the pipe. The extent to which the pipe will yield (or deflect) is governed by the relative stiffness of the pipe and soil. Terzaghi discovered that the region of arching extended to a height of two to three trap-door widths above the door itself. The consequence of this in the context of flexible pipes is that the loading on the pipe, when arching is accounted for, reaches an upper limit at a burial depth of two to three times the pipe diameter. The use of visual methods to monitor surround particle movements (Rogers et al, 1996) showed conclusively that arching does take place over flexible plastic pipes subjected to loading.

The presence of arching indicates that an equilibrium exists between a deflected pipe and its surround. In order for the arch to form, it is necessary for the pipe to deform, and the amount to which this will happen will depend broadly on the factors that make up Eq 2.7. When the pipe has deformed, the crown of the pipe will have moved downwards, allowing the onset of arching. The pipe crown will cease movement when the resistance offered by the pipe, by virtue of its ring stiffness and the passive resistance generated by the springers, balances the diminished (due to the arching) downward force on the pipe.

Arching can in general be quantified in two ways (Wu and Leonards, 1985):

- (i) the ratio of total vertical thrust in the pipe wall (usually located at the springers) to the loading of the overlying soil prism, or
- (ii) the ratio of the measured normal soil pressure at the pipe crown to the calculated free-field stress at the crown

The distribution of stresses in the soil around a buried flexible pipe is shown in Figure 2.6 (after Yapa and Lytton, 1989). The stress vertically above the pipe centreline decreases as the distance from the pipe centre decreases. The stress in the surround increases from the shoulder to the springer (for a given distance from the pipe centre). This will have the additional effect of increasing the density of the confined surround, thereby increasing its resistance to lateral movement of the pipe springer. The arrows indicate the flow (sic) of the stress in the soil due to arching, more accurately they show that the direction of increase of stress is from the crown to the springer. The primary factors affecting the ability of the soil to redistribute stress is the size of the solid particles within it and the water content of the soil. Soils such as clays exhibit smaller shear resistance (especially when wet) than sands or gravels, which have larger particle sizes.

2.2.3.2 Modes and Shapes of Deformation

Spangler's development of the Iowa formula (cf. 2.1.2) assumed that a flexible pipe under loading deformed to an elliptical shape, based on inspection of circular culverts. This type of deformation is referred to as ring compression.

More recent research has found that the shape of deformation (as well as the magnitude) depends on the stiffness of the pipe and the degree of support offered by the pipe surround material. A detailed study of single-wall PVC-U ducting (Rogers, 1985) defined three additional shapes of deformation, which are given in Figure 2.7.

The heart-shaped deformation occurred when the pipe was buried in a stiff bedding layer (up to the springers), with a less stiff material overlying it. The bottom half of the pipe maintains a near circular profile, but the upper half deforms more markedly. Because the springers are restrained by the stiffer lower layer, their outward movement is limited and this prevents the top half of the pipe from deforming elliptically. This causes the upper part of the pipe to flatten as shown, which in extreme cases would cause "snap through" and collapse. Inverted heart shape is the opposite of this and results from a poor bedding and better quality upper layer. This may occur on poorly supervised sites where the bedding is tipped and poorly compacted (usually manually), but the upper surround and backfill is more effectively compacted by mechanical means.

Square deformation results from the presence of very stiff surround material at the springers. The crown and invert quarters of the pipe flatten and the shoulders and haunches become

more curved. This type of deformation may occur where voids are left at the haunches (due to substandard workmanship), the surround at the springer is well compacted and the top layer of bedding is badly compacted. The phenomenon of “squaring” was also found by Prevost (1985) to occur in very flexible pipes in stiff soils, and collapse was seen to be initiated by the buckling of the pipe crown. This deformation case highlights the practical limitations of flexible pipes. If outward movement of the pipe springers is limited by the presence of a stiff surround, the pipe can only deflect under loading by severe deformation of the crown, in the form of snap-through buckling.

Further work by Rogers et al (1995) has found that the deformed shape of the pipe during the installation phase can be influenced significantly by site practice. An instance of this was the tipping of the surround material (gravel) on one side of the pipe only, causing an asymmetrical pipe shape.

2.2.4 Installation Environment

2.2.4.1 Trench Installations

The installation of a pipe in a trench (standard UK practice) has been shown to have beneficial effects for the deformation of flexible pipes. Frictional stresses generated at the trench wall oppose the downward imposed stress and thereby reduce the vertical stress experienced at the pipe crown. The extent of the frictional resistance depends on the native soil type, fill material type and density, the condition of the trench walls and the presence of temporary trench support.

The frictional force that resists the weight of the soil prism is related to the area of the trench walls and therefore increases as the trench depth increases. At a certain depth, it may become equal in magnitude to the downward soil loading on the pipe. Below this depth, the frictional resistance exceeds the weight of the soil prism, and the loading exerted on the pipe does not therefore increase further. The cross-sectional trench area (above the pipe crown) that causes this maximum loading can be approximated in terms of the trench width alone and may be taken as $4B_d^2$ for most installation conditions (Walton, 1970).

If the trench width is increased then the depth for which maximum loading occurs increases as the square of the depth. The effect of trench width has been quantified by Leonardt (1979), and is shown in Figure 2.8. An increase in trench width reduces the frictional effect of the trench walls. The central core of the soil prism, i.e. that furthest from the trench walls, may therefore slip appreciably and cause the loading on the pipe to increase further. If the trench width increases still further, the presence of the trench walls becomes insignificant and the pipe is

effectively subjected to the weight of the overlying fill as in the embankment case described below.

The use of trench boxes leads to the formation of voids as the boxes are removed. In the case of flexible pipes, the void may cause significant outward movement of the surround, leading to a reduction in the density of the surround and an increase in the pipe deflection under a given loading. This may be avoided if the tips of the box wall plates do not project below the springer level. This is usually done as it creates more working space at the pipe level to allow for jointing, for instance. It also allows more competent placing of the surround material.

The use of trench sheets may be more problematic. These normally extend to below the level of the trench floor so that they remain upright with a minimum of strutting, which tends to interfere with pipelaying operations. The sheets may be left in place until backfilling is complete. As the sheets have a profile depth of approximately 30mm, voids will be formed. An additional effect would be the formation of slip surfaces where the trench sheets had been, reducing the frictional resistance of the trench wall to the downward loading on the pipe. The progressive withdrawal of trench support as backfilling commences would reduce the effects of these phenomena, but this is not always done.

Analysis of a soil wedge adjacent to the pipe springer shows that the pressure exerted by the pipe on the trench wall can be small, and easily withstood by relatively poor soils (Watkins, 1995). An approximate maximum distance between the pipe and the trench wall of half of the pipe diameter, or a trench width of two pipe diameters would suffice without causing shear failure of the soil. The better the soil, the narrower the trench can be. The practical lower limit is governed by the need to place the surround easily and properly between the pipe and the trench wall, especially in the area of the pipe haunches. In the UK, the minimum acceptable value is 150mm.

2.2.4.2 Embankment Installations

Embankment installation involves the placing of the pipe on a bedding layer on the existing ground surface and the subsequent raising of the ground level in the form of an embankment over a large area above the pipe. This type of installation has not been common in the UK, but is becoming more so for the drainage of landfill sites, which are constructed upwards from an existing ground level.

In the absence of frictional trench walls, higher loads are transferred to the pipe and lower degrees of load reduction occur. Pipe deflections are therefore greater. However, it has been shown in model studies (Watkins, 1990) using soil cells containing the flexible pipe and acted on by hydraulic jacks that installation serviceable depths in excess of 50m can be achieved if a high

quality surround material is used in the region of the pipe, such as a well compacted well-graded sand.

2.2.4.3 Standard Installation Conditions in the United Kingdom

For the majority of highway drainage applications in the UK, the Specification for Highway Works (DoT, 1991) and advice document HA40/89 (DoT, 1990) provide a range of types of acceptable surround materials, fill materials and cover depths that will ensure the satisfactory performance of plastic pipes. The installation criteria were determined using Gumbel's method (see 2.3.2), a wholly theoretical method, as opposed to the semi-empirical approach of the Iowa formula which had hitherto been the norm.

Three loading conditions are quoted in the design guide:

- (i) Main road loading: equivalent to 8 wheels, each of weight 112.5kN, in the HB loading pattern (BSI, 1978),
- (ii) Field loading: equivalent to two static wheels, each of weight 60kN (incorporating an impact factor of 2), 0.9m apart, and
- (iii) Filter drain loading: equivalent to 8 wheels, each of weight 62.5kN, in the HB loading pattern.

Two types of installation are permitted for carrier drains. Installation type S (Figure 2.9) comprises a bedding and surround of granular material which may be graded aggregate of particle size limits between 5mm and 20mm for pipes between 140mm and 400mm diameter, and between 5mm and 40mm for larger pipes. Alternatively, single size aggregates may be specified. Type S may be used for all loading conditions. The permissible aggregate sizes are 10mm for pipes less than 140mm in diameter, 10mm, 14mm or 20mm for pipes between 140mm and 400mm diameter and 10mm, 14mm, 20mm or 40mm for larger pipes.

Installation type T is permitted for field loading only, and the surround material may be fine or all-in aggregate. Fine aggregate is simply defined within the overall limits of BS882 (BSI, 1992) and includes, for example, well-graded river sand. All-in aggregate may be of nominal maximum size 10mm (for pipes less than 140mm diameter), 10mm or 20mm (for pipes between 140mm and 400mm diameter) or 10mm, 20mm or 40mm for larger pipes.

Overlying the surround for installation Types S and T is 300mm of Class 8 fill material. This is selected fill material, and may simply be "as dug" material that is free from particles exceeding 40mm in size.

Allowable depths of cover depend on the surround type used and the design loading criteria:

(i) For Type S surround and main road loading are 0.9m to 6.0m for pipes up to 150mm in diameter. For larger pipes, the maximum depth is 5.5m, but with the odd exception of 400mm diameter pipes for which the maximum depth is 5.0m.

(ii) For Type S surround and field loading, the minimum cover depth is 0.6m and the maximum 6.0m, with the exception of 400mm pipe which may have a maximum cover depth of 5.5m.

(iii) Type T installation may only be used for field loading and the depth of cover must exceed 0.9m. Maximum allowable cover depths are 3.0m for pipes up to 150mm diameter, 2.7m for pipes up to 525mm diameter and 2.4m for pipes of 600mm diameter.

(iv) Filter drains may have any of the surrounds shown in Figure 2.11. Allowable depths of installation must exceed 0.9m, but be not greater than 6.0m for all pipes except 400mm diameter for which the maximum cover depth is 5.5m.

2.2.5 Loading

2.2.5.1 Static Loading

The general effects of static loads (caused mainly by the soil overlying the pipe) have been discussed in sections 2.1.1, and 2.2.4, and further characteristics of static loads will be discussed in 2.2.6. It is, however, appropriate to discuss some case studies as they relate to later work (see 2.3.7).

A test method for applying large pressures to pipes was developed (Selig, DiFrancesco and McGrath, 1994) and consisted of the apparatus shown in Figure 2.10. The pipe was installed in moist sand, and the maximum bladder pressure equated to a very deep burial on site (over 20m). The results showed diametral shortening of the order of 4% at an applied pressure of 240kPa. The change in diameter with time shows how the pipe deflection built up fairly quickly when the loading was applied, with the rate of deformation slowing as time progressed. The deformation of the pipe was physically manifested in rippling of the inner pipe wall, between the points at which the two walls were bonded, and did not affect the overall structural performance. However, if local stresses became high enough, or the deflection of the pipe increased markedly, it was predicted that the inner wall would fail by tearing. Removal of a pipe after testing to 380kPa bladder pressure revealed local buckling of the outer wall at the crest of the corrugation. This is more serious because the outer wall of the pipe has a large contribution to the structural rigidity of the pipe

Load testing of PVC-U pipe in a U-shaped test box found that, when the pipe was subject to static loading, the deflection of the pipe built up almost instantaneously and appeared to

reach a constant value (Bishop, 1981). Periodic measurement of the deformation of buried pipes over a six year period (Bauer, 1990) found that, after the first annual variation in the water table, they did not exhibit any significant further deformations, indicating that a very stable system had been established.

Failure of PVC-U pipes loaded in field installation conditions has been achieved (Sargand et al, 1995). The pipes were buried to cover depths of 0.3m and 0.6m, and excessive deflection was achieved at an applied surface stress of 500kPa (applied via hydraulic rams acting on a steel plate), equivalent to the dead weight of approximately 25m of overburden.

2.2.5.2 Dynamic Loading

The additional vertical stresses generated by a moving load can be visualised in terms of Boussinesq's theory, although it applies specifically to pressures caused by point loads. When the wheel is distant from the pipe, the amount of additional stress will be practically zero. As the load approaches the location of the pipe, the vertical stress increases as a "bell-shaped" curve until a maximum is reached when the wheel is directly over the pipe. This means that the deflection of the pipe will increase similarly. In larger diameter pipes, the approach of a wheel would be visible as a "wave" as the bell-shaped stress distribution passed over the trench from one side to the other. The change in vertical stress can be seen in Figure 2.11 (after Brown, 1996).

Early work on the impact of moving vehicles on a buried pipe was first carried out in the UK on buried concrete pipes (Page, 1966), over which a tipper wagon, heavy truck and HB wheel arrangement (BSI, 1978) were driven. Bumps of height 50mm had been created in the road surface. The results show that for HB loading, the most severe case, the impact factor increased with vehicle speed and reached a value of 1.6 (with low damping) at a speed of 8.9ms^{-1} . The impact factor was also influenced by the tyre pressure and the load on the wheel. The impact factor was not affected by the pipe diameter or the type of bedding and backfill used.

Later work (Leonard et al, 1974) found that impact factors considerably greater than those determined by Page could be experienced in normal conditions. Fully-laden commercial vehicles travelling at speed on roads with severe irregularities produced impact factors exceeding 3.

The above work concerned the forces that are generated by road vehicles travelling on highways of varying roughness. Of greater concern, however, are the forces that may be exerted on a buried pipe during the construction of the project of which the pipeline is a part. This will be a more severe case because of the heavier vehicles involved in the work (e.g. scrapers and dumptrucks). Also, there may be no pavement over the pipe trench to provide load spreading, and this will cause an increased loading to be passed to the pipe. It is also possible that depths of cover

may be lower than standard, since the pipes are likely to be laid before the layers of the overlying ground are built up to their finished levels. This, too, would mean that the pipe would experience unusually large loads. Design tables in the UK for rigid pipes (Young et al, 1986) include cases of loads caused by construction traffic.

A study was made of the impact and dynamic effects of construction scrapers by measuring the behaviour of a buried concrete slab when such vehicles were passed over it (Gemperline, 1985). Stress meters were used to measure the pressures exerted on the slab. The scraper was loaded to a total vehicle weight of 120 tonnes. Two distinct test regimes were planned. The static test phase consisted of the scraper travelling at approximately 1ms^{-1} (its lowest practical speed) along the trafficking surface. This phase was used to determine a “base value” of the stress applied to the slab when there were no additional impact effects caused by vertical oscillations of the vehicle. The dynamic tests used a selection of travelling speeds, up to a maximum of 14ms^{-1} . At this speed, large vertical oscillations of the vehicle would occur, thereby increasing the stress applied to the slab (i.e. impact would take place).

The impact factor (I_f) was defined as:

$$I_f = \frac{p_d(\text{max})}{p_s(\text{max})} \quad \text{Eq 2.15}$$

where:

$p_d(\text{max})$ =maximum dynamic pressure (Pa), and

$p_s(\text{max})$ =maximum static pressure (Pa).

Values of the computed impact factor were found to vary from 1.0 to 3.0. This is a larger range than that put forward by Marston (see 2.1.1).

The value of the impact factor was predominantly dependent on the vertical oscillation of the scraper, which was a function of the roughness of the trafficking surface and the vehicle speed.

Pipes buried under highways will experience many thousands of wheel loads, and the effect of repeated loading on flexible pipe is significant. A case study was carried out on a carriageway under construction, which entailed the installation of PVC-U pipes at a cover depth of 0.7m (Trott and Gaunt, 1976). Pipe deflections, wall strains and soil pressures were recorded during installation and whilst the buried pipes were traversed by motor scrapers of gross axle masses ranging from 15 tonnes to 32 tonnes. Approximately 100 passes of the vehicle over the trench were made. The mean vertical deflection following backfilling was 1.0% of the initial vertical diameter. Passing of the loaded scrapers over the pipe caused the deflection to accumulate, with the rate of accumulation decreasing after approximately ten passes. Passive soil pressures at the springers also increased markedly. This demonstrates that the increasing

deflection of the pipe springers under repeated loading caused the passive earth pressures to increase and act to reduce further deflection of the pipe (see Figure 2.12). The subsequent application of class HB loading (BSI, 1978), which was more severe than the loads imposed by the scraper, produced a slight increase in the pipe deflection, indicating that further movement of the springers caused the requisite (increased) passive pressure to develop. This study is one of the few that consider the effects of repeated loading on buried flexible pipes, although the number of loading cycles was not monitored when the road was open to traffic.

A full scale investigation of the effects of vehicular loading on corrugated polyethylene pipe (Watkins et al, 1993) was undertaken to determine the minimum and maximum depths of cover that would prevent pipe failure under repeated loading. The applied wheel load was varied from a minimum of 2.5 tonnes to a maximum of 7.25 tonnes. Back-calculation of the cover depth from measured deflection data yielded values ranging from -15mm (for a wheel load of 2.75t) to 175mm (for a wheel load of 7.25t) for 450mm diameter pipe. The negative values at low applied surface loads (2.75t) indicated that in theory no cover is needed. This means that the pipe may be exposed but that it possesses sufficient ring strength, and gains sufficient support from the surround adjacent to its springers, to carry the loading when applied directly to it. The case for the 7.25t load is also interesting because of the low depth of cover required compared to standard practice. At such low cover depths there is no possibility of significant soil arching. The inference is that the pipes tested would withstand an applied loading without the benefit of load reduction caused by soil arching. Conversely, the pipes seem to be excessively conservatively designed.

2.2.6 Time

2.2.6.1 Creep of the Pipe

As time passes, individual polymer chains within the body of a plastic pipe will move and reorientate. The results are either a reduction in the applied stress under a constant deformation or an increase in the pipe strain under a constant loading, amounting to deformation of the pipe. These phenomena are symptomatic of visco-elastic (creep) behaviour of the pipe material.

In order to predict pipe deformations after a significant period of loading, a long-term pipe stiffness was proposed, based on experimental observations of pipe samples under constant deflection, parallel-plate loading (Janson, 1995). In this work, stress relaxation occurred. The deflection was held constant and the stress decayed as the polymer chains reorientated during the creep process. Since the elastic modulus is proportional to the applied stress, in Janson's

experiment, the elastic modulus “decreased” with time. This is shown in Figure 2.13. The compliance C (defined as the reciprocal of E) demonstrates a linear relationship with logarithmic time, allowing determination of the “long term” E via linear extrapolation.

The reduction in E propounded by Janson is not a literal one. If a specimen of material is unloaded and allowed to recover, the elastic properties (i.e. the instant response of the pipe to an applied loading) will be the same as those of a specimen which had not been subject to stress over a long period. In practical terms, this means that pipe that had been buried and was later subject to transient loading (e.g. a loaded wheel) would deform and recover in much the same manner as a newly-buried pipe whose material had not had time to creep appreciably (Janson, 1990 and 1995).

2.2.6.2 Movement of the Soil

The soil surrounding a pipe is constantly subjected to stress from the overlying fill material. As well as causing the pipe to deflect, this stress gives rise to movements within the backfill (typically a clay) that continue as time progresses. The movements are due to consolidation, in which the relatively slow dissipation of local pore water pressures in the soil causes the effective stress in the region of the pipe to increase, leading to downward movement of the backfill and resulting in additional pipe deflection. Consolidation is less likely to occur in the surround as it is sufficiently permeable to allow rapid drainage of the local pore water within it. The surround also provides an additional drainage path which will reduce the overall effect of consolidation of the backfill.

There are other sources of soil movement. Individual particles of the surround may reorientate under the loading, causing settlement (or compaction) and allowing greater pipe deflection. This may ultimately have a beneficial effect as the result of densification is to cause a more rapid subsequent mobilisation of the passive earth pressure that resists pipe deflection (cf. 2.2.2.2). Wetter surrounds are thought to settle to a greater extent because of the “lubricating” effect of water on the soil particle surfaces (Petroff, 1990a).

The passing of time may cause the frictional interface of the trench wall to decay, leading to slippage of the soil prism and redistributing of load onto the pipe. The equilibrium in a soil arch would be destroyed if significant slippage took place, and this too would increase the loading on the pipe.

2.2.6.3 Creep of the Pipe-soil System

The combined effect of creep on the pipe-soil system depends on the relative stiffness of the two components. Studies of the behaviour of a buried pipe under loading

(Gehrels and Elzink, 1979) found that pipe deflections do not increase significantly after approximately five years. In cases where other loads were applied to the buried pipe, such as traffic loads, equilibrium was achieved after approximately two years.

An investigation of the time-dependent relaxation modulus of visco-elastic materials was made to derive an expression for the long-term pipe modulus ($E(t)$, in Pa) as a function of time (Chua and Lytton, 1989). This applies to plastic pipes buried in soils because the initial elastic response to an applied external loading is followed in the long term by slower, viscous behaviour as the two components in the pipe-soil system creep. The expression is:

$$E(t) = E_1 t^{-m} \quad \text{Eq 2.16}$$

where:

E_1 = modulus measured at one minute following application of the loading to a test piece (Pa).

t = time (s), and

m = constant (dimensionless).

The calculated effects of the creep on a buried pipe (PVC in this case) and soil (sand) on the pipe modulus are shown in Figure 2.14. The curve is approximately hyperbolic in shape. Comparing this with a typical curve from long-term tests on isolated pipes (Janson, 1995 (see Figure 2.13)) it can be seen that the reduction in modulus is more gradual in the buried pipe than in the isolated pipe. This indicates that the surround provides resistance to the movement of the pipe in the manner of a damper, with the elastic deflection of the pipe initially restrained but allowed to accumulate as time passes by the combined movement of the pipe and its surround.

In general, most of the deformation of a buried pipe, under static loading such as overburden, occurs soon after the loading is applied. Theoretical extrapolations of the deformation of both pipe and soil (Petroff, 1990b) found that, for the HDPE pipe buried in a clay fill (which is not common) 68% of the 100 year deformation occurred one day after application of loading, 76% occurred after one week, 81% occurred after month, 89% occurred after one year, and 95% occurred after ten years.

For a sand surround, the fractions of the 100 year deformation were 45%, 56%, 64%, 77% and 89% for the same time periods. The sand therefore exhibited a slower response to the applied loading than the pipe in this study, which would allow shedding of load to the sand. Chua (1986) found that the granular materials commonly used for pipe surrounds exhibit similar responses to loading, so the sand case is indicative of the response of granular surround media in general.

2.2.7 Acceptable Limits of Pipe Deflection

In assigning an upper limit of deflection to a flexible pipe, several factors need to be considered.

Firstly, the stability of the pipe in its deformed shape must be assured. This was considered by Spangler in his development of the Iowa formula (cf. 2.1.2), in which “snap-through” of the pipe crown at excessive pipe deflections precipitated collapse of the pipe. In his work, Spangler carried out a study of circular steel culverts under railways and concluded that VDS of 20% could be maintained before snap-through and collapse became a danger. A factor of safety of four was applied to this value to yield an upper limit of VDS of 5% for design purposes.

Secondly, the integrity of the pipeline may be compromised if there is sufficient deformation to affect the pipe joints, resulting in the opening of the joint at the location of the pipe springer and causing a leak.

Thirdly, deflection of the pipe will affect any structures that are adjacent to the pipe if the magnitude of the deflection causes appreciable settlement to the ground surface above it. This is important for very large structures such as culverts, where deflections may be large. It is also important for shallow burial depths where deformations under loading are larger and ground surface movements more pronounced.

Finally, the hydraulic capacity of the pipe is dependent on its cross-sectional area and excessive deflection will reduce this. It is unusual for gravity drainage to operate in “pipe-full” conditions, but pipelines are designed on this basis and it may indeed happen in exceptional circumstances. At low elliptical deflections the change in area is small, but becomes significant as deflection increases to levels indicative of pipe instability.

In the UK the limit of 5% VDS put forward by Spangler is still used (BSI, 1980), and applies when backfilling is completed. The British Standard further advises that this limit can only be met with proper compaction of the backfill material, and that it may be breached if the backfill is not properly compacted. More recently, a 6% limit has been recommended (WRc, 1986), and this applies to two years after construction, to allow for any settlement of the surround and continuing deformation of the pipe. It is also recommended that transient deflections resulting from installation practices be less than 8%, but that the 6% limit still be met after the maintenance period and two years after installation. The 6% limit is also stipulated in Germany (ATV, 1988 cf 2.3.4).

2.3 DEVELOPMENTS OF DEFLECTION THEORIES FOR FLEXIBLE PIPES

2.3.1 The USBR Equation

An empirical refinement of the Iowa formula based on back-calculated parameters from measured installations was derived for the US Bureau of Reclamation (USBR) by Howard (1981). It was considered an improvement on the Iowa formula in that:

- (i) vertical deflections are calculated,
- (ii) initial and long term deflections may be predicted,
- (iii) an inspection factor to account for differing levels of site supervision is included,
- (iv) a design factor is introduced for use of the equation in different circumstances (design, comparison of actual and theoretical deflections and in cases where deflection is the critical factor), and
- (v) a prism load, as opposed to the (smaller) “Marston” load (see 2.1.1) is used.

In addition, the modulus of soil reaction used by Spangler (and quantified in greater detail by Howard, 1977) is replaced by a soil stiffness term, S_f . The values used were derived from Howard’s work and are quoted for each soil type under the Unified Soil Classification System. The USBR equation is:

$$\delta y(\%) = T_f \left[\frac{0.07\gamma h}{\left(\frac{EI}{r^3} + S_f D_f \right)} + C_f \right] + I_f \quad \text{Eq 2.17}$$

The equation as written is valid only when the terms are expressed in the following Imperial units:

δy = vertical deflection (% of original diameter)

γ = backfill density (lb/ft³),

h = depth of cover (ft),

EI/r^3 = pipe stiffness factor (lb/in²),

S_f = soil stiffness factor (lb/in²),

D_f = design factor (dimensionless),

C_f = construction factor (%),

I_f = inspection factor (%), and

T_f = time factor (dimensionless).

The design factor D_f is intended to differentiate between applications of the equation, and depends on which of the following cases is relevant;

Case A is used for comparing field measurements with theoretical deflections.

Case B is used in design when the actual deflection is to be held at less than a theoretical value plus 0.5 percentage points.

Case C is used for design where deflection is the critical design criterion and should result in the actual deflection being not greater than the calculated value.

The time factor is analogous to the deflection lag factor D_L put forward by Spangler. T_f arises from the tendency of the soil loading on the pipe to increase with time, and for the soil at the springers to consolidate as the pipe continues to deflect under the increasing loading. The values of T_f were found by expressing the deflections recorded at periods following installation to the initial deflections.

The construction factor C_f is incorporated to allow for the variation in compaction that may occur on site. Surround media with low fines contents (e.g. single-size gravels) are assigned a lower value of C_f than well graded materials whose stiffness depends to a greater extent on the way in which their compaction is carried out.

The inspection factor I_f is intended to account for variations in workmanship during construction operations. The ideal case is where supervision is thorough and density tests are carried out on the placed fill material. This is rarely done in the UK as testing criteria were written when rigid pipes (which do not depend on their surround for strength) were the only type in use. Values for I_f for initial deflections are given as 2% and 5% for dumped and compacted surrounds respectively. The larger value for the compacted case shows both the effect of compaction on pipe deflection and the effect of probable variations in the compaction process. For the long-term case, these become 3% and 7% respectively. This implies a deflection lag factor of the order of 1.5 (similar to that of Spangler, see 2.1.2), although the “long term” is not defined in terms of elapsed time.

Howard used the simple soil prism load, not that calculated from Marston theory, in his work. This gives somewhat lower back-calculated values of E' than would be determined using Marston theory. Elliptical deformation was also assumed, allowing the horizontal deflection (predicted by the Iowa formula Eq 2.6) to be converted to a vertical deflection.

2.3.2 Greenwood and Lang's Development of the USBR Equation

A refinement of the USBR equation was developed by Greenwood and Lang (1990). The USBR method was the basis of the US standard for fibreglass pressure pipe (ANSI,

1988), and the aim of Greenwood and Lang was to produce a more accurate design method that took greater account of the variability of the factors affecting flexible pipe behaviour whilst retaining a method that could be easily used by the designer.

The pipe deflection is described as the sum of three parts:

$$\delta_{vp} = \delta_{vl} + \delta_{vo} + \delta_{va} \quad \text{Eq 2.18}$$

where:

δ_{vp} = upper limit of predicted vertical deflection,

δ_{vl} = deflection due to load,

δ_{vo} = deflection due to construction (or initial ovaling), and

δ_{va} = deflection due to field installation variability

Vertical deflection due to load is given by:

$$\delta_{vl} = \frac{W}{S_p + S_s} \quad \text{Eq 2.19}$$

where W is the gross load applied to the pipe and S_p and S_s the pipe and soil stiffnesses respectively. The effect of time on the static loading is accounted for by incorporating an arching factor C_L , which is equal to the Marston load coefficient (cf. Eq 2.1) in the short term case, thus taking account of the arching effects in the soil at that stage. For longer-term effects, complete decomposition of the soil arch is assumed to occur and C_L becomes unity, making the total static load simply the weight of the overlying soil prism. Live loads are calculated using conventional soil mechanics techniques (e.g. Boussinesq theory) and the resulting load added to the static load to give the total load on the pipe.

The pipe stiffness is the conventional expression (cf. Eq 2.1), but multiplied by the factor C_p , termed the pipe stiffness retention factor, to take account of creep. For the short-term case, C_p is unity, and longer-term values are obtained by extrapolation of creep modulus data.

The stiffness of the surrounding soil is considered in terms of soil type, density, burial depth, moisture content, trench configuration, lateral (passive) pressure distribution and time. The "soil modulus" adopted in this proof was determined using the one-dimensional consolidation method, with secant moduli being determined in relation to depth of burial and standard (Proctor) density for a number of soil types. A modified power law was developed to describe the reduction in soil stiffness with time:

$$E_s(50) = C_T(50) \cdot E_0 \quad \text{Eq 2.20}$$

where E_s is the secant modulus at fifty years, E_0 is the initial secant modulus and C_T is the soil retention factor. Values of C_T are given for different soil types.

Trench width effects are accounted for by using Leonhardt's (1979) factor, ζ , defined in Figure 2.10. In fact, the soil stiffness S_s term can be related to the soil secant modulus E_s :

$$S_s = 0.6\zeta E_s \quad \text{Eq 2.21}$$

The factor of 0.6 was included by Leonhardt to relate the backfill stiffness in a trench condition to that observed in confined laboratory compression testing.

The effect of non-uniform soil support will result in the deviation of the deformed pipe shape from the ellipse that is normally assumed. This factor is quantified in the theory by the ratio of the vertical deflection ΔV to the horizontal deflection ΔH . Values of this ratio are given as a function of the soil type, density and pipe stiffness and range from 1.0 to 3.5.

A dimensionless pipe-soil interaction coefficient C_1 was specified, which was a function of the pipe stiffness and degree of surround compaction:

$$C_1 = a \left(\frac{EI}{1250D^3} \right)^b \quad \text{Eq 2.22}$$

where a and b are dimensionless constants related to the standard Proctor density of the surround and EI and D the flexural rigidity per unit length and diameter of the pipe respectively. The factor 1250 has units of stress (Pa) and represents a "base pipe stiffness".

The component of the total pipe deflection caused during installation, δ_{v0} , was included as a simple additive term depending on pipe stiffness and soil density.

The factors found to affect the installation variability component δ_{va} were soil and density variations, variations in trench width and adherence to the project specification.

The inclusion of all of the above terms causes Eq 2.18 to be recast as:

$$\delta_{vp} = \frac{k_x (\Delta V / \Delta H) (C_1 \gamma H + W_L)}{8C_{TP} (EI / D^3) + 0.061(0.6)\zeta C_1 E_s} (\times 100\%) + \delta_{v0} + \delta_{va} \quad \text{Eq 2.23}$$

Deflection data were recorded from eighteen pipelines during and after construction, and it was found that Eq 2.23 predicted the pipe deflection data more accurately than the USBR equation (Eq. 2.17). An important improvement is the inclusion of a pipe-soil interaction coefficient. It is relatively easy to use because most of the terms can be taken directly from prepared tables. Compared to some of the theoretically justifiable methods described in 2.3, the method's simplicity would make it appropriate for use in routine drainage applications in the UK, provided that the effects of the difference in soil and installation conditions could be quantified.

2.3.3 Gumbel's Method

In 1982, a wholly theoretical method was introduced in which the pipe and its surrounding soil are considered as an entity (Gumbel, 1982).

The method defines excessive pipe deflection (which, in severe cases, leads to yielding of the pipe wall) and buckling of the pipe wall as the two primary failure criteria. The idealised analysis considers a long, thin-walled cylinder deeply buried in a uniform, weightless, linear elastic soil medium and subjected to two-dimensional loading in the plane of cross-section. The method applies to pipes with a ratio of thickness to diameter (commonly referred to as the Standard Dimension Ratio or SDR) of 20 or greater (Smith and Young, 1985).

The structural properties of the components in the system are defined in terms of the elastic moduli of the pipe and soil (E_p and E_s respectively), their Poisson's Ratios (ν_p and ν_s), the diameter of the pipe (D), the second moment of area of the pipe (I) and the area of cross-section of the pipe (A), such that;

$$(i) \text{ plane strain soil stiffness, } E_s^* = \frac{E_s}{(1 - \nu_s^2)} \text{ (in Pa),}$$

$$(ii) \text{ plane strain pipe modulus, } E_p^* = \frac{E_p}{(1 - \nu_p^2)} \text{ (in Pa)}$$

$$(iii) \text{ flexural stiffness of pipe ring, } S_f = \frac{E_p^* I}{D^3} \text{ (in Pa), and}$$

$$(iv) \text{ compression stiffness of pipe ring, } S_c = \frac{E_p^* A}{D^3} \text{ (in Pa).}$$

The influence of the relative stiffnesses of the pipe and the soil is accounted for by the following parameters:

(i) the flexural stiffness ratio $Y = E_s^* / S_f$ and

(ii) the compression stiffness ratio $Z = E_s^* / S_c$

Y is used to classify the pipe under consideration as rigid ($Y < 10$), flexible ($Y > 1000$) or intermediate ($10 < Y < 1000$), and it can be seen that this is dependent on the soil elasticity and the flexural stiffness of the pipe (i.e. the properties of the system). The ranges of Y for a selection of pipe materials and soil properties are given in Figure 2.15. The behaviour of systems of these categories can be summarised thus:

- (i) Rigid - over 90% of loading carried by pipe in bending,
- (ii) Intermediate - 10% to 90% of loading carried by pipe in bending, and
- (iii) Flexible - less than 10% of loading carried by pipe in bending.

The applied force is regarded as acting on the pipe-soil system, a fundamental departure from previous theory. The pressures on the system are assumed to be the free-field pressures due to the dead load of the overlying soil, and are designated p_{vd} and p_{hd} for the vertical and horizontal components respectively. The two are related by a dead load lateral pressure ratio k_d thus:

$$p_{hd} = k_d p_{vd} \quad \text{Eq 2.24}$$

These "external" forces are then expressed as uniform and distortional components (see Figure 2.17). Values of k_d and the other soil parameters are given in Table 2.2. Uniform deformation (i.e. hoop compression) is small and generally ignored for design. Distortional, or out-of-round, deformation is calculated as the sum of initial, first-order and second-order deformation:

$$\delta y = \delta y_o + \delta y_1 + \delta y_2 \quad \text{Eq 2.25}$$

Initial deformation (δy_o) is defined as the deformation when the fill material has reached the crown of the pipe. The first-order deformation, δy_1 , results from the external loading and is defined as:

$$\delta y_1 = \frac{4p_y}{108S_f + E_s} \quad \text{Eq 2.26}$$

where $p_y = 0.5 \times (p_{hd} + p_{vd})$.

Eq 2.26 is similar in form to the Iowa formula, but has the distortional pressure, not the vertical load, as numerator. This means that the frictional effects of the trench walls do not need to be taken into account as p_y is computed from the free-field stresses. Second-order deformation, δy_2 , relates to p_z (defined as $0.5 \times (p_{vd} - p_{hd})$) acting on the horizontal projections of the deformed pipe ring.

The mode of buckling of the pipe depends on the flexural stiffness ratio Y . Figure 2.17 demonstrates that a relatively flexible pipe will exhibit a larger number of "waves" when it buckles than would a relatively stiff pipe. In practice, short wavelength buckling would manifest itself by local buckling of the pipe wall. This would lead to an imbalance in the hoop stresses in the pipe wall and yielding of the wall. Thus the buckling would be more likely to lead to failure of the pipe by another mechanism.

Gumbel considered the effects of arching of the soil above the pipe using an "arching factor", α , which represents the proportion of p_z carried by the pipe, and is assumed to be unity for common installation conditions.

A set of design charts has been produced to determine δy directly, an example being Figure 2.18.

Field work, comprising box-loading tests on steel, aluminium and plastic (PVC-U) pipes was carried out to validate the model (Crabb and Carder, 1985). The pipes were buried in

both dry sand and sandy clay to a cover depth of 0.3m (an unusually shallow depth) and surface stresses of up to 725kPa were applied. The PVC-U pipe deformed elliptically in the loose sand, producing VDS in the range 2.7% to 7.9%.

Back-calculation of E_s^* was reported to give values ranging from 8.5MPa to 11.9MPa, corresponding to the “medium” compaction state as defined by Gumbel (see below). E_s^* values were determined for several deflection values. Figure 2.19 shows the trend of the results, emphasising the non-linear response of soils to the loads exerted by the pipe springer.

While Gumbel’s method has been proved by limited laboratory studies, difficulties arise in accurately defining E_s^* . Table 2.2 shows the range of values for different types and states of compaction. E_s^* is acknowledged to depend upon the soil surround, its placement and compaction, trench wall geometry, and the methods of insertion and withdrawal of trench supports. Gumbel acknowledges that E_s^* can only be defined by back analysis and, since little experience of applying the technique is available, this makes the method difficult to use (Rogers et al, 1995 gives worked examples). This is unfortunate since the inability to define accurately the soil elasticity parameter is also the primary weakness of the Iowa method which predated Gumbel’s theory by forty years. Since E_s^* is also the dominant component of the first order pipe deflection, the subtle improvements resulting from the inclusion of second-order effects are likely to be negated by uncertainties in the first order effects caused by estimating E_s^* . In addition, the effects of time are not accounted for. The method has, however been used for the compilation of the definitive UK Department of Transport document HA40/89 (1990), which specifies allowable installation conditions for pipes for highway drainage (see 2.2.4.3).

2.3.4 The ATV Method

The design standard used in Germany (ATV,1988) considers the pipe surround and backfill as comprising four regions, allowing a better definition of soil properties. Four classifications of soil are made and these are divided into sub-classes depending on their states of compaction. Each is assigned a value of the modulus of resilience (secant modulus), E_s . The effect of variations in compaction and workmanship is accommodated in the definition of the soil stiffness parameter (termed the secant modulus of resistance, E_s). External loads on the pipe are considered separately. Installation practice (i.e. type, spacing and duration of trench support) and bedding conditions are also included. The assumed stress distribution over the pipe is shown in Figure 2.21, and accounts for the redistribution of stress that occurs as a result of the difference in the stiffnesses of the two components. The amount of redistribution is governed by the concentration factor, λ which is a function of the relative projection of the pipe and the ratio of the

burial depth to the pipe diameter. The resultant pressure distribution is used to calculate the vertical diametral change of the pipe (Δd_v , measured in m) using the following equation:

$$\Delta d_v = c^*_v \frac{(q_v - q_h)}{S_R} . 2r_m \quad \text{Eq. 2.27}$$

where:

c^*_v = pressure coefficient depending on vertical and horizontal stress distribution (dimensionless),

q_v, q_h = vertical and horizontal pressure terms (Pa),

S_R = pipe stiffness term (Pa), and

r_m = mean pipe radius (m).

The allowable long-term deformation for non-railway applications is 6% of the original diameter, slightly larger than that allowed in the UK (BSI, 1980).

2.3.5 Gerbault's Method

A model for predicting the behaviour, including buckling, of flexible pipes under any condition or deflection shape represents the soil as a series of springs (based on the Winkler, 1957 model) of rigidity β (Gerbault, 1995). Gerbault modelled only half of the pipe, assuming the pipe and the loading to be symmetrical about the vertical axis of the pipe. A novelty was the definition of the second moment of area, I , thus:

$$I = \frac{t^3}{12(1 - \nu)} \quad \text{Eq 2.28}$$

where ν is Poisson's ratio of the pipe material.

This allowed the pipe to be considered as a shell and not a series of rings along its length. Figure 2.21 shows the basic model. The distribution of pressure around the pipe was simplified to vertical and horizontal contributions p_v and p_h respectively, and decomposed into "deviatoric" and "spherical" components, similar to the distortional and uniform components in Gumbel's method. The deviatoric component causes the pipe to become oval in shape, and the spherical component represents a hydrostatic pressure, which may be caused by the presence of water or an internal pressure.

The value of the vertical deformation is given by:

$$\frac{\delta D}{D} = p_v \left[\frac{k_\alpha - \frac{k_2}{12}}{8S + \frac{E_s}{9(1 - \nu_s^2)} - \frac{\bar{p}}{3}} \right] + 2(A - 1) \frac{e_o}{D} \quad \text{Eq 2.29}$$

where:

δD = change in pipe diameter (m),

D = initial pipe diameter (m),

k_α = bedding coefficient for bedding angle α (dimensionless),

k_2 = earth pressure coefficient (dimensionless) (such that $p_h = k_2 p_v$),

S = short term pipe stiffness (EI/R^3) (Pa),

E_s = soil elasticity modulus (Pa),

ν_s = Poisson's ratio of soil (dimensionless),

$\bar{p} = (p_v + p_h)/2$,

A = amplification factor (function of buckling pressure)(dimensionless), and

e_o = initial out-of-roundness (m).

The first term in the right-hand side of Eq 2.29 is similar in form to the first-order term in Gumbel's method (Eq 2.26). The vertical pressure term is used in the numerator. The coefficient of the soil stiffness term E_s reduces to 0.122, if a value of 0.3 is used for ν . The coefficient of E_s is twice that of the coefficient of E' in the Iowa formula. The reason for this is that the Iowa formula considered horizontal soil "springs" only, whereas Gerbault considered isotropic springs, effectively the superposition of vertical and horizontal springs of equal rigidity.

The method has been further refined to cope with changes in the soil stiffness. However, the effects of time are not considered.

2.3.6 Chua and Lytton's Method

This deflection prediction method uses a finite element model (FEM) and regression analysis applied to data for over 600 tests (Chua and Lytton, 1991). The method modelled the pipe-soil system as three components:

- (i) trench: the *in situ* soil, bedding layer and backfill were regarded as separate zones, as these may have distinctly different soil properties in practice,
- (ii) soil: this used a hyperbolic non-linear elastic model. It can accommodate the change in soil modulus that occurs as a result of remoulding or reloading and

thus is more relevant to the consideration of the long-term behaviour of the pipe-soil system, where remoulding and loading will affect soil properties, and (iii) pipe: a visco-elastic model is used to accommodate the behaviour of the pipe in the long term.

The inclusion of (ii) and (iii) allow the time-dependent behaviour of the pipe-soil system to be modelled. This is a distinct advantage over Gumbel's and Gerbault's methods.

The design equations were developed using the CANDE finite element analysis program (Katona et al, 1976) and as such are very complicated. The complexity of these equations would make the method time-consuming to use. As such, the method does not lend itself to manual calculations.

Regression analysis was used to produce relationships between the stresses and various soil and pipe parameters. The main factors influencing the behaviour of the model were found to be:

- (i) soil stiffness. Since the soil property E' is stress dependent, it is necessary to know the stress state, in particular the compaction state, of the soil. A poorly compacted backfill soil results in a higher stress level around the pipe and a larger surround soil modulus. A stiffer soil results in lower stresses in the soil elements around the pipe and produces a smaller modulus and, in addition, leads to the imposition of a smaller load on the pipe.
- (ii) Arching. This is quantified by an arching factor, which is a function of trench width, pipe diameter and the actual soil modulus. Stiffer surrounds cause a greater degree of arching.
- (iii) Trench width. This depends on the access requirement to compact the surround. Narrower trenches lead to greater arching effects and are preferable for arching purposes (Watkins, 1995) as well as economic ones.
- (iv) Groundwater. Hydrostatic stress is quantified by a multiplication factor.

Chua and Lytton proposed that the strain level at the fibre furthest from the neutral axis of the pipe wall would be an appropriate indicator of the integrity of the pipe. Comparison of field data with predicted deflections found that the FEM yielded an upper bound of deflection.

2.3.7 Moore's Finite Element Analysis of Corrugated Plastic Pipes

The response of twin wall annular corrugated HDPE pipe when installed in the ground has been predicted using FEM techniques (Moore and Hu, 1995). The FEM was used to model the compression of a pipe which was buried in the cylindrical test cell used by Selig et al

(described in 2.2.5.1). The test cell does not strictly represent pipe burial conditions but is used because of the controlled manner in which stresses can be applied.

A two-dimensional finite element mesh was generated around the pipe profile and is shown in Figure 2.22. The two-dimensional mesh was justified in the context of the situation modelled because the all-round pressure applied to the pipe and surround by the bladder will tend to confine the surround uniformly around the pipe and thereby prevent differential movement and slippage of the surround at its interface with the pipe. The polyethylene was modelled as having linear visco-elastic properties (see 2.2.1.1), an assumption which is valid for stresses approaching 50% of the yield stress. The surrounding soil was modelled as an isotropic linear elastic material, a good first approximation to most buried pipe applications (e.g. Katona, 1976).

The behaviour of the soil in shear is also of some interest. Shear failure may occur in a surrounding soil if the following inequality is observed:

$$\frac{\sigma_1}{\sigma_3} > \tan^2 \left(45 + \frac{\phi}{2} \right) \quad \text{Eq 2.30}$$

where:

σ_1 = major principal stress in soil,

σ_3 = minor principal stress in soil, and

ϕ = angle of internal friction of soil.

For a soil of moderate compaction (standard Proctor density of 80%), the critical value of σ_1/σ_3 is 4, and for a soil of good compaction (standard Proctor density of 98%) it is 10. Referring to Figure 2.23, it can be seen where shear failure would occur for these cases.

The stress distributions predicted by the FEM show the stresses generated both circumferentially and axially. The circumferential stresses (Figure 2.24) were predicted for the case of a bladder pressure of 35kPa applied for 1000 minutes. Compressive stresses are shown as negative quantities. The largest compressive stresses (0.8MPa) occurred at the junction of the two pipe walls, and the smallest on the outer face of the internal wall under the centre of the corrugation. Axial stresses are shown in Figure 2.24. The inner wall appeared to bend outwards whilst being constrained by the wall junctions. The outer wall showed a small region of axial compression but otherwise the axial stresses were small (0-0.2MPa). Rippling of the liner (observed by Selig et al, 1994) was predicted and was of the type found in the buckling of thin shell-type structures. This type of buckling is in fact quite stable and does not reduce the load capacity of the affected structure. The tearing of the inner wall was predicted to occur at the junction of the two pipe walls.

Parametric studies also showed that the secant moduli of the embankment and the surround materials increased as the embankment depth was increased. The degree of arching reduced the predicted stress on the pipe to only 8% of that of the vertical overburden pressure.

2.4 DISCUSSION

The individual factors that influence the structural response of buried plastic pipes to loading have been investigated and discussed. These factors were broadly identified in the early work on flexible culvert behaviour. In particular, Marston's analysis of installation conditions and the geotechnical mechanisms therein allowed the loads that actually bear on a buried pipe to be determined with greater accuracy and theoretical justification. Spangler's investigations of the means by which flexible pipes deform (and more importantly the consequences of deformation on the mobilisation of passive earth pressures as a limiting factor on that deformation) were the foundations of the "science" of flexible pipe behaviour that is now widely used for quite different types of pipes in a range of types of installations.

The effects of the material and geometry of the pipe have been discussed. Because of the commercial advantage that accrues from reducing the amount of material in the pipe, the trend will be for corrugated and helically-wound pipes to supplant the heavier and more expensive single-wall pipes. The design "limits" of these pipes were found to be influenced chiefly by the need for the pipe to pass a parallel-plate test in which the pipe deflection is extrapolated to fifty years and an equivalent stiffness is calculated. The weaknesses of this test in the context of buried pipes have been described and more appropriate means of testing (such as those used in the USA) have been identified. The degree of conservatism, if any, in the design of plastic pipes that the current specifications produce would be of interest to the plastic pipe and civil engineering industries.

The properties of the pipe are in most cases of secondary importance, since the soil that constitutes the pipe surround has a larger effect on the amount by which a plastic pipe will deform under loading. The degree to which adequate compaction can be achieved to resist pipe deflection depends partly on the type and particle size characteristics of the surround. However, selection of the surround must be carried out with regard to the ease with which compaction can be achieved because of productivity requirements on site and the need to achieve consistency of material density. The latter requirement is crucial as soil compaction has been shown to have a considerable influence on pipe deflection. In most civil engineering works, the installation of drainage is considered as a "low-technology" task, control of the quality of work being limited to checks on water-tightness and alignment. Therefore, the surround material for flexible pipes must

be such that the required density can be achieved without excessive monitoring or indeed disproportionate effort. This is why poorly-graded (or single-size) gravels are popular surround media. Accurate direct measurement of the critical soil parameters has been shown to be possible if parallels to pile behaviour are drawn or by the appropriate interpretation of standard laboratory tests. The favoured method has been back-calculation from observed deflection data but this can be affected by the effects of time and uncertainties in the static and dynamic loading histories of pipelines.

The effects of water on the surround have been described. Its effect on the density and stiffness of the surround, and the effective stresses in the soil is significant. All of these factors therefore affect the deflection of a buried flexible pipe. The presence of groundwater also adds to the forces on the pipe. In the long term, the decay of pore water pressure with time under a constant loading leads to higher effective stresses and causes an increase in deflection with time.

The magnitude of the static soil loading depends on the installation environment of the pipe. A pipe in a trench will experience a smaller loading because of the presence of the trench walls, which will resist the load of the soil prism by friction. This will not happen if the pipe is simply laid on the ground and fill placed above it. The phenomenon of arching, by which load is shed from the pipe, has been described and the development of an equilibrium between the deflected pipe and the surround explained. Both trench-wall friction and arching may deteriorate with time, which should be considered at the design phase.

The passing of vehicles repeatedly over some types of buried flexible pipes has been done in field studies. The general trend of pipe deformation is an initial increase in deflection which reduces in rate as the number of vehicle passes increases. The rate at which the deflection “stabilises” depends on pipe, soil, installation and loading characteristics. The controlled measurement of a large number of vehicle passes has not been carried out on the types of pipes investigated for this research work. This aspect of their behaviour is important from the point of view of the “lifespan” of a repeatedly loaded buried pipe before excessive deflection renders it unserviceable or structurally unstable. The longevity of structural components is becoming more important with the advent of Design, Build and Operate highway construction contracts, in which service lifetimes for all components (including buried flexible pipes) of thirty or perhaps fifty years are stipulated. On this point flexible pipes are at a disadvantage compared to rigid pipes, which have been in use for considerably longer times and are thus proven in terms of their long-term performance.

The effects of loading on the mechanisms of deformation depend on the relative stiffness of the pipe and its surround as well as those factors described above. The shape of deformation gives an indication of the likely mode of failure (i.e. excessive deflection or buckling).

The creep and consolidation behaviour of the pipe-soil system depends on the relative stiffness of the pipe and soil also, and this has been seen to cause time-dependent deflection of the pipe. This is important when considering the behaviour of the pipe during its lifetime. Long-term deflection limits currently used were derived from Spangler's observations of large steel culverts and as such may not be relevant in terms of the actual performance of smaller diameter plastic pipes under current UK conditions or indeed in terms of the potential performance of these pipes under more severe conditions.

Various methods of predicting pipe deflection have been described. These include the USBR equation, which is an empirically improved version of the Iowa formula, and Greenwood and Lang's refinement of it which is more complicated but goes into greater detail on the important soil properties (especially the effects of density). By the use of derived coefficients, it also takes account of time effects (on both pipe and soil) and pipe-soil interaction, the latter being a considerable advance on the Iowa and USBR formulae. The German ATV method uses a more rigorously-derived stress distribution in the calculation of deflection, which depends on the pipe stiffness. The soil properties are also dealt with in greater detail than the Iowa or USBR methods.

Theories by Gumbel and Gerbault looked anew at the pipe-soil system in its entirety and resulted in theoretical models which consider the effect of loading on the system itself. Whilst capable of producing more accurate results, Gumbel's method has been found to be awkward to use and requires assumptions to be made which detract from the improved accuracy that can be achieved. Gerbault's method models half of the pipe only and considers it as being supported by horizontal and vertical springs. As with Gumbel, the deformation is split into components that cause elliptical deflection and all-round diametral reduction. The Gerbault model itself is very versatile, but neither can take account of the long-term pipe performance which is an important practical shortcoming.

Finite element methods allow the pipe-soil system to be modelled and all manner of variables to be considered, including all of the factors that influence flexible pipe behaviour which have been described above. Chua and Lytton's work may be regarded as the epitome of this because it is based on the statistical analysis of hundreds of existing installations and uses the observations to develop the design equations. The method may be practically justifiable and indeed accurate but it is very complicated. The advent of structurally more complicated pipes (e.g. corrugated) and the complex stress patterns within them requires the use of finite element models such as Moore's to predict pipe behaviour. Failure mechanisms can be determined and the validated model can also be used as a research and development tool for the economical design of twin-wall pipe.

The increasing complexity of deflection theories is a good development in that it increases understanding of the pipe-soil system and allows for accurate pipe and pipeline design. However, the practical limitations are evident. When factors such as the variability in site practice are considered, it seems inappropriate to use exclusively a design method which produces precise solutions but is time-consuming to use and whose accuracy is undermined by possibly arbitrary additive or multiplication factors that account for uncertainties of site practices. For routine installations of proven pipes in common installation conditions and subject to normal applied loads, the more simple and quick design methods (the Iowa formula or the USBR equation) may be sufficient. However, in some circumstances, a more rigorous investigation would be quite justifiable. These include environmentally sensitive installations (where pipe failure and subsequent leakage may cause pollution), very shallow installations, very large diameter and/or very flexible pipes, very poor surrounds or very high live loading, any of which may result in the deformation mechanisms being outside the scope of assumptions made in the Iowa formula and its progeny and may lead ultimately to structural failure of the pipe.

2.5 RESEARCH PHILOSOPHY

In the above detailed review and discussion, the structural behaviour of buried flexible pipes has been described in terms of individual factors. From this exercise, the most influential of these factors can be defined. In addition, the aspects of pipe behaviour that require further investigation have been identified. These factors and aspects now form the basis for this research work and are summarised below.

The properties of the soil surrounding the buried pipe have a significant influence on the behaviour of the pipe. This influence is greater than that of the mechanical properties of the pipe. The properties of the surround are influenced to a considerable extent by the method and quality of its placement on site.

The deflection of a buried flexible pipe has been seen to occur when a static external stress (such as that produced by overburden) is applied to it. This deflection has been found by some laboratory and field observations to continue at a diminishing rate as time passes. The dominant factors influencing this phenomenon (for a given installation and applied stress) are the surround properties.

A very limited number of field observations of buried pipes subject to the repeated application of stress (such as may be experienced by pipes buried under a highway) have found that the pipe deflection increases as the number of stress cycles increases, but that the rate of

increase slows as the number of cycles increases. The observations were made some 20 years ago.

Laboratory testing has been carried out, much of it in the USA, to determine the behaviour of buried plastic pipes subjected to static stress. Some of the testing has been used for the prediction of field performance or for finite element modelling. In the UK, there has been no laboratory testing of the larger diameters of plastic pipes now in use. There has been little work carried out in the UK or elsewhere to determine whether field conditions (which may include the application of both static and dynamic stresses) can be accurately replicated in the laboratory.

Investigations that have been carried out in the UK relate mostly to pipes buried at normal cover depths in normal surrounds. More severe installation conditions have not been investigated in detail.

With the exception of a limited survey of PVC-U pipes, there is no documented research concerning the behaviour of the joints between pipes that have deflected.

From the above considerations, the areas of most importance and those where previous research work is inadequate in terms of the current design and usage of buried thermoplastic pipes can be established. These have been used to formulate the philosophy for the research work, the broad aspects of which are now elaborated upon as a prelude to the experimental work.

2.5.1 Determination of Long Term Plastic Pipe Performance

From the above discussion it is apparent that the structural performance of pipes in the long term requires investigation. In the first instance, the types of pipes tested must reflect those currently in use in UK civil engineering work. The diameters of the test pipes should be the largest that could be feasibly tested, since much of the research to date (especially in the UK) relates to smaller diameter (of the order of 100mm-200mm) pipes. Pipes of different materials must also be tested to determine whether this factor makes a significant difference both to pipe performance and costs of manufacture.

Having selected the subject pipes, the type and magnitude of the stresses applied to them needs to be quantified. It is apparent that both static stresses exerted by backfill overlying the pipe and transient stresses caused by the passage of vehicles over the buried pipe need to be considered.

For testing in laboratory conditions, the static stresses may be applied in one of the ways used in previous research work (e.g. hydraulic ram or bladder). The stresses need to be applied for such a length of time that continuing pipe deflection can be measured. More

importantly, the trend of deflection during the test needs to be defined sufficiently well to allow prediction of the deflection of the pipe in the long term. This is essential as a means of considering the structurally (and possibly contractually) important “lifetime” of the buried pipe. The test must nevertheless be of a reasonable duration in relation to the time allocated for the entire project.

The magnitude of the applied stresses must relate to both common and extreme depths of burial. This will allow determination of the extent of pipe deformation under “normal” and severe installation conditions. From these data, the margin of safety (quantified as the magnitude of pipe deformation in relation to that which may cause failure) under these two general conditions can be assessed.

The effects of cyclic stresses (due to traffic) on a buried plastic pipe requires the development of new test equipment, based broadly on that used for the application of static stresses. Again the test must be of sufficient (but practical) duration to allow the trends in deformation to be ascertained and longer-term deformation to be estimated with a degree of confidence. This relates to the need expressed above for a knowledge of the “lifetime” of the pipe. In addition, the likelihood of progressive failure or fatigue of the pipe may be determined.

Both the magnitude of deflection of the pipe ring and the shape of the deformed pipe must be recorded. The former quantity gives an indication of the integrity of the “macrostructure” of the pipe under loading and whether the pipe is approaching collapse or a reduction in fitness for use as a result of excessive deflection. The latter quantity gives an impression of the shape of the deformed pipe, knowledge of which will indicate the likely mode of failure of the pipe (e.g. buckling or excessive deflection, for instance). The effects of the installation conditions on the shape of deformation will yield information on the relative merits of each type of surround material and its means of placement.

In order to determine how the proposed laboratory testing related to the behaviour of the pipes in a real installation environment, field-based testing is essential. A test of this nature has not been carried out in the UK since the 1970s, since when there have been considerable advances in plastic pipe technology. The testing must reflect the extremes of current permitted installation practices and the vehicular loading must be the maximum that circumstances allow. Thus the testing (which will inarguably reflect “real” conditions) will also indicate the realistic performance limitations of the pipes. The field trial must also show whether, under typical but controlled site conditions, the specification and installation criteria are sensible or whether they may be widened without compromising the integrity of the pipeline in the long term. Existing tests for flexible pipes, such as those required by British Standards, may also be appraised in order to determine the relevance of their requirements to the

performance measured in the laboratory and field. The field testing will therefore be extensive and will be a significant element of the research. It will also be a key piece of research work in its own right as a contemporary and practical assessment of the performance of currently available plastic pipes under severe conditions.

2.5.2 Development of a Laboratory Test

The laboratory testing will necessarily be of a smaller than the field testing, and will consist of the testing of a small sample of pipe in a relatively small-scale installation environment. The boundary conditions in the laboratory will not therefore represent those on site. Although small-scale testing is not an apparent replication of site conditions (viz. a trench in a soil), the relatively constant boundary conditions will allow the relative performance of each type of pipe to be assessed in terms of their constructions, subject to control being exercised over the surround material. Thus, the reproducibility of the test will be increased. This is an important consideration in the possible adoption of these or similar testing procedures as a tool in the design of the pipes themselves.

However, any laboratory testing that is performed (in this or any other research) must be able to be considered in relation to realistic conditions. The inclusion of an extensive and controlled field test on the same pipes will justify the comparison of laboratory and field data. This will be essential in demonstrating the credibility of the laboratory environment in terms of the extent to which it represents the “real” environment. The differences between the two environments can therefore be accounted for and corrections applied to mitigate them, thereby allowing the use of a proven laboratory test as a research and development tool.

2.5.3. Better Definition of Soil Properties.

There is a relative dearth of reliable data to define accurately the elastic properties of the pipe surround; properties that have been shown to have considerable influence on the deflection of plastic pipes. Much of the data that has been published relates to the types of fills and trench conditions used in the USA, and these data are used widely in UK applications. Whilst this may not be inappropriate, the importance of the soil properties is such that there is a clear need to determine the properties of the common pipe surrounds used in UK civil engineering in the context of UK trenching practice. The deflection data obtained by laboratory and field testing will therefore be used to determine the soil stiffness parameters in the relevant design methods. These will be compared to those ^{6.5.1} recommended and used in the latest

Department of Transport Specifications to determine whether these values are realistic or whether they can be revised.

2.5.4 Integrity of Pipe Joints

This aspect must be considered to ensure that a pipeline (as opposed to the individual pipes tested in the aforementioned work) performs its primary function of providing an enclosed space for the passage of fluids. Samples of pipe, connected using proprietary jointing methods, will be installed in the testing box. The integrity of the joint will be monitored as the pipeline deforms ' under an applied surface stress.

2.5.5 Non-Standard Surrounds

Some tests will be carried out on pipes buried in non-standard surrounds and subject to more severe loading. This is to assess whether the range of surround materials could be increased without a deleterious effect on pipe performance, and to see if a plastic pipe would puncture, and thus in effect "fail", when sharp aggregates are used to surround the pipe and the pipe is subjected to sudden loading which produces a higher degree of impact.

Table 2.1. E' Values in MPa (after Howard, 1977).

COMPACTION STATE PIPE SURROUND TYPE	NONE Material Dumped	SLIGHT <85% Proctor Density	MODERATE 85-95% Proctor Density	HIGH >95% Proctor Density
Fine grained soils with medium to high plasticity	0	0	0	0
Fine grained soils with medium to no plasticity & <25% coarse grained particles	0.34	1.37	2.74	6.86
Fine grained soils with medium to no plasticity & >25% coarse grained particles	0.69	2.74	6.86	13.71
Coarse grained soils with <12% fines	1.37	6.86	13.71	20.57
Crushed Rock	6.86	20.57	20.57	20.57
Accuracy in terms of % deflection	±2	±2	±1	±0.5

Table 2.2. Soil Classification Parameters for use in Gumbel's Method.

(a) Soil Classification.

SOIL GROUP	DESCRIPTION	FINES CONTENT	COMMENTS
I	GRAVEL	<5%	Clean to slightly clayey/silty GRAVEL
II	SAND	<5%	Clean to slightly clayey/silty SAND
III	GRANULAR WITH FINES	5% - 35%	Clayey/silty or very clayey/silty GRAVEL or SAND
IV	COHESIVE (Liquid Limit < 50)	>35%	Inorganic CLAY/SILT of low to medium plasticity

Fines are particles passing a 63µm sieve.
Organic soils, high plasticity soils and chalk are not suitable surround media.

(b) Dead Load Lateral Pressure Coefficient k_d .

SOIL GROUP	UNCOMPACTED	COMPACTED
I	0.2 - 0.4	0.3 - 1.0
II	0.3 - 0.5	0.4 - 1.0
III	0.2 - 0.7	0.5 - 1.0
IV	0.1 - 0.8	0.6 - 1.0

(c) Plane Strain Soil Modulus, E_s^* (MPa).

SOIL GROUP	LOOSE	MEDIUM	DENSE
I	5 - 15	20 - 30	30 - 40
II	2 - 5	10 - 20	20 - 30
III	1 - 3	5 - 10	10 - 15
IV	0 - 0.2	0.5 - 2	1 - 3

First value is the worst probable value.
Second value is the average value

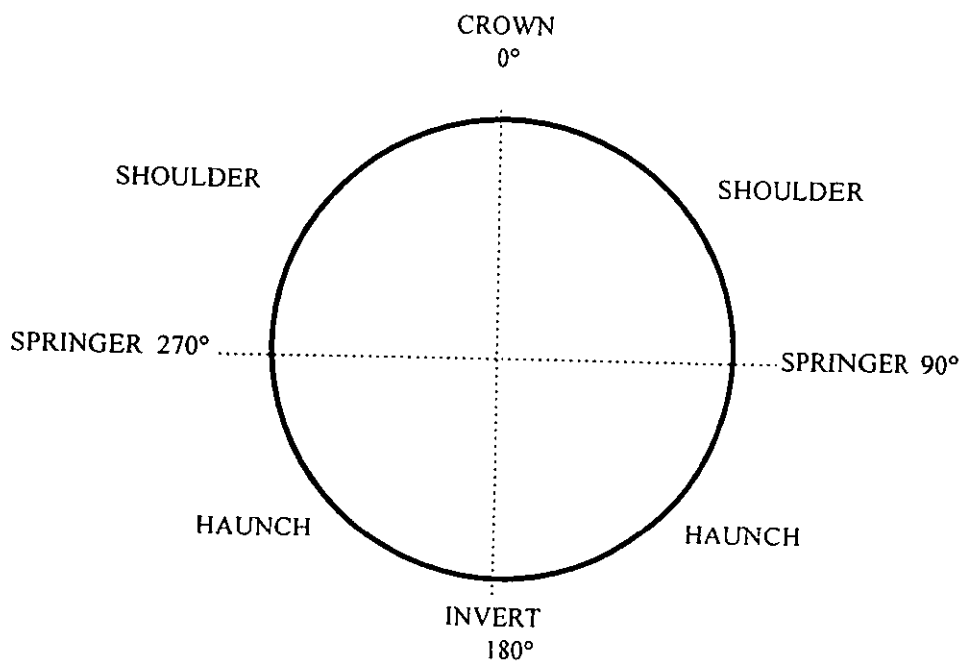
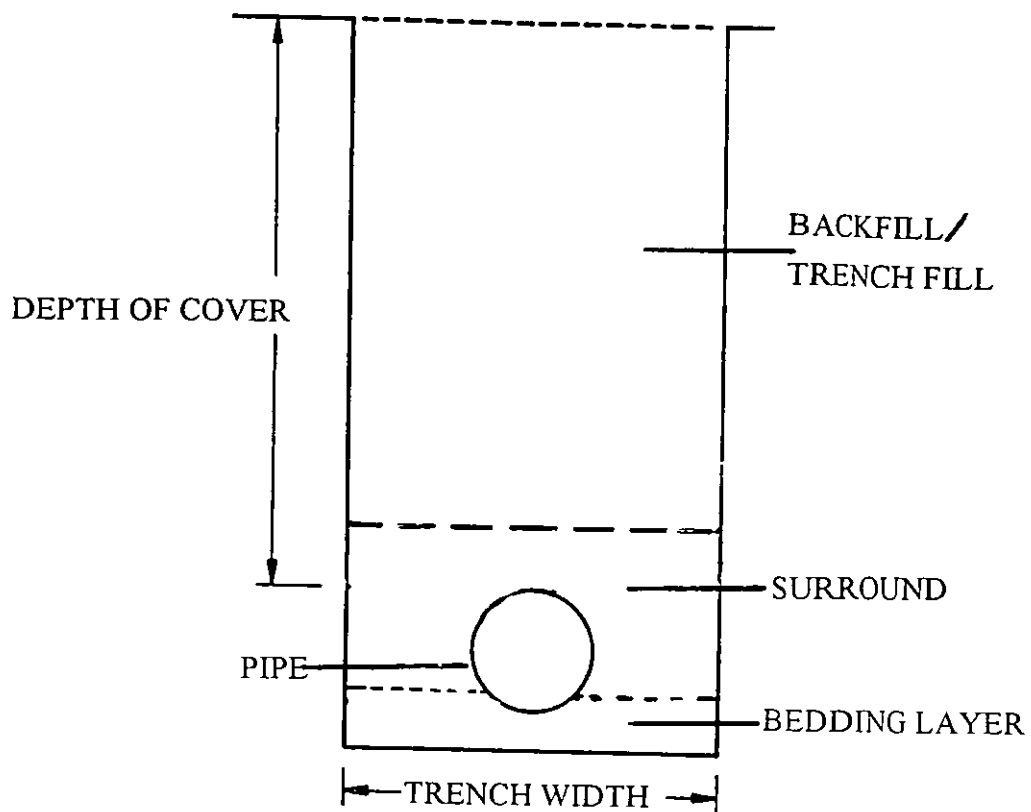


Figure 2.1. Installation of Pipe in Trench (including nomenclature).

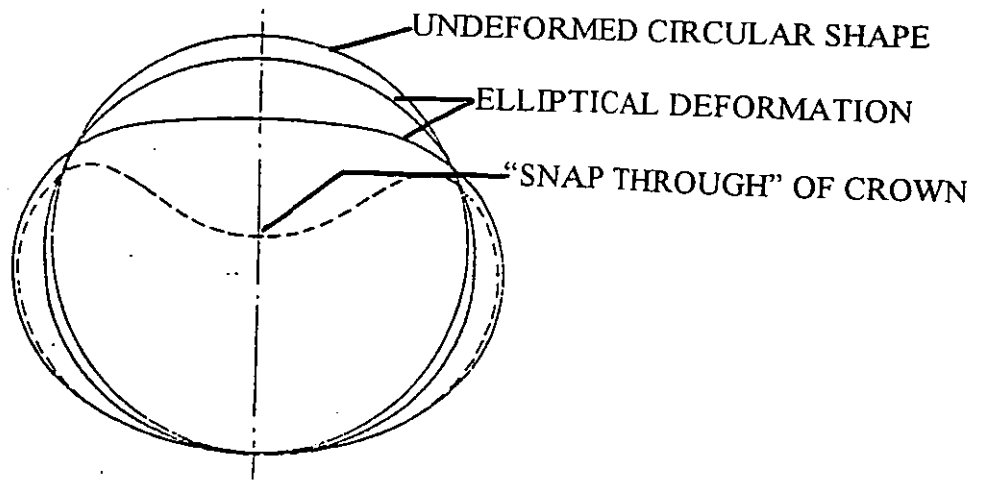


Figure 2.2. Mode of Pipe Deformation (after Spangler, 1941).

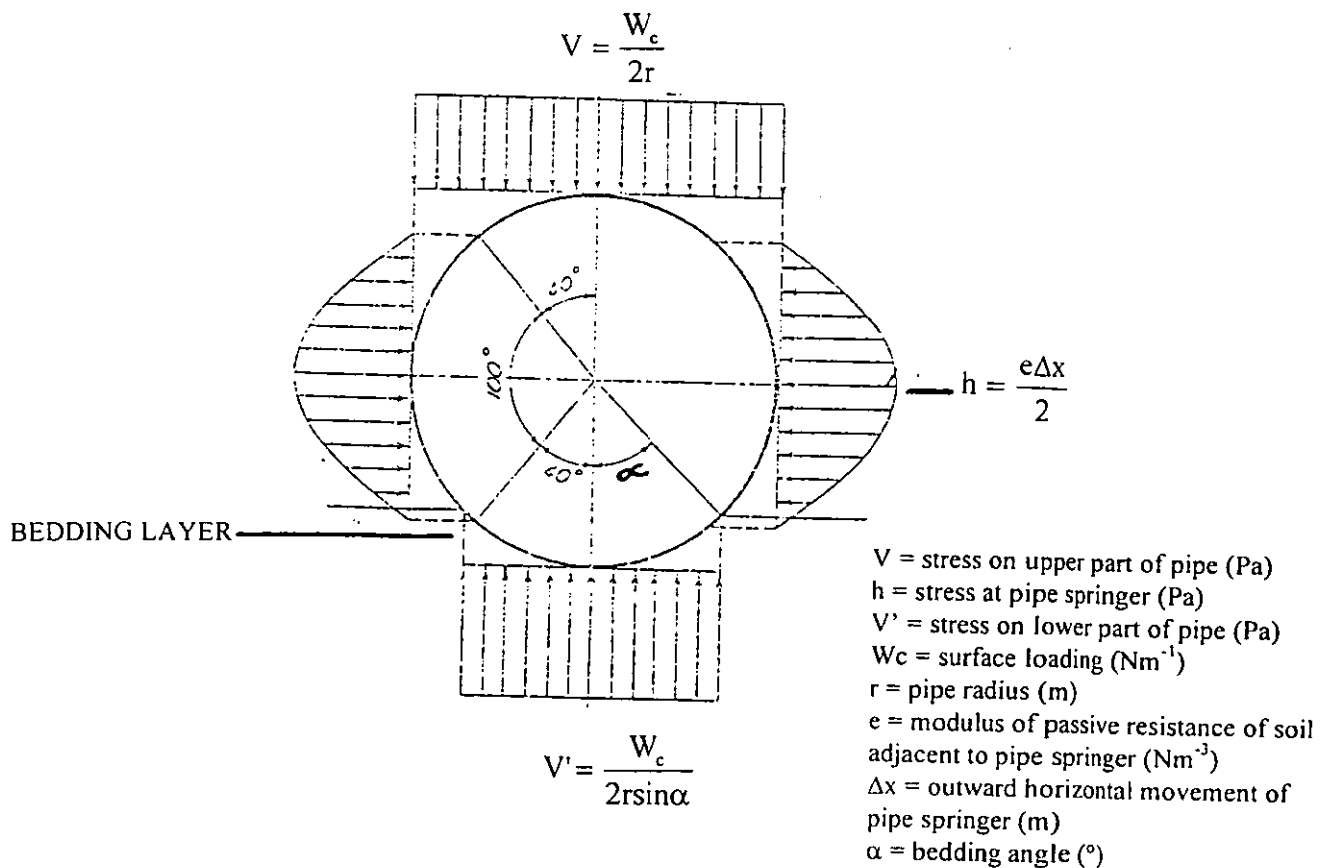


Figure 2.3. Stress Distribution around Flexible Pipe (after Spangler, 1941).

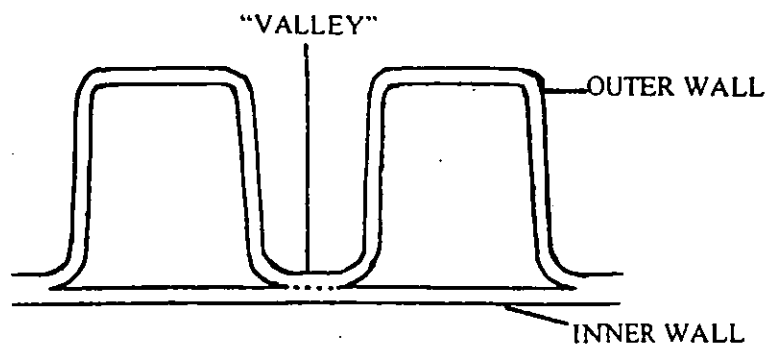


Figure 2.4. Typical Corrugated Pipe Wall Profile.

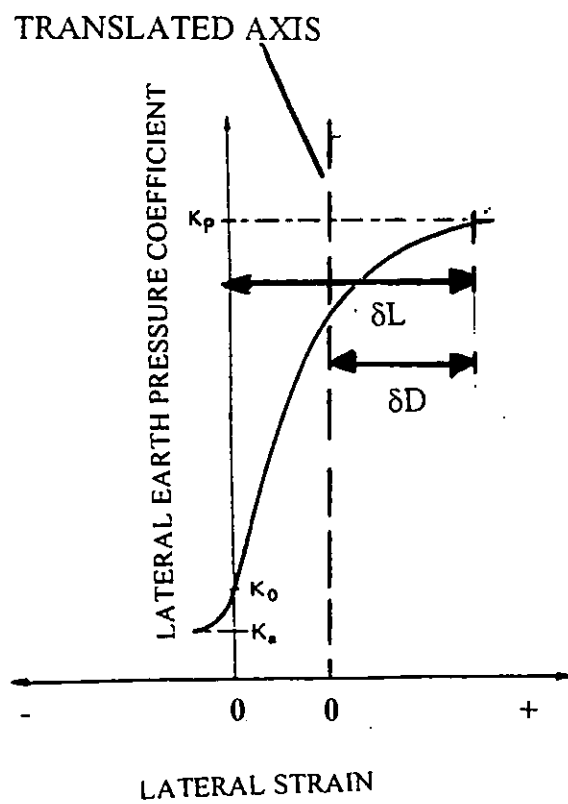


Figure 2.5. Effect of Compaction on Lateral Earth Pressure Coefficients.

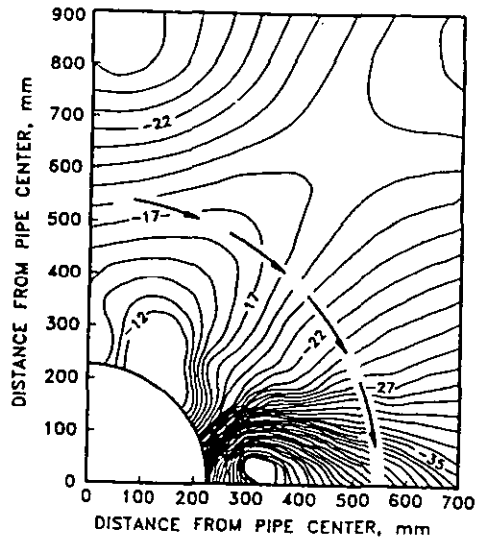


Figure 2.6. Arching as Illustrated by Horizontal Stress Distribution
(after Yapa and Lytton 1989).

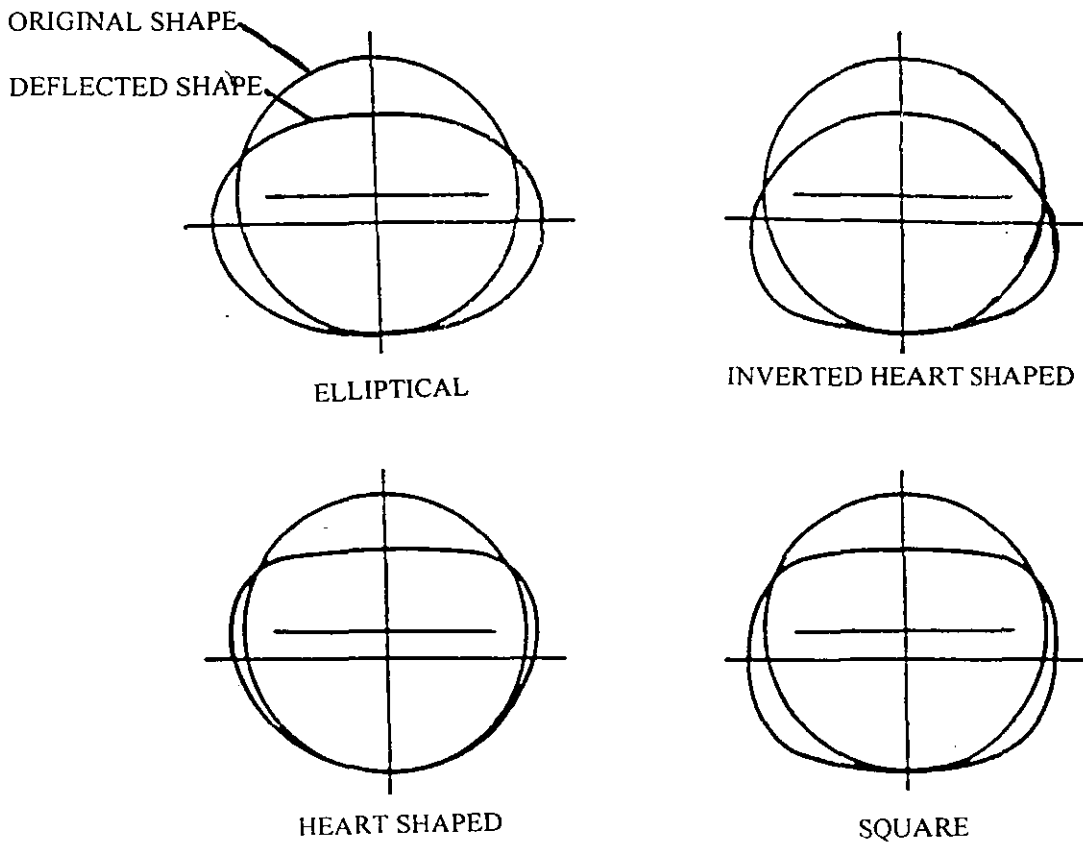


Figure 2.7. Shapes of Deformed Pipes (after Rogers, 1985).

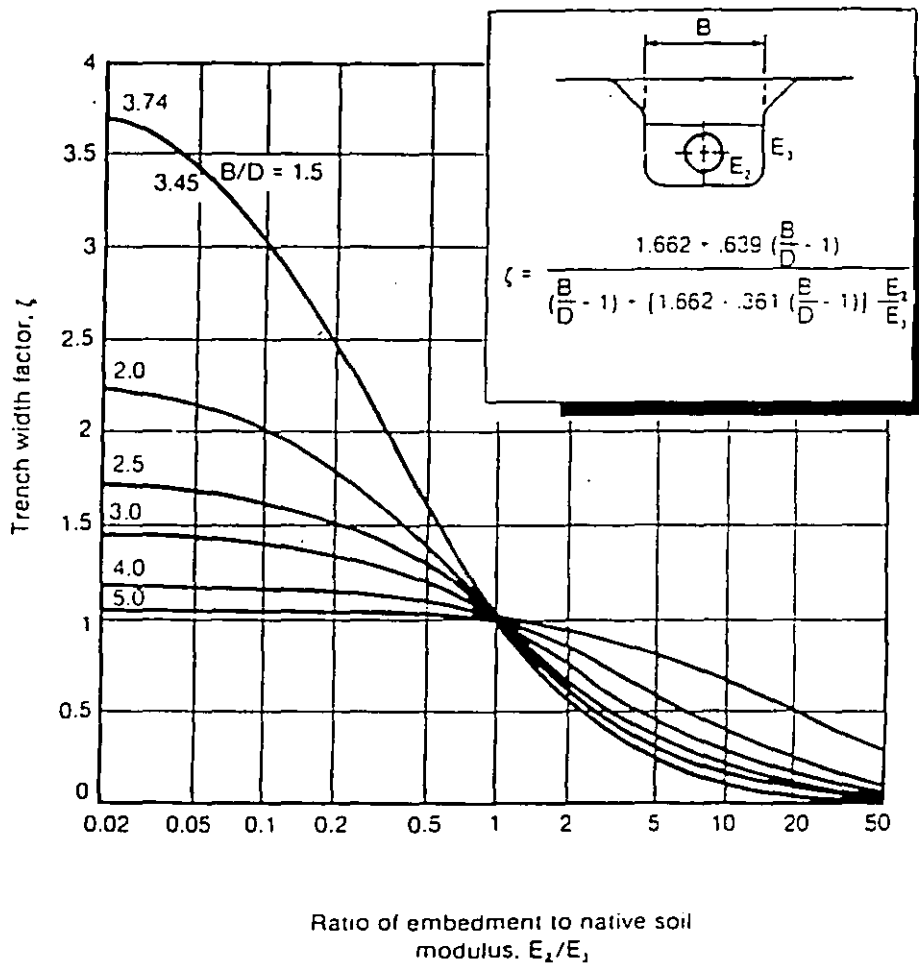


Figure 2.8. Effect of Trench Width (after Leonardt, 1979).

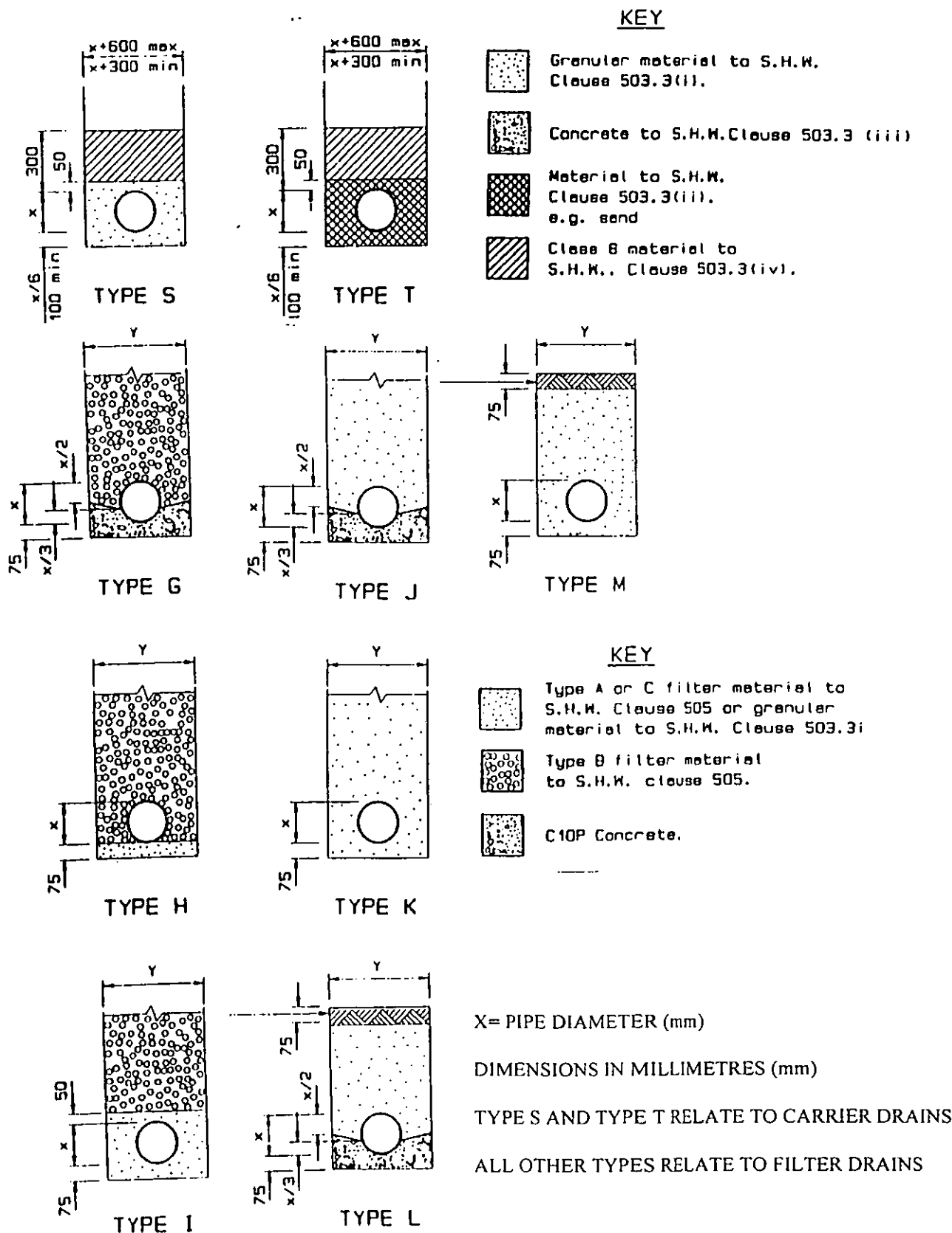


Figure 2.9. Standard Installation Details (after DoT, 1993).

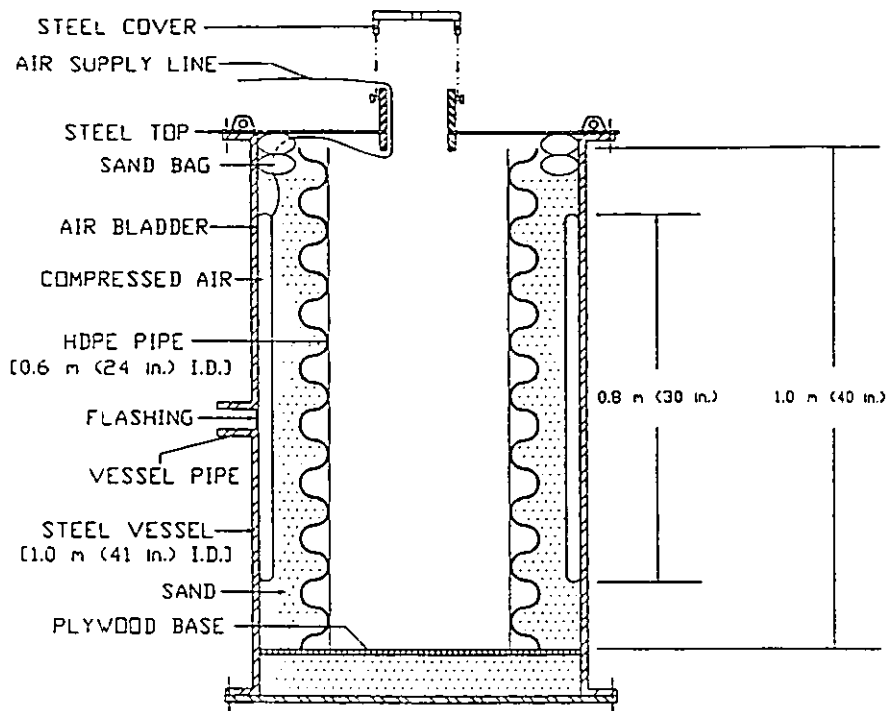


Figure 2.10. Pipe Testing Equipment (after Selig et al, 1994).

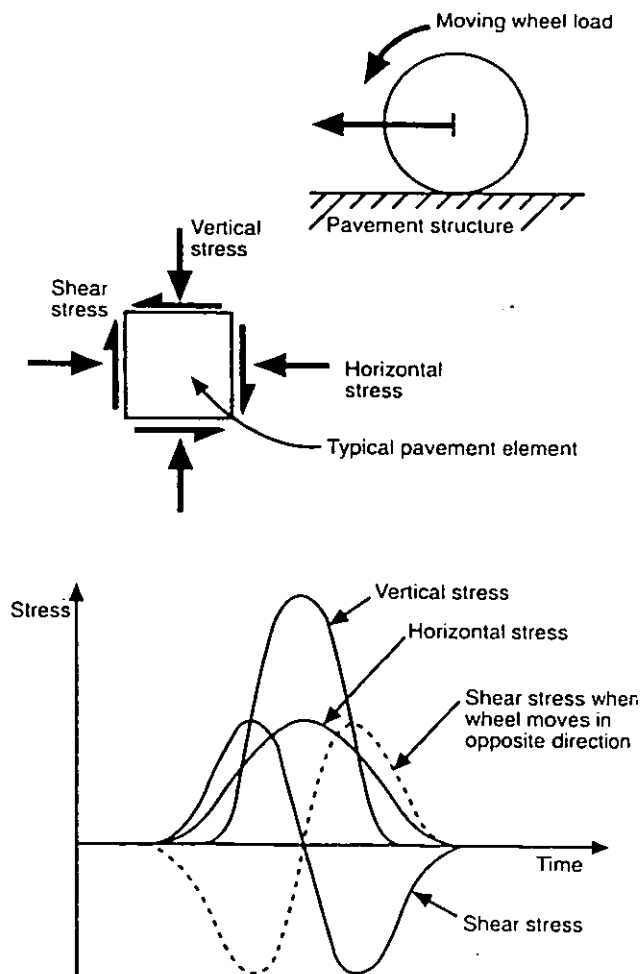


Figure 2.11. Changes in Soil Stress Caused by a Moving Load (after Brown, 1996).

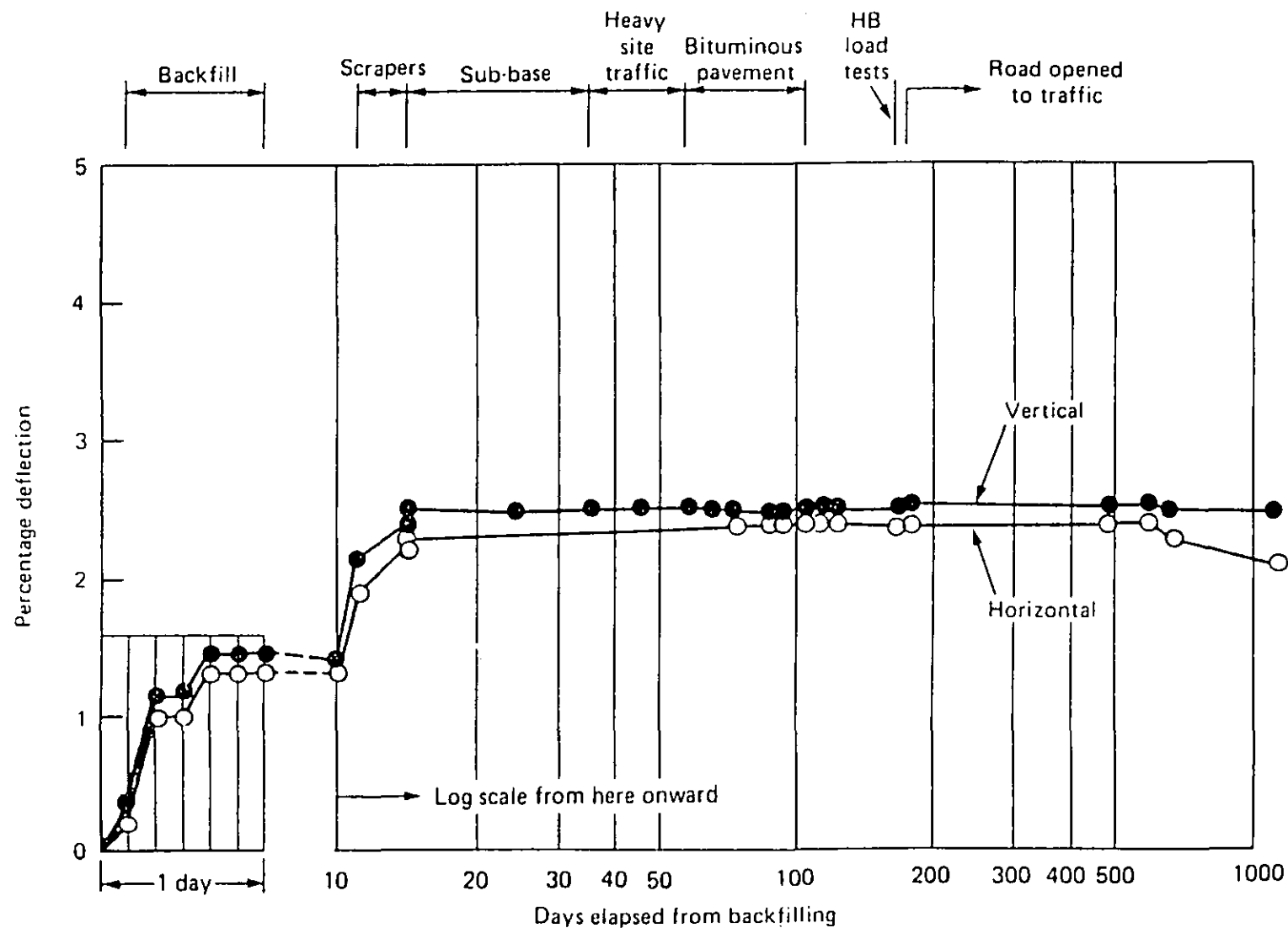


Figure 2.12. Effect of Repeated Loading on Pipe Deformation
(after Trott and Gaunt, 1976).

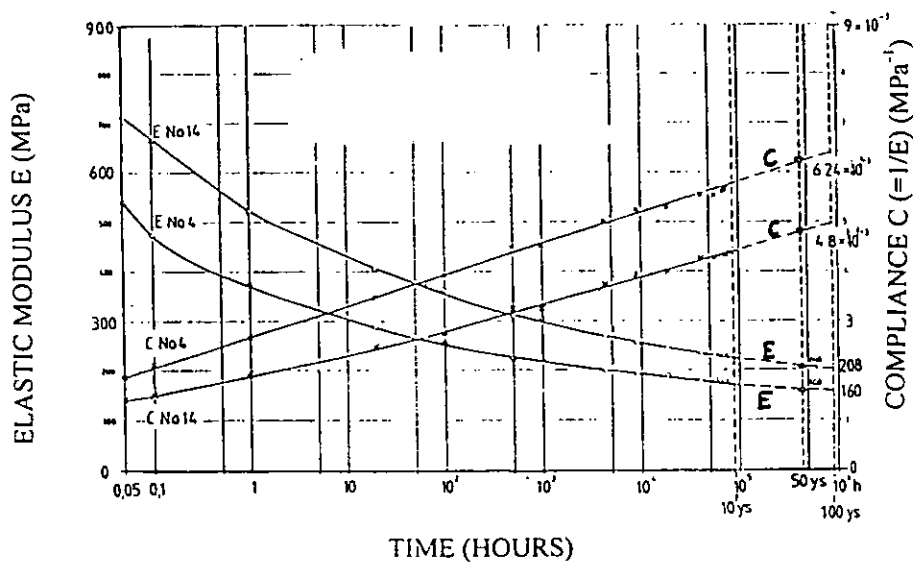


Figure 2.13. Effect of Time on Elastic Modulus of Constantly Deflected HDPE Pipe (after Janson, 1995).

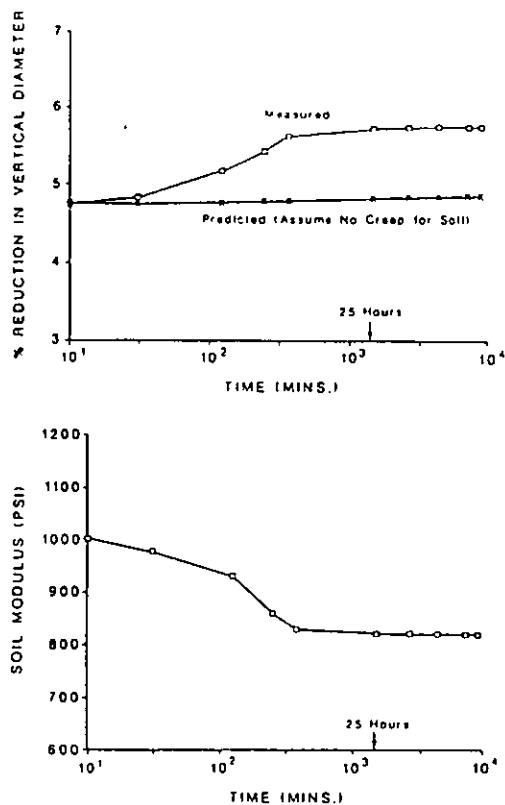


Figure 2.14. Change in Pipe Deflection and Soil Modulus Deflection with Time (after Chua and Lytton, 1989).

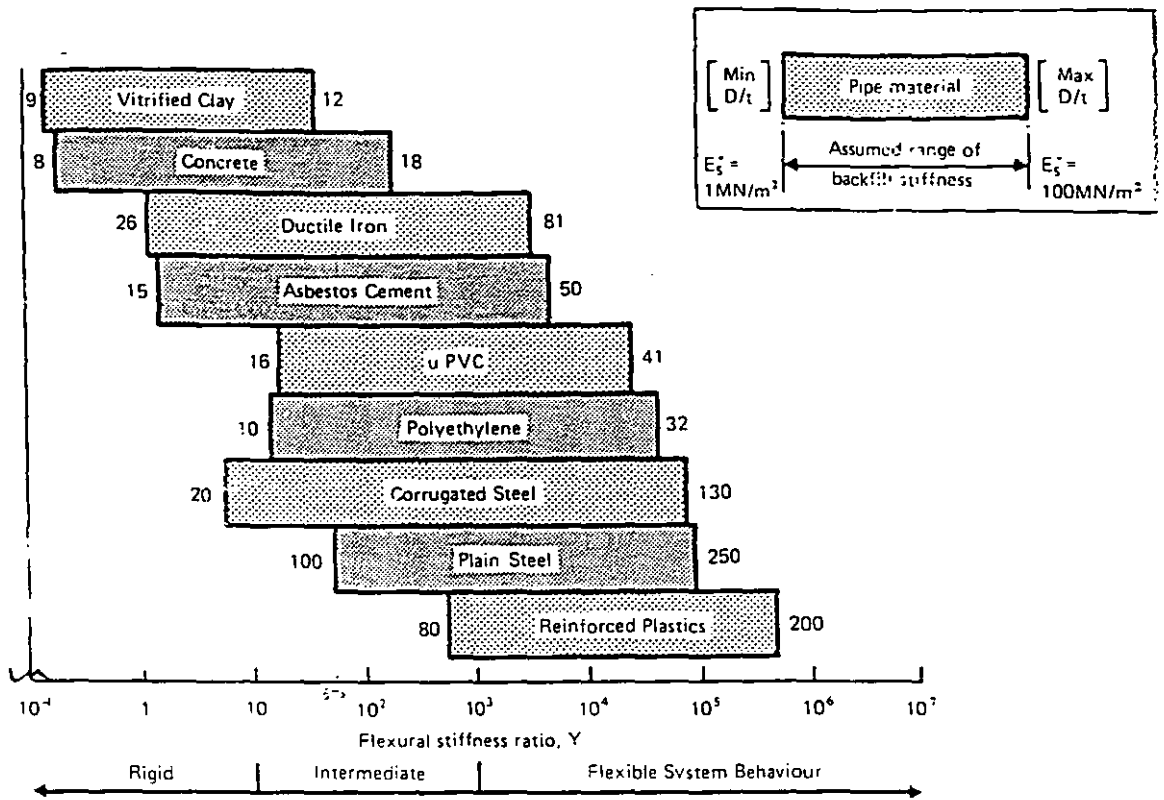


Figure 2.15. Flexural Stiffness Ratio Y (after Gumbel, 1982).

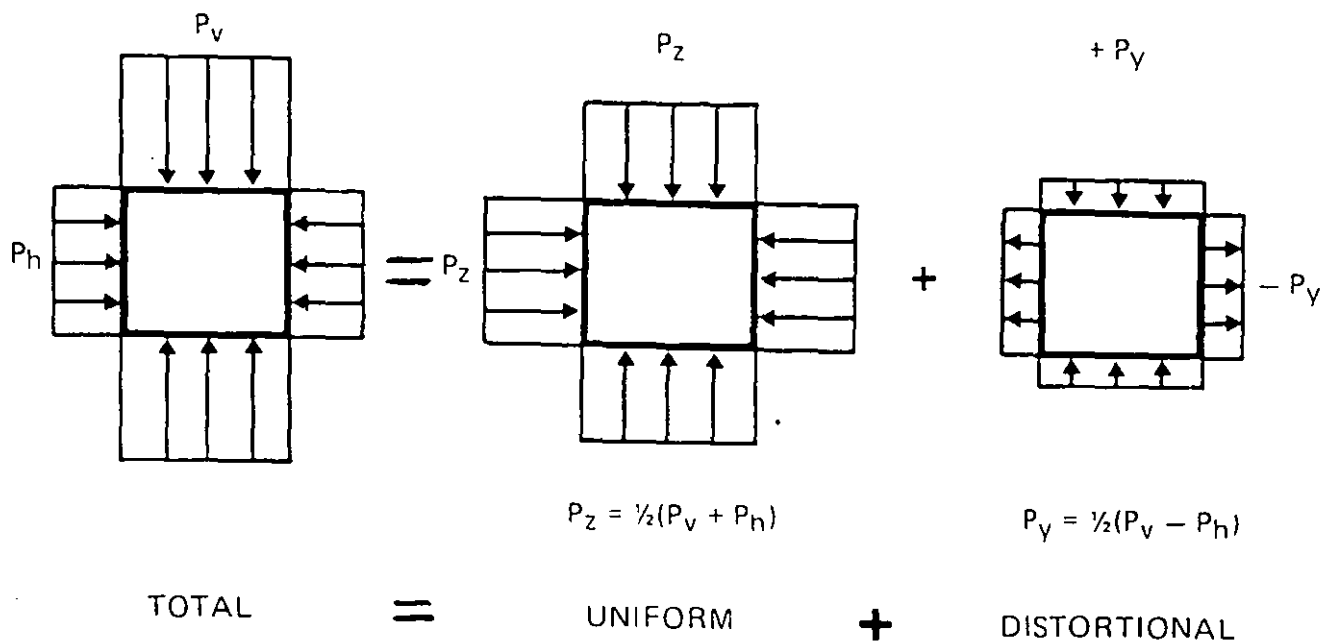


Figure 2.16. Representation of Stress Distribution around Pipe (after Gumbel, 1982).

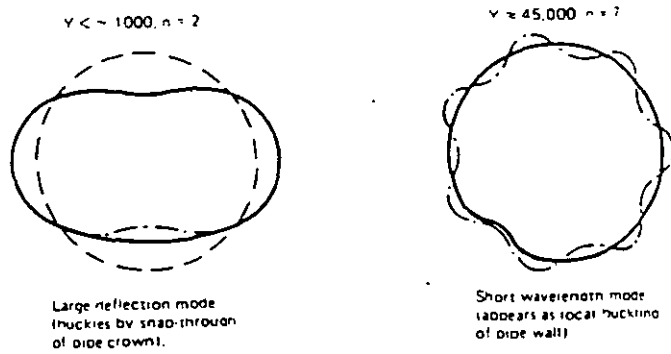


Figure 2.17. Modes of Pipe Buckling (after Gumbel, 1982).

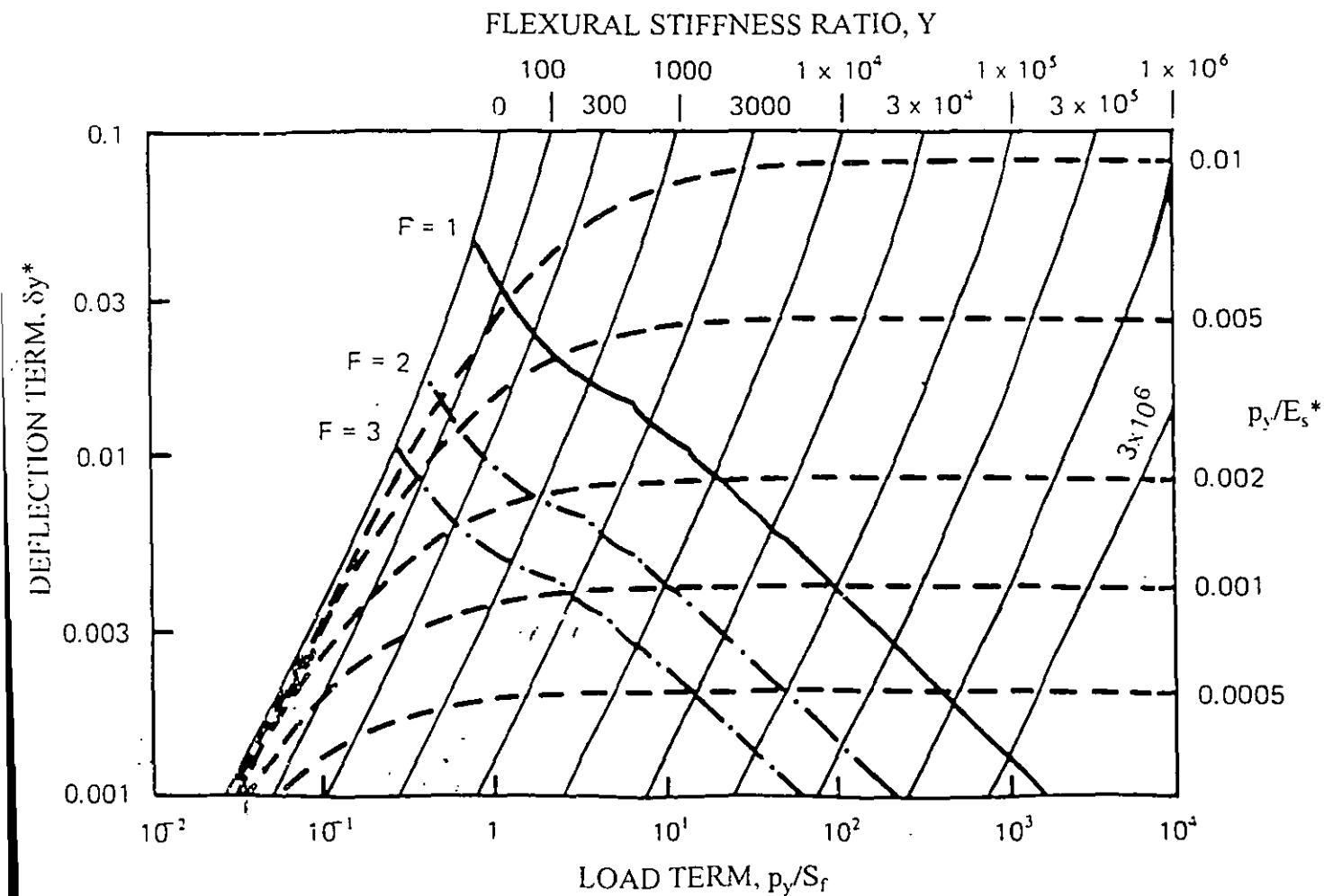


Figure 2.18. Design Chart for $p_y/\alpha p_z = 0.05$ (after Gumbel, 1982).

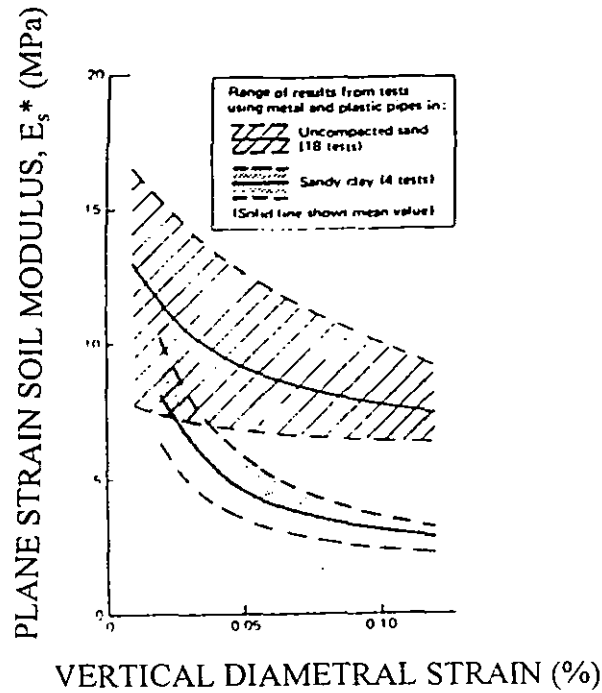
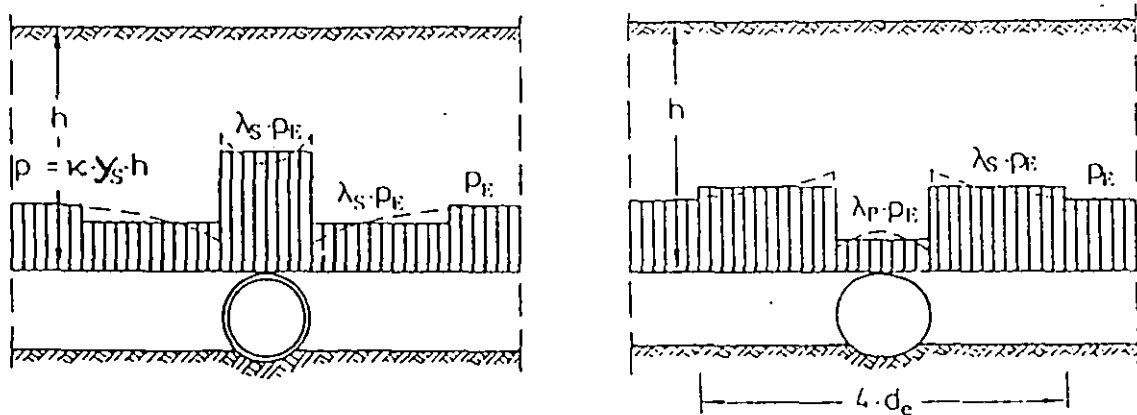


Figure 2.19. Variation of E_s^* with Deflection
(after Crabbe and Carder, 1985).



BEFORE REDISTRIBUTION

AFTER REDISTRIBUTION

d_e = external pipe diameter (m)

h = depth of cover (m)

λ_p = stress concentration factor above pipe (dimensionless)

λ_s = concentration factor in soil next to pipe (dimensionless)

p_e = applied external stress (Pa)

κ = stress reduction factor for trench (dimensionless)

γ_s = safety factor (dimensionless)

Figure 2.20. Stress Redistribution in Region of Flexible Pipe (after ATV, 1988).

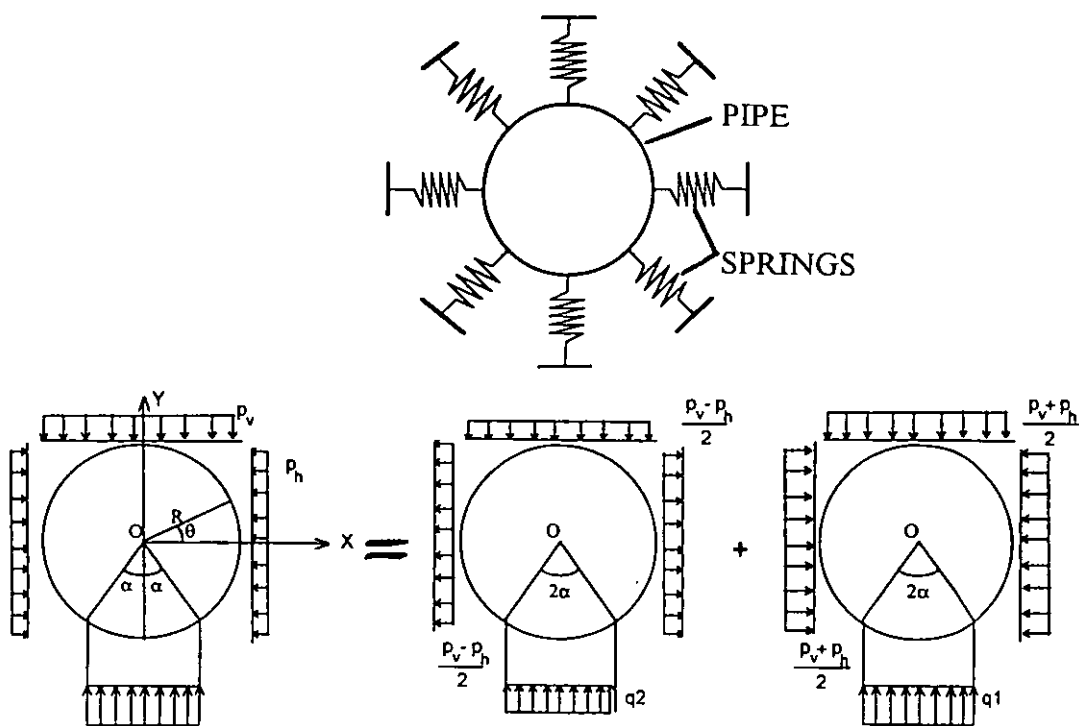


Figure 2.21. Winkler's Model and Stress Distribution around Pipe
(after Gerbault, 1995).

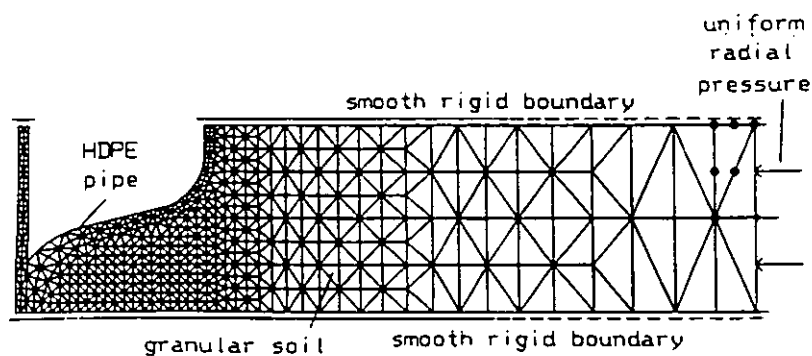


Figure 2.22. Finite Element Mesh for Annular Corrugated Twin-Wall Pipe
(after Moore and Hu, 1995).

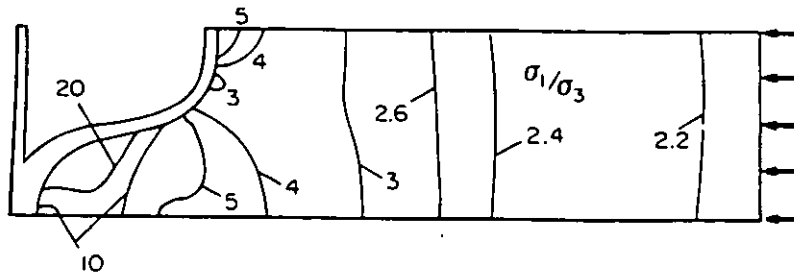


Figure 2.23. Principal Shear Stress Ratios in Soil and Failure Locations
(after Moore and Hu, 1995).

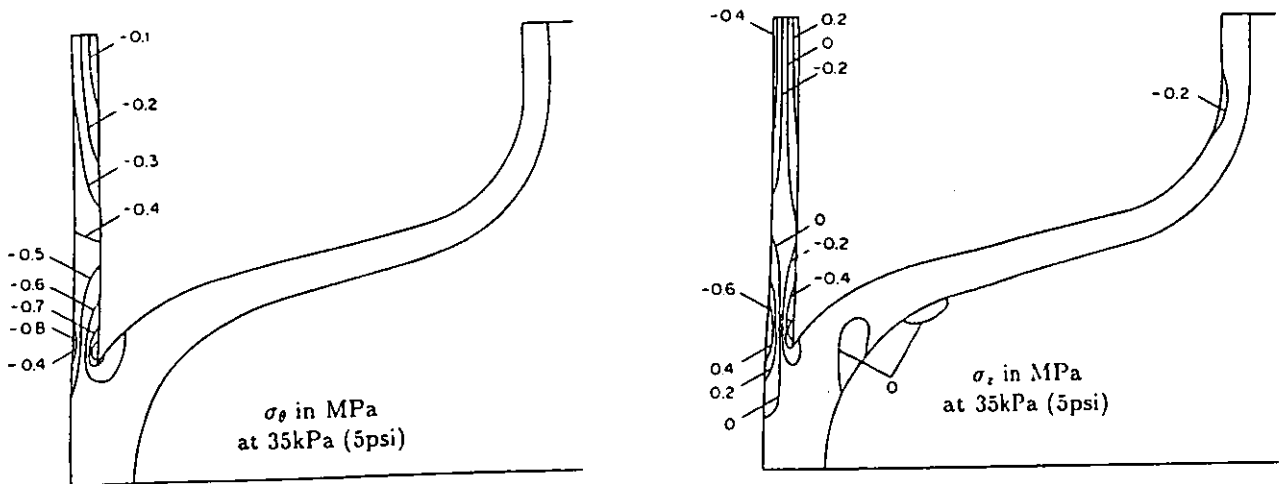


Figure 2.24. Circumferential and Axial Strains in Annular Corrugated Twin-Wall Pipe
(after Moore and Hu, 1995).

3 LABORATORY TESTING

This chapter describes the equipment and methods adopted for the laboratory test programme. The choice of an existing steel testing box is explained, and the boundary conditions described with reference to those that would be expected in practice. The development of the manual and electronic equipment that allowed the application of constant and variable loading to a buried pipe is described.

Following from this, the selection of the test pipes and surround types is explained. The pipes reflected a range of types of construction and were of a diameter that was compatible with the dimensions of the testing box. The two surround media used for the main testing programme were of types specified in the relevant design documents, with the additional feature that one of the media was installed in two states of compaction to reflect possible differences in the method of placement.

The magnitude and variation of the loading applied to a test pipe when buried is described. The loading pattern was designed to simulate the pressures caused by soil overlying a buried pipe and those caused when transient loading was applied to the pipe, for instance by a vehicle passing over the trench.

The deformation of a test pipe under the applied loading was measured in terms of deflections and wall strains. The measurement and logging equipment developed for this is described, along with the procedures adopted for their placement and securing.

The chapter then describes fully the events carried out during a test. This covers pipe preparation and installation, placement of the surround and fill material, density measurement, the application and removal of applied loading and the data collection procedures.

The chapter continues with a description of some additional testing that was carried out to investigate other aspects of the research subject. The effect of pipe deformation on the integrity of joints in a pipeline is investigated, as these may be thought to be possible locations of leakage. A very severe impact loading test was carried out on a pipe buried at shallow depth in an attempt to produce larger deflections than those recorded in the main test programme. The effect on the test pipe deflection of the trench box walls was also investigated by the use of wall facings that possessed low frictional properties in control tests. Finally, experimental repeatability was assessed by the use of duplicate tests.

3.1 TEST PARAMETERS AND EQUIPMENT

3.1.1 Testing Box

Many issues had to be considered when choosing the apparatus in which the pipes were to be tested, and these covered both experimental and economic matters.

The first issue was that of relevance of the laboratory testing environment to practical conditions. The construction of a trench in the laboratory was not possible. The construction of a trench outdoors in clay soil was feasible and would inarguably reflect realistic pipe installation conditions. There were, however, operational factors that militated against this option. The first was that the large number of tests planned for the work, involving repeated excavation and installation of the pipes, would result in the deterioration of, and an alteration to, the properties of the trench walls and the geometry of the trench. The loads imposed on the pipe and the pipe deflection would therefore change during the testing programme, preventing direct comparison of the test results. Deterioration of the trench would have been extensive because the soil around the laboratory building was relatively weak and consisted of areas of made ground. The option of excavating a test area and filling it with imported clay would have been expensive and arguably unrealistic in relation to a trench in virgin ground. In addition, the environmental effects of outdoor working, such as temperature variations, the possibility of water ingress to the trench and/or evaporation of water from the trench walls, and the sensitivity of the measurement and loading equipment to water were of serious concern. All of these factors favoured indoor testing.

The simulation of a trench in laboratory conditions has been achieved elsewhere (Rogers, 1985 and McDowell et al, 1994). Within the context of this research, the method adopted by Rogers for the testing of small diameter ducts (namely a purpose-built concrete tank filled with imported clay) was too time-consuming and costly to countenance because of the size of the pipes to be tested. The method used by McDowell et al for the testing of small diameter ducts at low cover depths involved the lining of a timber box with breeze-blocks to simulate a trench. This was a relatively low-cost option and minimised the deterioration of the trench walls during testing and allow the trench width to be adjusted to suit the diameter of the pipe to be tested. The properties of the trench walls so formed would not be representative of those of a trench cut in a soil (which would be more yielding under loading) and are therefore not appropriate to this research. However, the proposed loading regime involved larger pipes, considerably deeper burial depths, high loads and the repeated application of loads to the apparatus. A timber box would therefore need to be very robust to withstand the weight of the soil and the applied test loading.

The above factors led to the consideration of a steel box which had been constructed for a previous research project (see Figure 3.1). The box was constructed from 6mm thick steel plating and had been extensively reinforced around its perimeter with hollow square steel sections. The plan dimensions of the interior of the box were 1.8m by 1.5m. In terms of the size of the pipes to be tested (which were selected after consideration of the dimensions of the test box, see 3.1.3, and had nominal internal diameters of 600mm) the box was sufficiently small for the presence of the walls to influence the behaviour of the pipe. Finite element studies (Katona, 1976) had indicated that the soil in a region extending laterally 2.5 times the pipe diameter from the centre-line of the pipe has an effect on the behaviour of the pipe. The test box was therefore considered as the trench itself, but with very stiff walls.

The orientation of a "test" pipe (of approximate length 1.5m) centrally in the box so that its longitudinal axis was parallel to the shorter box walls would result in the box walls being approximately 0.6m from the pipe springers. This gave a slightly wider trench than would be allowed in practice (see 2.2.4.3), but resulted in the effects of the artificially stiff walls being minimised.

The box walls themselves had been roughened by corrosion and wear, and as a result they would generate frictional resistance to vertical loading. The walls were considered to be rougher than those of a trench cut in virgin clay, but in such conditions the filling of the trench with granular material during the installation process will cause particles of the fill to penetrate the clay wall, thereby increasing the friction coefficient of the interface. A trench cut in a granular material such as the sub-base used in highway construction, for example, would have rougher walls still, and this would cause a significant reduction in the loading exerted on the pipe. The subject of trench wall friction is described in more detail in 6.1.9.

The height of the box was 1.5m. Two access holes were located in the plan centres of the faces to which the pipe ends would abut, the distance from the floor to the bottom of the holes being 0.6m. The access holes were utilised for the placement, monitoring and repair of the measuring equipment in the pipe. The box floor was raised by the installation of a very dense sand base (approximately 0.45m deep), which represented a stiff trench bottom. In order to increase the cover depth from 0.3m to a more realistic value, an extension section of height 0.7m was fabricated. This resulted in a cover depth to the pipe of 1.0m, which was virtually the minimum allowed under UK installation guidelines (0.9m, see DoT, 1990).

3.1.2 Load Application Equipment

An external source of vertical stress was required to simulate cover depths exceeding the value of 1.0m provided by the fill in the test box. The test box was supplied with a 6mm thick steel lid, reinforced with 100mm square steel sections, which could be bolted to the box. To simulate the pressures caused by increased overburden, the test box lid was fitted with a 5mm thick natural rubber membrane on its underside, which extended to the inside edges of the box (see Figure 3.2). A seal was effected between the underside of the lid and the membrane by steel strips 40mm wide by 5mm thick, which were bolted to the lid and secured the membrane at 50mm centres around its perimeter. This arrangement is hereafter referred to as the water bag. An inlet hole was made in the box lid to allow for the connection of a water supply from the laboratory mains. The forcing of water into the water bag produced a downward static pressure on the surface of the fill material, which could be maintained by closing off the supply valve. The water pressure could be regulated by altering the amount of water in the water bag and monitored with a Bourdon gauge (see Figure 3.3). The maximum water pressure that could be achieved was approximately 160kPa, and the gauge could be read to an accuracy of $\pm 0.05\text{kPa}$.

In order to simulate the passing of a vehicle over the buried pipe it was necessary to produce cycles of variable pressure. By the simplification of a wheel passing over the pipe trench by a point load and the use of Boussinesq's theory (see 2.2.5.2), it is seen that the change in vertical stress at the crown of a buried pipe varies as an approximately "bell-shaped" curve as a load passes by. The shape of the curve bears a resemblance to a "stretched" sine wave.

A Dartec Model signal generator was used to provide a sinusoidal wave. A power unit was made that allowed the precise shape of this wave to be adjusted. This was used to drive an electro-pneumatic converter which was connected to the laboratory compressed air supply (see Figure 3.4). The converter produced an air supply with a similar waveform to the electrical input signal. This output air supply was then fed into the upper part of a steel pressure vessel that contained water. A pipe connected the pressure vessel to the lid of the test box via a valve. The converter drove air into the top of the vessel which had the effect of forcing the water out of the vessel, through the pipe and into the space between the membrane and the box lid. This resulted in pressure being applied to the surface of the soil in the box, which varied from zero to a maximum value under the influence of the input signal. The output current of the signal generator could then be adjusted using the power unit, which in turn allowed adjustment of the waveform of the pressure applied by the water bag. The maximum value was set by regulating the pressure of the compressed air supplied to the converter and by varying the gain on the power supply. The offset between consecutive cycles could be altered to prevent interference which may have given rise to

wave superposition and abnormal pressure variations. The frequency of the wave was controlled by the signal generator.

The determination of the magnitudes of the static and cyclic loading used in the testing programme is described in 3.1.5.

3.1.3 Sizes and Types of Pipes Tested

The maximum simulated trench width of 1.8m limited the diameters of the test pipes to 1.2m to 1.5m (DoT, 1993). The maximum diameter selected would have to be such that the cover depth did not become excessive, which would require significant amounts of time for burial and exhumation.

Consideration of the diameters of larger plastic pipes used in the UK found that the commonly specified nominal internal diameters were 0.300m, 0.375m, 0.450m, 0.600m, 0.750m and 0.900m. Concrete has generally been favoured for pipes of 0.750m diameter and above. Plastic pipes are, however specified for smaller diameters for a significant proportion of all pipework used in UK civil engineering. Experimental work had previously been carried out on pipes of 0.300m diameter (Rogers et al, 1994 and 0.375m diameter), so the adoption of pipes of this diameter would simply duplicate previous work. Pipes of 0.45m diameter were not appreciably larger, and the accurate placement of measurement equipment in them would have been difficult. Therefore pipes of 0.600m nominal diameter were selected for the laboratory work as being significantly larger than pipes tested previously in UK research, in widespread use in industry, broadly compatible with the dimensions of the test box, having sufficient working room for the accurate installation of measuring equipment and involving a sensible amount of work during installation in the laboratory.

A survey of the different types of flexible pipes available in the UK was carried out with distributors of these products. The range of pipes selected was limited to five so that a realistic timescale could be maintained for the proposed testing schedule. The pipes selected covered the three types of construction, namely single wall, annular corrugated twin-wall and helically-wound twin wall. The range included pipes manufactured from PVC-U, HDPE and PP.

Details of the size, construction and properties of each of the pipes were determined.. The elastic moduli of the pipe materials (E) were measured by testing small samples cut from the pipes (after the box loading tests) in an Instron compression/tension machine. The second moments of area (I) for the twin-wall pipes were determined by simplifying the pipe profile to an arrangement of rectangles as shown in Figure 3.5. To validate this simplification the resultant value of I for one of the pipes was compared with that obtained by capturing the image of a section

of the profile using a scanner linked to a computer, displaying the image as an AutoCAD drawing and determining I from this more accurate representation (MacGregor, 1995). The difference in the values of I calculated by the two methods was approximately 5%, which was an acceptable margin in the context of the relative influence of the pipe stiffness (see 2.2.1 and 2.2.2). STIS values were determined at the Berry and Hayward Laboratory at Boston. Parallel plate testing to ASTM D2412 was carried out in the Instron machine.

3.1.4 Types and States of Pipe Surround Media

Pipe surround materials that may be used are defined as the Department of Transport's (DoT) Types S and T (see section 2.2.4.3).

A rounded marine gravel of nominal particle size 10mm was selected for the type S surround (see Figure 3.6 for particle size distribution). This was the smallest of the permitted particle size range. Particles of river gravel of nominal size 20mm were found in earlier work (see 3.3.1) to interlock and bear onto the test box walls when a pressure was applied to them via the water bag. The gravel effectively formed a rigid, unyielding block of material that greatly reduced the pipe deflection. Larger particle sizes (e.g. 40mm) would have done so to a greater extent. Smaller sizes of particles would "flow" more easily when the loads were applied and would therefore result in a greater transfer of loading to the pipe. The choice of 10mm also reflects the fact that, as a particle size allowable for all diameters of pipes (DoT, 1993), it is more likely that it would be used for all drainage works on a site, rather than separate stockpiles of different sizes of gravel being maintained on site for different diameters of pipes. It also has the advantage of being the easiest to handle during the filling and emptying of the test box, as it is for pipe installation on site. For this material the coefficient of uniformity (C_u) was 1.55, the coefficient of curvature (C_c) was 0.95 and the diameter at which 10% of the particles pass, (D_{10}) was 5.5mm.

A river sand relating to DoT surround Type T was also used in the laboratory tests (see also Figure 3.6). For this material, C_u was 4.37, C_c was 0.65 and D_{10} was 0.19mm. As no density target is stipulated, the amount of compaction, hence passive resistance and ultimately pipe deflection (see 2.2.2.2), depends on the installation practices on site, and thus may be subject to appreciable variation. The current standard for plastic pipes (BS5955, 1980) states that mechanical compacting equipment may not be used within 300mm of a plastic pipe, which precludes its use for compaction of the surround. The remaining options are tamping, which is very rarely done, and treading, which is common.

The sand was initially drawn from an outdoor stockpile and therefore its water content was similar to the value it would have when in a stockpile on site. Excessive variations in this

important parameter (see 2.2.2.3) were avoided by monitoring the water content during the test programme and adding water when required.

To account for the possible variation in density, the laboratory tests were carried out with the sand in two states of compaction. In the first case, the surround was placed in layers of approximately 150mm, and compacted with a hand tamper of foot width 200mm and mass 10kg. The tamper was driven in a controlled pattern onto the surface of the surround such that three passes were made over the surface of each layer. The density of the material would therefore be relatively high and would be expected to lead to relatively smaller pipe deflections than those that would occur were the pipe buried in a less dense surround. This first surround case would represent extremely good workmanship on site. Such a degree of diligence may be rare in practice, but it was worthy of investigation because it showed the level to which pipe deflections could be reduced if more onerous compaction requirements were adopted, and it also allowed the establishment of an upper limit of soil stiffness parameters (e.g. E' in Eq 2.6).

The second state of compaction was achieved by placing the sand in the test box in layers of approximately 300mm. The sand was levelled and lightly tamped, with the tamper being held approximately 50mm above the surface and allowed to fall freely onto it. One pass only was made, merely to prevent "soft spots" at the corners of the box and excessive overall settlement of the sand during the loading, which may have caused the water bag to over-extend and tear. This compaction case simulated very poor workmanship, which would cause relatively large pipe deflections. These were regarded as "worst case" values and provided an important indication of the upper practical limit of deflection for poorly installed pipes. In addition, a lower bound for the soil stiffness could be determined. Pipe stiffness requirements, and hence profile design, could also be assessed in the light of pipe deflections measured for poor installation conditions and under severe loading.

It is worth noting that the specification for use on highway projects requires that fill material be compacted in layers of 150mm, which for type S and T surrounds would cause the 300mm limit in BS5955 to be violated. As the contractor is bound to adhere to the project specification, the pipes must be sufficiently strong to withstand the encroachment of mechanical compacting plant.

3.1.5 Loading Patterns

The magnitude of the applied loading was set to reflect relatively severe practical conditions. Three loading phases were developed that represent the different magnitudes and methods of application of the soil stresses that may act on a buried pipe.

The first phase was the application of a static pressure of 70kPa via the water bag. This was the equivalent of an additional 3.5m of overburden, assuming a soil unit weight of 20kNm^{-3} and no reduction in stress by the frictional effects of the trench walls. The total simulated depth of cover was therefore 4.5m, approaching the current maximum allowable installation depth (see 2.2.4.3). The 70kPa pressure was also the magnitude of pressure experienced by a pipe buried at a depth of 1.0m when an HB loading array (BS5400, 1978) with wheel masses of 112.5kN was parked on the trench. This represented the largest likely loading on UK roads and examples are given in BS5400 as the transport of electrical power transformers. The pressure was applied for a period of 24 hours. This was so that any increase in deflection of a buried pipe under a constant loading (such as trench fill) could be measured. After this period, the pressure was released and the pipe allowed to recover for at least four hours, it being determined during the first test that little significant further recovery takes place after this period.

There then followed a phase of repeated application of the 70kPa pressure, using the cyclic loading apparatus, which simulated the passing of the aforementioned HB loading array over a pipe buried to a cover depth of 1.0m. A total of 1000 cycles of the pressure was applied, considerably more than had been applied in previous laboratory tests on plastic pipes (e.g. Rogers and Loeppky, 1992). The behaviour of the pipes under repeated loading (caused by traffic in general) allowed the consequent long-term trends of deflection to be established. This information was also vital as an indicator of the longevity of the pipes in structural terms. It may be the case that the pipe continues to deflect under repeated loading, and in extreme cases this may lead to a loss of structural integrity by the development of excessive deflection or by fatigue. Excessive deflection may also cause excessive ground settlement, which would be problematic in some circumstances.

The period of the cycle was 100 seconds, the minimum permitted by the properties of the loading equipment. The relatively slow vehicle that this represents may be thought of as a more severe case than a faster vehicle, since the pipe-soil system is able to respond better (in terms of greater stress transfer through the fill and surround) to the slower loading. This will hold for relatively smooth road surfaces, but not for rougher surfaces where increased vehicle speeds would compound the impact effect caused by the surface irregularities. The repeated flowing of water between the pressure vessel and the box lid produced erratic, non-sinusoidal pressures if a signal of greater frequency was used. The effect of this relatively slow load application was increased by altering the gain of the input signal. The basic shape remained sinusoidal, but the rate of pressure application and removal was increased and the crest of the waveform was elongated. The offset of consecutive waves was set to ensure that the troughs of the signal remained unchanged so that, as soon as the pressure reached zero, it started to increase as the next cycle commenced. This

waveform resulted in a more rapid application of the pressure, which remained imposed for a longer period and remained at zero for a very short time. These refinements ensured a greater degree of loading impact, a greater duration of the loading on the pipe and a minimal degree of recovery on release of the loading.

The final loading phase was the application of a static pressure of 140kPa for 24 hours. This magnitude of pressure was twice the previous static pressure and approaching the limit of the test apparatus (160kPa). The pressure could be regarded as representing an unusually heavy vehicle, such as a motorised scraper used in construction work, or a very large overburden pressure (simulating a total cover depth of approximately 8m) in cases where no frictional resistance was offered by the trench walls to the applied vertical soil stress. It should be noted that heavy construction vehicles would not normally be permitted to traverse the trench without some degree of protection in order to ensure adequate care of the permanent works by the contractor. This test phase would indicate the behaviour of the pipes under extreme loading conditions and give an indication of the proximity to failure of the pipe under them or, conversely, the degree of safety inherent in the structural design of the pipe itself. In addition, the extent to which the deflection of a pipe under an applied loading depended on its loading history would be determined.

3.1.6 Deflection and Strain Measurement

3.1.6.1 Deflection Measurement

Vertical and horizontal diametral deformations were measured during all phases of the tests. Linear variable differential transformers (LVDTs) were used, and mounted on the mast arrangement shown in Figure 3.7. The mast was fixed to a heavy, semi-circular base which kept the LVDTs vertically and horizontally orientated and prevented their moving out of position during the test.

3.1.6.2 Wall Strain Measurement

Circumferential wall strains were measured with uniaxial foil/epoxy electrical resistance strain gauges placed at 45 degree intervals around the pipe (see Figure 3.8). For twin-wall pipes, the gauges were located at the internal face of the thicker wall. Moore and Hu's work (see 2.3.7) showed that larger stresses (and hence strains) were developed in the internal wall at this "valley" location than at locations where the two walls were separated by the corrugation void.

The gauges were affixed to the pipe using a cyano-acrylate (CN) adhesive. Until its recent development, successful bonding to materials such as HDPE and PP was difficult. CN

adhesive gives a strong bond, but it is hydrophobic and therefore the bond deteriorates in the presence of water. A brief study, following consultation with the manufacturer of the adhesive, found that the bond started to deteriorate after approximately two months in a naturally humid environment.

The position of the strain gauges allowed changes in the pipe circumference to be determined. Excessive all-round shortening would ultimately lead to failure of the pipe by ring buckling. Excessive changes in the curvature of the pipe wall would indicate severe overall deformation, ultimately resulting in local yielding of the pipe wall, the formation of plastic hinges and the collapse of the pipe. The strain gauges could therefore be used to determine the shape, and hence mode of deflection, of the pipe and the likely failure mechanism.

3.1.6.3 Data Processing Equipment

The outputs from the LVDTs and strain gauges were processed by an RDP Translog 500 datalogger (hereafter referred to as the datalogger), which converted the readings to linear displacements and strains respectively. Each device was connected to an individual channel, of which there were eight compatible with LVDTs and sixteen compatible with strain gauges. The LVDTs were connected via 5-pin plugs to a single circuit board in the datalogger that contained the electronic hardware for the eight channels. The hardware for the strain gauge channels was contained on two circuit boards. The channels on each board were wired to a "D" plug.

The datalogger was connected to a personal computer, on which was installed the bespoke software that controlled its operation. The various functions of the software were available as options on a menu format.

The datalogger was able to scan the active channels at intervals of one second or greater, the frequency of scanning being set by the operator. The number of scans of each frequency was also set, and these settings were saved into a "run profile" data file for each phase of the test, which was read by the computer during the test.

The data were stored into an "output" file on the computer as a series of numbers which represented the scan number, the date and time the scan was taken, the active channel number and the reading obtained from it. A BASIC program was devised to convert these files into a format that could be imported into a spreadsheet (in this case, Microsoft EXCEL) for subsequent analysis.

Calibration procedures for the LVDTs and strain gauges were included in the menu options of the datalogger software. Strain gauge calibration was carried out as part of the preparation of the pipe samples (see 3.2.1).

Calibration of the LVDTs was done using a feature of the datalogger software, and the device shown in Figure 3.9 (after Loeppky, 1992). The LVDT was placed in the central groove, secured and the plunger held at its mid-point (indicated by a reading of zero on the channel output). The channel was then cleared of existing calibration data. The travel of the plunger around the mid-point (25mm) was entered. The LVDT plunger was then extended to this value, as measured by the handwheel on the calibrating device. The datalogger recorded the resulting channel reading, and the process was repeated after the plunger had been moved to the lower travel limit (25mm below the mid-point). The datalogger then converted the difference in the channel readings for the two travel limits to a linear deflection scale in the range of $\pm 25\text{mm}$, and this was stored in a calibration file that the data collection program would use to convert input signals into linear deflections. The process was repeated for the other two LVDTs.

Because the LVDTs used were common to all tests, their calibration data were common as well, and were only altered if the LVDT circuit was altered (e.g. by rewiring the plug). These common calibration data were used in the "calibration files" that were compiled for each test pipe and contained the calibration characteristics of the LVDT and the strain gauges (see 3.2.1).

3.2 TEST PROCEDURES

For convenience, the test programme is summarised in Table 3.1, which shows the pipes and surround types used for the man testing programme.

3.2.1 Preparation of the Pipe Sample

A sample of the pipe to be tested was cut to a length of approximately 1.45m. In the case of the annular corrugated pipe, the cuts were made in the "valleys" to avoid affecting the corrugated sections, and the sample length maintained as closely to 1.45m as possible. In the case of the one helically-wound pipe tested, the cuts were made 1.45m apart, since it was impossible not to cut through the "corrugated" sections.

The internal diameter of the pipe was measured at not less than four locations and a mean diameter evaluated. The pipe circumference was calculated from the mean internal diameter, and the spacing of the strain gauges was determined by dividing the circumference by eight. Reference points for measurement were marked on the circumference at each end. In order to ensure that these points lay on a line parallel to the longitudinal axis, they were fixed by allowing a cylindrical to roll from the haunch towards the pipe invert at one end, which settled in the invert. The length of the rod ensured that it lay parallel to the longitudinal pipe axis. The point of contact of the rod on the pipe invert was marked. This exercise was then carried out at the other end of the

pipe. An external reference line was drawn along the pipe length between the two reference points to assist orientation of the pipe during installation in the test box.

The strain gauge spacing previously determined was measured around the circumference at each end of the pipe, starting from the reference points. A piece of thin line was pulled between corresponding points and a line drawn (with a scribe) near the centre of the pipe. The centre of the "valley" nearest to the centre of the pipe at the location of the line (for twin-wall pipe only) was found by measuring from one end and was marked off - the centre of the gauge would lie on this point. For the single wall pipe, the gauges were located on a plane half way along the pipe. The smooth surface of the pipe was then roughened slightly with emery paper to ensure a better bond. A patch of adhesive was deposited on the roughened area and the gauge placed on it. Correct orientation was achieved by aligning the reference marks on the gauge foil (which corresponded ^{to} its principal axes) with the marks inscribed on the pipe. The gauge was then held firmly in position until the adhesive set. Surplus adhesive, including that which had been expelled from under the gauge, was scraped off the pipe with a knife.

Connection of the gauges to the datalogger was achieved by soldering multi-core cables to the terminal wires on each gauge. Four gauges were connected to two cables. The cables extended to the end of the pipe, where the relevant wires were soldered into a "D" plug. These plugs mated with those emerging from the datalogger, and allowed the pipes to be changed with ease after testing by avoiding the need to rewire the strain gauge circuit boards on each occasion. The cables were fixed to the pipe walls by tie wire wrapped around screws driven into the walls. The ends of the wires that were soldered to the strain gauges were taped securely in position to prevent any movement that would have pulled the terminal wires off the strain gauges. The strain gauge wiring was checked using an ohmmeter, which established whether there was a complete circuit for each gauge.

The strain reading for the channel was set to zero and the gauge factor (2.13) and strain limit for the gauges (3%) entered. The calibration program then determined the amplification and additive factors that the datalogger software would apply to the input signal to yield the true strain value. This was loaded into the datalogger operating program at the start of the test on that pipe. The response characteristics for each strain gauge in a pipe, which would be affected by the electrical properties of the circuit or the state of the bond between the gauge and the pipe wall, were stored in the calibration file for the pipe that included the calibration data for the LVDTs.

The response of each gauge to loading was determined by placing the pipe in a parallel-plate testing machine and deflecting it to a vertical diametral strain of 5% over a period of one minute, holding the deflection for one minute and then reducing the deflection slowly to zero. The run profile was set so that the datalogger took readings of each strain gauge every second.

These were processed into the EXCEL format and plotted as a graph of strain versus time. A correctly-operating gauge responded linearly to the uniform rate of pipe deflection and exhibited a plateau when the deflection was held constant, whereas a malfunctioning gauge produced an erratic output. The cause of a non-linear responses was always a fault in the circuit rather than a deficiency in the bond between the gauge and the pipe wall. Once the circuit had been investigated and repaired, the gauge was recalibrated (and the calibration file updated) and its response checked by parallel-plate testing.

3.2.2 Installation of the Pipe

The 450mm layer of sand that represented the base of the trench was placed in the testing box and heavily tamped in layers of approximately 150mm. A bedding layer, 150mm thick, of the relevant surround type was placed on top of this. In the case of the gravel surround, a layer of 0.5mm thick polythene sheeting was first placed on the “trench floor” to prevent mixing of the sand and gravel. It is acknowledged that the sheeting may also reduce the degree of penetration of the trench base by individual gravel particles.

The prepared pipe sample was lowered by crane onto the bedding layer and centred in the testing box (Figure 3.10). The pipe was rotated so that the reference line formed the crown of the pipe, designated 0° (see Figure 3.8). The mast holding the LVDTs was placed in, and moved towards the middle of, the pipe so that the plungers of the LVDTs were as close as possible to the strain gauges at the 0° (crown), 90° and 270° (springer) locations.

The LVDTs and strain gauges were connected to the datalogger and the appropriate calibration file loaded. The run profile for data collection was set to record each channel reading every three minutes. A total of 100 such reading events (representing five hours) was programmed in order to allow a margin of safety so that recording did not terminate during installation. A menu option allowed the manual termination of data collection at any time during the program run.

The surround and fill material was then placed. Especial care was taken to ensure that the region around the pipe haunches was filled with the surround material, as a void may occur at this location. The surround material was fed into this region using a shovel and compacted inwards by foot. The gravel tended to flow to a greater extent, and it is probable that this minimised the likely formation of voids at the pipe haunches. The greater degree of diligence inherent in the heavily compacted sand case would also have helped to reduce the likelihood of voids at the haunches.

The sand surround was placed and compacted in one of the two ways described in 3.1.4. The gravel surround was initially poured from the skip, which could be tipped up using the

crane as shown in Figure 3.11. Care was taken to ensure that the surround was placed evenly at each side of the pipe to prevent sideways movement of the pipe which causes asymmetrical strain patterns (Rogers et al, 1996). After the extension piece had been added to the box, it too had to be shovelled. Compaction of the gravel surround was carried out in layers of approximately 300mm, and was achieved by treading on the surface, one pass only being made in accordance with observed site practice.

On completion of the installation process, the data collection program was terminated. For installations in sand, a sample of the surround was taken for determination of its water content. The density of the sand was determined by driving a U-100 tube into the surround and capping it. The tube was then carefully exposed and a piece of hardboard slid under the bottom so that none of the sand fell out and the sample maintained a cylindrical shape. The mass of sand in the tube was found, its volume determined and the density calculated. The area from which the sample was taken was carefully reinstated. For installations in gravel, the density was found by placing a 200mm square sampling box (Figure 3.12) in the surround material and compacting the gravel in the normal manner. The box was then excavated and the density of the compacted gravel determined.

A layer of rubber sheeting was placed over the surface of the fill material in the test box. This was to prevent damage to the water bag by particles of fill, which could have caused it to burst when pressurised with water. The drain valve on the test box lid (Figure 3.3) was opened and the lid lowered by crane onto the top of the box. Any water present in the water bag was able to drain, thereby preventing the premature application of pressure to the surface of the fill material. Finally, the lid was bolted in place.

3.2.3 70kPa Static Pressure Phase

Firstly, any air in the water bag was expelled. This was necessary to prevent the air dissolving into the water after the static pressure had been applied, which would decrease the volume of air in the water bag and cause the water pressure to drop. Bleeding of the air was achieved by opening the water inlet valve and allowing water to flow into the water bag. The (open) drain valve ensured that the water pressure remained at zero at this stage. An unsteady flow from the drain was first observed, which became more steady as the water drove out and replaced the air in the water bag and caused the membrane to flatten out onto the surface of the fill.

As the bleeding process continued, the datalogger was set up to collect deflection and strain data. The run profile was altered to provide several recordings in quick succession (every ten seconds) at the start of the phase, when the pipe deflection was expected to accumulate rapidly

owing to the increasing pressure. Thereafter, recordings were taken less frequently (quarter-hourly) because the rate of deformation was lower. This phenomenon is the “deflection lag” that was found empirically by Spangler (1941).

The datalogger was then activated. When water was seen to be flowing steadily out of the water bag, the drain valve on the test box lid was closed. The pressure within the water bag increased. When the pressure approached 70kPa, the water inlet valve was partly closed. Air trapped in the inlet pipework was expelled using the bleeding valves (Figure 3.3). A steady flow of water out of these indicated that no air remained in the inlet pipework. The small length of pipe between the box lid and the valve on the pipeline from the pressure vessel invariably contained trapped air, and was bled by opening the valve and allowing the air to escape back into the pressure vessel. When bleeding had been completed, the water pressure was allowed to increase slowly, and the inlet valve was closed when the pressure reached 70kPa.

The reading on the Bourdon gauge was monitored during the 24 hour period. It was observed that the water pressure would fall during this time, the magnitude of the fall being greater during the early part of the test. The pressure drop was caused by an increase in the volume of the water bag which was the result of compaction of the fill by the applied pressure. The magnitude of the pressure drop depended on the type of fill material in the box. The degree of compaction was most noticeable for the lightly compacted sand, with the gravel case showing a much smaller pressure drop. For the well compacted sand case, the pressure drop was negligible. Initially, the pressure was reset to 70kPa using the water supply at various periods during the test phase, which caused a “step-change” in the applied pressure. To allow for continuous monitoring and correction of the applied pressure, the water pressure used for the last three pipes tested was supplied through the compressor acting without the signal generator. The compressor was set to produce a constant pressure of 70kPa and the valve from the pressure vessel to the water bag was opened. Fine adjustment of the compressor setting was achieved by observing the Bourdon gauge. The compressor automatically compensated for any pressure drop caused by settlement of the fill material in the box. This resulted in a more realistic representation of a trench installation, since the backfill pressure would not normally dissipate with the passage of time under the fixed dead weight of the overburden. Indeed, the decay of both arching and frictional resistance to movement of the fill by the trench walls may occur. Both of these would lead to an increase of the pressure on the pipe, up to a maximum value of the weight of the soil prism per unit plan area of the trench.

At the end of the 24 hour period, the datalogger was reset to collect deflection and strain data for the unloading phase. The data were stored in a new file, but the same run profile was used for the unloading phase as for the loading phase. The valve from the pressure vessel (when used) was closed and the datalogger then activated. The drain valve was opened slowly and the

water pressure fell. When the pressure reached zero, the test box was left undisturbed for a minimum period of four hours. This allowed the pipe to recover as the backfill material relaxed following release of the pressure, and deflection and strain data were recorded during this time.

3.2.4 70kPa Cyclic Pressure Phase

3.2.4.1 Test Procedures

Following the recovery period, the water bag was bled as described in 3.2.3 above, save that the water inlet valve was closed as soon as the pressure in the bag started to increase. The pressure vessel was topped up with water and resealed. The datalogger run profile for this phase was then compiled (see 3.2.4.2).

The Dartec signal generator was turned on, connected to the compressor power unit, and the number (1005, i.e. with five extra cycles to allow for setting up procedures) and frequency (0.01Hz) of the cycles entered. The compressor was allowed to pressurise and de-pressurise for two cycles. At the peak of the third cycle, the valve to the water bag was opened and the datalogger was activated simultaneously. The maximum pressure was noted and the compressor air pressure adjusted if required.

At the end of the test, the valve to the membrane was closed at the peak of the 1003rd cycle (i.e. the 1000th cycle applied to the fill) and the compressor and Dartec signal generator was turned off. The pressure was released through the drain valve and the four hour minimum recovery period allowed.

3.2.4.2 Data Collection

Because of the potentially large amount of data that could be collected, the datalogger was programmed to record more frequently during the early part of the test, when these quantities were expected to change significantly. Recordings were made at intervals of 5 seconds for the first 25 cycles. No data were collected until the 150th cycle, whereupon recordings were made for five consecutive cycles. On these occasions, the interval between the recordings was set to 50 seconds, to coincide with the peaks and troughs of the cycles, and the process was repeated every 150 cycles and on the 995th cycle. This profile was changed after the first test because the Dartec signal generator and the computer tended to drift out of phase as the test proceeded, which had two effects. The first was the recording of data at points that moved gradually further from the peaks and troughs of the cycle (as will be shown in Chapter Five), and did not therefore cover the complete range of the pipe deformation during the pressure cycles. The second effect was that the phase difference was such that the run profile carried out its last sequence early, and stopped the datalogger before the 995th cycle was reached, thus resulting in the loss of detailed data for the last

pressure cycles. The latter effect was overcome by setting up an additional run profile that would operate at least to the end of the test and collect data every five seconds. The modified run profile maintained the large amount of data collection at the start of the test. This was followed by a period of 200 cycles during which no data were collected. There was then a period of approximately 300 seconds (i.e. three cycles) when data were collected every 5 seconds. This pattern continued to near the end of the test. The last sequence of data collection involved a long period of recordings at intervals of five seconds, which was set to start before the 980th cycle and continued until the datalogger was halted manually. A run profile for the recovery period was then set up, which took readings hourly.

3.2.5 140kPa Static Pressure Phase

This phase was carried out in the same way as the 70kPa static pressure phase. The only difference was that, for pipes buried in lightly compacted sand, the test box lid was removed and the settlement of the fill checked. Excessive settlement during the 70kPa pressure phases would have caused over-extension and tearing of the water bag during the 140kPa static pressure phase. The box was therefore topped up if required. For some tests, the approximate magnitude of the settlement was noted. When the lid had been replaced, testing was carried out as described in 3.2.3.

3.2.6 Removal of the Test Pipe

The test box lid and rubber sheeting were removed and the fill material excavated. Care was taken not to damage the pipe during shovelling. Although every effort was made not to disturb the pipe, the excavation of the surround material from the confined areas around pipe springers usually resulted in some small movement of the pipe. Deformation data were not recorded by the datalogger because of the likelihood of movement of the LVDTs if the pipe was displaced. However, the datalogger was able to monitor the active channels and display the results on the computer monitor without saving them in a data file. These were noted at the start of the removal phase and at the end if it was certain that the pipe had not been disturbed during excavation of the fill and surround.

When the pipe had been fully exposed, the strain gauges were disconnected and the LVDTs taken out. The pipe was removed using the crane and sling, and the bedding layer made ready to receive the next test pipe. Each pipe was installed in a different orientation for each surround case (i.e. the crown on one test became the springer on the next test) to minimise cumulative deviation from the initial circular shape.

3.3 ANCILLARY TESTING

3.3.1 Integrity of Deflected Pipe Joints

A pipeline was made, consisting of two sections of 300mm internal diameter pipe (B&H RidgiDrain), each 0.9m long, connected centrally by a coupler (see Figure 3.13). A rubber sealing ring was placed in the last corrugation valley of each pipe in accordance with manufacturer's instructions. The joined pipes were then placed centrally in the testing box (in the perpendicular direction to the larger pipes tested as part of the main programme), on a bedding layer of 200mm of 20mm nominal size rounded gravel, in order to create an installation with a cover depth of 1.0m. The pipe ends were braced against the framework of the test box to prevent them parting when air testing was carried out. When the pipeline was in place, a vertically pointing LVDT was placed in the centre of the pipeline to measure the deflection of the pipe crown.

Two types of surround were adopted. The first was the gravel used for the bedding layer. The testing box was filled (the extension piece was not used) and the lid placed on the box. An air test (DoT, 1993) was carried out on the pipeline, which involves applying an air pressure of 1kPa (using bungs and a manometer), allowing the pressure to stabilise for five minutes (and restoring it to 1kPa if necessary), then measuring the pressure drop over a further five minute period. For its applications, the DoT requires that the pressure does not drop below 0.75kPa. A static pressure of 20kPa was then applied to the pipeline via the water bag (see 3.1.2 and 3.2.3), which represented an additional 1 metre depth of burial, assuming a unit soil weight of 20kNm^{-3} . After a settlement period of one hour an air test was performed on the pipe. The static pressure was increased in increments of 20kPa up to 140kPa (representing an unusually deep installation depth of 8m with no trench wall friction over the upper 7m, or the long-term trench condition) and air tests were carried out at each stage. The total crown deflection (see 5.1.7) was very small and this was attributed to the behaviour of the gravel particles. As the static pressure increments were applied, the 20mm nominal size gravel in the testing box settled slightly and the particles bore onto each other, forming a rigid body. Further static pressure increments resulted in little settlement, and the gravel particles could be heard grinding against each other and the steel box walls. Significant settlement would have required the crushing of individual gravel particles. As this test was carried out before those that used gravel in the main testing programme, these observations assisted in the selection of a smaller particle size for the tests on the larger pipes.

Subsequent tests used the graded river sand as the surround and fill material. For the second test, the sand was placed in layers of 150mm and compacted with a rectangular tamp of mass 15kg. This method produced a backfill with a unit weight of 18.1kNm^{-3} . The static pressure

application and air tests were carried out as described above. For the third test, the sand was first placed loosely around the pipe using a shovel, to prevent movement of the pipe. The remainder of the sand was dumped in the box, effectively in one layer, and the top levelled off. This resulted in a sand unit weight of 15.6kNm^{-3} . The two methods of sand placement related to good and extremely poor site practice respectively.

3.3.2 Impact Loading of Pipes at Low Cover Depths

These tests were devised in the light of analysis of the deflection data from the main testing programme. The objectives were to determine whether the integrity of the pipe was compromised (either by puncturing or by excessive deflection) when buried at shallow depths in non-standard surrounds and subjected to more severe loading.

The two surround types used were a graded granodiorite granular sub-base to DoT grading Type 1 (a common road construction material comprising graded material of maximum particle size 37.5mm, see Figure 3.6), and a crushed flint of nominal particle size 10mm, believed to be one of the worst types of surround because of its hardness and sharp edges. The bottom 200mm of the testing box was filled with a concrete river sand which was compacted to provide a firm base for the pipe bedding and surround material. A sheet of polythene 0.5mm thick was placed on the surface of this layer to prevent contamination of the base layer. A bedding layer of 150mm was placed on the base layer. A section of 600mm diameter pipe 1.45m in length was placed in the box and a vertical LVDT was positioned at the centre and activated. The surround material was then added. The Type 1 sub-base was compacted, using a 15kg steel tamp, in layers of approximately 200mm to give a dry unit weight of 21kNm^{-3} . The flint, being a more uniformly graded material, did not compact significantly and therefore was trodden down evenly in layers of approximately 300mm. At the end of this stage, an air test was carried out on the pipe.

The depth of cover was 300mm, well below the minimum allowed by the DoT (600mm or 900mm, as described in 2.2.4.3). Repeated loading was applied by a ram operated by an electro-hydraulic system (as shown in Figure 3.14), which produced a truncated “saw-tooth” waveform of period 1.8 seconds. The load was therefore applied rapidly and resulted in a large degree of impact. The truncations allowed the pipe to experience the full load for a brief period before it was released. The load remained at zero for a very short time, to minimise the degree of strain recovery in the pipe and soil.

There were two loading phases. The magnitude and number of cycles of the first phase were determined from a (now withdrawn) prototype box-loading test for flexible ducts

such as those used for the protection of cable television services under footpaths (BSI, 1994). The first comprised 72000 cycles of a load of 40kN, this magnitude being that of a standard axle used in highway pavement design. The second load phase, which was not specified in the prototype BSI test comprised 5000 cycles of a load of 90kN, which was the maximum load that could be transmitted by the equipment and is equivalent to 36 units of HB loading (BSI, 1978). The load was transmitted to the surface of the surround material via a steel plate measuring 450mm x 300mm x 20mm thick which was designed to be similar in area to a loaded heavy vehicle tyre. The airtightness of the pipe was measured at the end of each loading phase.

The test using the flint surround was abandoned after the 6th load cycle because the nature of the surround caused it to "flow" under the applied load, which resulted in the loading plate being driven down to within 150mm of the pipe crown. An additional test was therefore carried out, in which the flint surround was confined by a layer of compacted Type 1 sub-base (properties as above) 150mm thick placed over its surface. This rudimentary pavement allowed the complete loading pattern to be performed.

3.3.3 Frictional Effects of Test Box Walls

The presence of a rough trench wall produces a frictional surface that counteracts the downward force of the prism of fill material over a buried pipe (see 2.1.1 and 2.2.4.1). The walls of the testing box were very stiff and relatively rough. These properties would influence soil strains and the stress exerted on the pipe by the applied pressure. Their effects on a pipe tested in the box were therefore investigated.

The influence of box wall friction was investigated by reducing the friction coefficient of the box walls. This was done by facing the box walls with smooth plywood sheets that had been coated with a phenolic resin, which made their surfaces hard and smooth (i.e. less frictional). The plywood was covered with polythene sheeting, which was applied loosely to the plywood and stapled in place. This arrangement produced two slip surfaces; one between the plywood and the polythene and the other between the polythene and the fill material. The polythene sheeting, by being loose, was able to accommodate movement of the surround. The minimal stapling allowed the sheeting to detach and move downwards *en masse* under an applied pressure if frictional forces built up, and this was found to happen on one of the tests on exhumation of the pipe. The conditions reproduced in this test therefore represented the deterioration of the trench wall interface.

Two tests were carried out using the above wall facings. The first used the lightly compacted sand surround and the second used the 10mm gravel surround. The tests were carried out in accordance with the procedures described in 3.2.

3.3.4 Experimental Repeatability

The test procedures described in 3.2 were followed as closely as possible for all of the tests to minimise the effect of slight changes in these on the measured pipe deflections. The boundary conditions were also constant, which removed another source of variability. The greatest opportunity for experimental variability in these circumstances lay with “human” sources, notably the control exercised over the water content, placement and compaction of the surround material. These have been seen (2.2.2) to have a significant effect on the modulus of soil reaction (E' in Eq 2.7). For the sand surround, both of these were measured during the installation phase of each test. For the gravel surround, the density only was measured (see 3.1.4). The ability to maintain these quantities within a narrow range was ascertained using the density and water contents from each test, and this range indicated the practical degree of repeatability of the testing methods. The repeatability of a particular test was determined by carrying out two tests on the same pipe (type B in Table 5.1) in heavily compacted sand and comparing the deflection data obtained from each of these tests. The tests were conducted in accordance with the procedures described in 3.2.

Table 3.1 Schedule of Laboratory Tests.

PIPE TYPE	LCS	HCS	GRAVEL	LCS (LFW)	GRAVEL (LFW)
A	√	√	√		
B	√	√ ∇	√	√	√
C	√	√	√		
D	√	√	√		
E	√	√	√		

Pipe type as Table 5.1

LCS - lightly compacted sand surround

HCS - heavily compacted sand surround

LFW - low friction box walls

∇— repeat test

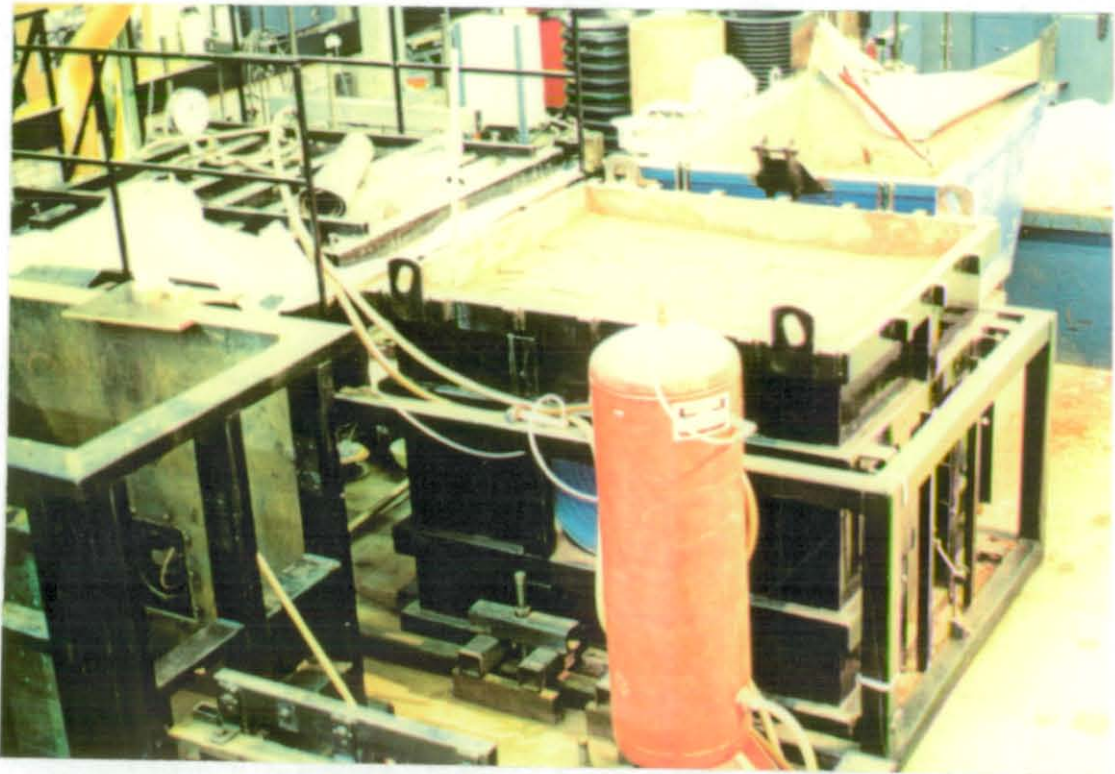


Figure 3.1. Pipe Testing Box (without Extension).

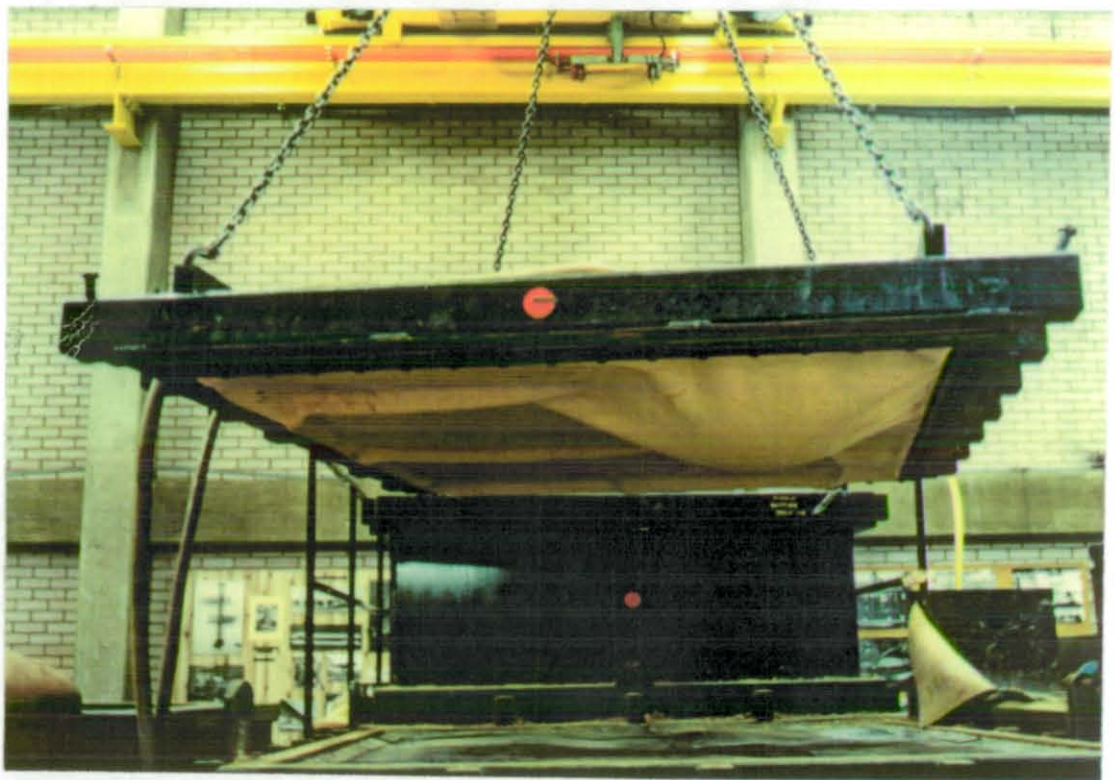


Figure 3.2. Testing Box Lid Showing Water Bag for the Application of Pressure.

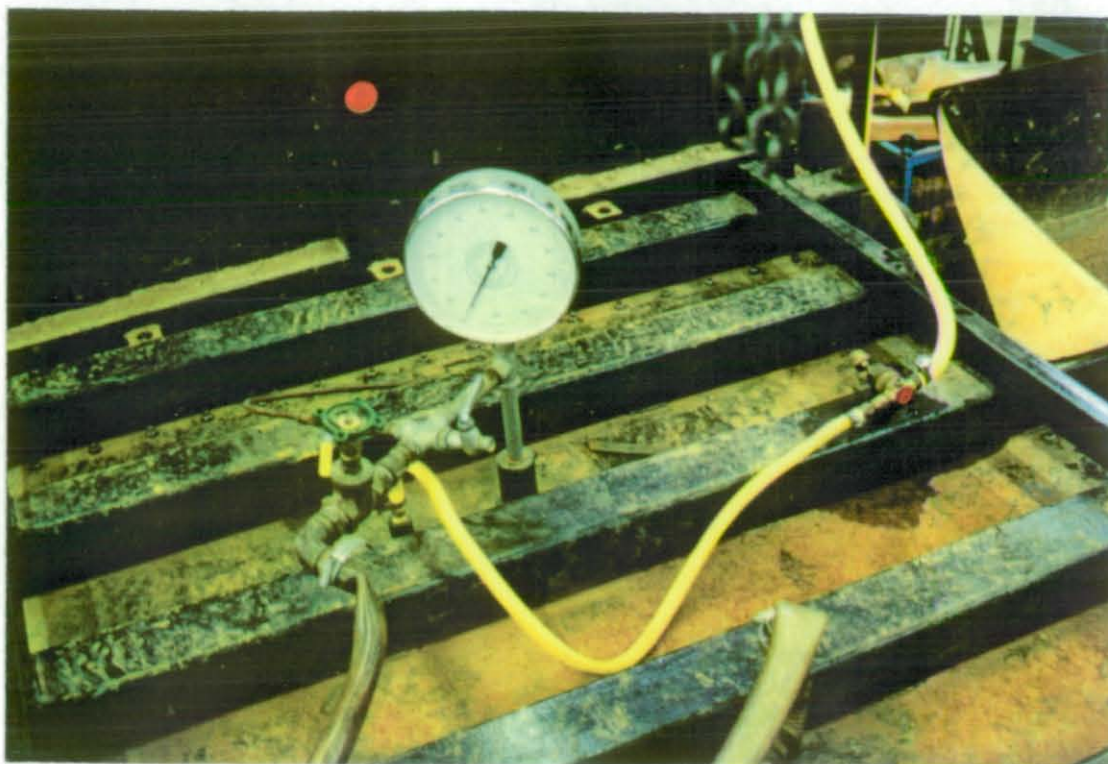


Figure 3.3. Pressure Application and Measurement Apparatus on Box Lid.

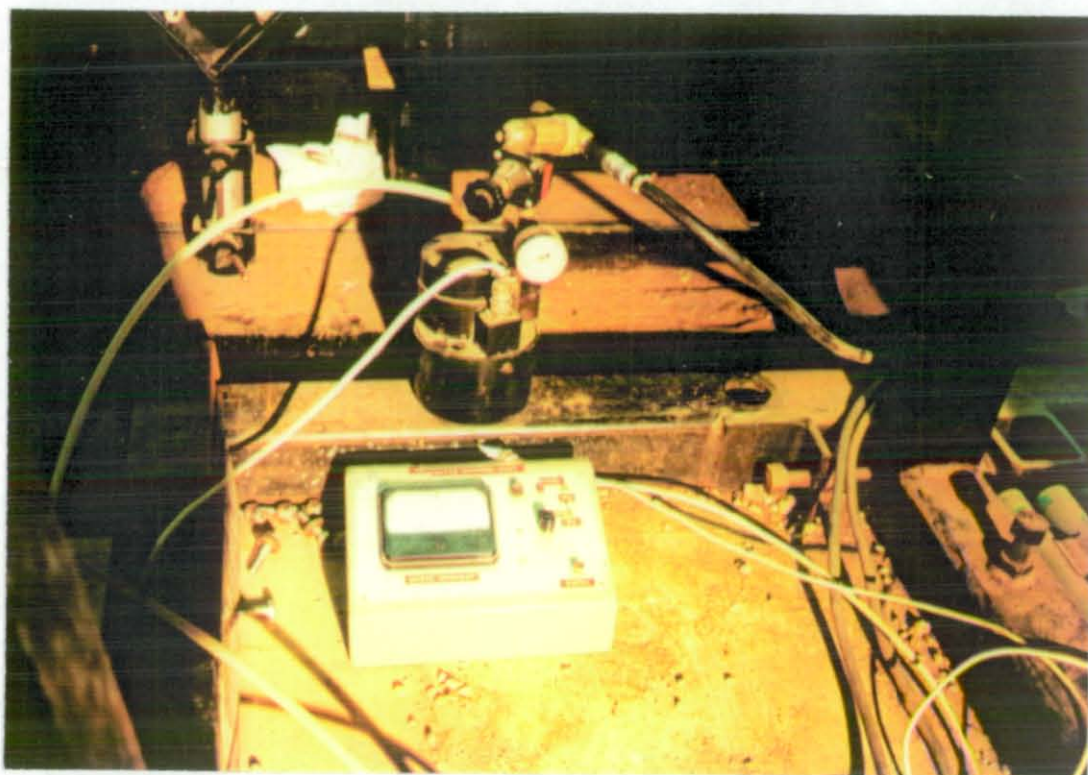
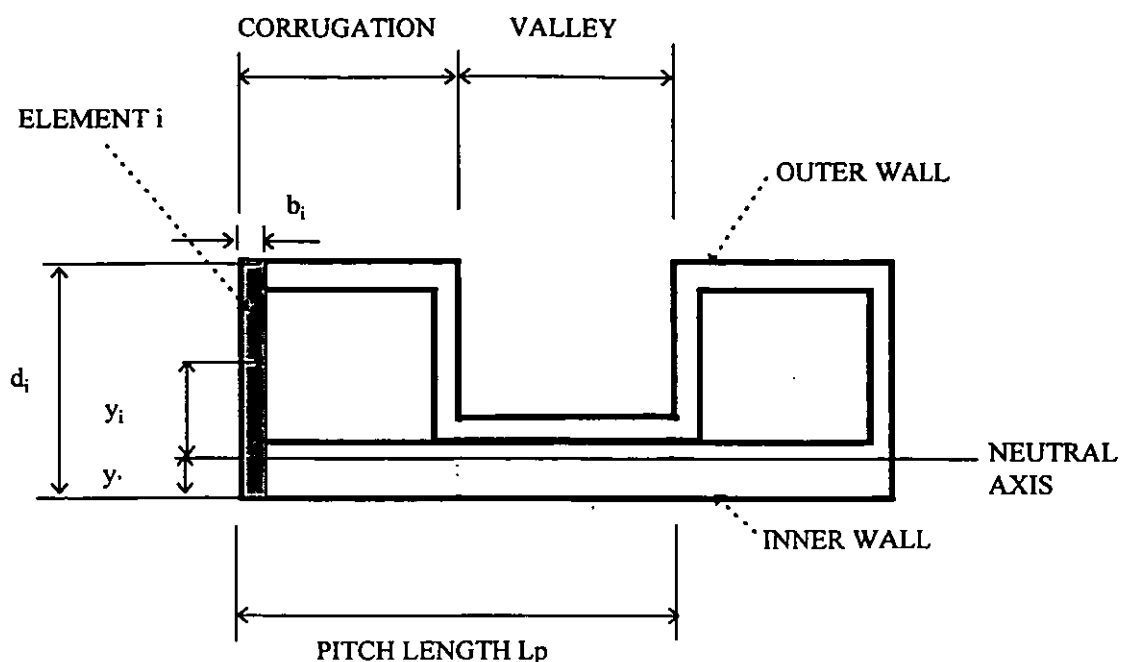


Figure 3.4. Electro-pneumatic Converter and Control Box.



One pitch length (comprising one whole corrugation and one whole valley) is simplified as a representation of rectangular elements.

Distance from inner face of internal wall to neutral axis, $y' = \frac{\sum A_i y_i}{\sum A_i}$

For element i , second moment of area about neutral axis, $I_i = \frac{b_i d_i^3}{12} + A_i (y_i - y')^2$

from the parallel axes theorem.

For one pitch length, the total second moment of area, $I_p = \sum I_i$

For the pipe, the second moment of area per unit length, $I = I_p / L_p$

Figure 3.5. Determination of Second Moment of Area of a Twin Wall Pipe.

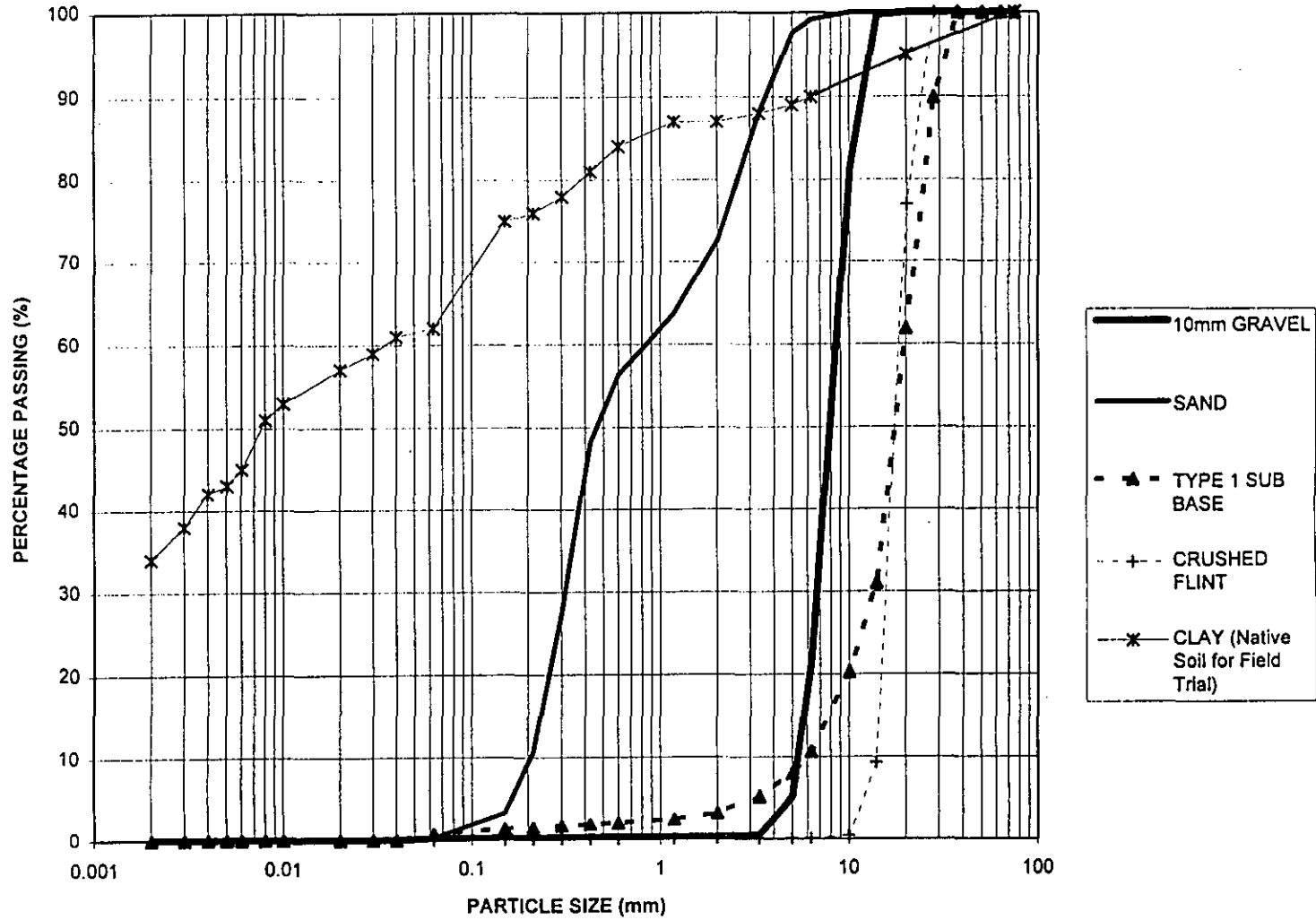


Figure 3.6. Particle Size Distributions of Surround Materials

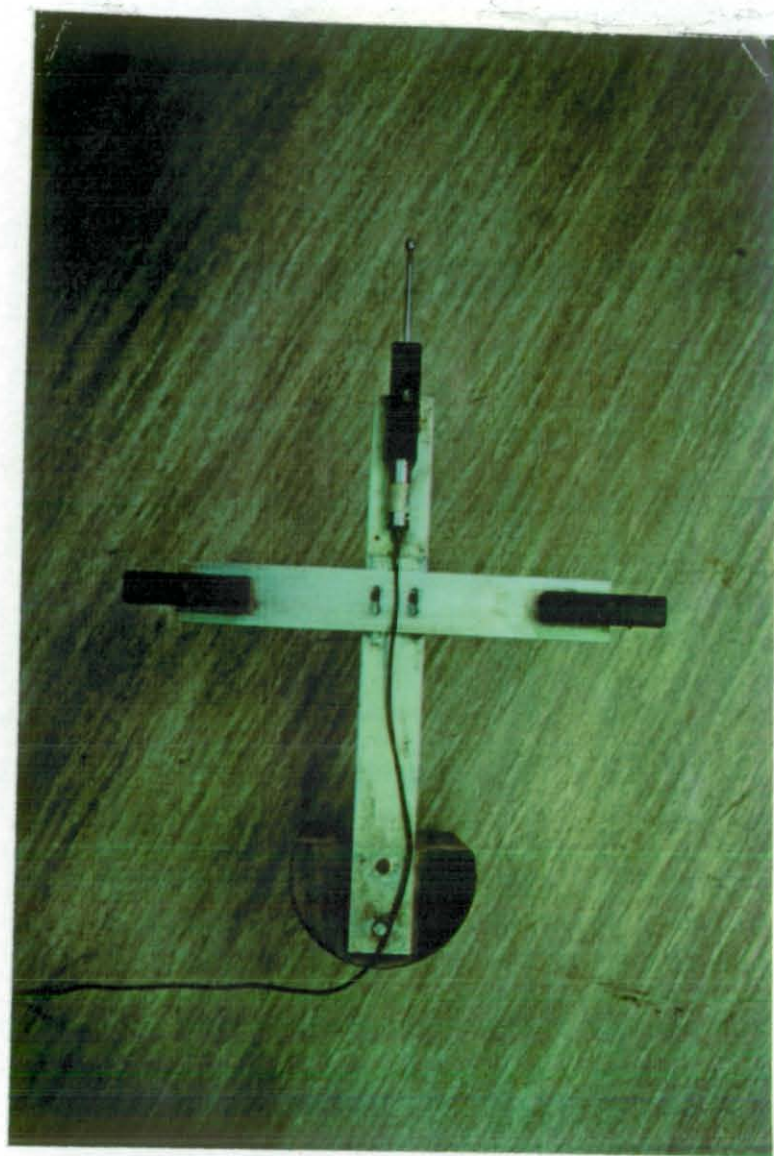


Figure 3.7. LVDT Mast.

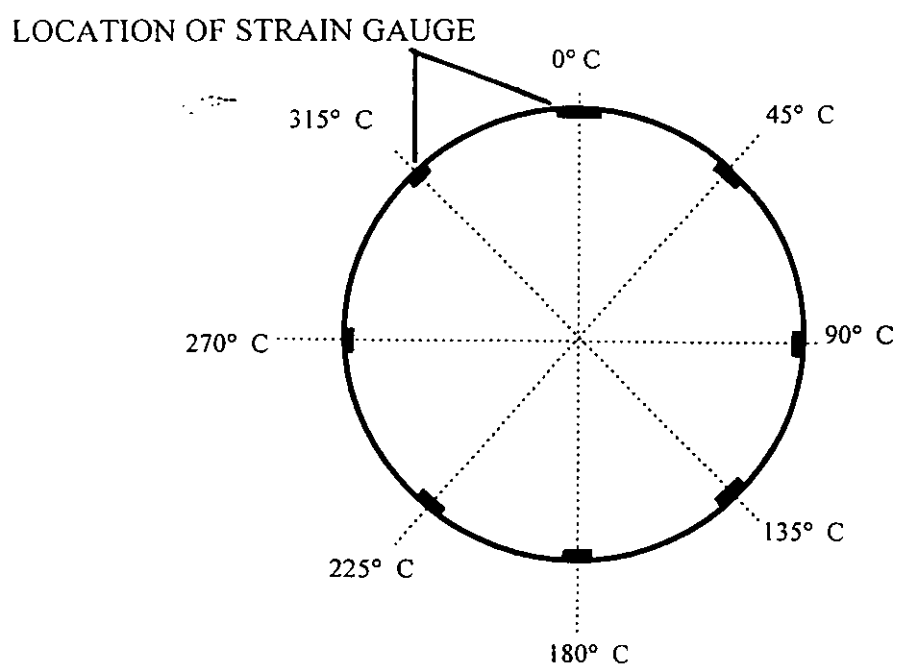
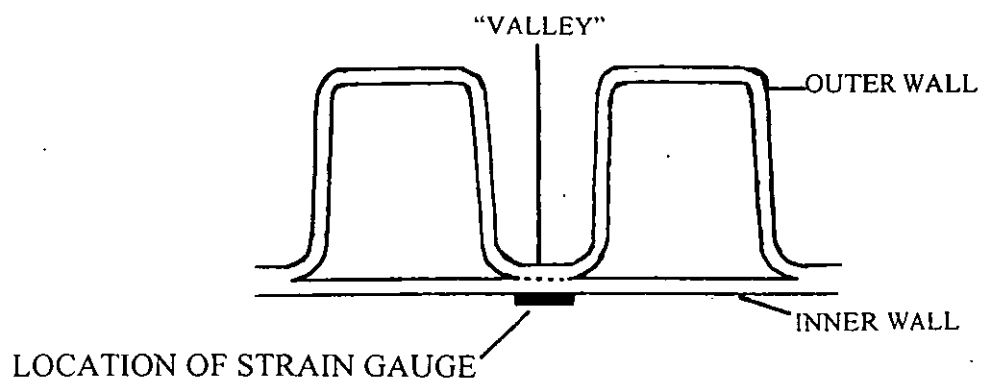


Figure 3.8. Details and Locations of Strain Gauges.

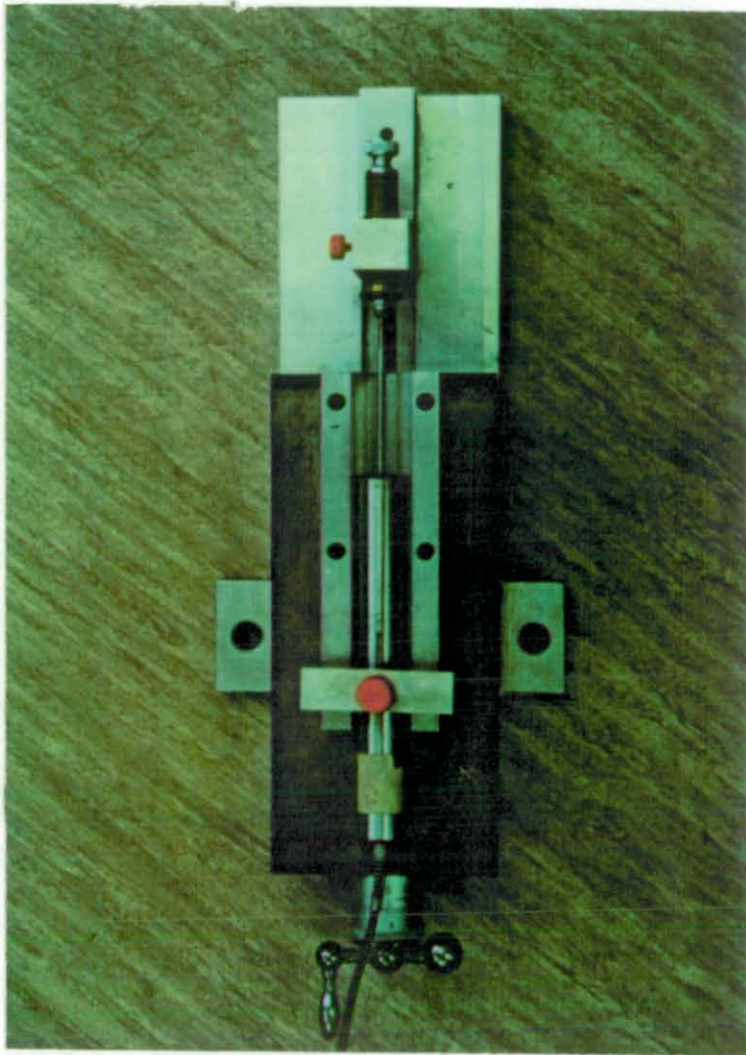


Figure 3.9. LVDT Calibration Device (after Loeppky, 1992).

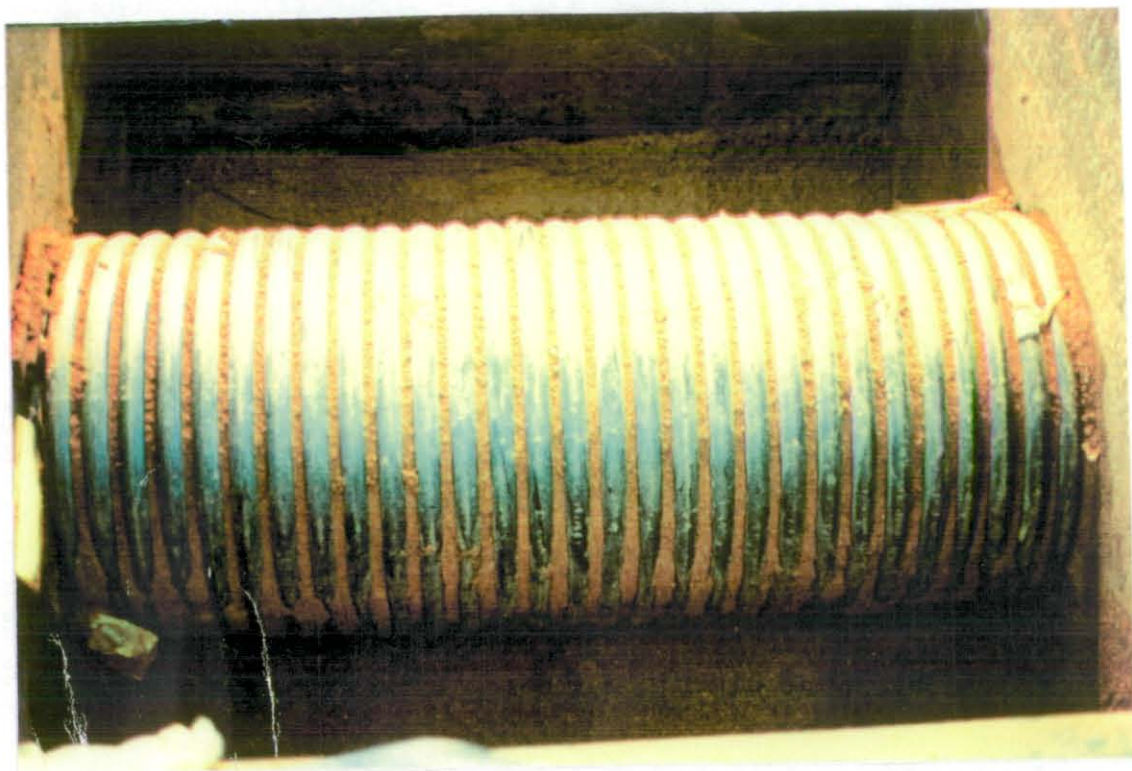


Figure 3.10. Test Pipe in Testing Box Prior to Filling.

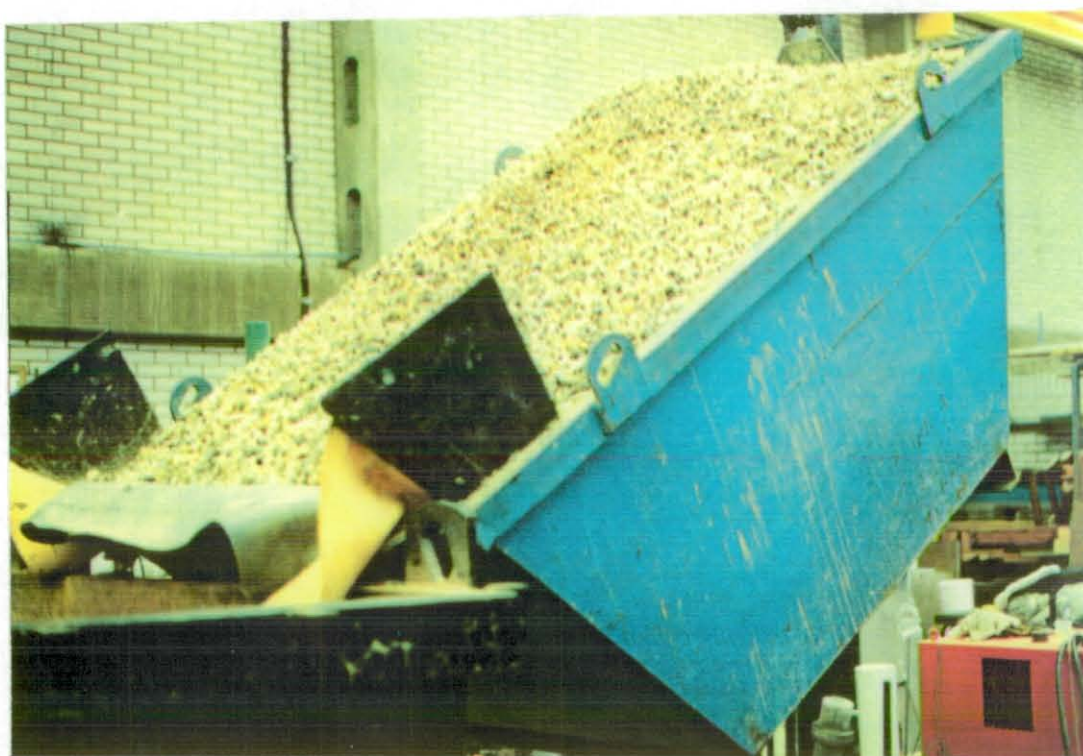


Figure 3.11. Tipping of Fill Material with Overhead Crane.

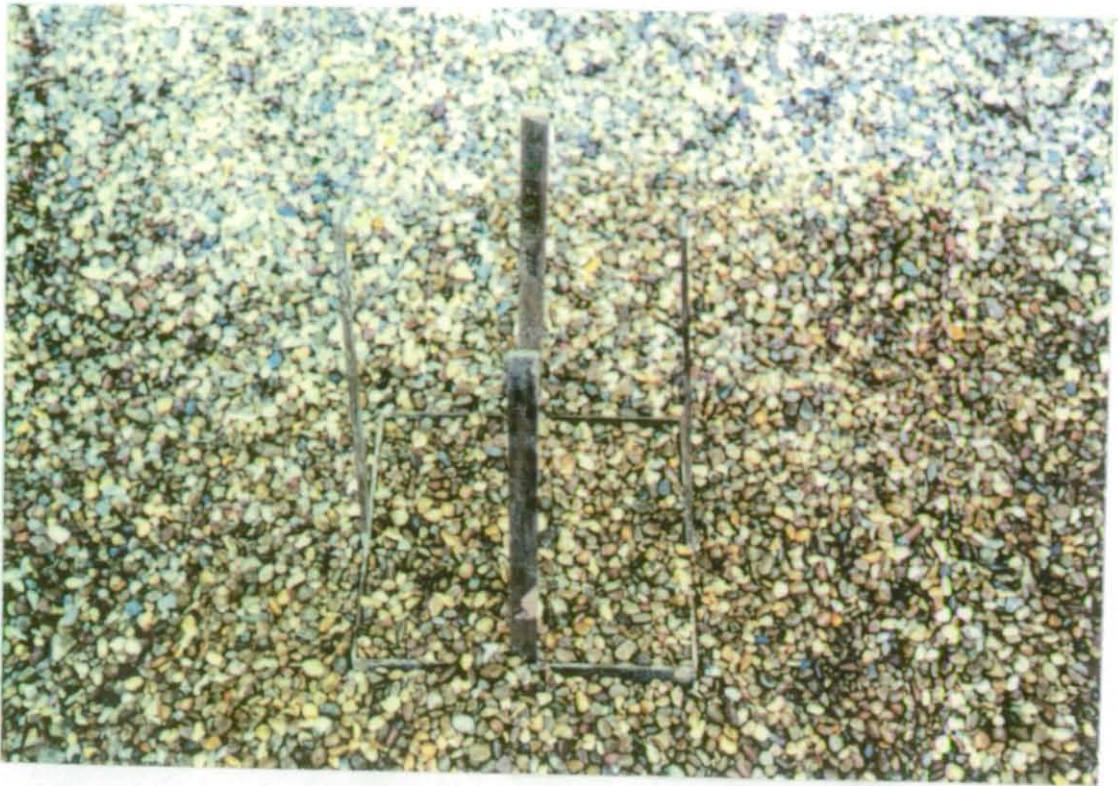
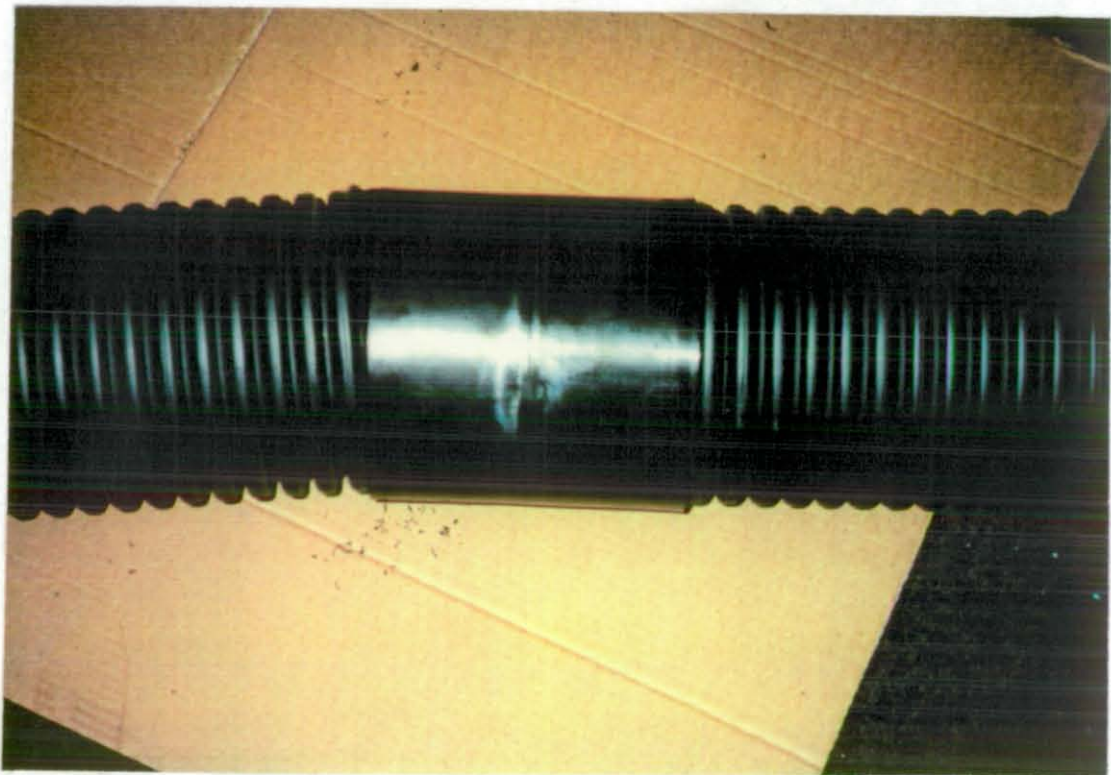


Figure 3.12. Determination of Density of Gravel Surround.



**Figure 3.13. Making of Joint in Pipeline with Coupling
(note Sealing Ring in "Valley" to Left of Coupling).**

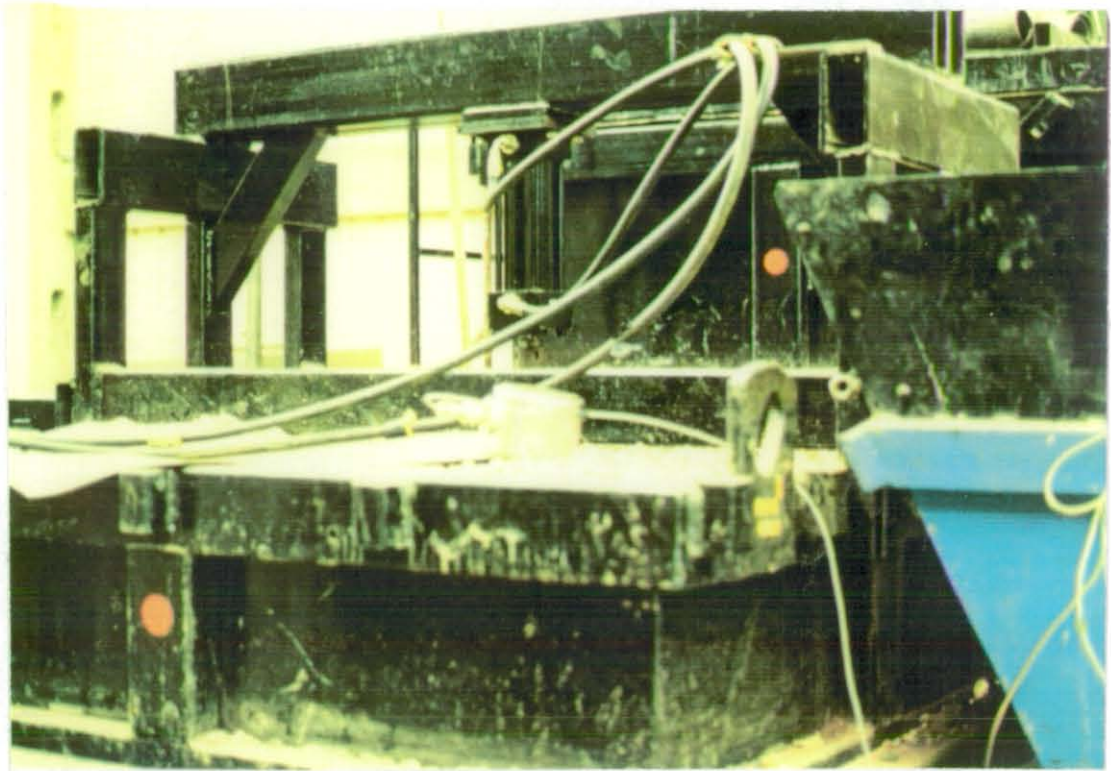


Figure 3.14. Loading Apparatus for Impact Load Testing.

4 FIELD TESTING

This chapter describes the experimental work that was carried out as full-scale field testing of the structural performance of the pipes that had been tested in the laboratory. One type of larger (1.05m internal diameter) pipe was also tested in the field alone to determine whether the increased diameter had a marked effect on structural performance.

The field testing adopted typical pipe installation practices, during which the deformation of the pipes were measured. This was followed the repeated (cyclic) application of loading to the buried via a heavily laden vehicle that traversed the pipe trenches 1000 times. This allowed the trends noted in the laboratory cyclic pressure phase to be confirmed and also provided valuable information on the cumulative deflection of flexible pipes under controlled field conditions. This latter subject has not hitherto been investigated in great detail, and such research as does exist (see 2.5.2) does not refer to the types of pipes that are the subject of this research.

This chapter includes reference to unfortunate flooding of the test site by heavy rainfall between the installation and cyclic loading phases, and observations on the pavement rutting that occurred during the cyclic loading phase. The effect of overloading of the cyclic loading vehicle on the magnitude of pipe deflection is also recorded.

4.1 TEST PARAMETERS AND EQUIPMENT

4.1.1 Test Site, Test Pipes and Ground Conditions

The test site was a field in Old Dalby near Loughborough which had the good access required for delivery of contractor's plant and surround materials. The geotechnical investigation (Salisbury and Fleming, 1993) found that the soil was a stiff gravelly clay (boulder clay), with occasional cobbles present. The particle size distribution is included in Figure 3.6. The water table at the time of the site investigation (September) was lower than the proposed depth of excavation.

Six types of pipes were tested (see 4.1.3). Five of these were of the same type as those tested in the laboratory (pipe types A to E in Table 5.1). The sixth (pipe type F) was a helically-wound pipe of 1.05m nominal internal diameter; which was made by the manufacturer of pipe type C (see 4.1.3).

The layout of the site was planned so that only one pipe received the test loading at any particular time. The site plan, showing the path of the loading apparatus (see 4.1.2) is given in Figure 4.1. The pipes were arranged in two runs of six pipes. Each run contained one type of each pipe (A to F) buried in a common surround material (of which there were two types, see 4.1.5).

The pipes were at centres of 8m, and the distance between the two runs was 2m, which was sufficiently large to allow the loading vehicle to turn easily at the end the run.

4.1.2 Dynamic Load Application Equipment

The repeated loading of the buried pipes was performed using a tractor and a trailer. The trailer was adapted to give a two-wheeled unit, thereby increasing the axle load to a practical maximum (see Figure 4.2). This arrangement was chosen because of its robustness which made it suitable for the site conditions and for travelling at the low speeds that would be necessary for data collection purposes. The use of a road vehicle, such as a two-axle tipper truck, was considered but this type of vehicle did not have sufficiently low gearing for steady low speed travel. Besides this, the maximum safe axle load was smaller than that achieved using the trailer. The most important advantage of the chosen loading apparatus was that the load of the trailer was concentrated almost entirely on the trailer axle. The contact pressures generated by the tractor were low because of this and the large dimensions of the tractor tyres. Secondary pipe deflection caused by the tractor was therefore kept to a minimum.

The trailer was filled with tarmac planings to give an axle load of 11.03t (108kN). This was considered to be the maximum load that the trailer could safely carry for the duration of the loading phase. The width of the contact area of the tyre that was to pass over the measuring equipment (see Figure 4.1 and 4.1.6) was determined by making a tyre-track in a relatively soft sand layer and measuring the width of the imprint. The length of the contact area was determined by pushing two steel rules (1mm thick) under each side of the tyre (in the direction parallel to the vehicle axle) until they touched it. The trailer was then driven off and the spacing of the two rules was measured. The contact area was measured at 450mm long by 290mm wide, giving rise to a contact stress of 413kPa. The track width (the distance between the tyre centres) was 2.75m. A higher axle load was used for a single pass at the end of the main cyclic loading phase (see 4.3.3).

4.1.3 Pipes Tested

Five types of test pipes were of the same types as those tested in the laboratory (see Chapter 3 and 4.1.1). The sixth type was a helically wound HDPE pipe of nominal internal diameter 1050mm, one of the largest sizes available in the UK. This pipe was not tested in the laboratory because of its large size relative to the resulting depth of cover and the dimensions of the testing box. It was tested in the field to ascertain whether there was an appreciable difference in the behaviour of a pipe that was substantially larger pipe than the others tested. Details of each type of pipe tested are again given in Table 5.1.

Four of the types of pipes (A, B, and E) were supplied in their standard lengths of 6.0m. The deflection and strain measurement instrumentation (as described in 4.1.7) was placed centrally in these pipes. Pipe type C was supplied as a 5.0m length, and in this case the instrumentation was placed 2.0m from one end so that the loading vehicle could travel in a straight line (see Figure 4.1). Pipe D was supplied as standard lengths of 3.0m. The instrumentation was placed centrally in one 3.0m length which was installed between two sections of length 1.5m. The joint was sealed with adhesive tape to prevent the ingress of water and surround material. This configuration allowed straight-line travel of the loading vehicle, but because the joint between the pipe sections was not structural the central section acted in isolation in terms of the applied surface loads and resultant deflections.

4.1.4 Trench Dimensions

The trench width for the 600mm nominal diameter pipes was 1200mm, the maximum permitted in highway construction (see Figure 2.10). This width was chosen over the alternative width of 900mm because the increased width led to proportionately smaller trench wall frictional effects. The effect of the stiff walls on the passive resistance to pipe springer movement was also diminished. These effects make the wider trench a slightly worse installation case.

The 1050mm diameter pipe was buried in a trench 1600mm wide, the minimum allowable width. This deviation from the use of the widest possible trench was made because at larger pipe diameters the cost of surround and fill material favours a narrow trench, and as such would be more likely to be used in practice.

Each pipe was buried to a cover depth of one metre, very nearly the minimum value of 0.9m allowed for pipes under trafficked surfaces (DoT, 1993). Trench details are given in Figure 4.3.

4.1.5 Pipe Surround, Trench Fill and Haul Road Materials

The surround materials used corresponded to the permitted types described in 2.2.4.3 (and DoT, 1993). A river gravel of 10mm nominal particle size was used to represent surround Type S, and a river sand was used represent surround Type T. Particle size distributions for both surrounds are assumed to be similar to those found for the relevant surround materials used in the laboratory tests (Figure 3.6).

Both surrounds were placed by treading, because this has been observed to be the normal mode of surround compaction on site and the resulting deflections would therefore be indicative of those achieved in real pipe installations. The use of treading is also justifiable because

mechanical compaction is not permitted within 300mm of the pipe (BSI, 1980). The density of the sand would be expected to lie within the range achieved in the laboratory tests.

The fill material overlying the surround was a granular, granodiorite (see Figure 3.6 for particle size distribution) of Type 1 sub-base (DoT, 1993). This material is used as sub-base for highway foundations and as a fill for trenches that are constructed in highways (except for cover depths of less than one metre where concrete is used). In both of these applications it is used in a compacted state. The use of materials permitted for trenches in other circumstances (such as the Class 8 fill described in 2.2.4.3, which is a general selected fill that must be free of particles exceeding 40mm nominal size and extraneous materials such as tree roots) would have produced a less stiff fill prism and as such may have led to higher subsequent pipe deflections.

The haul road over which the vehicle would be driven comprised a layer of Type 1 sub-base, approximately 250mm thick, placed on a layer of geotextile. The primary purpose of the geotextile was to assist in reducing lateral deformation, and hence the tendency to rutting, of the haul road by repeated loading over the track of the vehicle. The geotextile was cut at the location of the trench sides to prevent load spreading when the loading vehicle was over the trench, which would have reduced the stress on the pipe and led to lower deflections than would occur in practice.

4.1.6 Application of Dynamic Load

The loading vehicle was driven over each pipe 1000 times, to match the number of simulated vehicle loading applications used in the laboratory testing. A minimum speed of approximately 0.25ms^{-1} (0.9kmh^{-1}) was possible. This speed was used for those cycles during which deflection and strain data were collected (see 4.2.3.2), and permitted six deflection readings to be taken at intervals of 1s (the minimum allowed by the data collection equipment) as the vehicle passed over the trench for a 600mm pipe. The normal travelling speed for the remaining loading cycles (during which no data were collected) was approximately 3ms^{-1} (10kmh^{-1}).

The path of the trailer was such that one wheel passed directly over the measurement devices, as shown in Figure 4.4. This produced a greater stress on the pipe crown at the location of the measurement devices than would have been produced had the centre of trailer axle passed over this location.

4.1.7 Deflection and Strain Measurement

4.1.7.1 Deflection Measurement Equipment

The datalogger and computer was used for the collection of test data. The LVDTs, mounted on their mast (see 3.1.6.1), were used for the collection of detailed deflection data during individual passes of the load, and were moved from pipe to pipe throughout the test (the permanent provision of three LVDTs in each pipe being uneconomical). The result of moving the LVDTs during the testing was that the recorded data relating to an individual pass of the vehicle over the pipe under test did not represent the absolute deflection of the pipe as measured from the start of the cyclic loading phase. The data in fact represented only the transient change in the shape of the pipe during the particular loading cycle, as measured from the start of that cycle.

This problem required the use of additional measurement equipment that stayed in each pipe during the entire cyclic loading phase and which could be used to measure the absolute deflection during this loading phase. Calibrated, vertically aligned DC linear potentiometers of maximum travel 50mm were used for this purpose, which were less expensive than the LVDTs. The potentiometers were secured on masts at the crown of each pipe as near as possible to the location of the other measurement equipment. These were used to monitor the progressive change in the vertical diameter of the pipe, and were read manually by a portable digital voltmeter with combined power supply.

Three readings of the potentiometers were taken during a recorded pass of the load. The first was an initial reading prior to the passing of the load over the pipe, the second was a peak reading when the vehicle wheel was over the centre of the pipe and the third was a final reading when the vehicle had passed over the pipe. The peak deflection reading could then be matched to that recorded using the LVDT, thereby allowing the detailed deflection data obtained using the LVDT to be "normalised" to absolute values of pipe deflection.

The change in the horizontal diameter was not continuously monitored in the manner described above, but the horizontal deflection due to one pass of the vehicle was periodically measured with LVDTs.

The cycles during which deflection data were collected are described in 4.2.3.2.

4.1.7.2 Wall Strain Measurement Equipment

Wall strains were measured with the strain gauges described in 3.1.6.2. The gauges were placed on a circumferential plane which was located in the pipe shown in Figure 4.1. The layout of the strain gauges around the circumference is shown in Figure 4.5. The assumption, based on laboratory test results, was made that the pipe deformation would be broadly symmetrical about

the vertical axis. Strains were therefore measured on one side of the pipe, which allowed for greater detail on account of the closer gauge spacing.

Longitudinal (or axial) strain gauges were placed at key points to determine the extent of bowing of the pipe under wheel loading. This has functional implications, namely vertical alignment, ponding and silting of the pipe.

The ten gauges used to measure circumferential strains and the four used to measure axial strains were connected to the datalogger, the internal wiring of which was altered to activate the fourteen strain gauge channels necessary for the work.

4.2 TEST PROCEDURES

4.2.1 Preparation of the Test Pipes

The methods of installation and testing of the strain gauges was as described in 3.2.1. An additional feature for the field trial was that the gauges and exposed wiring were coated with molten wax, which was the recommended method of protecting them against the effects of the moist environment expected on site.

4.2.2 Installation of the Pipes

The topsoil was stripped from the site and stockpiled. The pipe trenches were set out and dug using an excavator (see Figure 4.6). Soil samples were taken during excavation using U-100 tubes.

The bedding layers (of finished thickness 100mm for pipes A to E and 200mm for pipe F) were placed on the trench bases and trodden down and the pipes lowered into their trenches (see Figure 4.7). The LVDTs were positioned in one pipe and were connected to the datalogger, as were the strain gauges. The datalogger run profile was set to read the input channels every three minutes. Data collection commenced and the surround material was placed and compacted by treading (see Figure 4.8). The fill material (Type 1 granular sub-base) was placed in layers of 150mm and compacted in six passes using a "Wacker" vibrating plate compactor (see Figures 4.9 and 4.10). This procedure was carried out for the remaining pipes.

When all of the pipes had been installed, the geotextile was placed over the site and cut where it crossed the trenches. The haul road was constructed over the site using the excavator and a Bomag 120 vibrating roller, which made ten passes over the Type 1 sub-base.

4.2.3 Application of Dynamic Loading

4.2.3.1 Test Procedures

The permanent linear potentiometers were secured on their masts in the pipes. The LVDTs were pushed up to the strain gauges (Figure 4.11) in the first pipe to be tested and all measuring equipment was made ready to record. The run profile of the datalogger was set to record the input channel readings at intervals of one second. The tractor was first driven over the pipe and stopped when before the trailer wheels entered the zone of influence of the trench. Observation of linear potentiometer readings as the tractor passed over the trench confirmed that the deflections caused by the tractor were extremely small.

An initial reading of the linear potentiometer was taken and the datalogger was then set to record. The trailer was then pulled across the trench at a speed of approximately 0.25ms^{-1} and stopped when the tractor and trailer straddled the next pipe to be tested. The pipe deflection was recorded for a further 10 seconds as the pipe recovered. A final linear potentiometer reading was then taken. This procedure was repeated for all of the pipes.

4.2.3.2 Data Collection Intervals

The laboratory tests showed that a large proportion of the deflection of a repeatedly loaded pipe occurred during the first cycles of load application. Therefore, more deformation and strain data were collected during the early load cycles. As the repeated loading test proceeded, the number of passes between those on which deformation and strain data were recorded with the datalogger were increased (see Table 4.1). Readings of the change in vertical diameter made using the linear potentiometers were taken more frequently throughout the test, again as shown in Table 4.1.

4.3 MISCELLANEOUS TEST OBSERVATIONS

4.3.1 Flooding of the Test Site

During the installation phase, the groundwater remained below the depth of the excavations. Between the installation and the vehicle loading phases there was a period of heavy rain that caused the access holes to the pipes, and the pipes themselves, to fill with water. The holes were pumped out, but water continued to flow from the adjacent soil. A filter drain was therefore installed with a sump containing a pump at its lower end (see Figure 4.1). This kept the water level below that of the trench bases. This caused severe and permanent damage to the strain gauges, all of which became erratic and highly inaccurate as a result. Therefore, no reliable wall strain data are presented in Chapter Five. In addition, the increase in water content of the clay and trench fill

material (and to a lesser extent and more temporarily that of the surround media), may have led to a reduction in the stiffness of these soils and a consequent increase in pipe deflection. Though highly inconvenient, this unfortunate event could have produced a slightly worse installation case and therefore was useful in the context of establishing the magnitude of pipe deflections in very poor site conditions.

4.3.2 Rutting of the Haul Road During Dynamic Loading

The repeated driving of the tractor and trailer around the test site on the same path caused the haul road to deteriorate somewhat during testing. Rutting occurred between the pipe trenches and the geotextile tore at some locations (see Figure 4.12). The deepest ruts were formed in the soil just to the side of the trench wall. This was caused by the cutting of the geotextile above the trench walls (see 4.1.5), and may have led to an additional impact loading on the pipe. Over the pipe trenches, rutting did not occur to a great extent, indicating that the fill material was stiffer than the native soil.

The haul road was repaired by spreading Type 1 sub-base over the affected areas with a dozer and compacting it with the roller. The linear potentiometers measured the deflections of the pipe crowns as reinstatement was carried out.

4.3.3 The Effect of One Pass of a High Load

Following the vehicle loading phase described above, the effect of the passage of a heavier vehicle was investigated. This was to determine whether the magnitude of deflection depended on the largest load experienced by a buried pipe or whether the repeated loading led to the formation of an appreciably stiffer pipe-soil system. The trailer was loaded further to give an axle load of approximately 150kN. The contact area produced by each tyre (measured in the manner described in 4.1.2) was 550mm by 300mm and the contact pressure was estimated to be 445kPa, which was approximately 7% higher than that determined for the main cyclic loading phase. The tractor and trailer were then driven once over each pipe, with the magnitude of the deflection recorded using a linear potentiometer.

4.3.4 Visual Observations of Pipe Deformation

During the vehicle loading tests, the opportunity was taken to observe, from inside the pipe, the manner in which the pipe responded to dynamic loading. When the axle passed over the trench wall and was directly over the surround to the side of the pipe, the pipe springer closest to the load deflected inwards by a small amount. This was due to the lateral earth pressure

generated by the advancing wheel. As the wheel passed over the pipe shoulder, deflection of the top of the pipe was seen to take place and travelled in a "wave" as the wheel passed over the pipe. True elliptical deformation was apparent when the wheel was over the centre of the pipe, and the "wave" continued as it proceeded to the other side of the trench, followed by a slight inward movement of the springer farthest from the load. The change in shape of the pipe is sketched in Figure 4.13. The effect at the crown was that of a downward deflection of an increasing rate as the wheel approached the crown, followed by an upward deflection of decreasing magnitude as the wheel departed. This is a visual representation of the rotation of principal stress at a point caused by a moving load (see 2.2.5.2).

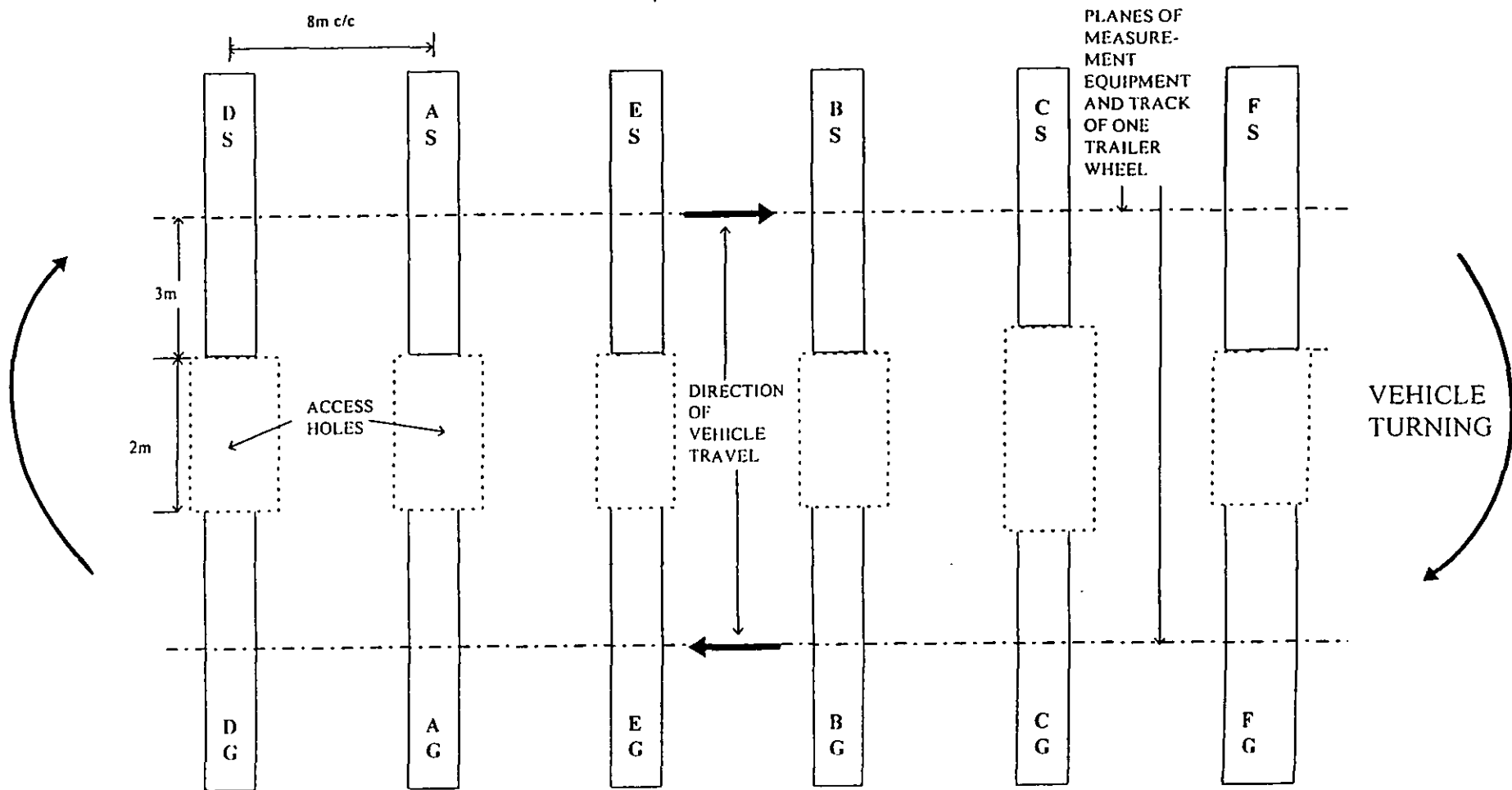
Table 4.1. Load Cycles During which the Measurement Devices Were Read.

DEVICE	READING CYCLES
LVDT, SG	1,2,5,10,15,20,25,50,100,400,1000
LP	1,2,3,4,5,6,7,8,9,10,11,12,13,14,15,20,25,30,35,40,45,50,60,70, 80,90,100,150,200,250,300,350,400,450,500,550,600,650,700, 750,800,850,900,950,999,1000

LVDT - Linear Variable Differential Transformers.

SG - Strain Gauges.

LP - Linear Potentiometers.



A B,C,D,E,F - PIPE TYPES (Table 5.1)
 S - SAND SURROUND
 G - GRAVEL SURROUND

Figure 4.1. Layout of the Test Site.



Figure 4.2. Tractor and Trailer Used for Repeated Load Application.

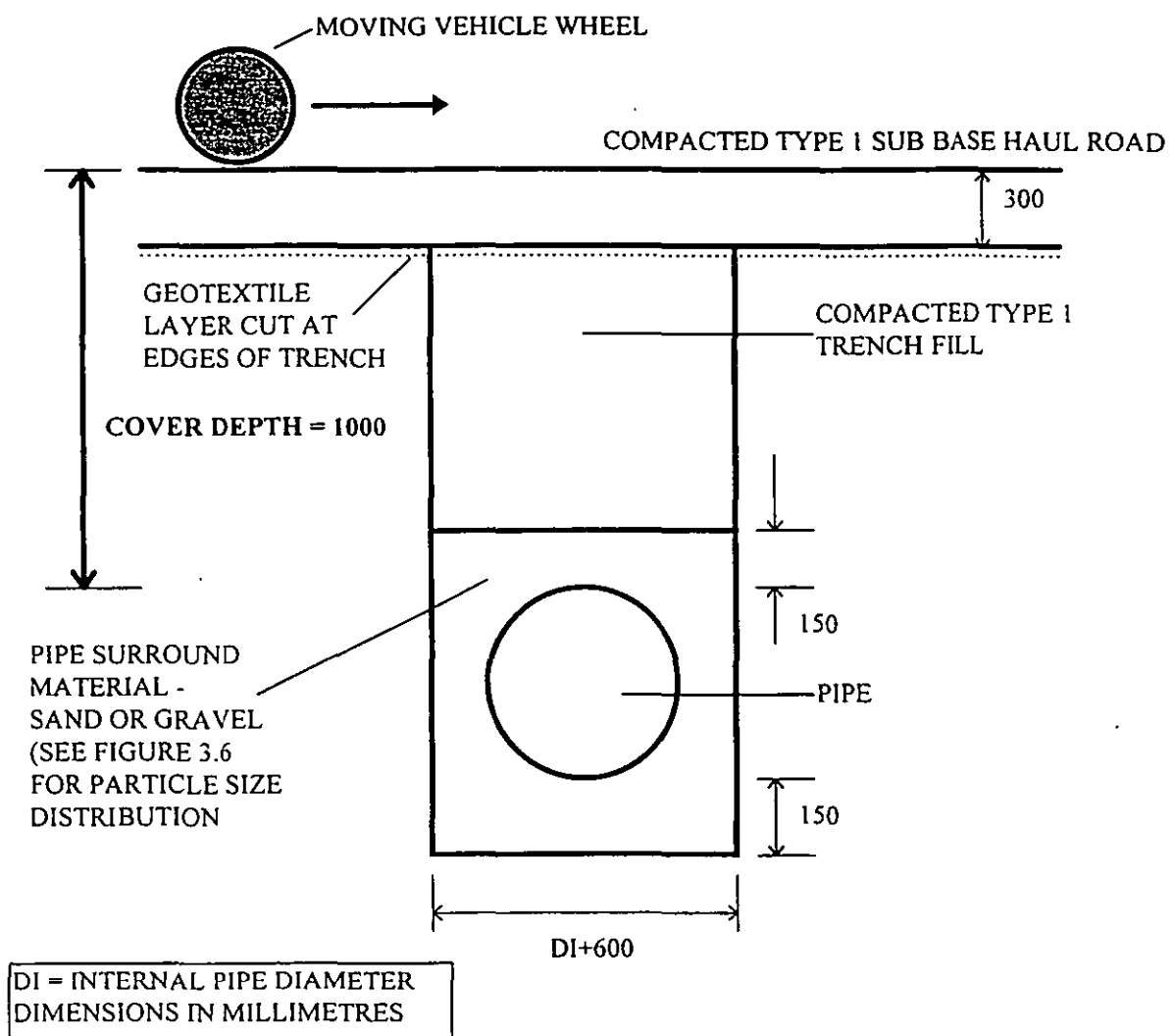


Figure 4.3. Pipe Trench Details.

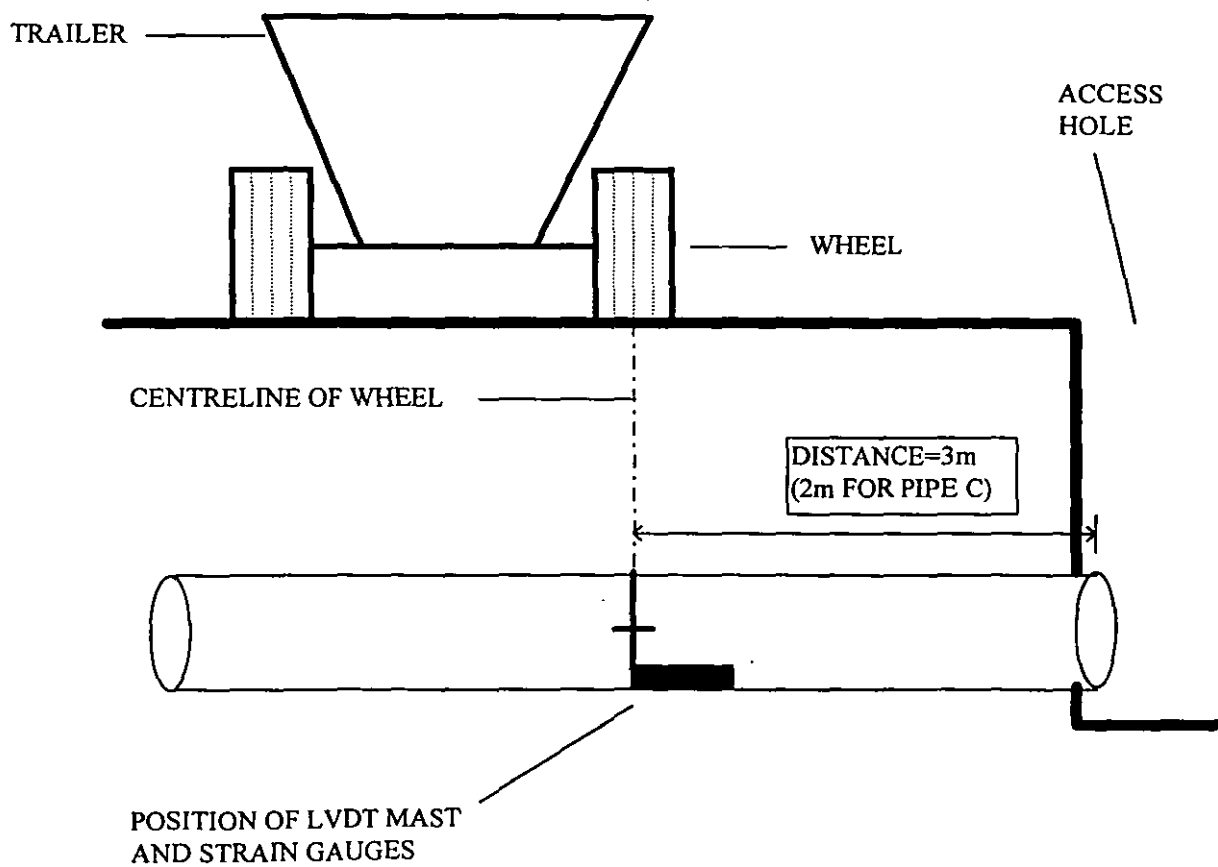


Figure 4.4. Position of Trailer with Respect to Measurement Devices.

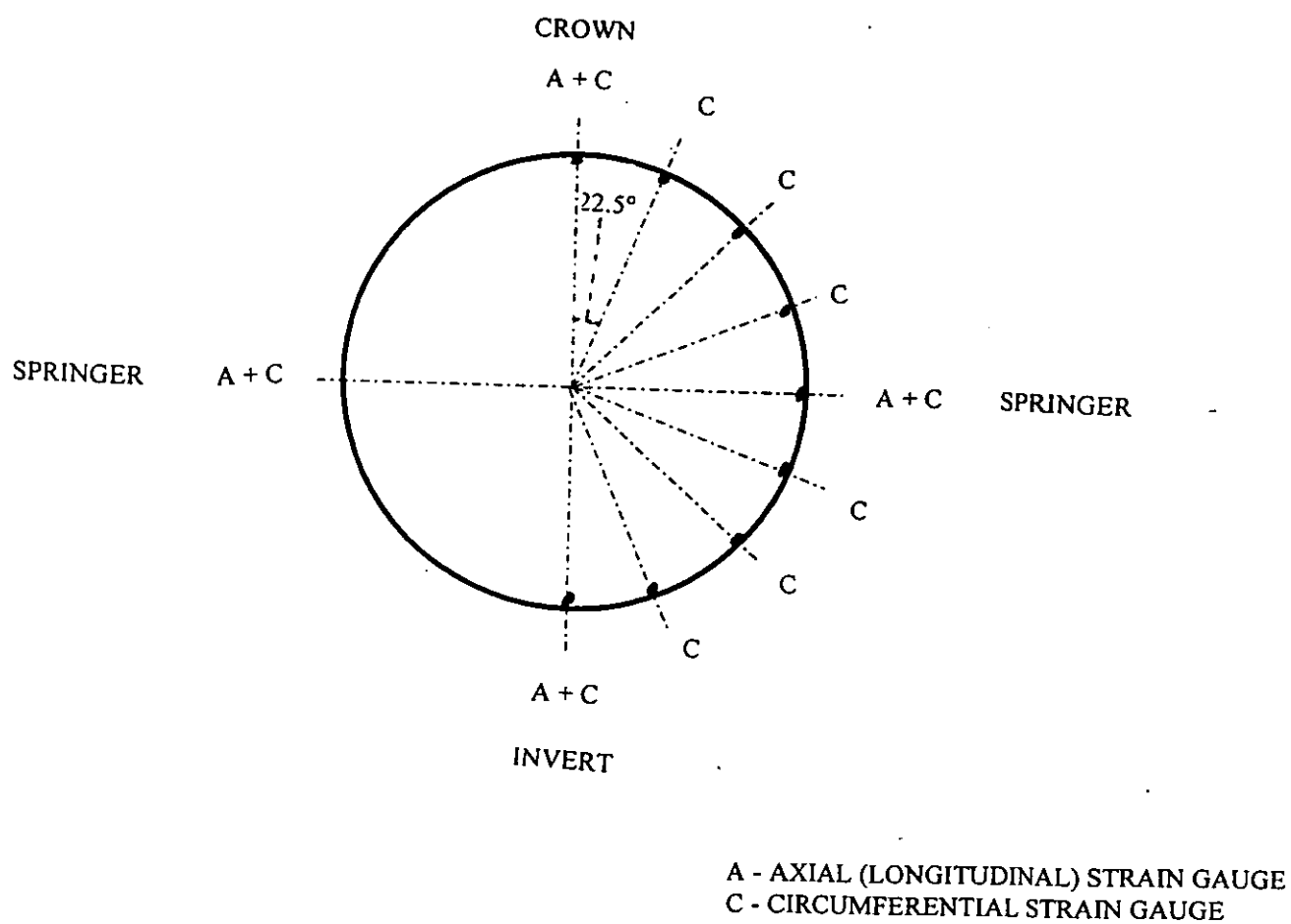


Figure 4.5. Layout of Strain Gauges.



Figure 4.6. Excavation of Trenches.



Figure 4.7. Lowering of Pipe into Trench.



Figure 4.8. Placing of Surround Material.



Figure 4.9. Placing of Trench Fill Material.



Figure 4.10. Compacting of Trench Fill Material.

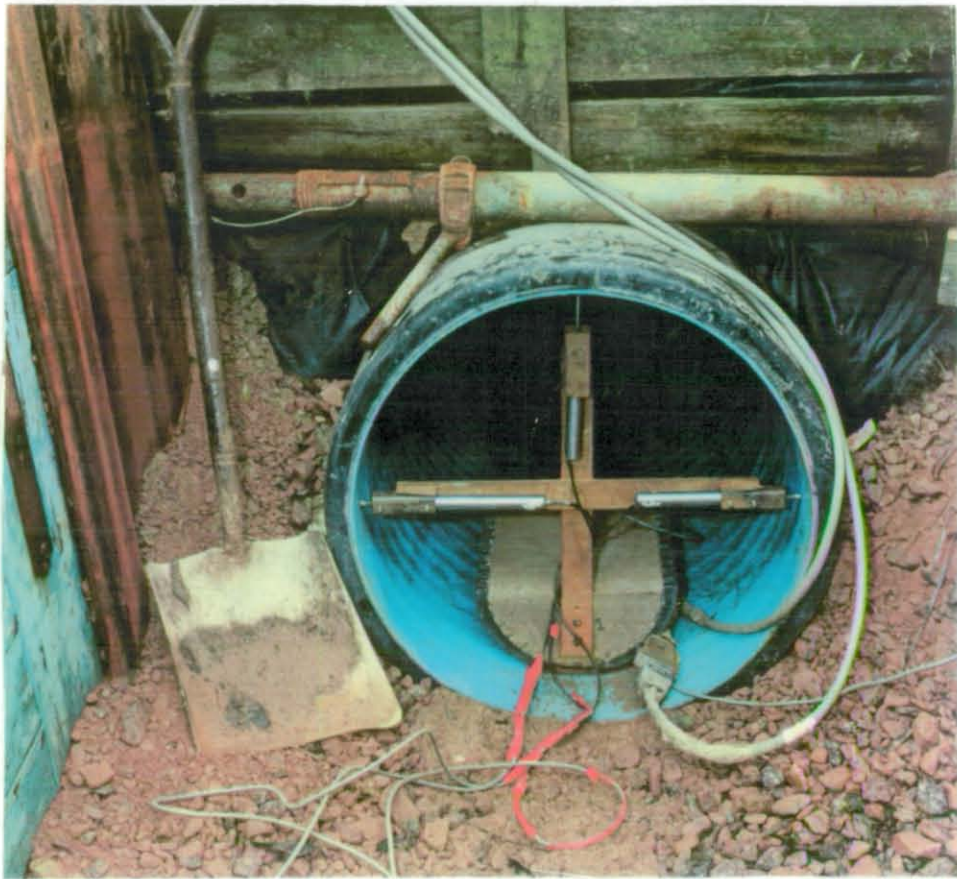


Figure 4.11. Measurement Equipment in the Pipe (Prior to Centring).



Figure 4.12. Rutting of Haul Road.

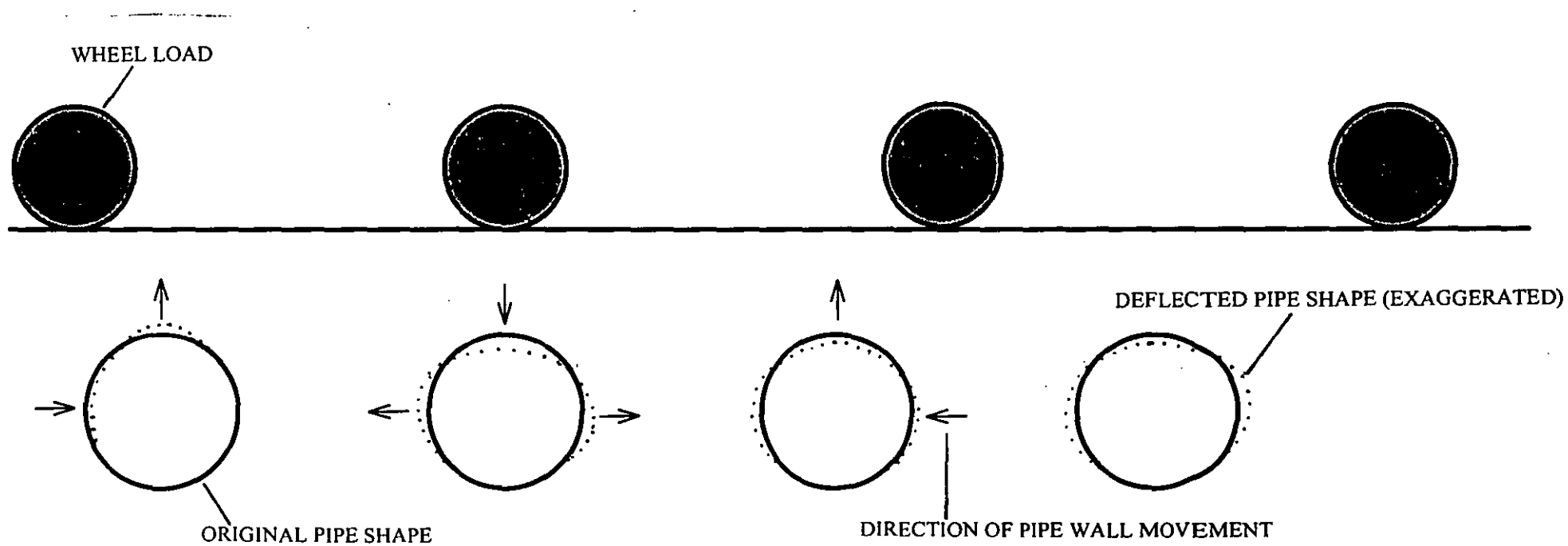


Figure 4.13. Exaggerated Change in Shape of Pipe as Wheel Passes Over Trench.

5 RESULTS

In this chapter, the data obtained from the laboratory tests are presented. The structural properties of the test pipes and the properties of the surround materials are included. The former allow the efficacies of the various manufacturing methods to be compared. Pipe stiffness data are also used for back-calculation of soil stiffness terms in Chapter 6. The properties of the surround materials (notably their unit weights) are discussed on terms of their consistency, which gives an indication of experimental repeatability, and their influence on the magnitude of pipe deflection, which is one of the main purposes of this research.

The deformation of the pipes tested in the laboratory (manifested as changes in the internal diameters and wall strains) is then explained. The data determined for key points of the tests are presented in tabular form. Complete sets of deflection data are then graphically presented for individual tests, with a broad introductory discussion of general trends. This is followed by a more detailed discussion of data relating to each test phase, including an extended recovery period after testing and the exhumation of the pipe. In this discussion, data are presented that represent the extreme cases (in terms of VDS and wall strain) that were noted for the phase, irrespective of the type of pipe. Examples of marked trends and/or unusual results are also given. Summary data tables have been compiled from the base test data to assist with the discussion.

The data recorded during the field trial are then presented. Deflection and wall strain data are presented that relate to the installation of the pipes. For the cyclic loading phase, the vertical deflection only are presented. The lack of wall strain data is the result of the flooding of the test site (see 4.3.1) prior to this phase, which caused terminal damage to the strain gauges.

5.1 RESULTS OF THE LABORATORY TESTING

5.1.1 Test Pipe Properties

Table 5.1 shows the materials, types of construction, the dimensions and stiffness properties of the pipes tested. The equivalent single wall of a profile-wall pipe thickness (t_e) was calculated from the measured value of I using Eq 2.8, and represents the thickness that a single wall pipe would require in order to maintain the same value of I . An impression of the amount of material saved by adopting a profile wall can be gained by comparing their equivalent wall thicknesses and masses per unit lengths with those of the single wall pipe (type E).

The pipe stiffness has been calculated and measured. The product (EI/D_i^3) is related to the pipe stiffness term in Eq 2.6, the difference being that the cube of the internal pipe diameter rather than the radius is used as the denominator. In calculations using Eq 2.6, the pipe stiffness term is often replaced by $8S_o$, where S_o is the short-term pipe stiffness and is implicitly assumed to be (EI/D_i^3) . The STISs for each pipe were determined using the appropriate test method (BSI, 1989, see 2.2.1.3). The STIS is the pipe stiffness value used in the UK for calculation purposes and is therefore normally termed S_o . The stiffness term measured in the USA (ASTM, 1987) is included for discussion.

Comparison of the pipe stiffness data in Table 5.1 (for pipes A to E) shows how the shape of the pipe profile affects the second moment of area of the pipe wall, I . The annular-corrugated and helically-wound pipes have values of I approximately ten times higher than that of the single-wall pipe. Single-wall construction is structurally inefficient, and also results in heavier pipes, as shown by the masses per unit length of each type of pipe.

The values of the elastic moduli, E , for each pipe show that PVC-U is appreciably stiffer than PP and HDPE, and this offsets partially the lower structural stiffness caused by single-wall construction. The range of stiffnesses for PP and HDPE exemplify the sensitivity of E to the factors described in 2.2.1.1, notably the raw material properties and the manner of extrusion. The values shown lie within the large ranges (400MPa to 1400MPa) quoted for such materials (Brandrup and Immergut, 1989).

The pipe stiffness values were calculated in three ways. The first was the determination of the product (EI/D^3) from the material and section properties of the pipe wall, while the second and third were the determination of the STIS and the stiffness to ASTM D2412 (see 2.2.1.3) by testing. The results indicate the relative merits of each method. The product (EI/D^3) exhibits the largest variation from pipe to pipe. This method is therefore the most sensitive to variations in the pipe properties (which may occur during the manufacturing process) and to individual aspects of the test methods used (such as the selection of a strain rate for determination of the elastic modulus). The value of 3.30kPa for pipe E is approximately 20% of the value for the stiffest pipe (C, which has a value of 15.91kPa). The range of values for STIS is appreciably smaller. This may be because the STIS test is carried out on a section of the pipe ring as opposed to a small tensile-testing sample, and therefore represents more accurately the stiffness of the pipe ring in deformation (which is the desired quantity) than an isolated sample. The presence of anisotropy and material impurities in a small sample would also effect the calculated value of (EI/D^3) . The values of STIS for a pipe were between 47% and 75% of (i.e. all lower than) the corresponding value of (EI/D^3) for the twin-wall pipes (A to D), resulting in more a conservative design when the STIS is used in, for example, Eq 2.6 or the method described in 2.3.2. The STIS

for the single-wall pipe was 50% larger than (EI/D^3) , and this means that the stiffness of the pipe ring is greater than the material and section properties would suggest when tested in isolation. Because this type of pipe is structurally the most simple, it would be expected that the two values would show close agreement. That they do not indicates that the pipe ring does not seem to perform in the manner assumed by the theories that include the product (EI/D^3) as the pipe stiffness term. This observation is a strong indication that "ring theory" is a simplification of pipe behaviour, and that the pipe-soil system behaves more as a three-dimensional entity than has hitherto been supposed. The difference in the two stiffness values may also be due to factors such as sample size, strain rates and the stress regime. The STIS test has been found by use to produce consistent results and the test conditions (notwithstanding the reservations given in 2.2.1.3), are more appropriate to the circumstances of a buried pipe than the tensile testing of small samples.

Determination of the pipe stiffness using the ASTM method yields considerably larger stiffnesses. This is partly because of the constant rate of strain that the ASTM test adopts, which does not reflect the observed change in deflection of a buried pipe with time (see 5.2 et seq). The test method forces the pipe quickly into a pre-set deformed shape and records the resistance offered by the deformed pipe ring. The rapid rate of strain has the effect of neglecting the effects of creep that tend to reduce the stress within a pipe held at a constant deflection (see 2.2.6.1). The testing method, whilst simple enough for quality monitoring processes, is not therefore suitable for the design of buried flexible pipes.

5.1.2 Surround Properties

The unit weights and moisture contents of the surround types used are given in Tables 5.2, 5.3 and 5.4.

The mean value of the (wet) unit weight of the lightly compacted sand was 17.51 kNm^{-3} , whereas that of the heavily compacted sand was 18.23 kNm^{-3} . The difference between the unit weights of the lightly and heavily compacted sand surrounds (see Tables 5.2 and 5.3) was approximately 5%. Thus, the two extremes of workmanship that these cases were designed to represent resulted in unit weights that were relatively similar. However, the deflection data for these two cases were markedly different in magnitude. This is due in large part to the effect of compaction on the lateral earth pressure coefficient k_0 which is explained in 2.2.2.2 and demonstrates that the small magnitude of the increase in density (being the unit weight divided by the gravitational constant g) that was produced by a considerably larger compactive effort was sufficient to allow much larger passive pressures to be mobilised in the case of the heavily compacted sand. The "overlap" in the range of unit weights for the two compaction states

(compare 17.70kNm^{-3} for pipe B in heavily compacted sand and 17.80kNm^{-3} for pipe E in lightly compacted sand) may have been partly due to inaccuracy in the determination of the unit weight in individual tests, but it also shows that there were differences in compaction procedures between tests. Based on the deflection data which showed appreciable differences between the two compaction cases (see chapter 5) the two compaction regimes did produce surrounds of quite different stiffnesses.

The standard deviations of the wet unit weights was 0.40kNm^{-3} (or 2.2% of the mean) for the lightly compacted sand case and 0.69kNm^{-3} (or 3.8% of the mean) for the heavily compacted sand case. The relatively small amount of compactive effort utilised in the lightly compacted sand case resulted in more uniform densities between individual tests, whereas the larger compactive effort utilised for the heavily compacted sand case gave rise to a greater variability in the densities achieved in individual tests. The variability in compaction between tests also gives an indication of the variability in compaction in individual tests, and the results suggest that this may be larger than expected given the tight control exercised over the compaction procedures. Nevertheless, it is certain that the degree of control exercised in the laboratory was greater than that which would be exercised on site, and as such the laboratory procedures approximate to the upper limit of achievable consistency.

The mean wet unit weight of the gravel surround (15.16kNm^{-3}) was smaller in relation to the sand cases because of the voids that existed between the relatively large gravel particles. This leads to a packing arrangement wherein there are high point forces between the particles. In confined locations, this would be advantageous as it leads to a relatively stiff material. The standard deviation of the sample was 0.22kNm^{-3} , or 1.4% of the mean. This demonstrates the superior natural ability of the gravel to attain a uniform density with a small amount of compactive effort.

5.1.3 Pipe Deflections and Deformed Shapes

5.1.3.1 Presentation of Results

Deformation data for the pipes are summarised at key test points in Tables 5.5. to 5.21. The pipe deflections are given as cumulative vertical and horizontal diametral strains (VDS and HDS), defined as the change in internal diameter divided by the original internal diameter.

The cumulative internal pipe wall strains are quoted in microstrains ($\mu\epsilon$, being the measured strain $\times 10^6$), the location of the gauge being defined as ϵ_n , where n is the angle between the crown and the gauge location (thus the invert is located at 180° and the

springers are located at 90° and 270°). Positive strains indicate compression or an increase in curvature of the pipe wall, whereas negative strains indicate tension or flattening of the pipe wall.

The test phases are defined thus:

SI	Start of installation
EI	End of installation
E7SL	End of application of 70kPa static pressure (i.e. loading of the buried pipe)
E7SC	End of 24 hour period of 70kPa static pressure application
E7SU	End of removal of 70kPa static stress (i.e. unloading of the buried pipe)
E7SR	End of 4 hour recovery period following removal of 70kPa static pressure
CnP	Peak of nth cycle of 70kPa cyclic pressure
CnT	Trough of nth cycle of 70kPa cyclic pressure
E7CR	End of 4 hour recovery period following last pressure cycle
E14SL	End of application of 70kPa static pressure (or loading of the buried pipe)
E14SC	End of 24 hour period of 70kPa static pressure application
E14SU	End of removal of 70kPa static pressure (or unloading of the pipe)
E14SR	End of 4 hour recovery period following removal of 70kPa static pressure

The VDS data are then summarised in Tables 5.22 and 5.23 for key test phases.

These are:

EI	End of installation
E70S ON	End of 70kPa static pressure phase with loading applied (=E7SC above)
C1000P	Peak of 1000th pressure cycle
C1000T	Trough of 1000th pressure cycle
E140S ON	End of 140kPa static pressure phase with loading applied (=E14SC above)

Table 5.22 comprises the total VDS at the end of each test phase, that is measured from zero at the start of the installation phase. Table 5.23 comprises the incremental VDS for each test phase, with the VDS taken as zero at the start of the test. These tables also express the ratio of the VDSs recorded under the 140kPa and 70kPa static pressure phases.

Experimental data are also presented graphically. General data of complete tests are presented first in Figures 5.1 to 5.3, in order to show the trend of deflections caused by the full programme of loading. Figures 5.1 to 5.3 relate to the pipes that showed the largest deflections in each of the three surround types. The data are discussed in 5.1.3.2.

The deformation of the pipe during individual test phases is then discussed in 5.1.3.3 to 5.1.3.6. In these sections, the data discussed relate to the largest changes in deformations recorded for each type of surround in the test phase, regardless of the type of pipe.

The variation of VDS during the installation phase : is shown in Figures 5.4 and 5.5 for the two sand surround cases. Figure 5.6 shows an initially negative VDS that becomes positive as the installation phase proceeds and Figure 5.7 relates to an installation phase in which the VDS remained negative.

Wall strains for the installation phase are given in Figures 5.8 and 5.9 for the same pipes for which VDS data were presented in Figures 5.4 and 5.5. The gravel surround case is not included as it is similar to the lightly compacted sand case. The strain gauge positions are described in Figure 3.8, so that Position 1 represents the pipe crown and Position 5 represents the invert.

The deflections caused by the application of the 70kPa static pressure are shown in Figures 5.10 to 5.12 for the three surround cases. Corresponding wall strains are shown in Figures 5.13 and 5.14 for the lightly and heavily compacted sand cases respectively (these representing the extremes of measured wall strains).

The accumulation of VDS during the 70kPa cyclic pressure phase is shown in Figures 5.15 to 5.17 for each surround type. The appearance of the curves was influenced by the problems experienced with the synchronisation of the loading and recording equipment described in 3.2.4.2. Trend lines for VDS have been added to overcome this and to show the development of transient and permanent deformation. Wall strains measured at the end of this phase for the pipe in gravel are given in Figure 5.18, which displayed flattening of the crown (see later discussion). The rapid accumulation of VDS during the early cycles of loading is shown in Figure 5.19.

The deflections caused by the 140kPa static pressure phase are shown by Figures 5.20 to 5.22 for each surround type. Figure 5.23 shows the effect of an accidental release and re-application of the water bag pressure.

Figures 5.24 and 5.25 show two unusual strain distributions that were found to occur in a well compacted sand surround at the end of the 140kPa static pressure phase. These are discussed further in 6.1.1.

5.1.3.2 Overview of Results from Complete Loading Phases

This section is intended as a general introduction to the pipe deflection data that were recorded in the laboratory tests. The VDS trends and relative effects of the surround types are briefly discussed in broad terms. The individual test phases and specific effects of static and cyclic

loading, and the influence of the surround properties are discussed in much greater detail in the following sections of this Chapter.

Figures 5.1 to 5.3 show the change in VDS during the laboratory loading phases for pipes in each type of surround. The pipes that exhibited the greatest VDS at the end of testing are presented in each case. The installation phases are not shown since these were of variable duration, but the VDS arising from installation has been added to the data so that the figures relate the total VDS for each pipe.

In Figure 5.1, the VDS can be seen to increase rapidly at the start of the 70kPa static pressure phase to a value of 1.54%, before decreasing slightly when the pressure was released. The 70kPa cyclic pressure phase led to a greater VDS, but the rate of increase slowed as the number of pressure cycles increased. The 140kPa static pressure phase resulted in a further increase in VDS which again levelled off rapidly when the pressure had been applied. The peak VDS recorded under the 140kPa static pressure (3.73%) was over double that recorded under the 70kPa static pressure. On release of this pressure, the pipe recovered slightly, but retained an appreciable component of VDS.

Figure 5.2 shows the change in VDS for a pipe in heavily compacted sand. The overall trend appears similar to that of the lightly compacted sand case. However, there are considerable differences. The VDS under the 70kPa static pressure phase was 0.44%, and at the end of the cyclic phase had increased to a peak of only 0.62%. The maximum value recorded under the 140kPa static pressure phase was 0.86% (again virtually double the value for the lower static pressure phase). The magnitude of these VDSs was much smaller (approximately one fifth) compared to the lightly compacted sand case. The rate of increase of VDS during the cyclic pressure phase was slower and more uniform. The degree of recovery on release of the applied pressures was proportionately larger than in the lightly compacted sand case.

For the gravel case (Figure 5.3) the pipe VDS were 0.86% under the 70kPa static pressure, a peak of 1.30% at the end of the 70kPa cyclic pressure phase and 1.60% under the 140kPa static pressure. These values were within the range of those recorded for the two sand cases, but were closer to those of the lightly compacted sand case. Gravel is the most common type of surround material of the three, and the pipes demonstrated good structural performance exhibited under the relatively severe loading by remaining stable under applied loading and not approaching the 5% deflection limit (BSI, 1980). The lightly compacted sand represents an unusually poor surround, but the pipes again performed well when buried in it and subjected to loading. The heavily compacted sand represents an unusually good surround and gave a high degree of support to the pipe, which displayed minimal deflection under the applied loading.

These general observations of pipe deflection are now elaborated on significantly in the remainder of this Chapter, and the factors that influence them are discussed in terms of the surround conditions and the magnitude and nature of applied loading.

5.1.3.3 Deformation During the Installation Phase

This section describes the pipe deformation (in terms of deflection and changes in wall strain) that occurred in each of the surround cases. In each surround case, the pipe that exhibited the largest deflection is considered. This is followed by a discussion of two cases in which the compaction processes themselves led to other shapes of pipe deformation, and the effect of these shapes on subsequent pipe deformations is also considered.

The largest recorded values were 0.27% (pipe A), 0.35% (pipe C) and 0.31% (pipe E) for pipes buried in lightly compacted sand, heavily compacted sand and gravel respectively. The deflection built up during the first 200 to 300 minutes in the case of the lightly compacted sand surround, which corresponded to the time during which the sand was placed in the test box. On completion of filling, the deflection in these cases tended to continue, although at a greatly reduced rate (see Figure 5.4). This phenomenon is the “deflection lag” referred to by Spangler (1941) and is thought to continue as long as the pipe is subjected to a constant loading.

The effect of the placement of surround material on pipe deformation depends on the amount of subsequent compaction. In the case of light compaction (Figure 5.4) there is no significant change of shape until filling has proceeded some distance above the pipe, whereupon the weight of the overburden causes the pipe to deform to an oval shape. In the case of heavy compaction, the initial compaction of surround material around the pipe springers can be to cause the springers to move inwards. This is facilitated by the absence of loading on the pipe crown, which is unrestrained and therefore able to move upwards. The overall effect is a “reverse ovaling” of the pipe. The change in VDS is shown in Figure 5.5. The VDS is negative (indicating diametral extension) and the HDS positive for the first 250 minutes of testing. As filling proceeds upwards, the pipe crown moves downwards under the increasing weight of the overlying soil and the VDS becomes more positive. The initial negative VDS in cases such as this leads to smaller overall pipe deflections during the service lifetime of the pipe. The most severe example of this was for pipe type B in heavily compacted sand (Figure 5.6), for which the VDS at the end of installation was -0.35% and did not become positive at any time during the test (see also Table 5.9).

The pipe buried in a gravel surround (Figure 5.7) showed a more gradual deflection as the gravel was placed around and over the pipe. The amount of compactive effort (applied by treading) was small and it did not cause negative values of VDS during the this phase of any of the tests.

The above observations apply only to particular tests. There was no clear correlation between the magnitude of deflection and surround type. In one case (pipe A), the pipe buried in lightly compacted sand showed the largest VDS of the three surround types at the end of installation, and in the case of pipe E the VDS was negative after installation in lightly compacted sand. The small magnitude of VDS all cases, and the scatter of results (irrespective of pipe or surround type) indicate that the pipe deflection is influenced significantly by individual installation events and small changes in shape of any type may occur depending on site practice.

Particular shapes of deformation are indicated by the circumferential wall strain distributions, which are given in Figures 5.8 and 5.9.

In Figure 5.8 the pipe has assumed an approximately oval shape, with the crown and invert showing (negative) tensile strains. Tensile strains represent a decrease in the curvature or flattening of the pipe wall. The springers displayed compressive strains, confirming that they were becoming more curved. This location is important in terms of the likelihood of failure of the pipe by excessive elliptical deformation. At the springers, excessive compressive strains at the inner wall will be accompanied by large tensile strains on the outer wall (whether the pipe is single-wall or twin-wall) and in extreme cases these may cause local yielding. The plastic hinges that result from excessive strain will allow the collapse of the pipe ring. This is less critical at the crown because although large tensile forces occur on the inner face as the pipe flattens, a plastic hinge would result only if the curvature of the wall was reversed. This requires "snap-through" of the crown which occurs only at excessive pipe deflections (a VDS of the order of 20-30%) and under exceptionally high stresses. The deflections recorded at the end of this phase are therefore a very small proportion of those required to cause failure.

The strains in the walls of the pipe buried in heavily compacted sand (Figure 5.9) show the effect of compaction of the material adjacent to the springers. This case represents the "reverse ovalling" case described above. As the horizontal diameter was reduced, the inner walls of the springers flattened and tensile strains resulted. The initially unrestrained crown was able to move upwards and increase in curvature. This also occurred at the invert, which is notable because this part of the pipe is assumed to be restrained from downward movement by the bedding layer. A possible explanation is that the large amount of compaction, especially around the haunch areas, caused the pipe to lift slightly off the bedding layer. This allowed the invert to move downwards as compaction of the fill adjacent to the springers caused the vertical diameter to increase. It should

be emphasised that the resultant strains were small (of the order of $1400\mu\epsilon$ 0.14%), but the effects were very much concentrated at the invert. The compressive strains recorded at the haunches were smaller than those recorded at the shoulders, which suggest that support to the pipe was concentrated at the haunch area. This may have been the result of careful placement of surround material. Again the effects at the areas of tensile strain (the springers) were more localised than those of compression. This occurrence would be beneficial in the case of subsequent elliptical deformation that resulted from an applied surface loading. The strain pattern represented by Figure 5.9 is effectively the “reverse” of that obtained from elliptical deformation (see Figure 5.8), in that the compressive and tensile strains are interchanged. Thus, if the installation procedures were to produce a strain pattern similar to Figure 5.9, the superposition of an elliptical strain distribution on it would cause an overall reduction of the total strain in the pipe wall.

The wall strains recorded for pipe E in a gravel surround described a similar deflected shape to the elliptical deformation recorded for a lightly compacted surround. The magnitudes of the strain during installation (Table 5.19) varied from $-429\mu\epsilon$ to $287\mu\epsilon$. The crown of the pipe exhibited a smaller degree of tensile strain than would occur for purely elliptical deformation, whereas the shoulders exhibited less compression. This portion of the pipe seemed to remain quite circular during this test phase, which may have been due to a combination of the relatively small compactive effort and the comparatively low density of the overlying surround material, which would give rise to a relatively small overburden stress compared to the sand surround cases.

5.1.3.4 Deformation During the 70kPa Static Pressure Phase

The cumulative VDSs recorded after 24 hours of static pressure application are summarised in Table 5.22 and 5.23. The maximum cumulative values recorded were 1.67% (pipe A in lightly compacted sand), 0.44% (pipe C in heavily compacted sand) and 0.92% (pipe B in gravel).

The VDS built up rapidly as the static loading was applied for all surround types (see Figures 5.10, 5.11 and 5.12). The accumulation of VDS was somewhat more gradual for the lightly compacted sand case (Figure 5.10) than the other surround types. This was due to the greater amount of non-recoverable volumetric strain that the relatively loose particle packing allowed. The applied pressure caused the sand particles to reorientate and take up a closer packing arrangement. This phenomenon represents densification of the surround material (see 6.1.3), and will be seen to have significant and beneficial effects on pipe performance. The increment in VDS for this test was 1.35%.

In the case of the heavily compacted sand surround, the deflection built up more rapidly on application of the static pressure (Figure 5.11). The increment of VDS for this test (0.21%) was approximately seven times that recorded for the lightly compacted sand case. In this case, the higher degree of compaction of the surround material reduced the amount of particle packing that took place within it, leading to smaller volumetric strains and a more rapid mobilisation of the passive earth pressures that tend to oppose deformation of the pipe. The reduced facility for volumetric strain also reduced the “lag” in the deflection.

In the case of the gravel surround (Figure 5.12) the increase in VDS was similar in rate to the heavily compacted sand phase, indicating that the reorientation mechanisms may be similar in the two cases. The increment in VDS (0.62%) for this surround lay between those recorded for the two sand cases.

The wall strains at the end of the 24-hour phase are shown in Figures 5.13 and 5.14 for the lightly and heavily compacted sand surrounds respectively. In the former case, the deformed shape was essentially elliptical. Tension was apparent at the crown and invert, with slight compression at the shoulders, greater compression at the haunches and maximum compression at the springers. In the latter case, there was a greater component of tension at the haunches (which occurrence is discussed in more detail in 6.1.1.2), although the strains at all points measured were compressive. The overall magnitude of the wall strains in the lightly compacted sand case (both tensile and compressive) was larger than for the heavily compacted sand case. This confirms that the pipe was undergoing a more severe change in shape in the lightly compacted sand, or conversely that the heavily compacted sand was more effective at restraining the pipe from deformation.

The wall strains tended to increase with time under the application of the static loading as shown in Tables 5.5 to 5.21. As suggested by the trends in VDS (shown in Figures 5.10, 5.11 and 5.12) the wall strains increased at the largest rate in the case of pipes buried in lightly compacted sand. In some cases of pipes buried in heavily compacted sand (e.g. gauge locations 1, 2, 7 and 8 of pipe D (Table 5.15)) the increase in wall strains was very small. This indicates that there was little creep of the pipe under these test conditions. There were isolated cases of the strain reducing under the constant pressure, for instance at gauge locations 4, 5 and 6 of pipe B in heavily compacted sand (Table 5.9) and locations 2, 4, 6 and 7 of pipe E in gravel (Table 5.19). This would indicate that some visco-elastic behaviour (i.e. creep) was taking place at these locations in these tests.

In the light of this, it can be seen that tests of the type used by Janson (1990 and 1995, see 2.2.6.1) that assume that a buried plastic pipe is held under a constant deflection which gives rise to stress relaxation are not entirely relevant to the case of a buried flexible plastic pipe.

Rather, the pipe is subject to a constant or increasing loading (depending in practice on the change in the frictional resistance offered by the trench walls with time) and the deflection varies as a result. In general, this causes an increase in pipe wall stress (and strain), the degree of which is influenced by the capacity for movement (or volumetric strain) within the material surrounding the pipe.

On release of the static loading the deflection of the pipe buried in lightly compacted sand reduced quickly. A substantial amount of the deflection (approximately 90%) was not recovered. Even after the pipe had been left for 76 hours (Figure 5.10) little further reduction in the deflection took place (approximately 0.02 percentage points or a further one hundredth of the existing deflection). Similar trends were observed for the heavily compacted sand, but in this case only about 40% of the deflection was not recovered. The proportionally large amount of recoverable strain in this case was the result of the relatively small amount of non-recoverable volumetric strain that occurred during pressure application. In the lightly compacted sand case, the large volumetric strain (resulting from particle packing) led to a smaller degree of recoverable strain in the soil and (as a result) in the pipe.

The gravel surround case exhibited a recovery of deflection between these two extremes, approximately 80% was not recovered. Whilst less volumetric reduction took place than for the lightly compacted sand case, some particle reorientation was nevertheless possible in the gravel, and this would have led to a reduced recovery of the pipe deflection.

5.1.3.5 Deformations During the 70kPa Cyclic Pressure Phase

The largest cumulative deflections at the last pressure cycle were 3.09% (lightly compacted sand case), 0.57% (heavily compacted sand surround case) and 1.25% (gravel surround case).

In every test the VDS built up rapidly during the early applications of the cyclic pressure (see Figures 5.12, 5.13 and 5.14). The relative rate of accumulation was dependent on the type of surround. The lightly compacted and heavily compacted sand cases achieved 50% of their peak VDS for this phase at around 125 and 70 cycles respectively, and 90% of the peak at 500 and 560 cycles respectively. The pipe in the lightly compacted sand surround accumulated deflection at a slower rate because of continuing particle reorientation and packing of the sand surround. The repeated loading and unloading of the surround would have agitated the surround particles, causing the packing arrangement to change with time and the surround to become progressively more dense. However, by about 500 pressure cycles, the rates of VDS accumulation for the two surround

cases had almost equalised, although the absolute values of deflection were still markedly larger for the lightly compacted sand case.

The pipe in the gravel surround achieved 50% of its peak deflection after only 25 cycles and 90% of its peak after approximately 300 cycles, which is considerably earlier than either of the sand surround cases. The relatively large and uniform grading of the gravel caused (large) contact forces to be developed between individual particles more quickly than for the sand surround, thus leading to the more rapid attainment of a closely-packed, stable structure. Agitation of the gravel by the repeated loading resulted in a reduced level of additional particle movement, and consequently a reduced accumulation of pipe deflection.

The behaviour of the pipes during repeated loading implies that the stiffness of the surround increases as the cyclic loading continues. The rate of accumulation does not become zero, but it is apparent that the deflections would tend to a limiting value after a great number of loading cycles. This observation is important in terms of prediction of the service lifetime of a buried pipe that is subject to repeated (vehicular) loading, the effects of which are additional to long-term pipe behaviour under static loading. This is discussed further in 6.1.11.3 and 6.2.3.

Wall strains during the cyclic loading phase increased in a similar manner to the diametral strains, and the effect in most cases was to magnify the strain patterns that existed at the end of the 70kPa static pressure phase. However, other strain patterns were noted. In Figure 5.18 (which relates to pipe E in a gravel surround), increasing tension was apparent at the crown. This is representative of "heart-shaped" deformation (Rogers, 1985, see 2.2.3.2), and is indicative of good support at the lower part of the pipe combined with poorer support at the top part. This type of strain pattern was found to occur for some of the tests carried out using gravel or lightly compacted sand surrounds.

The amplitude of the final cycle for the lightly compacted sand and gravel cases was in general approximately one tenth of the amount recorded during the first cycle. In the heavily compacted sand case, the amplitude of the deflection cycles remained virtually constant. This indicates that little instantaneous volumetric reduction was possible under individual loading cycles (because of the already tight particle packing), but that a gradual volumetric reduction took place over the long term which allowed the slight accumulation of permanent pipe deflection.

The effect of the first cycles of pressure is shown in greater detail in Figure 5.16, which relates to pipe B in a gravel surround and displays the accumulation of VDS during the first ten cycles of pipe B in a gravel surround. The flattish peaks and relatively pointed troughs confirm that the profile of the cyclic pressure was transmitted to the pipe with a reasonable degree of accuracy (see 3.1.5). The increase in VDS during this test phase was 0.52%, and by the tenth cycle

approximately half of this deflection had been reached. The rate of can be seen to decrease markedly after the second pressure cycle.

5.1.3.6 Deformations During the 140kPa Static Pressure Phase

The trends of the deflections (Figures 5.17, 5.18 and 5.19) were similar to those observed in the 70kPa static pressure phase, in that the deflection accumulated rapidly as the pressure was applied and increased at a much slower and diminishing rate when the pressure was constant. The largest cumulative VDSs were 3.73% (pipe B in lightly compacted sand), 0.86% (pipe C in heavily compacted sand) and 1.69% (pipe B in gravel).

The magnitudes of cumulative VDS (Table 5.22) for this pressure phase were larger than those recorded in the 70kPa static pressure phase. For the lightly compacted sand case, the ratio of the total VDS (for each pipe) varied from 2.0 to 3.0 (neglecting an anomalous value of 0.1), with a mean of 2.5. For the heavily compacted sand case, the ratios ranged from 1.3 to 2.0, with a mean of 1.7 (neglecting the anomalous result pipe B). For the gravel case the ration ranged from 1.8 to 2.1, with a mean of 1.9. If deflection is assumed proportional to load (as is the case in the principal design criteria), this ratio would be expected to be 2. The mean ratios for each surround type lay around this expected value, and were reasonably close to it. This finding indicates that the total deflection of a buried pipe is approximately proportional to the largest stress applied to it in its lifetime.

The ratios of the increments of VDS for the 140kPa pressure phase to those for the 70kPa pressure phase (Table 5.23) ranged from 0.3 to 0.8 for lightly compacted sand, 0.8 to 2.8 for heavily compacted sand and 0.6 to 1.5 gravel. This shows that the pipe deflection was not strictly proportional to the applied loading, and that the measured deflections were smaller than expected if proportionality was assumed. The smaller than expected incremental deflection confirms that the surround material became stiffer as a result of the previously applied static and cyclic loading. Thus, the stiffness of the surround is dependent on its stress history.

The pipes buried in lightly compacted sand generally exhibited a larger ratio than this, due in part to further non-recoverable volumetric strain in the sand. The heavily compacted sand produced a wider range of values of the deflection ratio, but the displacements were very small in all cases. The gravel surround case resulted in lower values than the lightly compacted sand case.

In the gravel cases, the shape of deformation was generally elliptical. In the lightly compacted surround cases, the deformed shape occasionally deviated from the elliptical at the invert, with the pipe exhibiting “heart-shaped” deformation overall. This may have been the result

of good support of the lower portion of the pipe, the cause of which may have been the ability of the gravel to flow under the pipe haunches during the installation phases.

The effect of unloading and reloading a pipe was observed for pipe B (Figure 5.23) where an equipment malfunction caused the loss of static pressure at the start of the test. The water bag had to be bled and re-pressurised about 750 minutes into the test. The VDS reached approximately 0.44% before reducing slowly (as the static pressure diminished) and dropping to 0.26% after the loading was released. This amount of recovery was about twice that recorded during the 70kPa static pressure phase. Re-application of the static pressure caused a higher VDS, indicating that the pipe-soil system responded to this “cyclic” pressure (albeit of a low frequency) in much the same trend as it did to the 70kPa static pressure. During the second “cycle” the VDS rose slightly as normal and the recovery period produced a recovery of similar proportion (relative to the peak strain) as the earlier unloading event.

Since this test phase produced the maximum pipe deflections, it is possible to assess clearly the efficacy of the three surround types. The sand, in its two states of compaction, provides the best and worst cases. The use of heavily compacted sand as a surround leads to a stable pipe-soil system in which the pipe will deflect by only a small amount and will not in normal circumstances become unstable (that is, approach levels of VDS of 20-30% at which “snap-through” buckling would occur). The use of heavily compacted sand as a surround would therefore be appropriate in all installations, but especially in extreme cases, where there are low depths of cover or where high levels of traffic loading are expected on the pipe.

The deflection of pipes buried in gravel are closer to those recorded for pipes buried in heavily compacted sand than lightly compacted sand. This is encouraging and shows that, despite the lack of care with which it can be (and in practice sometimes is) placed, the support it offers to the pipe is of a high standard. The well compacted sand is more effective in limiting pipe deflection, but the effort required to place it weighs against it on the grounds of economy. The pipe buried in lightly compacted sand showed the largest deflection, but it was not severe in terms of the permitted limit (5% VDS) and the magnitude of the applied pressure. Therefore, a gravel surround offers good support to the pipe combined with relative ease of placement, and is suitable for all but the most onerous installations, where a heavily compacted sand surround should be considered.

5.2 RESULTS OF THE FIELD TESTING

5.2.1 Presentation of Data

Deflection data (in terms of the VDS) are presented for all of the test pipes (A to F) for the whole of the field testing programme (i.e. installation and cyclic loading) in Table 5.24 (for the sand surround) and Table 5.25 (for the gravel surround) for the end of the installation phase. Test phases are generally as described in 5.1.3.1. For pipe C in sand, the linear potentiometer failed at the 400th cycle and the final VDS was obtained by physical measurement. For pipe D in sand, the linear potentiometer did not function correctly (giving spurious readings) and the final VDS was again obtained by physical measurement. The “peak” VDS values are those obtained when the trailer wheel was directly above the pipe crown, and the “trough” values were those obtained when the trailer had passed over the trench.

Strain gauge data are presented for the end of the installation phase in Tables 5.26 and 5.27 for the sand and gravel surround cases respectively. The nomenclature for these tables is:

C_n = circumferential strain recorded at n° from the pipe crown, and

A_n = axial (i.e. longitudinal) strain recorded at n° from the pipe crown.

The layout of the strain gauges is shown in Figure 4.5. Because of the flooding of the test site after the pipes had been installed (see 4.3.2), there are no meaningful strain gauge data for the cyclic loading phase.

Table 5.28 shows the amplitudes of the VDS cycles at the first and last loading cycles, and also as a result of the one pass of the heavier axle. These are expressed as ratios for further comment.

Figures 5.26 and 5.27 show the accumulation of VDS during the cyclic loading phase for the pipes buried in sand and gravel respectively. Figure 5.28 shows the amplitude of transient deflection during the cyclic loading phase for a pipe buried in sand and 5.29 shows the same quantity for a pipe buried in gravel.

5.2.2 Pipe Deflections and Wall Strains During the Installation Phase

5.2.2.1 Pipe Deflections

The VDSs recorded at the end of the installation phase for each pipe and surround case are given in the row designated “EI” in Tables 5.22 and 5.23. The values ranged from 0.1% (for pipe B in gravel surround) to 1.01% (for pipe A in sand surround). The mean value of VDS was 0.75% for the pipes installed in sand and 0.59% for those installed in gravel. Pipes A, B, C and D exhibited greater deflection for installation in sand, whereas pipes E and F deflected more when buried in a gravel surround. The order of deflections for the pipes in sand (from largest to smallest)

was A, B, C, F, D, E, and for gravel the order was E, F, A, C, D, B. The STIS values of the test pipes A to E (Table 5.1) were ranked (least stiff first) in the order E, C, B, D, A. Both the range of VDS (the extreme values differing by a factor of 10) and the lack of a discernible trend in relation to the pipe stiffness or the type (and stiffness) of the backfill show that the deflection caused by installation procedures is influenced to a significant extent by the events that occur on site during particular installations. These include tipping of the surround material around the pipe and its compaction by treading and the tipping, levelling and mechanical compaction of the backfill material.

The compaction applied to the Type 1 sub-base was sufficient to form a stiff material (evinced by the lack of rutting over the trench), indicating that the backfill experienced a large degree of compaction. This may not be the case for backfill types such as as-dug clay, which is used for pipe installation in verges (and other non-highway environments) and as such are subject to less stringent compaction requirements (DoT, 1993). The installation case used in the field testing therefore represented a relatively severe compaction case and the maximum deflection recorded (1.01%) may approach the upper limit for the majority of practical installation cases.

5.2.2.2 Pipe Wall Strains

Circumferential internal wall strain data for the installation phase are given in Tables 5.24 and 5.25. The results indicate that the area of tension in the region of the pipe crown in general did not extend the entire distance from the crown (0°) to the shoulder (45°). This means that the pipe has not deformed to an elliptical shape (in which tension is apparent between the crown and shoulder and compression is apparent between the shoulder and the springer (90°)). In four cases, tensile strains (indicating flattening of the pipe wall) were measured at the crown and compressive strains were measured at 22.5° either side of it. In five cases tension was measured by the gauges located at 22.5° either side of the crown, but in none of the cases were tensile strains recorded at the shoulders (45° from the crown).

At the bottom of the pipe, tension was generally recorded within 22.5° of the invert, and in one instance tension was recorded at the haunch (45° from the invert). The slightly larger regions of tension at the bottom of the pipe indicate that areas of poor compaction or voids may have been present, which allowed greater flattening of this portion of the pipe.

The areas of compression extended over half of the pipe circumference, in most cases including the haunches and shoulders. The higher degree of compression indicates that the pipe is well supported by the surround at these areas.

5.2.3 Pipe Deflections During the Dynamic Loading Phase

Tables 5.24 and 5.25 show the peak and residual values of VDS recorded for key loading cycles. The change in VDS during the cyclic loading phase for both surround cases are also shown graphically in Figures 5.31 and 5.32. Data for pipe D are omitted from Figure 5.31 because the linear potentiometer did not produce accurate readings.

The VDS accumulated rapidly during the initial cycles of loading, with the rate of deflection reducing as more passes of the trailer were made over the pipes. There was no clearly defined trend between the surround types, with three of the pipes exhibiting larger deflections in sand. This again shows that the installation practices govern the behaviour of the pipe to a large extent. The largest total VDS measured at the end of the test was 3.18% for pipe B in a sand surround, and the lowest was 0.95%, also in a sand surround, for pipe E. The scatter of final VDS for the pipes buried in gravel was smaller than that for the pipes buried in sand, indicating that the gravel can be compacted to a more uniform degree.

The rate at which VDS accumulated ... differed slightly between the surround types. For the pipes in a sand surround, half of the VDS recorded at the 1000th loading cycle was achieved after approximately 100 loading cycles. In the case of the gravel surrounds, half of the VDS recorded at the 1000th loading cycle was achieved after between approximately 10 and 100 loading cycles. The tendency of the pipes buried in gravel to accumulate VDS more rapidly (which indicates that an equilibrium of deformation would be attained more quickly) than those buried in sand confirms the results from the laboratory tests that the gravel forms a stable surround more quickly.

The amplitude of the deflection (i.e. the transient deflection) as the loaded vehicle passed over the pipe was typically 0.1% at the 1000th loading cycle for all of the pipes, regardless of the surround type. This constant value was reached after relatively few passes of the load (see Figures 5.28 and 5.29).

The field test deflection data must be considered in the context of the test conditions. The wheel load (approximately 55kN) was similar to that of a dumptruck on site, but the tyre contact area was much smaller, leading to a contact stress of approximately 415kPa. However, in comparison to the heaviest legal road vehicle (380kN distributed over five axles, giving a mean axle load of 76kN) the trailer used in the field test (which had an axle load of 108kN) represented a severe case. To compound the effects of the loading, the cover depth was near the minimum allowable value and there was no flexible or rigid pavement layer overlying the sub-base layer that constituted the haul road, which would have reduced the stresses at the pipe crown. In view of

these considerations, the pipes performed well during the vehicular loading phase, and the 5% VDS limit was not breached.

5.2.4. Effect of One Pass of Very High Load

The loading of the trailer to produce an axle load of approximately 150kN (i.e. 75kN per wheel) caused the tyre contact area to increase and the contact stress was approximately 445kPa, an increase of approximately 7%. This is relatively small in comparison to the 35% increase in the axle load. The amplitudes of deflection caused by the passing of the vehicle (see Table 5.28) varied from 0.09% to 0.23%, with the larger values for each pipe generally being recorded for the sand surround case. The larger amplitudes (which were between 1.1 and 2.2 times those recorded for the case of the 108kN axle load) show that the larger loading did have a significant effect on the deflection of the pipe, although the absolute values of the amplitudes were small and may have been influenced by greater impact effects of the heavier vehicle.

The flooding of the site that occurred prior to the start of the vehicular loading phase led to the failure of the strain gauges and no accurate data were collected for this test phase.

Table 5.1. Materials, Construction and Properties of Test Pipes.

PIPE REF	MATERIAL OF CONST ^N	TYPE OF CONST ^N	MASS PER METRE (kgm ⁻¹)	I PER UNIT LENGTH (mm ⁴ mm ⁻¹)	t _e (mm)	D _i (mm)	E (MPa)	EI/D _i ³ (kPa)	STIS (kPa)	ASTM (kPa)
A	PP	TW AC	26.82	2627	31.59	603.5	1260	15.58	10.57	554
B	HDPE	TW AC	22.18	4960	39.04	607.1	558	12.40	6.90	523
C	HDPE	TW HW	17.40	3216	33.79	609.6	1121	15.91	6.52	518
D	PP	TW AC	19.65	2393	30.62	548.1	889	12.92	9.68	502
E	PVC-U	SW SP	44.67	331	15.84	598.0	2130	3.30	4.97	249
F*	HDPE	TW AC	-	9917	49.19	1066.8	-	-	-	-

Key.

PP-polypropylene

HDPE-high density polyethylene,

PVC-U-unplasticised polyvinyl chloride,

SW-single wall,

SP-smooth profile,

TW-twin wall,

AC-annular-corrugated,

HW-helically wound,

I-second moment of area,

t_e-equivalent thickness of single-wall pipe having same value of I (determined by substitution in Eq 2.8)

D_i-internal diameter,

E-elastic modulus per BS2782, Method 320, at a strain rate of 25mm min⁻¹,

STIS-specific tangential initial stiffness per BS4962.

ASTM-Load at 5% VDS per ASTM D2412, at a loading rate of 12.5mm min⁻¹.

* Pipe F was used in the field tests but not in the laboratory tests. Stiffness data were unobtainable because testing equipment to accommodate pipes of this diameter not available.

Table 5.2 Properties of the Lightly Compacted Sand Surrounds for the Laboratory Tests

PIPE REF	UNIT WEIGHT OF SURROUND (kNm ⁻³)	WATER CONTENT (%)	DRY UNIT WEIGHT (kNm ⁻³)
A	17.52	5.1	16.67
B	17.28	5.2	16.42
C	17.40	4.8	16.60
D	17.60	4.1	16.91
E	17.80	5.6	16.86
B-F	17.50	6.1	16.49

B-F - Test carried out on pipe B using low friction test box wall facings

Table 5.3 Properties of the Heavily Compacted Sands Surrounds for the Laboratory Tests

PIPE REF	UNIT WEIGHT OF SURROUND (kNm ⁻³)	WATER CONTENT (%)	DRY UNIT WEIGHT (kNm ⁻³)
A	18.10	3.1	17.56
B	17.70	3.7	17.07
C	18.30	4.8	17.46
D	18.30	4.1	17.57
E	18.39	4.9	17.53
B-R	18.60	3.2	18.02

B-R - Repeat test carried out on pipe B

Table 5.4 Properties of Gravel Surrounds for the Laboratory Tests

PIPE REF	UNIT WEIGHT OF SURROUND (kNm ⁻³)	WATER CONTENT (%)	DRY UNIT WEIGHT (kNm ⁻³)
A	15.05	4.7	14.37
B	15.20	5.5	14.41
C	15.29	4.2	14.67
D	15.14	4.0	14.55
E	15.22	3.7	14.67
B-F	15.03	5.2	14.28

B-F - Test carried out on pipe B using low friction test box wall facings

Table 5.5. VDS, HDS and Circumferential Wall Strain Laboratory Test Data for Pipe A (PP TW AC) in Lightly Compacted Sand Surround.

PHASE	VDS(%)	HDS(%)	$\epsilon_0(\mu\epsilon)$	$\epsilon_{45}(\mu\epsilon)$	$\epsilon_{90}(\mu\epsilon)$	$\epsilon_{135}(\mu\epsilon)$	$\epsilon_{180}(\mu\epsilon)$	$\epsilon_{225}(\mu\epsilon)$	$\epsilon_{270}(\mu\epsilon)$	$\epsilon_{315}(\mu\epsilon)$
SI	0.00	0.00	0	0	0	0	0	0	0	0
EI	0.27	-0.18	-454	317	417	213	-129	345	462	253
E70L	1.33	-0.95	-2013	1234	2015	1065	-604	1477	2299	858
E70C	1.67	-1.15	-2162	1504	2769	1703	-518	2104	3130	1110
E70U	1.54	-1.09	-2244	1379	2063	1125	-697	1484	2407	918
E70R	1.52	-1.11	-2251	1310	1880	758	-791	1311	2262	785
C1P	1.64	1.17	-2230	1408	2361	1165	-711	1747	2774	903
C1T	1.54	-1.12	-2222	1322	1849	742	-758	1299	2254	771
C2P	1.73	-1.34	-2225	1479	2557	1309	-720	1912	3005	940
C2T	1.62	-1.18	-2364	1389	1994	851	-863	1426	2423	790
C5P	1.85	-1.33	-2454	1542	2670	1354	868	1971	3167	928
C5T	1.76	-1.28	-2516	1457	2178	957	1001	1546	2665	803
C10P	1.99	-1.45	-2630	1600	2793	1382	-1045	2022	3347	907
C10T	1.91	-1.41	-2693	1530	2394	1049	-1159	1670	2923	805
C25P	2.20	-1.63	-2910	1467	2976	1396	-1337	2080	3598	855
C25T	2.16	-1.61	-2950	1632	2759	1214	1408	1882	3367	802
C50P	2.36	-1.77	-3101	1711	3072	1382	-1558	2086	3738	805
C50T	2.36	-1.77	3121	1701	3072	1381	-1599	2093	3743	793
C100P	2.54	-1.91	-3263	1763	3382	1553	-1750	2297	3758	787
C100T	2.50	-1.90	-3264	1718	3055	1311	-1798	2022	2050	723
C250P	2.72	-2.05	-3407	1786	3569	1676	-1947	2437	4320	733
C250T	2.67	2.03	-3409	1749	3248	1411	-1980	2158	3995	676
C500P	2.84	-2.14	-3483	1822	3662	1800	-2029	2567	4460	706
C500T	2.81	-2.12	-3464	1771	3255	1571	-2048	2319	4178	667
C750P	2.88	-2.17	-3471	1838	3659	1842	-2037	2600	4492	706
C750T	2.86	-2.16	-3454	1827	3547	1747	-2035	2495	4357	691
C1000P	2.95	-2.21	-3477	1842	3780	1960	-2049	2719	4616	706
C1000T	2.94	-2.12	-3480	1825	3709	1908	-2074	2657	4551	688
ECR	2.83	-2.18	-3487	1731	3147	1320	-2204	2061	3949	568
E140L	3.27	-2.39	-3382	2059	4819	2608	-1866	3442	5736	976
E140C	3.39	-2.41	-3195	2248	5508	3127	-2849	3922	6378	1251
E140U	3.17	-2.33	-3323	2070	4262	2161	-1849	2946	5133	957
E140R	3.14	-2.35	-3304	1923	3912	1892	-1999	2669	4805	795

Table 5.6. VDS, HDS and Circumferential Wall Strain Laboratory Test Data for Pipe A (PP TW AC) in Heavily Compacted Sand Surround.

PHASE	VDS(%)	HDS(%)	$\epsilon_0(\mu\epsilon)$	$\epsilon_{45}(\mu\epsilon)$	$\epsilon_{90}(\mu\epsilon)$	$\epsilon_{135}(\mu\epsilon)$	$\epsilon_{180}(\mu\epsilon)$	$\epsilon_{225}(\mu\epsilon)$	$\epsilon_{270}(\mu\epsilon)$	$\epsilon_{315}(\mu\epsilon)$
SI	0.00	0.00	0	0	0	0	0	0	0	0
EI	0.23	-0.16	816	475	-47	-88	947	106	357	146
E70L	0.34	-0.23	910	823	439	70	1029	194	858	623
E70C	0.37	-0.23	1007	982	605	120	1061	243	1040	793
E70U	0.32	-0.21	995	732	377	101	1075	211	775	597
E70R	0.32	-0.21	1026	737	370	72	1075	223	730	549
C1P	0.31	-0.20	1046	701	337	85	1095	227	684	518
C1T	0.31	-0.20	1035	674	326	83	1107	222	655	503
C2P	0.28	-0.19	1046	528	170	56	1114	205	503	360
C2T	0.27	-0.19	1046	486	126	53	1117	199	459	314
C5P	0.27	-0.19	1044	473	119	47	1117	188	421	303
C5T										
C10P	0.32	-0.21	1026	737	370	72	1075	223	730	549
C10T										
C25P	0.27	-0.19	1040	458	112	47	1121	188	409	292
C25T										
C50P	0.27	-0.19	1041	445	96	52	1115	188	402	280
C50T										
C100P	0.27	-0.19	1032	439	91	43	1112	185	390	273
C100T										
C250P	0.26	-0.19	1027	416	69	37	1107	181	377	268
C250T										
C500P	0.27	-0.19	1022	433	71	32	1109	181	391	284
C500T	0.28	-0.19	1022	475	98	40	1101	191	450	321
C750P	0.44	-0.28	1140	1127	875	211	1170	331	1277	931
C750T	0.44	-0.28	1138	1131	884	202	1175	328	1274	938
C1000P	0.44	-0.28	1126	1122	877	182	1151	311	1271	931
C1000T	0.44	-0.28	1121	1123	878	188	1149	314	1265	920
ECR	0.31	-0.22	1005	428	172	42	1124	186	490	259
E140L	0.47	-0.30	1087	1061	901	174	1151	309	1286	852
E140C	0.49	-0.31	1105	1152	1012	188	1143	322	1394	916
E140U	0.43	-0.29	1099	776	658	200	1206	274	991	736
E140R	0.36	-0.26	991	451	295	46	1125	193	611	259

Table 5.7. VDS, HDS and Circumferential Wall Strain Laboratory Test Data for Pipe A
(PP TW AC) in Gravel Surround.

PHASE	VDS(%)	HDS(%)	$\epsilon_0(\mu\epsilon)$	$\epsilon_{45}(\mu\epsilon)$	$\epsilon_{90}(\mu\epsilon)$	$\epsilon_{135}(\mu\epsilon)$	$\epsilon_{180}(\mu\epsilon)$	$\epsilon_{225}(\mu\epsilon)$	$\epsilon_{270}(\mu\epsilon)$	$\epsilon_{315}(\mu\epsilon)$
SI	0.00	0.00	0	0	0	0	0	0	0	0
EI	0.23	0.01	93	326	697	369	-340	455	709	1320
E70L	0.73	-0.35	66	1078	1882	760	-1114	-61	2006	2576
E70C	0.77	-0.39	1710	1197	2054	831	-1067	-189	2191	2742
E70U	0.66	-0.33	1619	773	1484	681	-1093	44	1537	2267
E70R	0.65	-0.33	1625	725	1427	649	-1125	52	1481	2214
C1P	0.75	-0.39	1670	1046	1821	754	-1126	207	1938	2599
C1T	0.69	-0.36	1619	786	1485	678	-1100	89	1558	2293
C2P	0.81	-0.42	1665	1170	1984	811	-1120	285	2108	2748
C2T	0.72	-0.38	1589	846	1561	705	-1105	121	1643	2364
C5P	0.84	-0.44	1617	1232	2040	837	-1127	312	2172	2853
C5T	0.77	-0.41	1547	915	1639	736	-1103	164	1723	2472
C10P	0.88	-0.47	1559	1273	2090	849	-1120	337	2236	2926
C10T	0.81	-0.44	1508	973	1710	764	-1090	195	1827	2579
C25P	0.91	-0.50	1507	1330	2140	878	-1152	349	2323	3047
C25T	0.84	-0.46	1473	1039	1780	796	-1124	233	1916	2717
C50P	0.97	-0.53	1455	1431	2225	928	-796	462	2388	1153
C50T										
C100P	1.01	-0.56	1427	1507	2282	980	-820	509	2576	1539
C100T										
C320P	1.07	-0.60	1373	1628	2358	1025	-873	568	2804	2083
C320T	1.04	-0.59	1361	1542	2243	1001	-867	530	2679	1987
C630P	1.07	-0.60	1395	1556	2278	1045	-1007	583	2731	2197
C630T	1.10	-0.61	1390	1681	2436	1066	-1025	632	2897	2338
C750P										
C750T	1.07	-0.60	1398	1521	2249	1038	-983	581	2701	2223
C1000P	1.13	-0.63	1368	1731	2519	1083	-1102	679	2993	2548
C1000T	1.10	-0.62	1364	1600	2347	1050	-1091	629	2815	2403
ECR	1.02	-0.59	1276	1254	1966	947	-1117	481	2379	2062
E140L	1.34	-0.76	1528	2101	3181	1437	-414	1511	3576	2909
E140C	1.39	-0.78	1693	2265	3392	1542	172	1673	3832	3073
E140U	1.19	-0.69	1382	1447	2383	1222	106	1271	2678	2255
E140R	1.16	-0.69	1294	1276	2214	1169	-451	1266	2540	2084

Table 5.8. VDS, HDS and Circumferential Wall Strain Laboratory Test Data for Pipe B (HDPE TW AC) in Lightly Compacted Sand Surround.

PHASE	VDS(%)	HDS(%)	$\epsilon_0(\mu\epsilon)$	$\epsilon_{45}(\mu\epsilon)$	$\epsilon_{90}(\mu\epsilon)$	$\epsilon_{135}(\mu\epsilon)$	$\epsilon_{180}(\mu\epsilon)$	$\epsilon_{225}(\mu\epsilon)$	$\epsilon_{270}(\mu\epsilon)$	$\epsilon_{315}(\mu\epsilon)$
SI	0.00	0.00	0	0	0	0	0	0	0	0
EI	0.16	-0.11	392	822	2116	902	800	1065	1788	1366
E70L	1.30	-1.04	-978	2481	5736	1658	531	2002	4700	3702
E70C	1.54	-1.15	-594	3254	6909	2152	901	2665	5652	4710
E70U	1.42	-1.09	-717	2689	6042	1927	818	2453	4915	4012
E70R	1.39	-1.09	-936	2401	5729	1725	658	2229	4600	3685
C1P	1.60	-1.21	-796	3294	7022	2063	864	2612	5727	4749
C1T	1.48	-1.16	-940	2705	6122	1861	764	2403	4980	4052
C2P	1.69	-1.28	-912	3484	7308	2109	894	2695	5964	4995
C2T	1.57	-1.23	-1080	2897	6418	1894	763	2468	5217	4293
C5P	1.82	-1.40	-1230	3626	7585	2082	800	2702	6175	5182
C5T	1.71	-1.35	-1381	3098	6816	1889	672	2527	5519	4559
C10P	1.95	-1.53	-1568	3727	7848	2052	677	2701	6377	5325
C10T	1.87	-1.49	-1707	3283	7203	1880	567	2536	5824	4789
C25P	2.17	-1.73	-2118	3836	8190	1970	438	2668	6639	5467
C25T	2.11	-1.71	-2222	3542	7778	1848	361	2558	6286	5133
C50P	2.35	-1.90	-2567	3947	8498	1900	269	2650	6876	5614
C50T	2.35	-1.90	-2637	3904	8435	1855	227	2607	6821	5561
C100P	2.52	-2.07	-2973	4007	8690	1801	156	2620	6992	5718
C100T	2.60	-2.11	-3038	4358	9180	1864	128	2677	7411	6119
C250P	2.80	-2.27	-3422	4655	9621	1807	56	2680	7773	6472
C250T	2.75	-2.26	-3431	4340	9179	1734	73	2619	7352	6090
C500P	3.03	-2.45	-3699	5124	10222	1836	121	2803	8202	7018
C500T	3.00	-2.44	-3659	4940	9950	1826	141	2780	7968	6797
C750P	3.12	-2.52	-3747	5388	10459	1882	195	2870	8439	7310
C750T	3.10	-2.51	-3711	5292	10326	1875	217	2866	8277	7199
C1000P	3.18	-2.55	-3739	5546	10676	1934	240	2951	8597	7475
C1000T	3.17	-2.55	-3780	5460	10550	1901	236	2911	8485	7375
ECR	3.09	-2.53	-3811	4947	9923	1761	197	2778	7940	6764
E140L	3.58	-2.80	-3508	6573	12842	2448	864	3733	10469	8664
E140C	3.73	-2.83	-3005	7239	13976	2949	1241	4339	11528	7075
E140U	3.51	-2.72	-3193	6152	12242	2618	1086	4015	10026	6306
E140R	3.46	-2.74	-3337	5780	11697	2380	983	3841	9579	6217

Table 5.9. VDS, HDS and Circumferential Wall Strain Laboratory Test Data for Pipe B (HDPE TW AC) in Heavily Compacted Sand Surround.

PHASE	VDS(%)	HDS(%)	$\epsilon_0(\mu\epsilon)$	$\epsilon_{45}(\mu\epsilon)$	$\epsilon_{90}(\mu\epsilon)$	$\epsilon_{135}(\mu\epsilon)$	$\epsilon_{180}(\mu\epsilon)$	$\epsilon_{225}(\mu\epsilon)$	$\epsilon_{270}(\mu\epsilon)$	$\epsilon_{315}(\mu\epsilon)$
SI	0.00	0.00	0	0	0	0	0	0	0	0
EI	-0.35	-1.14	1378	948	-85	313	1397	384	-273	1045
E70L	-0.27	-0.11	1495	1422	373	409	1529	560	244	1427
E70C	-0.25	-0.11	1496	1551	532	386	1528	543	385	1547
E70U	-0.29	-0.11	1490	1206	198	347	1526	478	35	1284
E70R	-0.29	-0.11	1496	1199	189	347	1529	480	32	1286
C1P	-0.23	-0.11	1505	1631	615	381	1528	558	484	1631
C1T	-0.28	-0.11	1521	1240	217	356	1548	493	69	1323
C2P	-0.28	-0.11	1524	1229	217	363	1548	495	71	1318
C2T	-0.28	-0.10	1518	1234	220	362	1550	491	73	1327
C5P	-0.25	-0.10	1495	1503	463	369	1526	532	336	1533
C5T	-0.28	-0.10	1513	1270	244	360	1541	500	103	1350
C10P	-0.23	-0.10	1505	1609	542	375	1525	547	411	1624
C10T	-0.28	-0.10	1534	1287	229	360	1546	503	99	1358
C25P	-0.23	-0.10	1519	1660	548	378	1525	559	432	1669
C25T	-0.27	-0.10	1544	1330	223	358	1556	505	98	1392
C50P	-0.22	-0.10	1529	1725	568	380	1536	564	450	1729
C50T	-0.27	-0.10	1554	1377	227	356	1559	516	110	1423
C100P	-0.21	-0.10	1534	1798	586	376	1543	587	473	1796
C100T	-0.26	-0.10	1558	1441	228	346	1569	540	127	1479
C250P	-0.20	-0.10	1530	1866	594	371	1554	605	495	1859
C250T	-0.24	-0.10	1559	1565	285	343	1579	562	186	1585
C500P	-0.19	-0.09	1567	1915	580	393	1585	670	496	1907
C500T	-0.22	-0.09	1562	1762	420	376	1594	645	338	1774
C750P	-0.17	-0.08	1571	2044	706	416	1606	705	626	2035
C750T	-0.23	-0.08	1607	1689	333	384	1630	655	265	1710
C1000P	-0.19	-0.07	1588	1948	579	400	1629	709	505	1959
C1000T	-0.19	-0.07	1579	1932	561	399	1625	709	482	1936
ECR	-0.22	-0.07	1676	1748	334	422	1710	769	308	1770
E140L	-0.07	-0.10	1857	2519	1332	638	1904	1071	1294	2512
E140C	-0.04	-0.09	1946	2761	1623	723	1985	1162	1599	2732
E140U	-0.15	-0.06	1892	2017	769	631	1989	1014	775	2064
E140R	-0.17	0.10	1875	1834	581	622	1973	939	586	1906

Table 5.10. VDS, HDS and Circumferential Wall Strain Laboratory Test Data for Pipe B (HDPE TW AC) in Gravel Surround.

PHASE	VDS(%)	HDS(%)	$\epsilon_0(\mu\epsilon)$	$\epsilon_{45}(\mu\epsilon)$	$\epsilon_{90}(\mu\epsilon)$	$\epsilon_{135}(\mu\epsilon)$	$\epsilon_{180}(\mu\epsilon)$	$\epsilon_{225}(\mu\epsilon)$	$\epsilon_{270}(\mu\epsilon)$	$\epsilon_{315}(\mu\epsilon)$
SI	0.00	0.00	0	0	0	0	0	0	0	0
EI	0.28	-0.14	111	695	690	651	-411	523	785	720
E70L	0.84	-0.48	-13	1925	2050	1569	-1193	1322	2297	1946
E70C	0.92	-0.49	317	2267	2454	1666	-1039	1577	2712	2297
E70U	0.82	-0.46	131	1655	1741	1517	-1073	1427	2054	1745
E70R	0.81	-0.46	80	1576	1700	1481	-1099	1393	1977	1677
C1P	0.92	-0.51	143	2098	2163	1614	-1135	1525	2506	2164
C1T	0.92	-0.51	162	2011	2061	1627	-1117	1541	2400	2081
C2P	0.99	-0.54	144	2308	2346	1690	-1172	1609	2716	2370
C2T	0.91	-0.51	44	1865	1928	1602	-1172	1513	2242	1967
C5P	1.02	-0.56	74	2398	2387	1714	-1236	1646	2763	2455
C5T	0.95	-0.53	9	1963	1982	1639	-1217	1568	2316	2061
C10P	1.07	-0.59	16	2514	2477	1759	-1296	1711	2854	2574
C10T	1.01	-0.57	-32	2093	2096	1692	-1275	1643	2432	2201
C25P	1.11	-0.62	-32	2595	2532	1801	-1359	1757	2920	2678
C25T	1.05	-0.59	-67	2216	2177	1733	-1313	1694	2523	2324
C50P	1.17	-0.65	-89	2754	2608	1836	-1417	1816	3008	2840
C50T										
C100P	1.22	-0.67	-96	2910	2626	1881	-1448	1879	3116	3016
C100T										
C250P	1.28	-0.69	-70	3156	2715	1929	-1446	1951	3259	3221
C250T	1.24	-0.68	-75	2922	2496	1888	-1423	1926	2997	3005
C500P	1.29	-0.70	-43	3262	2774	1965	-1435	1995	3323	3310
C500T										
C750P	1.31	-0.71	-9	3361	2848	2029	-1427	2031	3386	3392
C750T	1.28	-0.69	-7	3151	2648	1984	-1392	1997	3151	3191
C1000P	1.34	-0.72	9	3475	2895	2019	-1410	2076	3475	3486
C1000T	1.24	-0.68	-86	2910	2422	1979	-1336	1979	2897	2917
ECR	1.23	-0.68	-121	2815	2350	1930	-1345	1968	2819	2829
E140L	1.63	-0.88	221	4257	3919	2525	-1478	2677	4642	4163
E140C	1.69	-0.88	454	4472	4211	2760	-1343	2858	4967	4417
E140U	1.60	-0.87	95	3549	3392	2687	-1433	2728	3997	3573
E140R	1.59	-0.88	8	3379	3264	2635	-1466	2680	3802	3403

Table 5.11. VDS, HDS and Circumferential Wall Strain Laboratory Test Data for Pipe C (HDPE TW HW) in Lightly Compacted Sand Surround.

PHASE	VDS(%)	HDS(%)	$\epsilon_0(\mu\epsilon)$	$\epsilon_{45}(\mu\epsilon)$	$\epsilon_{90}(\mu\epsilon)$	$\epsilon_{135}(\mu\epsilon)$	$\epsilon_{180}(\mu\epsilon)$	$\epsilon_{225}(\mu\epsilon)$	$\epsilon_{270}(\mu\epsilon)$	$\epsilon_{315}(\mu\epsilon)$
SI	0.00	0.00	0	0	0	0	0	0	0	0
EI	0.03	0.08	566	666	663	381	374	319	616	947
E70L	1.16	-0.93	-479	2227	4116	852	-469	901	3332	3197
E70C	1.37	-0.98	125	3283	5651	1137	157	1344	4459	4529
E70U	1.27	-0.93	41	2855	4921	1067	96	1274	3804	3988
E70R	1.25	-0.93	-2	2769	4786	1051	59	1274	3693	3871
C1P	1.48	-1.06	21	3547	6022	1138	179	1389	4773	4813
C1T	1.35	-0.99	-116	2991	5103	1069	44	1322	3959	4122
C2P	1.57	-1.12	-90	3695	6265	1151	127	1419	4979	5006
C2T	1.44	-1.06	-233	3144	5358	1077	-1	1343	4164	4302
C5P	1.70	-1.22	-372	3815	6499	1148	-40	1448	5147	5141
C5T	1.58	-1.17	-493	3315	5695	1084	-128	1386	4431	4502
C10P	1.85	-1.34	-667	3939	6782	1145	-181	1473	5368	5296
C10T	1.72	-1.28	-720	3482	6019	1092	-236	1407	4692	4714
C25P	2.07	-1.53	-1132	4088	7148	1138	-440	1498	5656	5478
C25T	2.01	-1.50	-1219	3830	6715	1095	-486	1470	5246	5145
C50P	2.25	-1.68	-1521	4202	7393	1108	-591	1525	5807	5618
C50T	2.24	-1.67	-1573	4125	7260	1090	-629	1490	5707	5516
C100P	2.58	-1.93	-2075	4588	8154	1075	-814	1544	6426	6104
C100T	2.53	-1.91	-2105	4297	7686	1051	-835	1520	6010	5740
C250P	2.86	-2.13	-2485	4950	8767	1034	-927	1559	6925	6589
C250T	2.80	-2.11	-2478	4706	8351	1011	-894	1533	6528	6271
C500P	3.03	-2.24	-2579	5311	9222	993	-838	1548	7226	7091
C500T	3.00	-2.22	-2563	5188	9012	979	-814	1552	7006	6938
C750P	3.12	-2.28	-2622	5487	9426	986	-775	1564	7333	7374
C750T	3.10	-2.27	-2595	5431	9321	990	-762	1581	7239	7295
C1000P	3.16	-2.31	-2692	5582	9472	960	-747	1568	7321	7493
C1000T	3.15	-2.31	-2720	5545	9402	951	-765	1543	7281	7439
ECR	3.06	-2.27	-2700	5190	8888	984	-736	1593	6832	6920
E140L	3.50	-2.50	-2471	6380	11520	1121	-343	1742	9293	8626
E140C	3.68	-2.52	-1903	6325	13392	1238	146	1942	10989	9750
E140U	3.41	-2.41	-2155	5539	11348	1053	-52	1783	9082	8357
E140R	3.34	-2.44	-2320	5432	10537	943	-58	1630	8251	7814

Table 5.12. VDS, HDS and Circumferential Wall Strain Laboratory Test Data for Pipe C (HDPE TW HW) in Heavily Compacted Sand Surround.

PHASE	VDS(%)	HDS(%)	$\epsilon_0(\mu\epsilon)$	$\epsilon_{45}(\mu\epsilon)$	$\epsilon_{90}(\mu\epsilon)$	$\epsilon_{135}(\mu\epsilon)$	$\epsilon_{180}(\mu\epsilon)$	$\epsilon_{225}(\mu\epsilon)$	$\epsilon_{270}(\mu\epsilon)$	$\epsilon_{315}(\mu\epsilon)$
SI	0.00	0.00	0	0	0	0	0	0	0	0
EI	0.22	0.58	1493	1066	102	84	1478	270	108	761
E70L	0.39	0.19	1584	1843	1076	288	1642	331	1095	1551
E70C	0.44	0.10	1721	2238	1530	361	1706	349	1516	1910
E70U	0.36	0.20	1753	1816	1023	303	1739	331	1013	1492
E70R	0.36	0.20	1755	1810	1012	301	1742	331	1000	1486
C1P	0.43	0.18	1737	2204	1445	349	1726	361	1430	1862
C1T	0.37	0.20	1763	1836	1026	304	1758	347	1028	1503
C2P	0.44	0.17	1754	2296	1550	370	1728	355	1546	1963
C2T	0.37	0.20	1775	1885	1077	312	1765	337	1073	1569
C5P	0.45	0.17	1772	2378	1583	372	1734	363	1554	2031
C5T	0.39	0.19	1787	1997	1155	320	1765	350	1139	1655
C10P	0.46	0.16	1792	2410	1582	381	1743	352	1561	2071
C10T	0.40	0.19	1803	2049	1170	333	1777	350	1145	1714
C25P	0.47	0.16	1804	2495	1589	389	1762	365	1558	2126
C25T	0.45	0.17	1793	2334	1409	361	1772	352	1369	1977
C50P	0.49	0.15	1787	2556	1605	396	1773	337	1558	2206
C50T	0.47	0.16	1828	2456	1482	386	1797	337	1443	2111
C100P	0.53	0.13	1788	2795	1782	422	1774	352	1717	2421
C100T	0.47	0.16	1833	2387	1336	371	1822	335	1281	2033
C250P	0.58	0.11	1771	3047	1929	451	1797	358	1863	2637
C250T	0.50	0.14	1818	2592	1427	399	1842	337	1362	2219
C500P	0.61	0.10	1777	3256	2038	500	1819	388	1956	2838
C500T	0.54	0.13	1827	2824	1564	445	1866	379	1508	2421
C750P	0.62	0.09	1799	3339	2057	534	1853	422	1987	2902
C750T	0.57	0.11	1848	3075	1746	501	1892	402	1683	2672
C1000P	0.62	0.09	1813	3341	2008	559	1871	446	1940	2925
C1000T	0.61	0.10	1844	3316	1965	561	1895	443	1910	2899
ECR	0.57	0.11	1856	3032	1689	526	1906	420	1622	2633
E140L	0.81	0.00	1924	4193	3313	803	2038	561	3300	3704
E140C	0.86	-0.01	2065	4638	3840	965	2132	666	3822	4108
E140U	0.71	0.06	2068	3791	2775	818	2161	601	2749	3316
E140R	0.68	0.06	2035	3520	2385	738	2139	544	2352	3055

Table 5.13. VDS, HDS and Circumferential Wall Strain Laboratory Test Data for Pipe C (HDPE TW HW) in Gravel Surround.

PHASE	VDS(%)	HDS(%)	$\epsilon_0(\mu\epsilon)$	$\epsilon_{45}(\mu\epsilon)$	$\epsilon_{90}(\mu\epsilon)$	$\epsilon_{135}(\mu\epsilon)$	$\epsilon_{180}(\mu\epsilon)$	$\epsilon_{225}(\mu\epsilon)$	$\epsilon_{270}(\mu\epsilon)$	$\epsilon_{315}(\mu\epsilon)$
SI	0.00	0.00	0	0	0	0	0	0	0	0
EI	0.19	-0.10	223	778	825	452	-67	346	8528*	463
E70L	0.59	-0.35	275	2317	2356	966	27	742	10073	1664
E70C	0.65	-0.35	556	2831	2832	1201	174	868	10646	2087
E70U	0.57	-0.32	464	2350	2299	1080	201	817	10073	1670
E70R	0.57	-0.32	430	2275	2194	1054	188	804	9910	1579
C1P	0.69	-0.37	501	2951	2811	1259	135	912	10581	2130
C1T	0.60	-0.34	407	2449	2255	1125	184	834	10006	1690
C2P	0.71	-0.38	478	3040	2848	1272	141	931	10626	2192
C2T	0.62	-0.35	395	2539	2310	1153	174	854	10063	1757
C5P	0.74	-0.40	431	3208	2919	1332	98	965	10723	2300
C5T	0.67	-0.37	365	2712	2418	1211	143	917	10181	1878
C10P	0.78	-0.42	366	3371	2968	1358	76	980	10774	2422
C10T	0.71	-0.39	321	2900	2504	1258	132	939	10264	2023
C25P	0.82	-0.44	318	3533	3035	1389	44	1012	10857	2537
C25T	0.75	-0.41	289	3077	2583	1305	118	970	10355	2151
C50P	0.88	-0.47	262	3797	3117	1448	16	1076	10938	2747
C50T										
C100P	0.93	-0.49	260	4112	3212	1498	21	1102	11068	2958
C100T										
C250P	1.00	-0.52	298	4575	3394	1582	-10	1166	11271	3268
C250T	0.95	-0.50	304	4282	3087	1530	37	1130	10967	3009
C500P	1.02	-0.53	316	4771	3471	1657	7	1230	11621	3374
C500T										
C750P	1.04	-0.53	350	4884	3561	1700	59	1340	11490	3518
C750T	0.99	-0.52	366	4604	3269	1659	124	1312	11184	3278
C1000P	1.06	-0.54	395	5046	3651	1744	79	1362	11600	3615
C1000T	1.02	-0.52	424	4768	3386	1702	153	1346	11279	3389
ECR	1.00	-0.52	433	4616	3240	1698	171	1382	11161	3281
E140L	1.31	-0.68	752	6039	5004	2314	363	1697	13049	4452
E140C	1.38	-0.69	934	6375	5461	2471	386	1739	13074	4655
E140U	1.17	-0.62	582	5029	4015	2157	391	1589	11477	3539
E140R	1.16	-0.63	530	4866	3835	2108	393	1570	11259	3387

* - High strain due to broken connection to strain gauge. If ϵ_{270} is corrected to $800\mu\epsilon$ at the end of the installation phase (approximately the value of ϵ_{90} at this stage), the strains at 270° become similar to those recorded at 90° , viz:

$$(\epsilon_{270}) = (\epsilon_{90}) - 8528 + 800$$

EI becomes $800\mu\epsilon$ (to approximate ϵ_{270})

E70L becomes $2345\mu\epsilon$ (compare $2317\mu\epsilon$ at 90°)

E70C becomes $2918\mu\epsilon$ (compare $2831\mu\epsilon$ at 90°)

E70U becomes $2345\mu\epsilon$ (compare $2350\mu\epsilon$ at 90°)

E70R becomes $2182\mu\epsilon$ (compare $2275\mu\epsilon$ at 90°)

C1000P becomes $3872\mu\epsilon$ (compare $3651\mu\epsilon$ at 90°)

C1000T becomes $3551\mu\epsilon$ (compare $3386\mu\epsilon$ at 90°)

E140L becomes $5321\mu\epsilon$ (compare $5004\mu\epsilon$ at 90°)

E140C becomes $5346\mu\epsilon$ (compare $5461\mu\epsilon$ at 90°)

E140U becomes $3749\mu\epsilon$ (compare $4015\mu\epsilon$ at 90°)

E140R becomes $3531\mu\epsilon$ (compare $3835\mu\epsilon$ at 90°)

**Table 5.14. VDS, HDS and Circumferential Wall Strain Laboratory Test Data for Pipe D
(PP TW AC) in Lightly Compacted Sand Surround.**

PHASE	VDS(%)	HDS(%)	$\epsilon_0(\mu\epsilon)$	$\epsilon_{45}(\mu\epsilon)$	$\epsilon_{90}(\mu\epsilon)$	$\epsilon_{135}(\mu\epsilon)$	$\epsilon_{180}(\mu\epsilon)$	$\epsilon_{225}(\mu\epsilon)$	$\epsilon_{270}(\mu\epsilon)$	$\epsilon_{315}(\mu\epsilon)$
SI	0.00	0.00	0	0	0	0	0	0	0	0
EI	0.16	-0.05	232	459	587	178	2811	305	537	639
E70L	0.73	-0.44	-14	1495	2183	642	2348	763	2010	2214
E70C	0.93	-0.54	199	1976	2829	915	2507	1002	2635	2939
E70U	0.76	-0.48	-115	1272	1938	562	2336	764	1706	1968
E70R	0.73	-0.48	-175	1138	1835	618	2213	693	1563	1762
C1P	0.89	-0.56	-8	1723	2530	864	2204	891	2309	2558
C1T	0.79	-0.53	-210	1274	1949	652	2169	756	1686	1933
C2P	0.95	-0.60	-36	1875	2662	908	2151	945	2456	2745
C2T	0.86	-0.58	-245	1402	2069	695	2092	797	1820	2085
C5P	1.10	-0.75	-254	2058	2905	950	1845	1013	2666	2988
C5T	0.97	-0.70	-484	1489	2209	700	1800	820	1924	2195
C10P	1.15	-0.79	-347	2092	2958	940	1753	1020	2704	3025
C10T	1.03	-0.75	-565	1578	2332	712	1729	855	2042	2325
C25P	1.32	-0.95	-583	2271	3221	962	1534	1081	2942	3271
C25T	1.28	-0.93	-662	2091	2986	878	1524	1022	2694	3025
C50P	1.42	-1.03	-744	2373	3362	967	1485	1106	3060	3422
C50T	1.35	-1.01	-854	2058	2959	814	1483	1009	2630	3003
C100P	1.49	-1.10	-900	2373	3348	920	1660	1096	3007	3428
C100T	1.48	-1.10	-948	2319	3290	879	1648	1087	2941	3364
C250P	1.64	-1.23	-1286	2533	3547	818	1931	1136	3114	3633
C250T	1.63	-1.23	-1309	2436	3406	774	1929	1109	2964	3482
C500P	1.76	-1.33	-1459	2626	3632	796	1798	1154	3144	3762
C500T	1.76	-1.33	-1484	2609	3618	793	1781	1139	3124	3732
C750P	1.82	-1.37	-1472	2759	3780	840	1760	1195	3282	3949
C750T	1.80	-1.36	-1497	2641	3623	799	1762	1151	3126	3773
C1000P	1.89	-1.41	-1543	2946	4008	791	2180	1220	3469	4198
C1000T	1.84	-1.39	-1574	2703	3680	706	2210	1160	3146	3864
ECR	1.72	-1.37	-1893	2075	3157	504	2809	1010	2600	3087
E140L	2.14	-1.56	-1381	3501	4991	1161	2808	1520	4585	4950
E140C	2.30	-1.62	-880	4021	5760	1541	2904	1765	5466	5737
E140U	2.00	-1.52	-1533	2685	4116	917	2738	1342	3673	3947
E140R	1.96	-1.53	-1809	2359	3760	720	2700	1219	3304	3507

Table 5.15. VDS, HDS and Circumferential Wall Strain Laboratory Test Data for Pipe D (PP TW AC) in Heavily Compacted Sand Surround.

PHASE	VDS(%)	HDS(%)	$\epsilon_0(\mu\epsilon)$	$\epsilon_{45}(\mu\epsilon)$	$\epsilon_{90}(\mu\epsilon)$	$\epsilon_{135}(\mu\epsilon)$	$\epsilon_{180}(\mu\epsilon)$	$\epsilon_{225}(\mu\epsilon)$	$\epsilon_{270}(\mu\epsilon)$	$\epsilon_{315}(\mu\epsilon)$
SI	0.00	0.00	0	0	0	0	0	0	0	0
EI	0.21	0.61	1011	654	-299	-719	908	416	-203	663
E70L	0.29	0.57	1040	907	60	-1625	994	518	119	990
E70C	0.30	0.57	1047	945	119	-1939	972	541	177	1019
E70U	0.26	0.58	1065	750	-130	-1986	985	507	-61	782
E70R	0.25	0.58	1053	719	-188	-2022	968	492	-107	734
C1P	0.27	0.58	1030	800	-73	-2009	965	505	0	831
C1T	0.26	0.58	1074	717	-180	-2011	983	517	-105	726
C2P	0.31	0.56	1057	944	102	-1949	957	539	203	1001
C2T	0.26	0.58	1078	724	-175	-2003	982	506	-89	742
C5P	0.31	0.56	1071	960	117	-1924	951	559	205	1010
C5T	0.26	0.58	1085	738	-165	-1998	979	511	-73	750
C10P	0.31	0.55	1066	969	124	-1945	965	549	200	1032
C10T	0.27	0.58	1097	750	-156	-1987	978	522	-68	758
C25P	0.32	0.55	1071	988	118	-1940	951	549	219	1044
C25T	0.27	0.57	1093	766	-147	-2004	986	522	-69	781
C50P	0.31	0.56	1069	964	60	-1978	964	549	170	1022
C50T	0.28	0.57	1069	807	-121	-2037	990	530	-27	831
C100P	0.32	0.55	1085	978	96	-2021	984	558	176	1041
C100T	0.28	0.57	1112	826	-92	-2062	1011	537	-15	859
C250P	0.33	0.54	1095	1034	163	-2000	1017	571	238	1114
C250T	0.29	0.56	1122	830	-102	-2049	1041	535	-13	864
C500P	0.34	0.54	1077	1033	133	-1897	959	588	230	1097
C500T	0.30	0.56	1100	858	-87	-1947	996	548	12	896
C750P	0.32	0.55	1109	980	73	-1888	941	575	149	1036
C750T	0.32	0.55	1126	951	31	-1877	957	570	116	986
C1000P	0.35	0.53	1092	1092	224	-1867	957	610	306	1173
C1000T	0.30	0.55	1122	875	-53	-1932	996	568	30	905
ECR	0.30	0.55	1113	857	-91	-1993	979	554	-6	872
E140L	0.26	0.58	1143	639	-370	-2050	1007	521	-287	597
E140C	0.42	0.49	1239	1179	441	-1803	1020	726	612	1292
E140U	0.32	0.54	1224	737	-152	-1970	1037	641	-25	742
E140R	0.30	0.54	1183	668	-282	-2069	1054	616	-130	633

**Table 5.16. VDS, HDS and Circumferential Wall Strain Laboratory Test Data for Pipe D
(PP TW AC) in Gravel Surround.**

PHASE	VDS(%)	HDS(%)	$\epsilon_0(\mu\epsilon)$	$\epsilon_{45}(\mu\epsilon)$	$\epsilon_{90}(\mu\epsilon)$	$\epsilon_{135}(\mu\epsilon)$	$\epsilon_{180}(\mu\epsilon)$	$\epsilon_{225}(\mu\epsilon)$	$\epsilon_{270}(\mu\epsilon)$	$\epsilon_{315}(\mu\epsilon)$
SI	0.00	0.00	0	0	0	0	0	0	0	0
EI	0.26	-0.11	250	750	686	552	-299	473	4	466
E70L	0.80	-0.44	78	1794	1954	1252	-668	937	1449	1530
E70C	0.88	-0.47	220	2060	2273	1407	-547	1094	1131	1909
E70U	0.76	-0.44	-9	1506	1637	1187	-593	941	514	1223
E70R	0.75	-0.44	-60	1433	1548	1154	-612	916	415	1126
C1P	0.91	-0.51	72	2041	2171	1424	-622	1067	1088	1801
C1T	0.80	-0.47	-93	1548	1635	1235	-628	952	517	1232
C2P	0.93	-0.52	38	2099	2212	1452	-645	1080	1135	1863
C2T	0.83	-0.49	-117	1607	1681	1270	-628	958	573	1293
C5P	0.98	-0.56	-38	2187	2272	1491	-692	1103	1183	1968
C5T	0.88	-0.53	-171	1714	1765	1321	-682	997	678	1396
C10P	1.02	-0.60	-115	2255	2320	1521	-755	1118	1261	2011
C10T	0.93	-0.57	-228	1812	1852	1368	-731	1018	775	1508
C19P	1.07	-0.63	-187	2331	2392	1545	-797	1138	1314	2114
C19T	0.99	-0.60	-280	1926	1946	1415	-751	1049	868	1626
C50P	1.13	-0.67	-287	2448	2466	1597	-877	1161	1407	2234
C50T										
C100P	1.19	-0.70	-343	2572	2545	1634	-895	1185	1484	2370
C100T										
C250P	1.24	-0.73	-372	2711	2628	1681	-938	1229	1559	2511
C250T										
C321P	1.25	-0.74	-380	2742	2641	1695	-940	1232	1598	2549
C321T	1.20	-0.72	-399	2472	2343	1616	-896	1190	1290	2238
C630P	1.29	-0.76	-388	2842	2716	1743	-937	1268	1672	2675
C630T	1.24	-0.74	-399	2595	2435	1670	-886	1215	1388	2383
C1000P	1.32	-0.77	-374	2919	2787	1774	-925	1272	1748	2773
C1000T	1.28	-0.76	-392	2734	2574	1719	-877	1238	1519	2552
ECR	1.21	-0.74	-527	2297	2199	1613	-862	1148	1139	2051
E140L	1.57	-0.90	-154	3452	3574	2304	-833	1646	2611	3398
E140C	1.63	-0.91	-11	3641	3815	2440	-718	1778	2846	3645
E140U	1.44	-0.85	-363	2752	2847	2092	-742	1577	1850	2547
E140R	1.42	-0.86	-465	2613	2694	2029	-782	1536	1705	2359

Table 5.17. VDS, HDS and Circumferential Wall Strain Laboratory Test Data for Pipe E (PVC-U SW SP) in Lightly Compacted Sand Surround.

PHASE	VDS(%)	HDS(%)	$\epsilon_0(\mu\epsilon)$	$\epsilon_{45}(\mu\epsilon)$	$\epsilon_{90}(\mu\epsilon)$	$\epsilon_{135}(\mu\epsilon)$	$\epsilon_{180}(\mu\epsilon)$	$\epsilon_{225}(\mu\epsilon)$	$\epsilon_{270}(\mu\epsilon)$	$\epsilon_{315}(\mu\epsilon)$
SI	0.00	0.00	0	0	0	0	0	0	0	0
EI	-0.11	0.00	39	173	-49	-105	3025	-450	29	145
E70L	1.03	-0.97	-827	1069	771	41	3201	-197	1224	741
E70C	1.23	-1.14	-1059	1188	874	77	2588	-115	1359	826
E70U	1.10	-1.03	-1176	822	535	1	2443	-309	926	568
E70R	1.08	-1.01	-1196	751	498	-18	2107	-362	876	519
C1P	1.95	-1.06	-1239	1075	730	34	2158	-222	572	736
C1T	1.99	-1.10	-1332	1019	681	52	2162	-171	650	694
C2P	2.01	-1.11	-1342	1066	711	45	2100	-211	596	739
C2T	1.98	-1.09	-1389	951	619	40	2095	-226	729	654
C5P	2.10	-1.18	-1445	1139	761	70	2025	-191	544	799
C5T	2.09	-1.18	-1492	1051	686	72	2031	-187	635	726
C10P	2.28	-1.33	-1584	1316	921	126	1956	-111	355	934
C10T	2.24	-1.30	-1624	1173	792	109	1957	-134	521	831
C25P	2.43	-1.46	-1774	1405	977	165	1821	-64	301	1018
C25T	2.39	-1.42	-1810	1245	836	146	1819	-91	469	900
C50P	2.59	-1.59	-1939	1533	1071	208	1711	-13	194	1128
C50T	2.52	-1.54	-1992	1300	876	181	1711	-61	427	952
C100P	2.71	-1.68	-2062	1604	1111	251	1641	23	151	1191
C100T	2.68	-1.67	-2127	1481	1006	231	1628	3	280	1105
C250P	2.91	-1.85	-2302	1708	1154	292	1743	64	110	1288
C250T	2.90	-1.84	-2335	1655	1113	287	1846	57	162	1247
C500P	3.05	-2.00	-2532	1825	1234	340	3129	111	18	1387
C500T	3.02	-1.98	-2563	1717	1147	328	3129	94	120	1299
C750P	3.18	-2.05	-2589	1887	1294	368	2714	143	-30	1449
C750T	3.12	-2.01	-2631	1690	1134	349	2703	107	157	1292
C1000P	3.18	-2.06	-2676	1826	1233	352	2663	131	17	1393
C1000T	3.13	-2.03	-2693	1659	1108	343	2675	103	175	1258
ECR	3.08	-2.03	-2784	1499	1076	327	2672	85	241	1159
E140L	3.46	-2.34	-2686	2286	1792	399	2884	292	1042	1771
E140C	3.61	-2.45	-2692	2393	2000	452	2552	341	1249	1851
E140U	3.34	-2.26	-2933	1569	1344	361	2447	133	491	1209
E140R	3.34	-2.25	-2945	1515	1293	322	3019	90	449	1158

Table 5.18. VDS, HDS and Circumferential Wall Strain Laboratory Test Data for Pipe E (PVC-U SW SP) in Heavily Compacted Sand Surround.

PHASE	VDS(%)	HDS(%)	$\epsilon_0(\mu\epsilon)$	$\epsilon_{45}(\mu\epsilon)$	$\epsilon_{90}(\mu\epsilon)$	$\epsilon_{135}(\mu\epsilon)$	$\epsilon_{180}(\mu\epsilon)$	$\epsilon_{225}(\mu\epsilon)$	$\epsilon_{270}(\mu\epsilon)$	$\epsilon_{315}(\mu\epsilon)$
SI	0.00	0.00	0	0	0	0	0	0	0	0
EI	-	-	143	-90	-812	-665	1587	-119	-387	218
E70L	0.04	-0.03	165	18	-711	-667	1604	-102	-282	319
E70C	0.04	-0.03	150	27	-711	-668	1622	-97	-269	320
E70U	0.01	0.00	143	-73	-803	-674	1619	-109	-367	235
E70R	0.00	0.00	141	-106	-830	-678	1616	-111	-385	208
C1P	-0.01	0.00	144	-111	-836	-682	1628	-104	-387	212
C1T	-0.05	0.03	126	-251	-711	-695	1642	-118	-514	92
C2P	-0.01	0.00	140	-110	-831	-681	1638	-106	-387	208
C2T	-0.05	0.03	122	-252	-710	-696	1640	-122	-519	90
C5P	-0.01	0.00	141	-108	-830	-683	1640	-109	-382	210
C5T	-0.05	0.03	123	-249	-710	-693	1651	-121	-518	87
C10P	-0.01	0.00	145	-103	-836	-675	1657	-106	-384	210
C10T	-0.05	0.03	124	-243	-710	-690	1656	-123	-509	89
C25P	-0.01	0.01	144	-129	-811	-683	1812	-104	-409	196
C25T	-0.04	0.03	126	-201	-742	-687	1821	-118	-474	128
C50P	-0.03	0.02	138	-170	-764	-687	2669	-112	-456	155
C50T	-0.02	0.01	134	-150	-790	-685	2697	-100	-428	179
C100P	0.00	0.00	134	-103	-829	-685	4011	-97	-390	215
C100T	-0.05	0.03	119	-239	-707	-696	4056	-112	-515	96
C250P	0.00	0.00	152	-85	-857	-650	3900	-96	-388	220
C250T	-0.04	0.03	132	-223	-730	-671	3913	-117	-514	102
C500P	0.01	0.00	141	-88	-843	-656	3835	-96	-385	219
C500T	-0.04	0.03	129	-221	-731	-666	3836	-109	-513	107
C750P	0.01	0.00	130	-102	-834	-654	3870	-82	-397	214
C750T	-0.03	0.02	121	-199	-740	-661	3880	-104	-499	116
C1000P	0.00	0.00	118	-117	-802	-667	7416	-94	-421	197
C1000T	-0.02	0.02	116	-176	-744	-670	7456	-100	-484	138
ECR	-0.03	0.02	107	-209	-724	-667	7470	-97	-510	114
E140L	0.07	-0.07	171	47	-428	-682	7610	-67	-207	335
E140C	0.08	-0.08	178	69	-396	-670	7646	-75	-186	335
E140U	-0.01	-0.01	107	-217	-665	-693	7601	-121	-471	102
E140R	-0.01	-0.01	105	-227	-677	-701	7581	-121	-472	97

Table 5.19. VDS, HDS and Circumferential Wall Strain Laboratory Test Data for Pipe E (PVC-U SW SP) in Gravel Surround.

PHASE	VDS(%)	HDS(%)	$\epsilon_0(\mu\epsilon)$	$\epsilon_{45}(\mu\epsilon)$	$\epsilon_{90}(\mu\epsilon)$	$\epsilon_{135}(\mu\epsilon)$	$\epsilon_{180}(\mu\epsilon)$	$\epsilon_{225}(\mu\epsilon)$	$\epsilon_{270}(\mu\epsilon)$	$\epsilon_{315}(\mu\epsilon)$
SI	0.00	0.00	0	0	0	0	0	0	0	0
EI	0.31	-0.24	-113	80	287	238	-429	240	333	80
E70L	0.83	-0.66	-441	369	879	330	-754	229	985	369
E70C	0.86	-0.70	-471	355	893	314	-754	220	1002	355
E70U	0.77	-0.63	-527	164	649	266	-750	185	748	164
E70R	0.76	-0.63	-527	145	625	268	-755	185	724	145
C1P	0.88	-0.72	-522	358	878	322	-807	211	988	358
C1T	0.80	-0.66	-571	168	643	275	-799	182	737	168
C2P	0.91	-0.74	-544	389	899	331	-832	214	994	389
C2T	0.83	-0.68	-596	199	664	283	-812	179	755	199
C5P	0.96	-0.77	-601	417	929	332	-881	213	1012	417
C5T	0.88	-0.72	-653	225	693	290	-865	180	786	225
C10P	1.01	-0.81	-669	436	946	331	-916	199	1037	436
C10T	0.93	-0.77	-713	253	731	296	-900	172	815	253
C19P	1.06	-0.85	-732	462	962	328	-936	193	1057	462
C19T	0.99	-0.81	-776	284	754	294	-912	166	850	284
C50P	1.13	-0.91	-814	500	991	326	-957	193	1093	500
C50T										
C110P	1.18	-0.96	-877	541	1028	326	-981	187	1117	541
C110T										
C260P	1.25	-1.02	-947	579	1061	328	-1010	176	1159	579
C260T										
C630P	1.26	-1.03	-957	587	1077	333	-1015	179	1167	587
C630T	1.21	-1.00	-981	454	923	315	-996	162	1016	454
C750P	1.30	-1.07	-992	610	1103	331	-1036	173	1194	610
C750T	1.26	-1.04	-1015	486	959	317	-1015	159	1051	486
C1000P	1.34	-1.10	-1016	647	1132	340	-1037	176	1222	647
C1000T	1.30	-1.08	-1033	558	1018	324	-1024	168	1112	558
ECR	1.25	-1.04	-1069	408	884	302	-1010	148	982	408
E140L	1.57	-1.23	-1011	780	1419	430	-1115	215	1544	780
E140C	1.60	-1.26	-1051	778	1447	431	-1130	207	1600	778
E140U	1.44	-1.16	-1204	374	1010	342	-1127	172	1135	374
E140R	1.43	-1.15	-1215	353	983	329	-1142	162	1115	353

Table 5.20. VDS, HDS and Circumferential Wall Strain Laboratory Test Data for Pipe B (HDPE TW AC) in Lightly Compacted Sand Surround in Low Friction Box.

PHASE	VDS(%)	HDS(%)	$\epsilon_0(\mu\epsilon)$	$\epsilon_{45}(\mu\epsilon)$	$\epsilon_{90}(\mu\epsilon)$	$\epsilon_{135}(\mu\epsilon)$	$\epsilon_{180}(\mu\epsilon)$	$\epsilon_{225}(\mu\epsilon)$	$\epsilon_{270}(\mu\epsilon)$	$\epsilon_{315}(\mu\epsilon)$
SI	0.00	0.00	0	0	0	0	0	0	0	0
EI	0.32	-0.30	-140	956	1719	3314	3348	-36	1482	956
E70L	1.42	-1.35	-1266	2912	6408	2507	4695	-489	5530	2912
E70C	1.65	-1.52	-844	3819	8035	2742	5518	-303	6826	3819
E70U	1.47	-1.42	-1191	2742	6403	2571	5060	-580	5366	2742
E70R	1.47	-1.42	-1429	2375	5802	2469	4771	-711	4904	2375
C1P	1.65	-1.55	-1436	3126	6848	2488	5056	-588	5842	2660
C1T	1.66	-1.57	-1437	3047	6819	2462	5202	-605	5755	2806
C2P	1.69	-1.59	-1520	3256	7032	2450	5109	-602	5990	2713
C2T	1.70	-1.60	-1514	3149	6954	2430	5223	-623	5871	2827
C5P	1.79	-1.67	-1709	3479	7339	2372	5182	-631	6228	2786
C5T	1.79	-1.67	-1701	3336	7212	2365	5274	-649	6066	2878
C10P	1.92	-1.73	-1876	3487	7418	2302	5287	-681	6226	2891
C10T	1.92	-1.75	-1927	3706	7659	2298	5229	-661	6475	2833
C25P	2.11	-1.91	-2281	4136	8243	2185	5296	-716	6922	2900
C25T	2.11	-1.89	-2281	3798	7829	2167	5307	-775	6515	2911
C50P	2.23	-2.02	-2570	4401	8606	2100	5297	-747	7205	2901
C50T	2.24	-1.98	-2602	3872	7949	2059	5270	-852	6578	2874
C100P	2.38	-2.15	-2890	4679	8998	1963	5399	-823	7427	3003
C100T	2.37	-2.15	-2912	4527	8757	1949	5396	-869	7240	3000
C250P	2.60	-2.33	-3411	4868	9328	1769	5385	-934	7663	2989
C250T	2.57	-2.32	-3453	4685	9058	1735	5344	-988	7415	2948
C500P	2.80	-2.48	-3732	5380	9937	1603	5454	-982	8093	3058
C500T	2.81	-2.47	-3760	5130	9596	1570	5431	-1041	7754	3035
C750P	2.88	-2.51	-3800	5220	9684	1564	5457	-1043	7786	3061
C750T	2.88	-2.54	-3800	5650	10225	1597	5465	-961	8303	3069
C1000P	2.94	-2.58	-3900	5842	10471	1554	5312	-941	8433	2916
C1000T	2.94	-2.55	-3855	5391	9891	1550	5319	-1026	7916	2923
ECR	2.93	-2.59	-3860	5654	10224	1571	5328	-982	8243	2932
E140L	2.62	-2.76	-3508	6878	12403	1311	6597	-865	10154	4155
E140C	2.79	-2.83	-2769	7837	13927	1501	7574	-573	11740	5114
E140U	2.45	-2.67	-3298	5668	10962	1177	6809	-1141	9006	2945
E140R	2.38	-2.69	-3834	5001	10188	822	6448	-1414	8271	2278

Table 5.21. VDS, HDS and Circumferential Wall Strain Laboratory Test Data for Pipe B (HDPE TW AC) in Gravel Surround in Low Friction Box.

PHASE	VDS(%)	HDS(%)	$\epsilon_0(\mu\epsilon)$	$\epsilon_{45}(\mu\epsilon)$	$\epsilon_{90}(\mu\epsilon)$	$\epsilon_{135}(\mu\epsilon)$	$\epsilon_{180}(\mu\epsilon)$	$\epsilon_{225}(\mu\epsilon)$	$\epsilon_{270}(\mu\epsilon)$	$\epsilon_{315}(\mu\epsilon)$
SI	0.00	0.00	0	0	0	0	0	0	0	0
EI	0.68	-0.49	-393	929	7990	519	-780	640	1929	823
E70L	1.71	-1.26	-1353	2578	11014	934	-1407	1038	4953	2365
E70C	1.94	-1.36	-1007	3226	11997	1276	-1026	1376	5936	3043
E70U	1.81	-1.31	-1152	2503	11053	1022	-1142	1211	4992	2278
E70R	1.79	-1.32	-1251	2320	10831	939	-1214	1126	4770	2107
C1P	2.00	-1.42	-1280	3115	11876	1177	-1148	1274	5815	2978
C1T	1.89	-1.38	-1361	2511	11123	1011	-1190	1184	5062	2344
C2P	2.03	-1.45	-1340	3194	11963	1161	-1154	1287	5902	3056
C2T	1.92	-1.41	-1408	2586	11236	1009	-1187	1207	5175	2431
C5P	2.09	-1.49	-1477	3271	12085	1178	-1212	1299	6024	3175
C5T	1.99	-1.46	-1518	2716	11412	1049	-1214	1225	5351	2585
C10P	2.16	-1.54	-1606	3367	12203	1220	-1265	1321	6142	3276
C10T	2.06	-1.50	-1626	2874	11573	1077	-1252	1251	5512	2725
C25P	2.22	-1.59	-1738	3459	12321	1208	-1292	1329	6260	3391
C25T	2.13	-1.55	-1737	2963	11722	1092	-1305	1271	5661	2866
C50P	2.32	-1.66	-1937	3588	12446	1223	-1371	1354	6385	3556
C50T										
C100P	2.40	-1.71	-2052	3720	12597	1231	-1416	1368	6536	3721
C100T										
C250P	2.49	-1.77	-2155	3910	12773	1254	-1441	1409	6712	3983
C250T	2.43	-1.75	-2117	3592	12361	1173	-1423	1385	6300	3622
C500P	2.51	-1.79	-2145	3931	12722	1241	-1413	1430	6661	3985
C500T										
C750P	2.55	-1.81	-2172	4065	12898	1293	-1426	1446	6837	4146
C750T	2.49	-1.78	-2138	3770	12506	1203	-1394	1417	6445	3818
C1000P	2.60	-1.84	-2227	4138	12960	1247	-1427	1449	6899	4239
C1000T	2.54	-1.81	-2179	3854	12587	1198	-1409	1423	6526	3913
ECR	2.44	-1.79	-2280	3272	11935	1033	-1520	1288	5874	3247
E140L	2.95	-2.05	-2043	4954	14447	1543	-1125	1772	8386	5009
E140C	3.15	-2.09	-1654	5619	15615	1921	-686	2180	9554	5707
E140U	2.85	-2.01	-2019	3996	13601	1443	-732	1787	7540	3913
E140R	2.80	-2.04	-2276	3540	13033	1202	-814	1520	6972	3390

Table 5.22. Summary Table of Total VDS for Laboratory Tests.

PHASE	AL	AH	AG	BL	BH	BG	CL	CH	CG	DL	DH	DG	EL	EH	EG
EI	0.27	0.23	0.23	0.16	-0.34	0.28	0.02	0.07	0.19	0.16	0.21	0.26	-1.00	0.00	0.31
E70S ON	1.67	0.37	0.77	1.54	-0.25	0.92	1.37	0.44	0.65	0.92	0.30	0.88	1.22	0.04	0.86
C1000 P	2.95	0.44	1.12	3.18	-0.91	1.33	3.16	0.62	1.06	1.89	0.35	1.31	3.17	0.00	1.34
C1000 R	2.83	0.31	1.02	3.09	-0.22	1.23	3.06	0.57	1.00	1.72	0.30	1.20	3.08	-0.03	1.25
E140S ON	3.39	0.49	1.39	3.73	-0.03	1.69	3.68	0.86	1.38	2.29	0.42	1.63	3.61	0.08	1.60
E140/E70	2.0	1.3	1.8	2.4	0.1	1.8	2.7	1.9	2.1	2.5	1.4	1.9	3.0	2.0	1.9

Table 5.23. Summary Table of Incremental VDS for Laboratory Tests.

PHASE	AL	AH	AG	BL	BH	BG	CL	CH	CG	DL	DH	DG	EL	EH	EG
EI	0.27	0.23	0.23	0.16	-0.34	0.28	0.02	0.07	0.19	0.16	0.21	0.26	-0.10	0.00	0.31
E70S ON	1.40	0.14	0.54	1.38	-0.09	0.64	1.35	0.37	0.46	0.76	0.09	0.62	1.32	0.04	0.55
C1000 P	1.43	0.12	0.47	1.79	0.10	0.52	1.91	0.26	0.49	1.16	0.10	0.56	2.09	0.00	0.58
C1000 R	1.31	-0.10	0.37	1.70	0.10	0.42	1.81	0.21	0.43	0.99	0.05	0.45	2.00	-0.03	0.49
E140S ON	0.56	0.18	0.37	0.64	0.17	0.46	0.62	0.29	0.37	0.57	0.12	0.42	0.52	0.11	0.35
E140/E70	0.3	1.3	1.5	0.5	2	0.7	0.5	0.8	0.8	0.8	1.3	0.7	0.4	2.8	0.6

A, B, C, D, E = test pipe types (Table 5.1)

L - lightly compacted sand surround

H - heavily compacted sand surround

G - gravel surround

EI - end of installation

E70S ON - end of 24 hour period of 70kPa static pressure application

C1000P - peak pf 1000th cycle of 70kPa pressure

C1000R - release of 1000th cycle of 70kPa pressure

E140S ON - end of 24 hour period of 140kPa static pressure application

E140/E70 - ratio of VDS at end of 140kPa static phase to that at end of 70kPa static phase

Table 5.24. VDS Data for Field Test Pipes in Sand Surround.

PHASE	PIPE A	PIPE B	PIPE C	PIPE D	PIPE E	PIPE F	MEAN
SI	0.00	0.00	0.00	0.00	0.00	0.00	0.00
EI	1.01	0.92	0.73	0.66	0.48	0.69	0.75
C1P	1.12	1.10	0.91	-	0.58	0.88	0.92
C1T	1.10	1.01	0.82	-	0.53	0.81	0.85
C2P	1.13	1.14	1.02	-	0.59	1.04	0.98
C2T	1.12	1.03	0.87	-	0.54	0.95	0.90
C5P	1.24	1.25	1.11	-	0.69	1.15	1.09
C5T	1.13	1.10	0.98	-	0.56	0.98	0.95
C10P	1.29	1.33	1.21	-	0.69	1.20	1.14
C10T	1.17	1.19	1.05	-	0.56	1.06	1.01
C25P	1.35	1.52	1.35	-	0.71	1.32	1.25
C25T	1.24	1.37	1.20	-	0.58	1.20	1.12
C50P	1.45	1.66	1.50	-	0.72	1.39	1.34
C50T	1.33	1.53	1.39	-	0.63	1.29	1.23
C100P	1.61	1.94	1.77	-	0.79	1.46	1.51
C100T	1.53	1.80	2.64	-	0.64	1.38	1.60
C250P	1.94	2.55	2.19	-	0.81	1.90	1.88
C250T	1.81	2.33	2.03	-	0.71	1.78	1.73
C500P	2.03	3.01	2.49	-	0.84	2.22	2.12
C500T	1.98	2.87	2.36	-	0.76	2.12	2.02
C750P	2.14	3.23	-	-	0.91	2.26	2.13
C750T	2.03	3.04	-	-	0.83	2.17	2.02
C1000P	2.22	3.31	-	-	0.94	2.29	2.19
C1000T	2.11	3.18	-	2.20	0.85	2.23	2.11

Table 5.25. VDS Data for Field Test Pipes in Gravel Surround.

PHASE	PIPE A	PIPE B	PIPE C	PIPE D	PIPE E	PIPE F	MEAN
SI	0.00	0.00	0.00	0.00	0.00	0.00	0.00
EI	0.70	0.10	0.65	0.36	0.91	0.84	0.59
C1P	0.81	0.14	0.78	0.44	1.02	0.99	0.70
C1T	0.75	0.11	0.66	0.41	0.92	0.95	0.63
C2P	0.87	0.20	0.84	0.51	1.07	1.16	0.78
C2T	0.78	0.13	0.67	0.45	0.93	1.13	0.68
C5P	0.90	0.29	0.89	0.58	1.07	1.32	0.84
C5T	0.78	0.13	0.77	0.46	0.97	1.24	0.73
C10P	0.92	0.29	0.92	0.59	1.09	1.48	0.88
C10T	0.81	0.15	0.79	0.48	0.98	1.39	0.77
C25P	0.95	0.32	0.98	0.72	1.13	1.50	0.93
C25T	0.86	0.21	0.85	0.60	1.00	1.41	0.82
C50P	1.00	0.49	1.05	0.76	1.15	1.57	1.00
C50T	0.91	0.34	0.94	0.60	1.04	1.47	0.88
C100P	1.09	0.59	1.09	0.79	1.19	1.68	1.07
C100T	1.00	0.45	0.97	0.61	1.06	1.57	0.94
C250P	1.24	0.81	1.37	0.86	1.24	1.96	1.25
C250T	1.12	0.66	1.25	0.75	1.14	1.87	1.13
C500P	1.36	1.10	1.50	0.93	1.36	2.20	1.41
C500T	1.26	1.02	1.41	0.82	1.25	2.12	1.31
C750P	1.43	1.15	1.54	1.02	1.40	2.27	1.47
C750T	1.33	1.03	1.45	0.93	1.29	2.20	1.37
C1000P	1.47	1.18	1.68	1.12	1.47	2.33	1.54
C1000T	1.36	1.08	1.56	1.03	1.36	2.25	1.44

Table 5.26. Circumferential and Axial Strains (in $\mu\epsilon$) for Field Test Pipes in Sand Surround During Installation Phase.

GAUGE	PIPE A	PIPE B	PIPE C	PIPE D	PIPE E	PIPE F
C0	-175	-736	-896	-886	-419	-495
C22.5	-1229	-757	-	568	-162	-
C45	318	285	-	-	289	-
C67.5	661	1393	993	832	359	-
C90	1203	2174	2020	865	310	429
C112.5	-	1811	1320	627	-	-
C135	1340	797	477	-35	-241	-
C157.5	-256	-550	538	-250	-	-
C180	-2107	-2437	-1912	-682	-	-1157
C270	1292	1645	2174	1166	358	470
A0	-488	-169	-299	-	-	-184
A90	103	-507	-714	-	113	233
A180	-57	-800	680	-1397	-574	-251
A270	-1014	-398	-921	-148	-419	264

Table 5.27. Circumferential and Axial Strains (in $\mu\epsilon$) for Field Test Pipes in Gravel Surround During Installation Phase.

GAUGE	PIPE A	PIPE B	PIPE C	PIPE D	PIPE E	PIPE F
C0	-813	-179	-236	-333	-682	-490
C22.5	177	-283	203	-	-652	-
C45	202	572	755	-	313	-
C67.5	1048	1218	1860	-	665	-
C90	1317	1380	1354	496	639	389
C112.5	1137	1446	1462	-	1007	-
C135	246	679	674	-	710	-
C157.5	-866	-229	-242	-	-771	-
C180	-1136	-831	-2133	-	-1521	-1157
C270	1234	1292	1528	557	-	470
A0	-200	-	-	-436	-187	-349
A90	-224	-396	-	133	-	-
A180	102	-1026	194	-896	-75	-495
A270	-432	-298	-	-	-	-

Cn = circumferential strain gauge at location n° measured from crown (see Figure 4.5)

An = axial (longitudinal) strain gauge at location n° from crown

Table 5.28. Amplitudes of VDS Cycles for Field Test Pipes Under 55kN and 75kN Wheel Loads.

PIPE	A55(1)	A55(1000)	A75	A75/A55(1)	A75/A55(1000)
AS	0.020	0.117	0.220	11.000	1.880
BS	0.095	0.130	0.230	2.421	1.769
CS*	0.090	0.135	0.180	2.000	1.333
DS	0.017	-	-	-	-
ES	0.051	0.091	0.150	2.941	1.648
FS	0.073	0.064	0.140	1.918	2.188
AG	0.050	0.108	0.130	2.600	1.204
BG	0.260	0.121	0.200	0.769	1.653
CG	0.117	0.126	0.150	1.282	1.190
DG	0.036	0.089	-	-	-
EG	0.103	0.112	0.170	1.650	1.518
FG	0.035	0.081	0.090	2.571	1.111

A, B, C, D, E, F = test pipe type (Table 5.1)

S = sand surround,

G = gravel surround,

A55(1) = amplitude of change in VDS during 1st passage of 55kN wheel load

A55(1000) = amplitude of change in VDS during 1000th passage of 55kN wheel load

A75 = amplitude of change in VDS during one pass of 75kN (approx.) wheel load.

* - data relate to 400th passage of wheel load, not 1000th

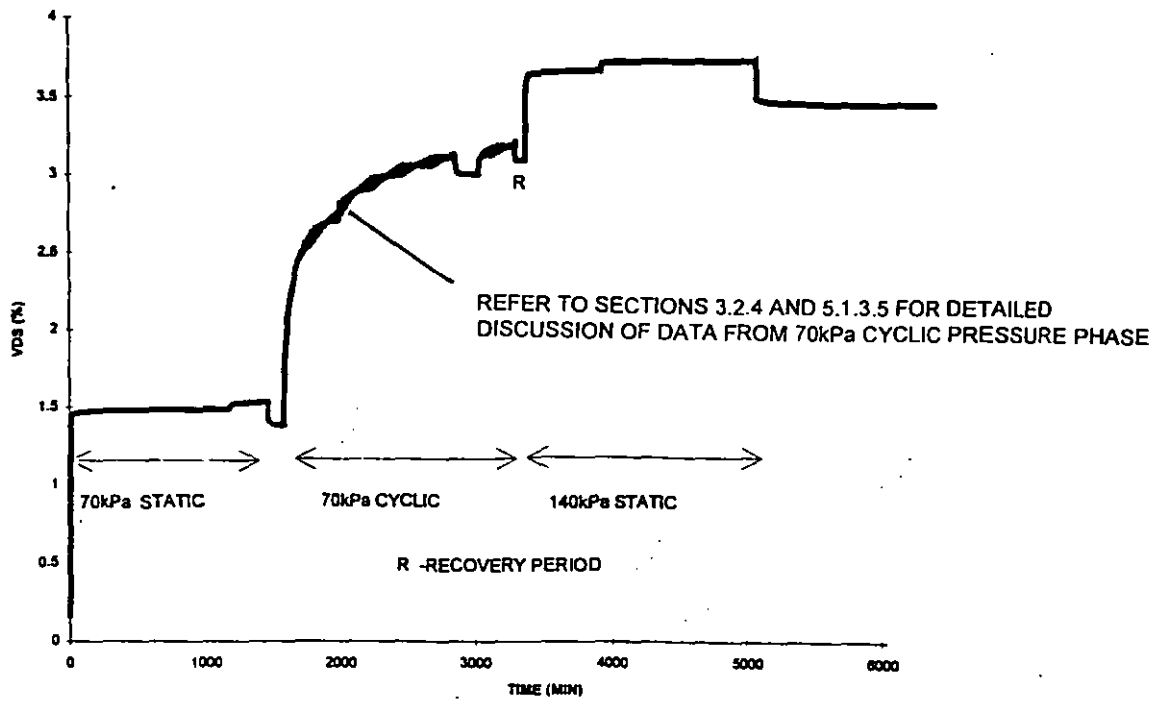


Figure 5.1. VDS for Pipe B in Lightly Compacted Sand For All Pressure Phases.

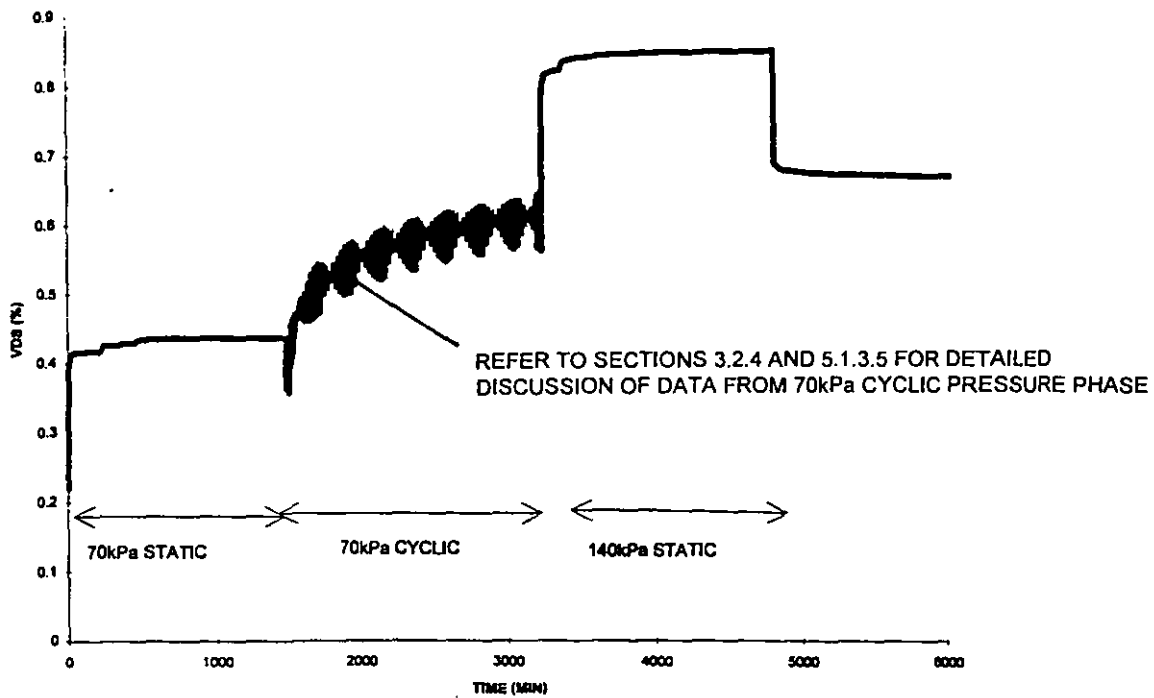


Figure 5.2. VDS for Pipe C in Heavily Compacted Sand For All Pressure Phases.

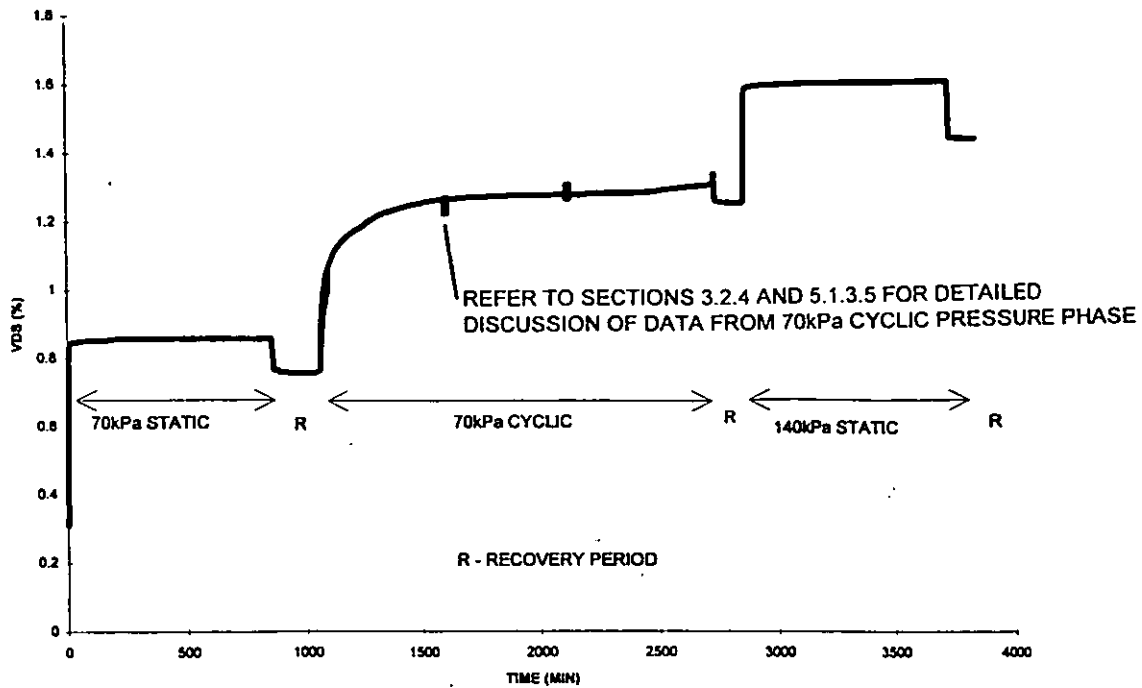


Figure 5.3.VDS For Pipe E in Gravel for All Pressure Phases.

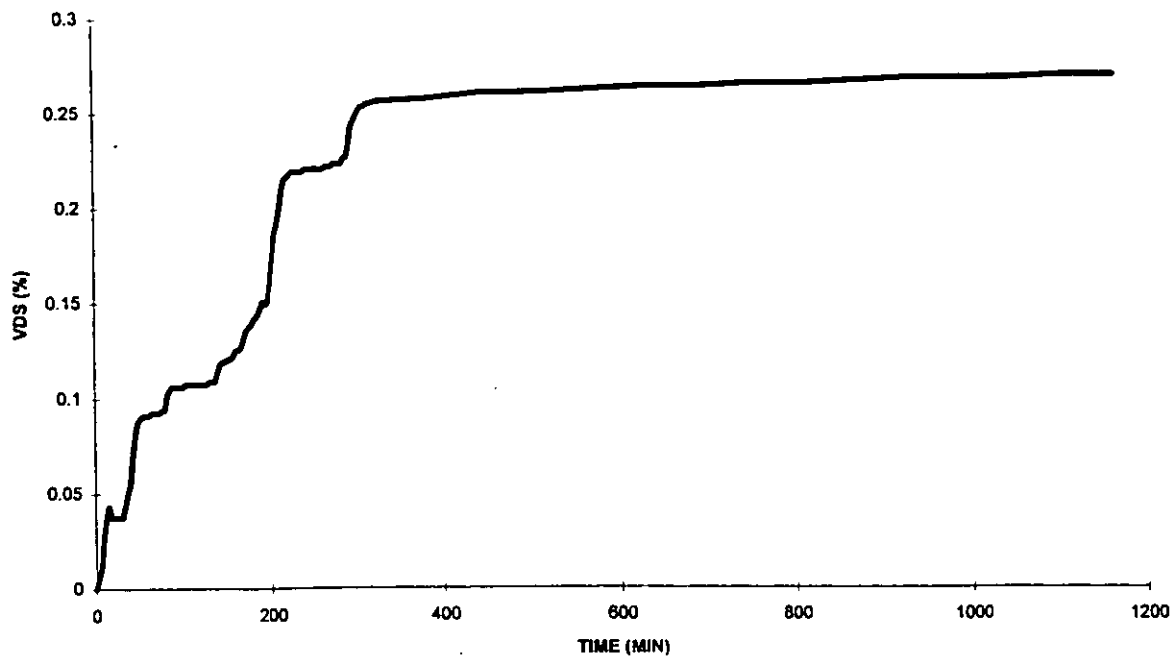


Figure 5.4. VDS for Pipe A in Lightly Compacted Sand During Installation Phase.

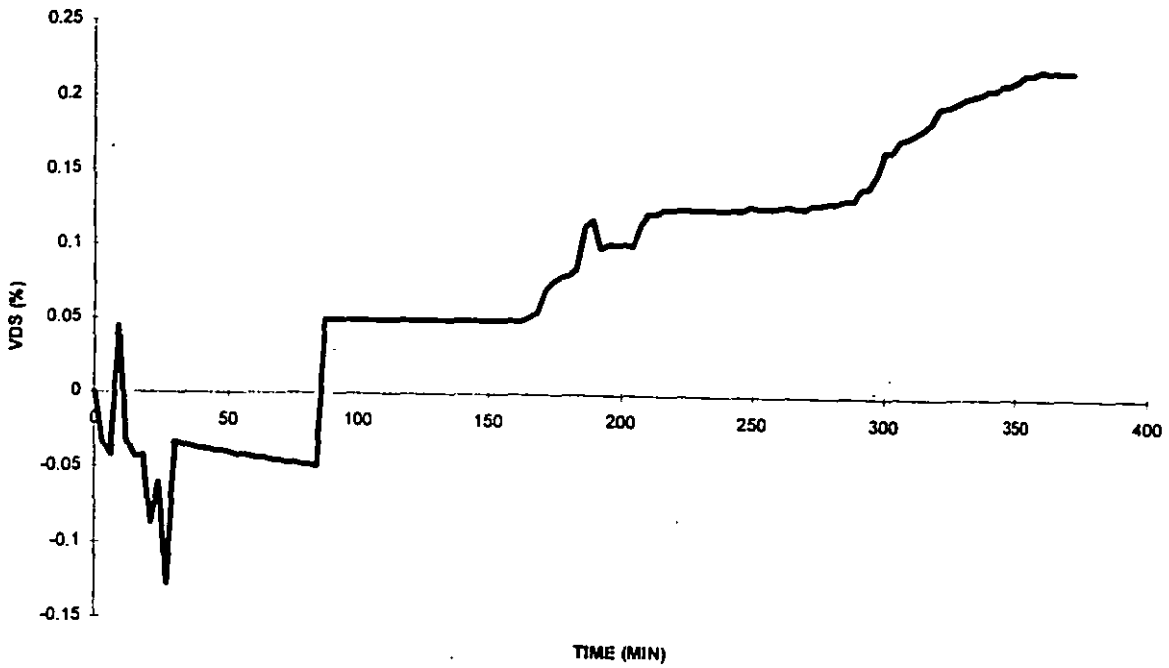


Figure 5.5. VDS for Pipe C in Heavily Compacted Sand During Installation Phase.

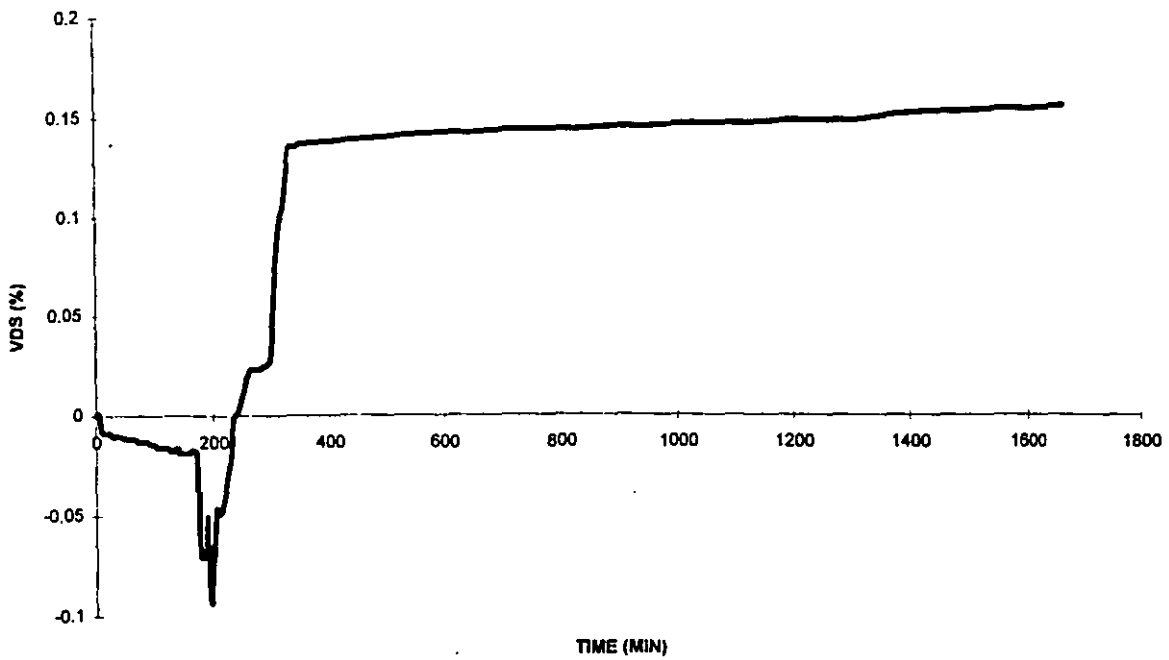


Figure 5.6. VDS for Pipe F in Heavily Compacted Sand During Installation Phase

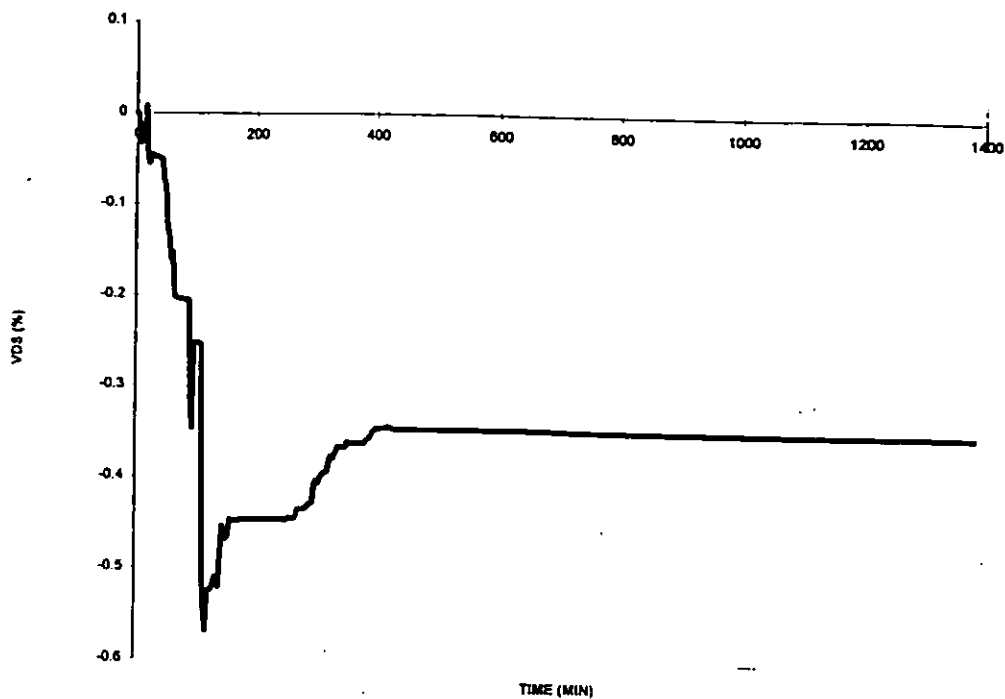


Figure 5.7. VDS for Pipe B in Heavily Compacted Sand During Installation Phase.

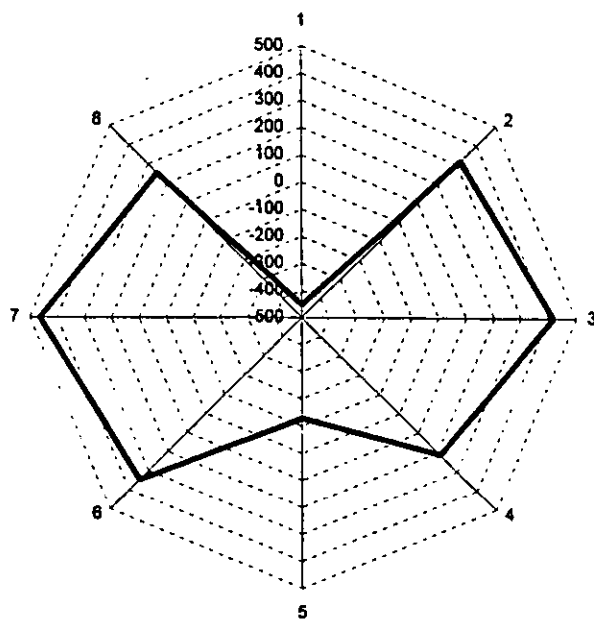


Figure 5.8. Circumferential Strains for Pipe A in Lightly Compacted Sand at End of Installation Phase.

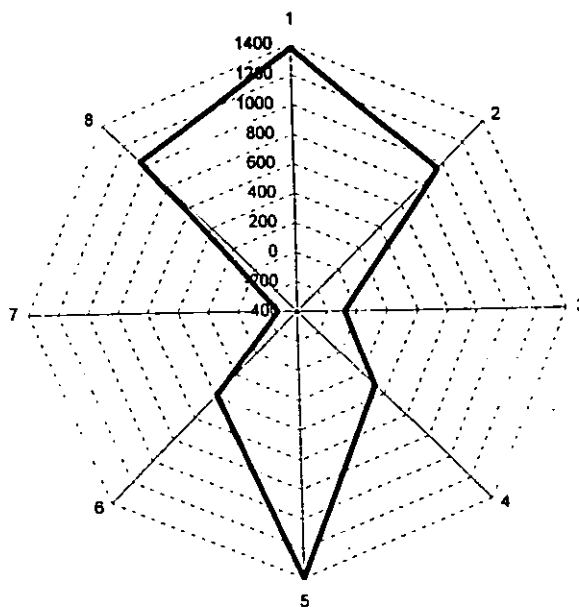


Figure 5.9. Circumferential Strains for Pipe B in Heavily Compacted Sand at End of Installation Phase.

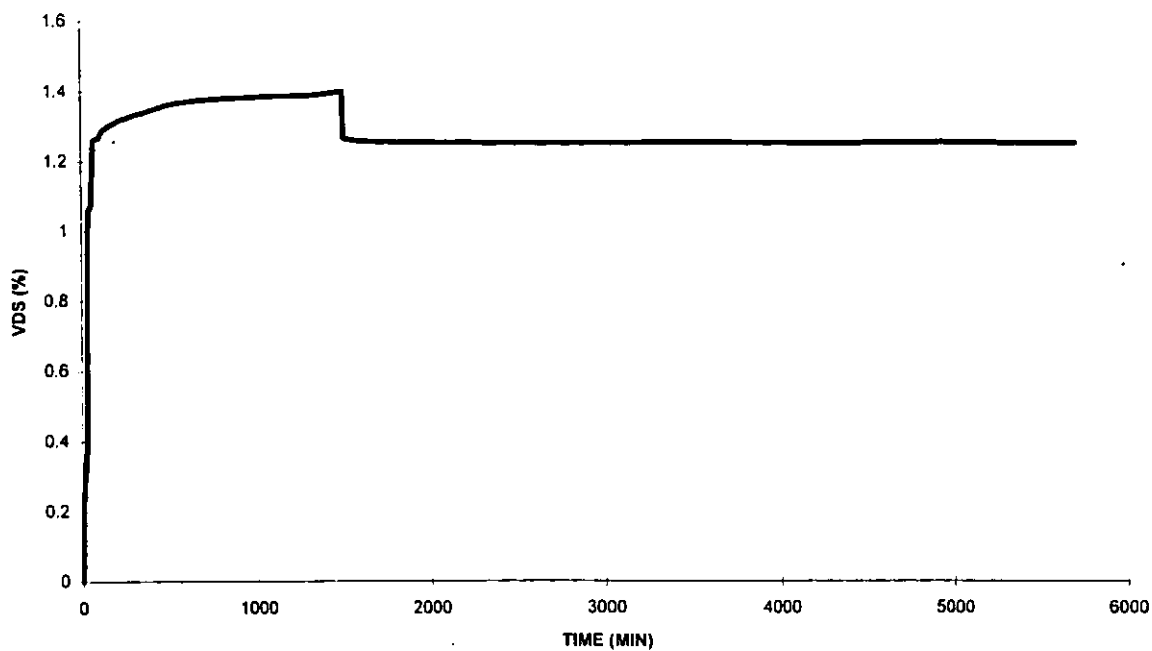


Figure 5.10. VDS for Pipe A in Lightly Compacted Sand During 70kPa Static Pressure Phase.

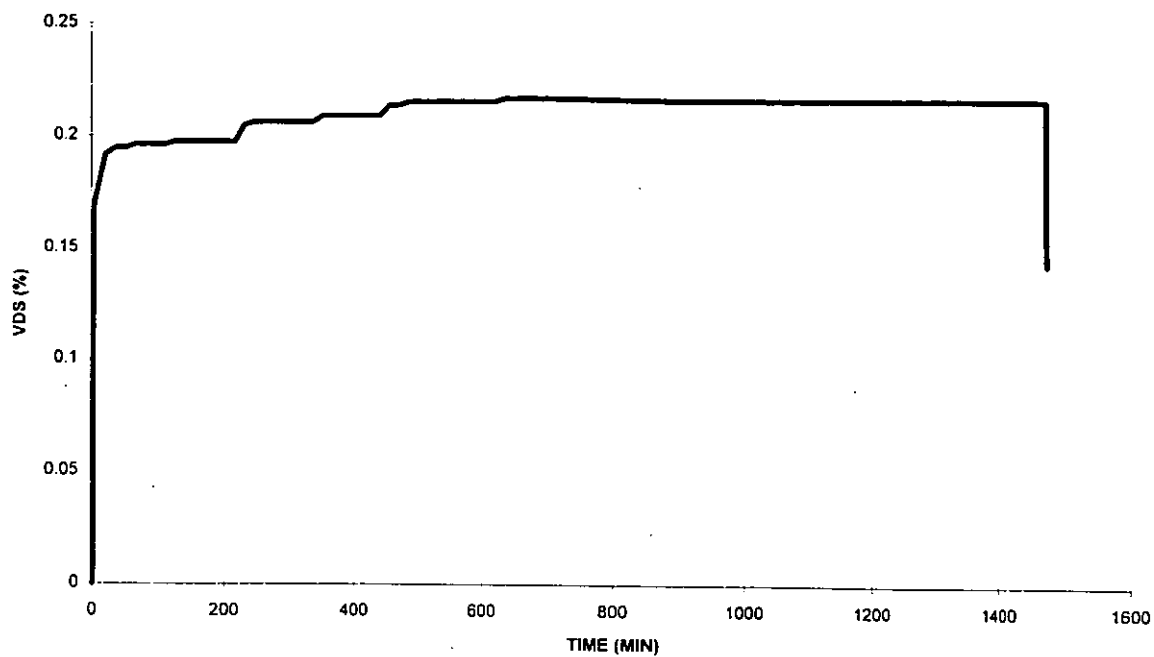


Figure 5.11. VDS for Pipe C in Heavily Compacted Sand During 70kPa Static Pressure Phase.

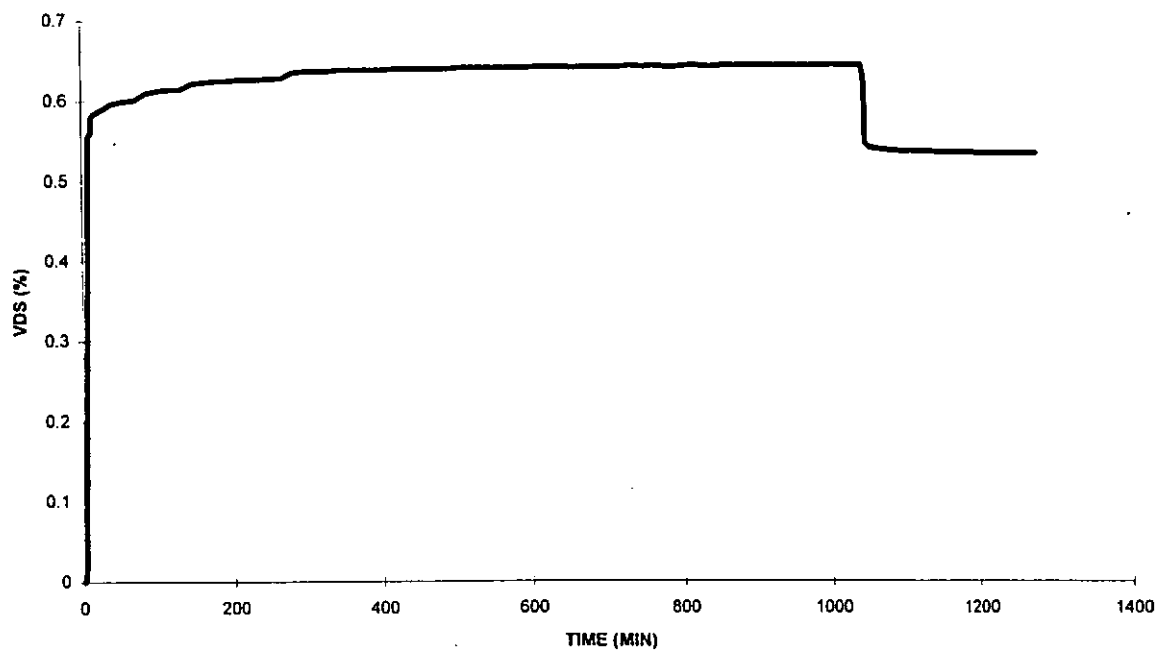


Figure 5.12. VDS for Pipe B in Gravel Surround During 70kPa Static Pressure Phase.

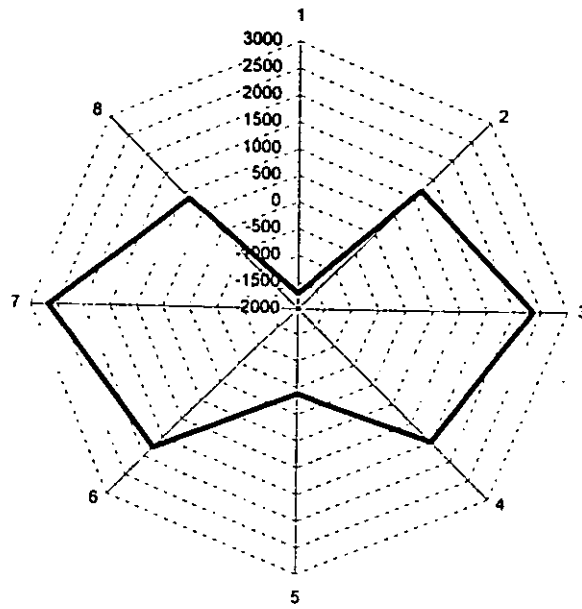


Figure 5.13. Circumferential Strain for Pipe A in Lightly Compacted Sand at End of 70kPa Static Pressure Phase

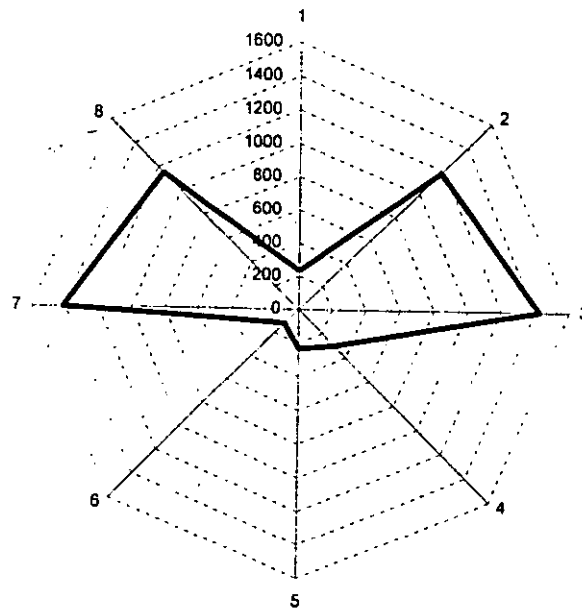


Figure 5.14. Circumferential Strain for Pipe C in Heavily Compacted Sand at End of 70kPa Static Pressure Phase.

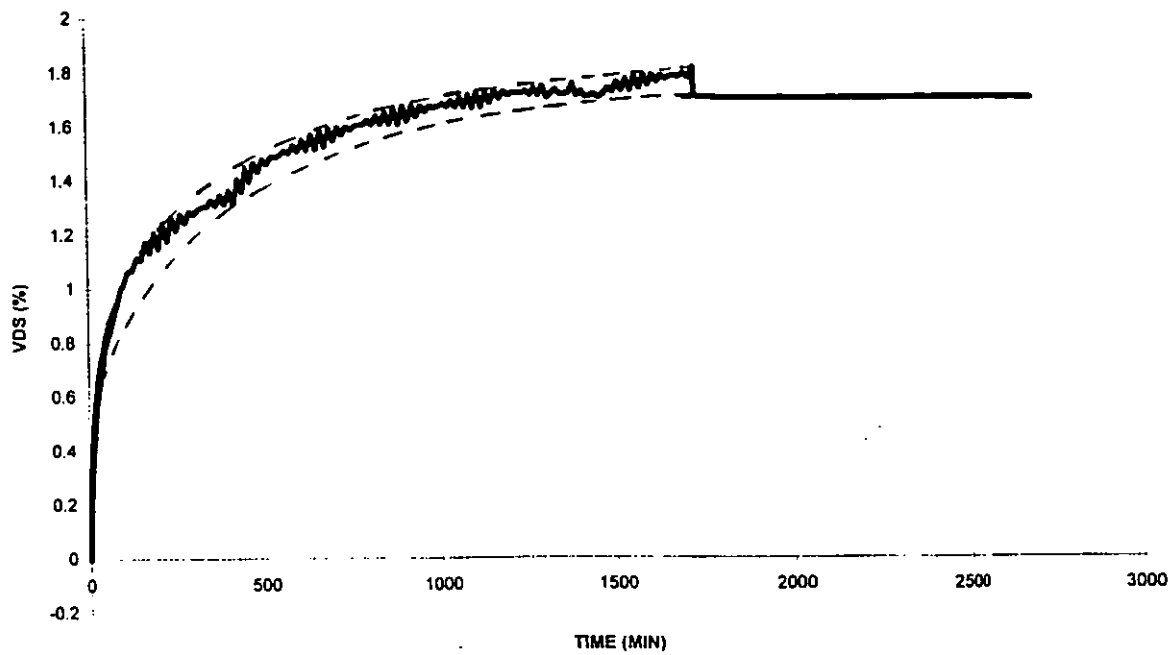


Figure 5.15. VDS for Pipe B in Lightly Compacted Sand During 70kPa Cyclic Pressure Phase.

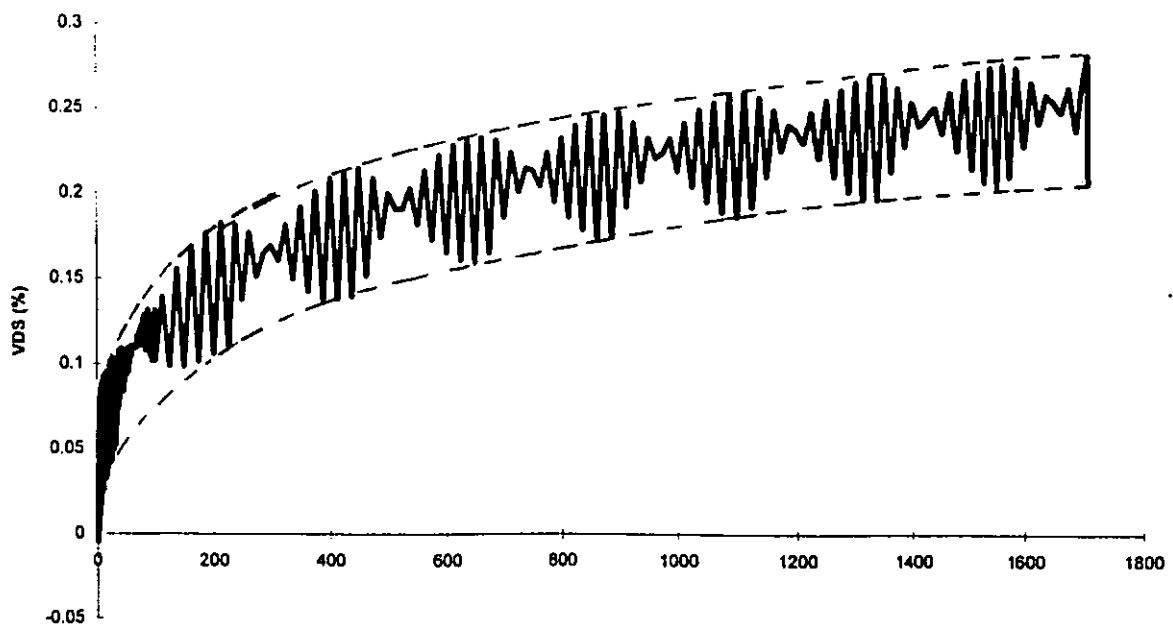


Figure 5.16. VDS for Pipe C in Heavily Compacted Sand During 70kPa Cyclic Pressure Phase.

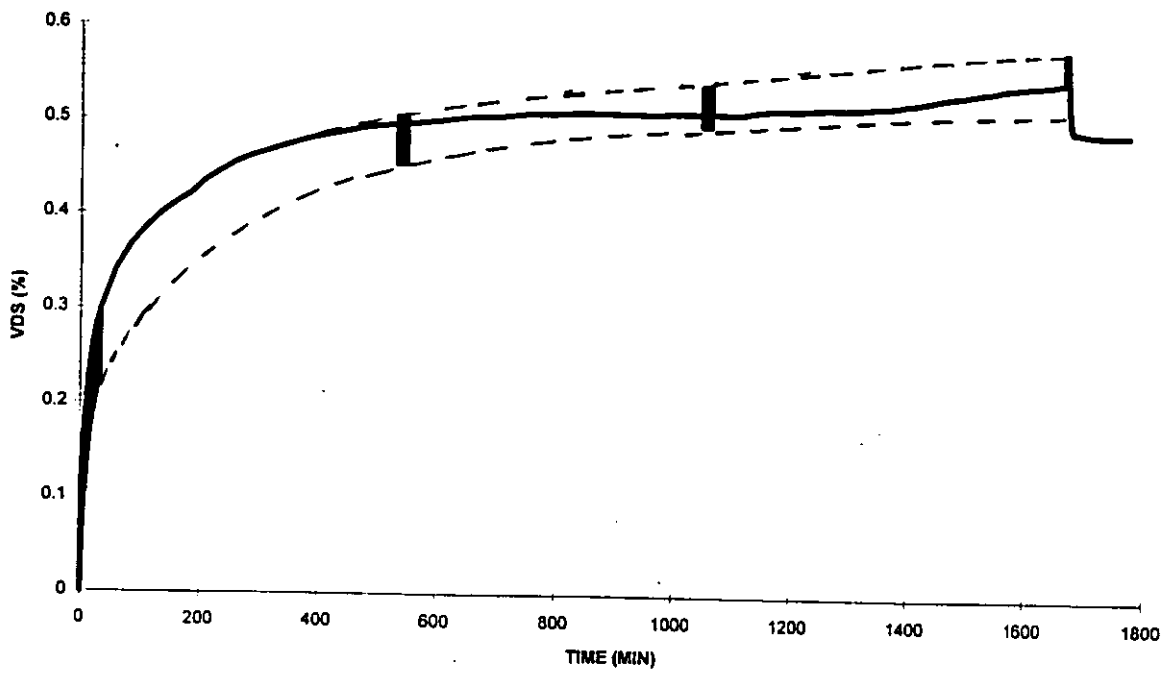


Figure 5.17. VDS for Pipe E in Gravel During 70kPa Cyclic Pressure Phase.

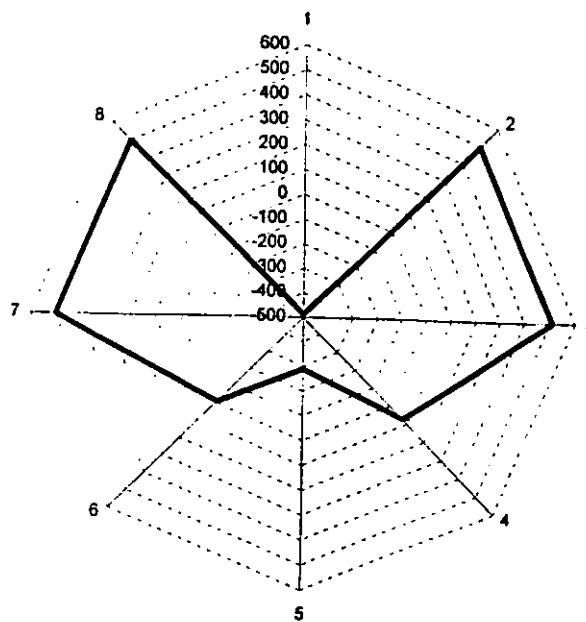


Figure 5.18. Circumferential Strains for Pipe E in Gravel Surround at Peak of 1000th Pressure 70kPa Cycle

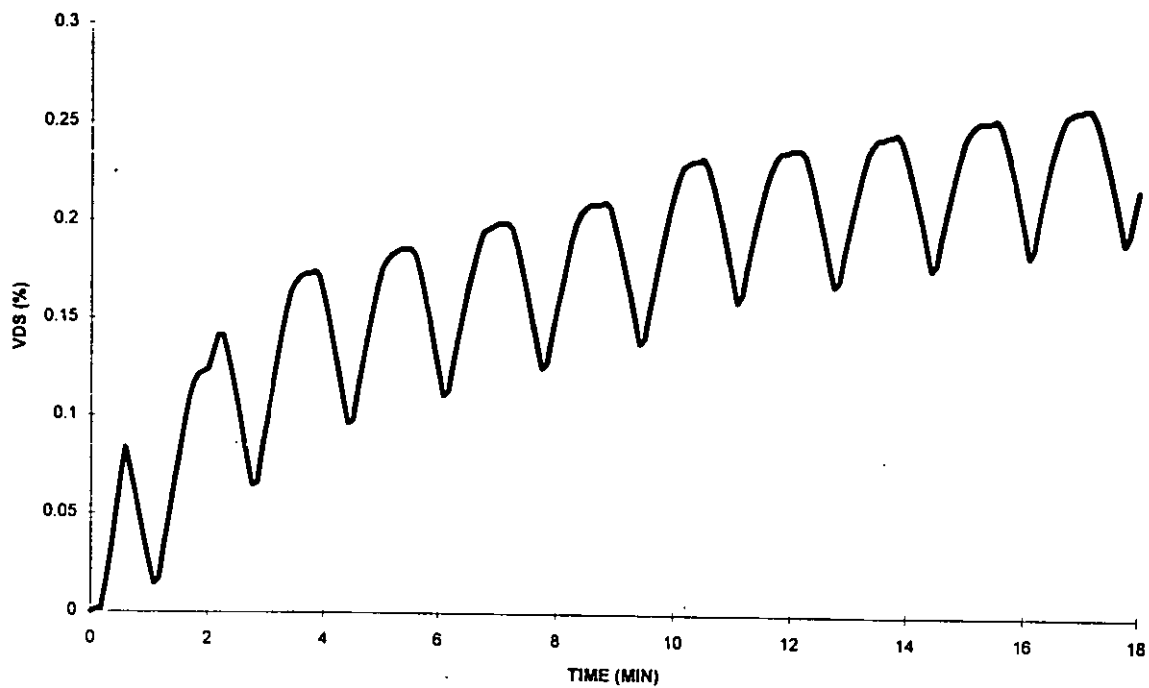


Figure 5.19. Typical Trend of Accumulation of VDS During Early Load Cycles.

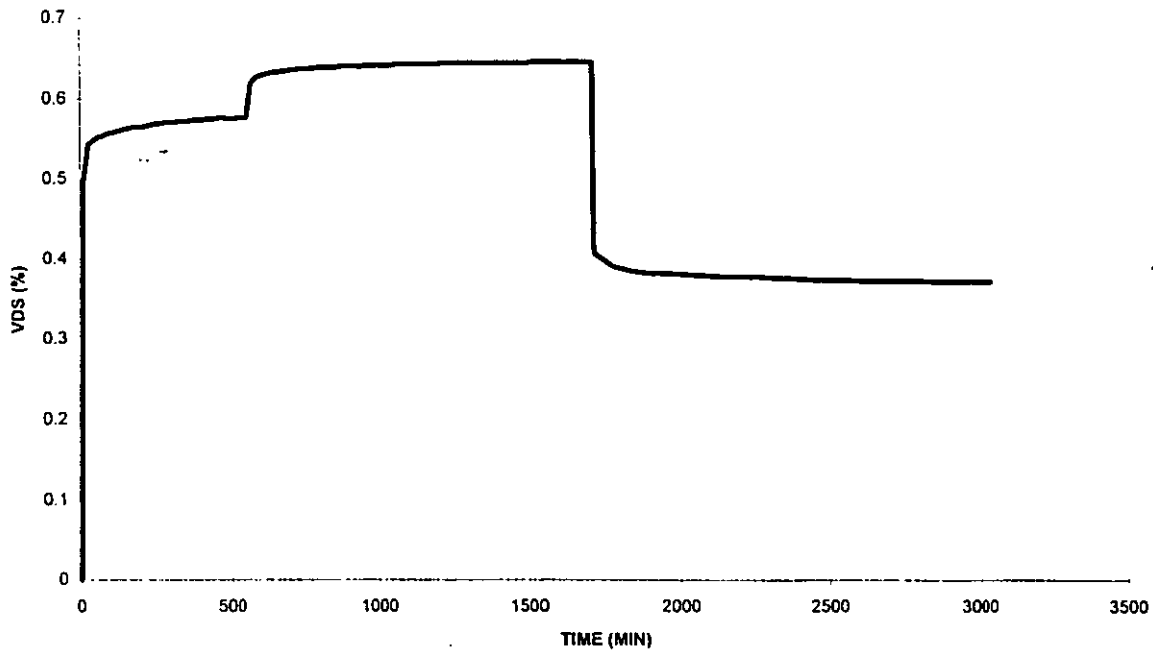


Figure 5.20. VDS for Pipe B in Lightly Compacted Sand During 140kPa Static Pressure Phase.

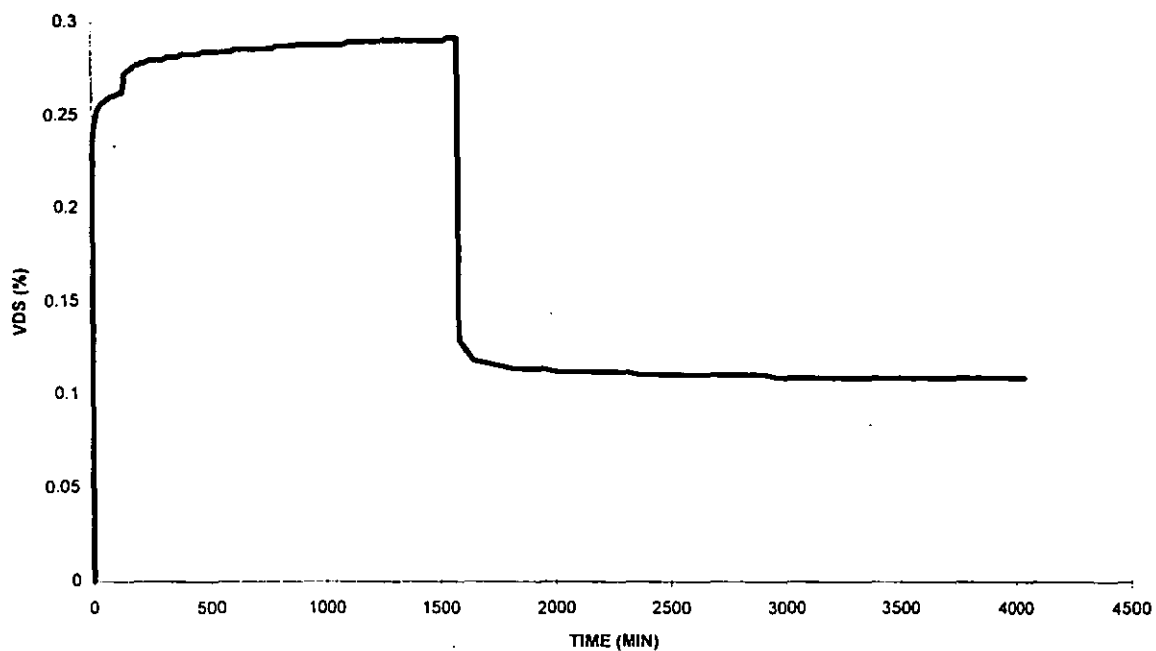


Figure 5.21. VDS for Pipe C in Heavily Compacted Sand During 140kPa Static Pressure Phase.

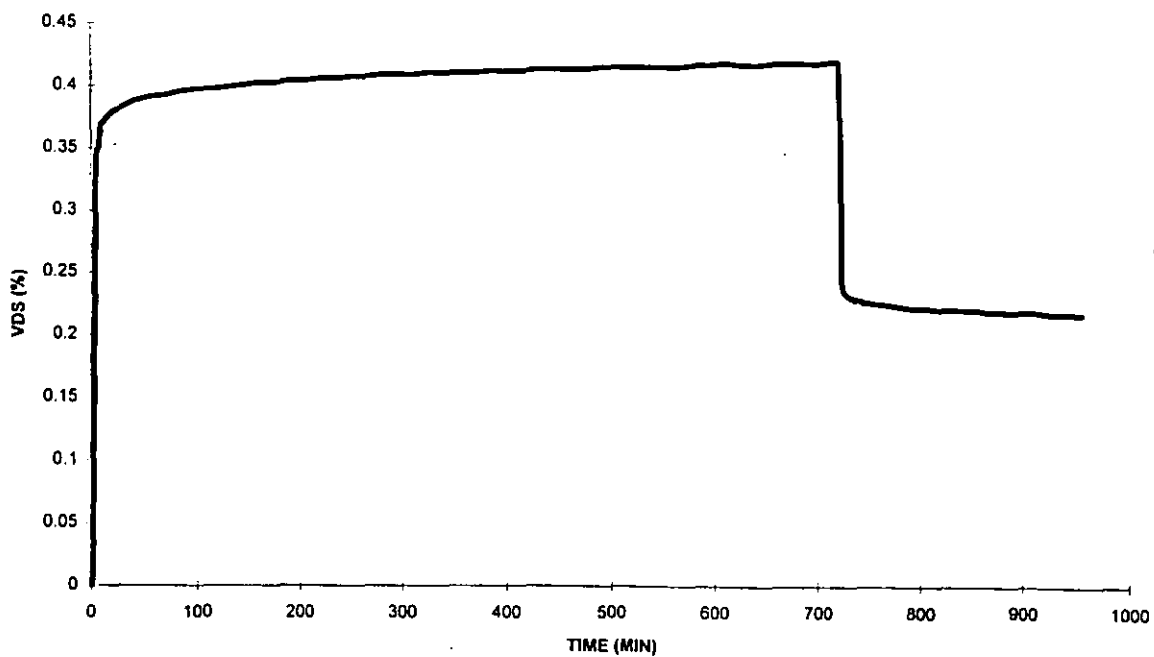


Figure 5.22. VDS for Pipe D in Gravel During 140kPa Static Pressure Phase.

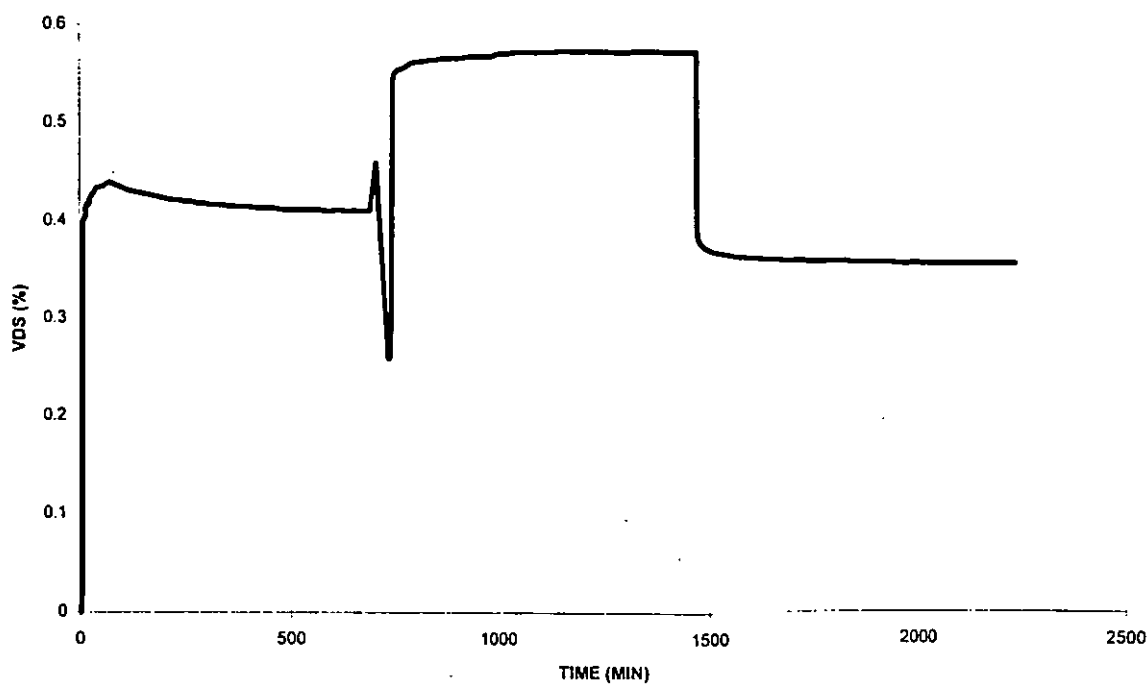


Figure 5.23. Effect of Accidental Release and Reapplication of 140kPa Static Pressure.

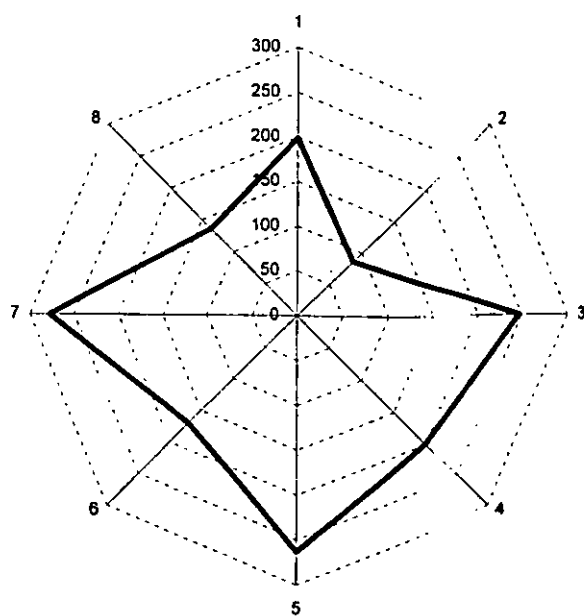


Figure 5.24. All-Round Compression of the Pipe Wall.

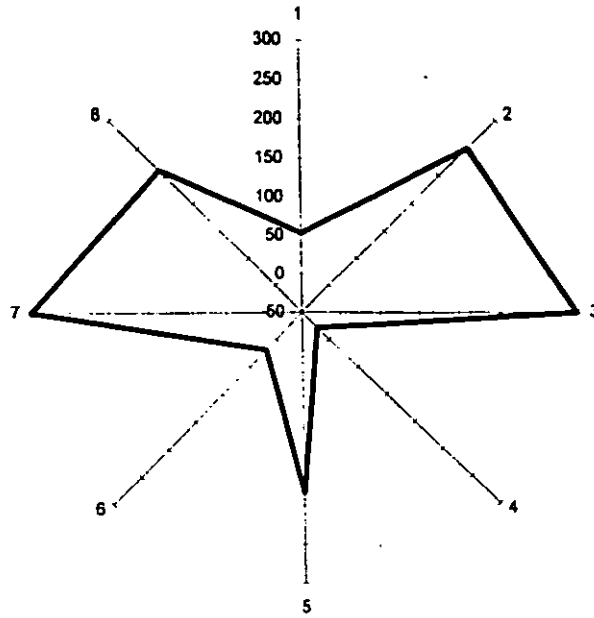


Figure 5.25. Effect on Wall Strain of Lifting of Pipe off Bedding Layer During Installation.

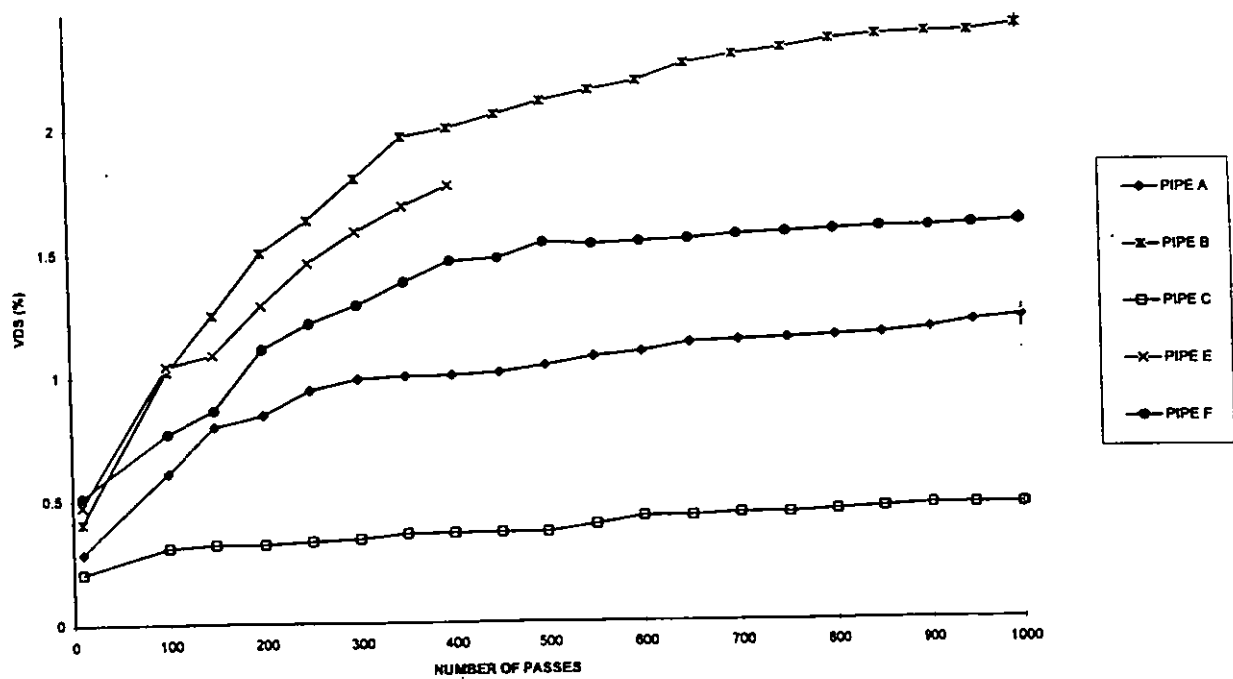


Figure 5.26. VDS for Pipes in Sand During Field Test Cyclic Loading Phase.

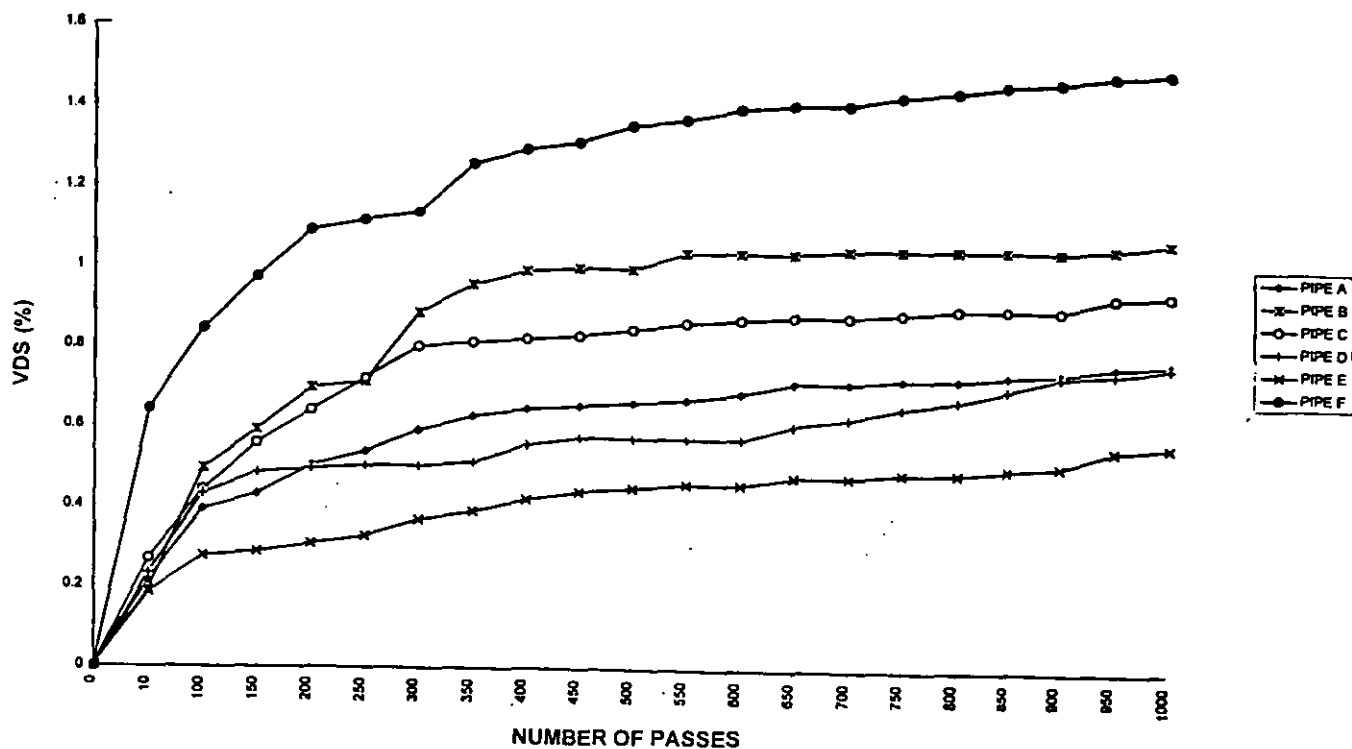


Figure 5.27. VDS for Pipes in Gravel During Field Test Cyclic Loading Phase.

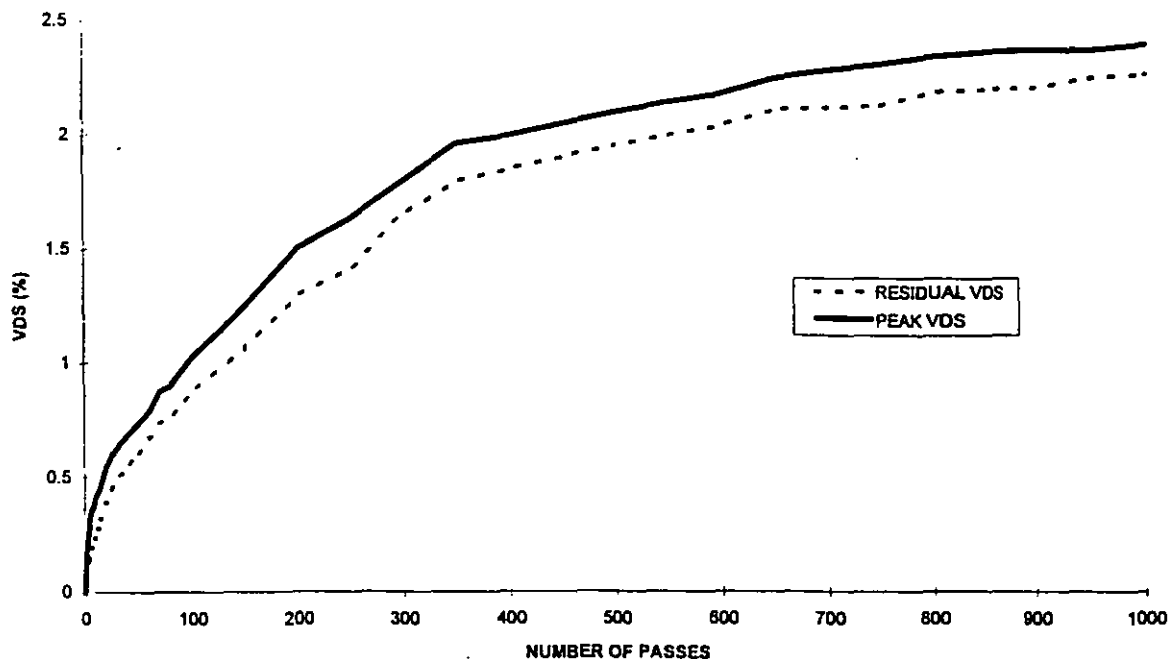


Figure 5.28. Peak and Residual VDS for Pipe B in Sand Surround During Field Test Cyclic Loading Phase.

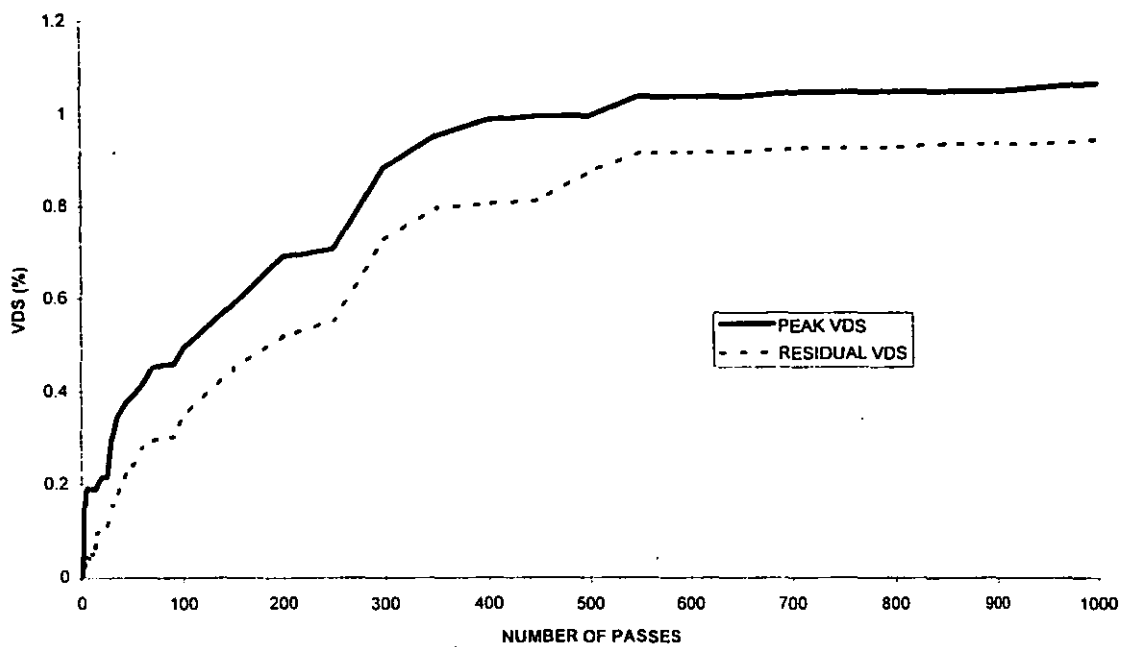


Figure 5.29. Peak and Residual VDS for Pipe B in Gravel During Field Test Cyclic Loading Phase

6 DISCUSSION

This chapter includes a more detailed treatment of the basic laboratory and field data that were presented and described in Chapter 5. The data are discussed in greater depth to determine more accurately the mechanisms of pipe deformation. The implications of the test data in terms of current practice relating to pipe specification and installation criteria are also discussed.

The effect of the type of surround on the shape of pipe deformation is first investigated in greater depth. Examples of two other shapes of deformation are presented, which are not covered by standard shape descriptions (Rogers, 1985, see Figure 2.8). The subject of deformed shapes is discussed further by consideration of the effects of the surround materials on them. This is of considerable importance since it indicates the mechanism of pipe deformation which, in extreme cases, is an indicator of the failure mechanism of the pipe. Thus, the stability of the deformed pipe can be assessed and the effects of the surround type on this factor are discussed.

The effect of an applied surface stress (simulated by water pressure) on the pipe surround material is also discussed. During the static and cyclic pressure phases of the laboratory tests, the surface of the surround material in the testing box was observed to settle as a result of the applied pressures. This is indicative of an increase in the density of the surround material, and is therefore an important development in relation to the degree of progressive deflection of a buried pipe.

Experimental repeatability is considered by the comparison of the data from two tests carried out on the same pipe with the same specified surround type and subject to the standard test loading pattern. The unit weights of a particular type of surround measured in each relevant test are also compared and the variations in them discussed. The data show that the unit weight of the material may vary somewhat despite the close control adopted. Because of the significant effect of the surround density on pipe deflection (see 2.2.2.2) these findings are important and indicate the uncertainty inherent in the laboratory and (to a greater degree) on site.

The boundary conditions of the laboratory test are discussed. This is done theoretically by the use of Marston's load theory (see 2.1.1). The frictional properties of the box walls and the pipe surround are determined, and their effects on the stress applied to the pipe are computed. This exercise is followed by a discussion of the results of the comparative testing carried out using the low-friction testing box wall facings. These test data serve to place the frictional effects of the trench walls in context with the overall uncertainties of the testing methods.

The results of tests carried out on a pipeline (composed of two lengths of pipe connected by a patent coupler) are discussed. The findings are of considerable importance because

of the large deflections produced for one of the tests, which exceeded the 5% limit on vertical diametral strain that has its origins in Spangler's work (1941, and see 2.2.7). Since the pipe was seen to maintain its functionality (by not leaking) this result calls into question the strain limit and, by implication, pipe design, installation and loading specifications.

The significance of the tests carried out on pipes buried at low cover depths in novel surround types and subject to severe loading is discussed. These results, too, are of considerable significance since the good performance of the pipes under this testing regime causes specification and loading criteria to be questioned.

6.1 FURTHER DISCUSSION OF TEST RESULTS

6.1.1 Other Shapes of Pipe Deformation

In addition to the elliptical, reverse elliptical and heart-shaped deformations recorded above, other deflected shapes were observed. These are now described, and their causes explained.

6.1.1.1 All-round Compression

This phenomenon was observed for pipes buried in heavily compacted sand, and an example is given in Figure 5.21. The strains at the measurement locations were relatively small but wholly compressive. The all-round compression implies that the pipe received virtually uniform support from the heavily compacted surround which prevented any significant change in the original circular shape. This relatively uniform strain distribution implies a similarly uniform (near-hydrostatic) stress distribution on the pipe. This implies that the lateral earth pressure coefficient (K_0) is near unity, which is the case in a very dense sand. This result may also relate to a deeply-buried pipe buried, since K_0 is known to increase with depth in a soil stratum. Because of the near-uniform restraint given to the pipe, it is prevented from significant out-of-round (e.g. elliptical) deformation, and the extreme case of failure by excessive deflection is considerably less likely to occur. The only alternative mode of failure is by buckling of the pipe wall, in which very large stresses on the (constrained) pipe wall lead ultimately to instability and buckling failure in the shape shown in Figure 2.18. The pressures required to cause this are of the order of ten times those that typically cause elliptical deformation in less stiff surrounds (using Gumbel's Method, see 2.3.3), which again pertain only in deep installations and/or where the pipe is deeply buried below the water table.

For this shape of deformation, the circumferential shortening (estimated from the strain gauge readings) was generally less than 0.5%.

6.1.1.2 High Tensile Strains at the Pipe Invert

In some of the heavily compacted sand cases (see Figure 5.22) the top half of the pipe exhibited elliptical deformation but the bottom half behaved quite differently. The haunches displayed greater tension and the invert displayed markedly high compression. Although the magnitude of the strains was relatively small in the case shown, the overall effect was one of a modest tendency towards reversal of curvature at the haunches with an increase in the curvature of the invert. The impression is given that the pipe is supported at the haunches and that the invert is not restrained from downward movement. This is assumed to be the result of the placing of surround material at the haunches, the careful compaction of which may have caused the pipe to be lifted slightly off its bedding layer. The invert would therefore have been free to move downwards as a loading was applied to the pipe.

6.1.2 The Effect of Surround Type on the Shape of Pipe Deformation

Figures 6.1 to 6.5 describe the variation of the ratio of vertical diameter to horizontal diameter during the entire test programme for each pipe buried in the three types of surround. This ratio may be used to determine the degree to which the initially circular pipe has deformed to an ellipse. For small deflections, a value of 1.000 for the ratio of vertical diameter to horizontal diameter indicates that the pipe remains circular. A value of 0.908 indicates that the pipe has deformed to a VDS of 5% (the current limit) and is of the elliptical shape that would occur in a parallel-plate loading test (Spangler, 1941).

The lightly compacted sand produced the most out-of-round deformation in all cases. The largest deviation from a circular shape was exhibited by pipe B (Figure 5.24). At the start of the 70kPa static pressure phase, the ratio of vertical diameter to horizontal diameter changed from 1.000 to 0.977 almost instantaneously and remained at that value until the pressure was removed at approximately 3900min. The pipe then re-rounded slightly. During the 70kPa cyclic pressure phase, the rapid early build-up in deflection caused a similarly rapid change in the shape of the pipe as the ratio reduced further to approximately 0.948 at the end of the test phase (5700min). The minimum value of the ratio was reached during the 140kPa static pressure phase (6800min onwards), and was approximately 0.938.

By contrast, the heavily compacted sand surround case resulted in very small vertical and horizontal deflections, which caused little change in the shape of the pipe. The ratio of horizontal diameter to vertical diameter for pipe B remained very close to unity for the 70kPa static and cyclic pressure phases. The minimum value reached was approximately 0.997 during the

140kPa static pressure phase, indicating that the pipe deviated very little from its initial circular shape.

The pipe buried in a gravel surround deformed to a larger extent than the pipe buried in heavily compacted sand. However, the deformation was not as severe as the lightly compacted sand case. After an initial reduction in the ratio from 1.000 to 0.990 during the 70kPa static pressure phase, little further deformation took place. The 70kPa cyclic pressure phase resulted in a reduction in the ratio to about 0.988, which did not reduce significantly during the 140kPa static pressure phase for this pipe or any of the others. This confirms that the gravel was able to form a stable surround medium relatively quickly upon the initial application of loading, due to its relatively poor grading.

An important point is that the ratio of the vertical diameter to the horizontal diameter remained in the range of 0.938-1.000, thus never reaching the value of 0.908 which defines “pure” elliptical deformation. This confirms that the pipe, when buried, is subject to a more complex stress distribution than (amongst others) Spangler’s simplified model, and that as a result the pipes are rather stiffer than is necessary for current installation and loading requirements. The implication is that their stiffnesses could be reduced without a dramatic reduction in performance. Alternatively, it may be feasible to specify less stiff surround materials or less onerous compaction requirements. These would have to be subject to appropriate factors of safety to guard against failure by leakage or collapse.

6.1.3 Compaction of the Surround Media by the Applied Test Pressures

The depression of the surface of the surround materials in the testing box that was noted during the tests (see 3.2.5) indicated that compaction of the surround material took place under the influence of the applied test pressures. This phenomenon is significant because of the effect that the surround density has on the deflection of a buried flexible pipe (see 2.2.2.2). The surface depression was especially significant in the case of the lightly compacted sand surround. However, this case represents a worse condition than that which would exist in a practical installation case, in which the surround would be overlaid by a stiffer (compacted) backfill material which would limit the amount of settlement observed at the surface of such an installation. Nevertheless, a surface depression of the order of 50mm, if assumed to result from the compaction of all of the sand in the box, represents a mean increase in the density of the lightly compacted sand in the box of approximately 4%. This is the same as the difference in mean densities of the sand in its lightly and heavily compacted states. In effect, the lightly compacted sand has, by the action of the repeated loading, become heavily compacted. Since the heavily compacted sand

surround resulted in small pipe deflections, the resulting further deflection of a pipe whose surround has been compacted to a similar density over time should be small. This is an important finding in that it shows that the long-term performance of a pipe buried in a “poor” surround may be acceptable once the deformation in the shorter term has been determined.

The heavily compacted sand in the testing box also densified during the test, with surface settlements of the order of 20mm. Therefore a smaller increase in density (approximately 2%) did take place, which will have caused the surround to stiffen. The increase in stiffness would however not be proportional to that achieved in the lightly compacted sand surround case, because the passive soil resistance tends to a maximum value as the total amount of settlement (represented by the lateral strain in Figure 2.5) increases. The gravel surround also compacted during testing, causing an increase in density of around 3%. This showed that, despite the notionally “self compacting” nature of uniform and rounded materials of this particle size, applied loading can agitate the particles and allow them to settle and re-orientate into a more tightly packed arrangement.

The magnitudes of the surface settlements (4% for lightly compacted sand, 3% for gravel and 2% for heavily compacted sand) show the same general trend as the pipe deflections, that is that the sand cases are extremes and the gravel case is intermediate, although the surface settlement of each surround case was not proportional to the pipe deflection recorded. The trend may indicate that surface settlement is an indicator (albeit a very crude one) of pipe deflection, since pipe deflection is dependent on surround density and density (in these cases) is dependent on settlement.

6.1.4 Experimental Repeatability

A repeat test was carried out on pipe B in a heavily compacted sand surround. Comparative test data for the installation and static pressure phases are given in Table 6.1. The lack of test data for the cyclic loading phase was due to a computer breakdown during the repeat test. The magnitude of displacements during each test was small, but the order thereof was similar for the two tests. The installation phases produced similar deflections. The 70kPa static pressure phase produced similar incremental VDSs of 0.10% and 0.09% for tests 1 and 2 respectively. The 140kPa static pressure phase (the most onerous) produced deflection increments of 0.25% and 0.10%. This was a proportionally large difference but the overall magnitude of deflection was similar in the context of the small deflections recorded.

The material unit weights in the two tests were 17.70kNm^{-3} and 18.60kNm^{-3} , a difference of approximately 5%. This would have been sufficient to give rise to the difference in

deflections (see 2.2.2.2). Therefore the installation pattern condition that required the most rigorous degree of control produced a surround that was sufficiently variable in density to cause a noticeable difference in pipe deflection. The observed difference highlights the significant effect of small variations in surround density on its stiffness and hence pipe deflection.

6.1.5 Frictional Effects of Testing Box Walls

6.1.5.1 Parametric Study of Wall Friction

It is necessary to recall Marston's Load Equation (cf 2.1.1)

$$W_c = C\gamma B_d^2 \quad \text{Eq 6.1}$$

The coefficient C was defined as follows:

$$C = C_d = \frac{1 - e^{-2k\mu'H/B_d}}{2k\mu'} \quad \text{Eq 6.2}$$

for the trench condition, where:

μ' = coefficient of friction between the surround material and the trench wall,

H = distance between top of pipe and ground level, i.e. cover depth (m),

B_d = trench width (m), and

$k = (1 - \sin\phi)/(1 + \sin\phi)$ for a soil of angle of friction ϕ (the lower case k having been adopted by Marston to avoid confusion with the bedding factor K in Eq 2.5).

The walls of the testing box were first considered as those of a wide trench. The coefficient of friction (μ') of the steel walls was determined empirically using one of the cover plates for the access holes. A bottomless concrete cube mould was placed on the steel surface and driven along it at a constant rate using a motor. This was to determine the magnitude of the frictional forces generated by the mould alone. A proving ring was used to record the load required to do this. The cube mould was then filled with surround material (sand or gravel) and a normal force of stress of 9.5kPa applied to the surface of the material using known masses. The mould was again driven along the steel surface and the shearing force measured via the proving ring. The ratio of the shear force to the normal force (corrected to allow for the presence of the cube mould) defined the coefficient of friction of the surround material on the box walls (μ'). The values of μ' were 0.31 and 0.42 for the gravel and sand surrounds respectively.

The value of k for the gravel was found to be 0.4 from shear box tests. For the sand, the extremes of 0.35 and 0.6 were assumed for the dense and loose cases respectively

(Craig, 1992). Design guides for pipes (Young et al, 1986) state that a value of 0.13 should be used as an upper limit for the product $k\mu'$.

The theoretical loads on a pipe of 0.6m diameter at a cover depth of 1.0m were calculated for trenches in normal soils having widths of 0.9m and 1.2m (the extreme values for pipes of diameter 0.6m (according to DoT, 1993), assuming $k\mu'=0.13$, and a soil unit weight of 20kNm^{-3} . The theoretical loads were 15.6kNm^{-1} and 21.6kNm^{-1} respectively.

The loads predicted using the measured frictional parameters and a trench width equal to that of the box (viz. 1.8m) were 33.6kNm^{-1} (gravel), 33.2kNm^{-1} (well compacted sand) and 31.40kNm^{-1} (lightly compacted sand) for a soil unit weight of 20kNm^{-3} and a cover depth of 1.0m. These were all considerably higher than that expected for conventional trench situations. However, the influence of the remaining two box walls must be accounted for. The computed values of C_d for these were 0.61, 0.60 and 0.57 for gravel, well compacted sand and lightly compacted sand respectively. These coefficients must be reduced to reflect the narrower trench that they represented, since the loading on a pipe in a trench varies as the square of the trench width. This had the effect of reducing the loads predicted in the testing box to 14.2kNm^{-1} , 13.8kNm^{-1} and 13.1kNm^{-1} for the three surround cases. These represent, respectively, 91%, 88% and 84% of the load predicted for a 0.9m wide trench and 66%, 64%, and 61% of the load predicted for a 1.2m wide trench. Thus the box walls were sufficiently distant to allow for a reasonable representation of a narrow trench, but underestimated the load applied to a pipe in the widest permitted trench.

The presence of the trench walls clearly affected the magnitude of the loads applied to the pipe, and because deflection is assumed dependent on load, the pipe deflections recorded in the laboratory will underestimate the realistic deflections of a pipe buried on site by a proportionate amount. The largest discrepancies between predicted and actual loads relate to the lightly compacted sand case, for which an extreme value of k (0.6) was selected. Since it is unlikely that a sand surround would be placed in the extremely loose state that this value represents (as the densities quoted in Tables 5.2 and 5.3 show) these discrepancies may be unnecessarily pessimistic. Nevertheless, the values of the applied loading, and hence deflection should be corrected by between 10% and 50% depending on the trench width.

6.1.5.2 The Effect of the Less Frictional Box Wall Facing

The effect of facing the box walls with the polythene-wrapped plywood can be seen by comparing the results in Tables 5.8 and 5.20 (for pipe B in the lightly compacted sand surround) and Tables 5.9 and 5.21 (for pipe B in the gravel surround).

For the lightly compacted sand case, the VDS at the end of installation was twice the value recorded for the un-faced box walls, (0.32% compared to 0.16%) Some of this discrepancy may be ascribed to variations in the state of compaction of the sand within the test box. This is confirmed by the observation that the difference in these results is comparable to the range of VDSs observed for the installation phase for all of the tests in the main programme, mostly as a result of particular installation events. Therefore the frictional effects of the box walls are insignificant at this stage.

During the 70kPa static pressure phase, the maximum VDSs recorded were 1.54% (faced walls), and 1.65% (or 7% greater) for the unfaced walls case.

At the peak of the 1000th cycle of the 70kPa cyclic pressure, the VDSs were 3.80% and 2.94% for the unfaced and faced wall cases respectively, and the values following the four hour relaxation period were very close, with that for the faced wall case (2.93%) being slightly less than that for the unfaced case (3.09%).

The 140kPa static pressure phase produced instantaneous values of VDS of 2.62% (faced walls) and 3.58% (unfaced walls). Following 24 hours of loading, the deflections were 3.73% and 2.79% for the respective cases. On release of the pressure, the pipe recovered to a larger extent when buried in the faced box. It would appear, therefore, that the lower friction of these walls allowed upward movement of the soil plug after it was unloaded.

The effect of reducing the box wall friction was considerably more marked when the pipe was buried in gravel (see Tables 5.10 and 5.21). The VDS at the end of the installation phase was 0.68%, compared to 0.28% for the unfaced wall case. The maximum loads reached during the 70kPa static pressure phase were 1.94% and 0.92% for the faced and unfaced cases respectively. This very large difference shows that the gravel is more susceptible to the frictional effects of a trench wall than is sand. One explanation is that the gravel particles, which are relatively smooth, can slide easily down the polythene surface whereas the sand, behaves more as a single body and moves downwards as a "plug" of material.

The maximum VDSs observed during the 140kPa static pressure phase were 3.15% and 1.69% for the faced and unfaced cases respectively. The change in deflection during the 24 hours that the pressure was applied was more marked in the latter case. This indicates that the gravel surround continued to move as a result of the lower frictional resistance of the box walls.

There was some variation in the results for the lightly compacted sand surround case which did not clearly show that the frictional test box walls had a marked effect on the pipe deflection. This suggests that the effects of the test box walls are small in comparison to those of the surround material stiffness. However the two tests carried out using the gravel surround, which gave a more uniform surround (see Table 5.4), did confirm clearly that the frictional effects of the

test box walls were significant. It would therefore be prudent to adopt low-friction box walls for future testing, both to represent a worst case of installation and to obtain larger pipe deflections.

6.1.6 Integrity of Deflected Joined Pipes

The maximum VDS achieved at an applied static pressure of 160kPa was 1.2% for the gravel surround and 7.8% for the (very) lightly compacted sand surround. At these deflections, the integrity of the pipelines was maintained and no pressure drop was observed when air tests (DoT, 1993) were carried out.

The deflection of 7.8% recorded for the lightly compacted sand is significant for three reasons. The first is that such large deflections do not disrupt the sealing mechanism, and thus pipes that experience these deflections (very deep burial or accidental heavy loading by construction traffic where unprotected being examples) will not leak. The second reason concerns the 5% VDS limit commonly applied to buried pipes (see 2.2.7). The result suggests that this limit is unnecessarily onerous for the purposes of pipe leakage control. The third reason, which is related to the foregoing two, is that the use of a very poor surround caused pipe deflections that, although large, were not excessive (and did not approach the 20-30% limit at which “snap-through” buckling may occur) and did not cause a leak in the pipe. In the light of these observations, it may be possible to reconsider the deflection limit and (although appropriate factors of safety would have to be defined) pipe design and installation criteria.

The deflection data cannot be compared directly with those of the main test programme because of the difference in loading patterns. Nevertheless, the maximum VDS of 7.8% recorded for the very lightly compacted sand case is interesting because it is more than twice the maximum recorded in the main test programme (3.73% for pipe B at the end of the 140kPa static pressure phase). The result demonstrates the disproportionately large benefit to the buried pipe of even minimal compaction such as that provided for the lightly compacted sand case in the main test programme. The difference in the unit weights of the sand in each case was approximately 10%, but this caused a much larger difference in pipe deflections. Thus the very lightly compacted sand allowed wholly acceptable pipe performance (since the pipe did not leak), but the effect of minimal compaction (quite possibly less than would be provided on site during placement and incomplete treading) was to produce markedly better pipe performance.

6.1.7 Application of Impact Loading to a Shallowly Buried Pipe

These tests were carried out on pipes of 600mm nominal internal diameter buried to cover depths of 300mm. For the pipe buried in Type 1 sub-base, the first loading phase

(comprising 72000 cycles of a load of 40kN acting on a plate of plan dimensions 450mm by 300mm) produced a final peak value of VDS of 2.5%. The second loading phase (comprising 5000 cycles of a load of 90kN acting on the plate) produced a peak final VDS of 3.7%.

The pipe buried in flint alone showed a peak VDS of 4.2% before the loading plate sank excessively into the surround after 65 cycles of the 40kN load. The plate travelled to within 100mm of the pipe crown. Following the placing of the Type 1 sub-base layer, the peak VDS recorded at the end of the 40kN phase was 5.5%. The 90kN load phase produced final VDSs of 5.9% (under loading) and 5.8% (with loading released), including the VDS remaining at the end of the previous test (i.e. that due to excessive settlement of the plate). The outer wall had some scratches from the movement of flint particles, but no damage was found on the internal wall and the pipe remained airtight.

These results showed that the pipes tested were sufficiently robust to withstand severe loading at very low cover depths. The 5% deflection limit (BSI, 1980) was not exceeded when the pipe was buried in Type 1 sub-base. The limit was breached during testing of the pipe buried in flint, but this was partly the result of the excessive movement of the loading plate through the flint surround. Notwithstanding this, the slight breach of the limit occurred only under extreme conditions of installation and loading and the pipes performed well in this context. In addition, it was seen that surround materials that are considerably more angular than those generally permitted do not cause significant damage to the pipe.

6.2 CALCULATION OF SOIL STIFFNESS, DEFLECTION LAG

FACTORS AND TRAFFICKING FACTORS FROM TEST DATA

6.2.1 Determination of Soil Stiffness and Deflection Lag Factors from Laboratory Test Data

The Iowa Method is acknowledged as the simplest method of pipe deflection prediction of those discussed in Chapter Two, and is widely used in routine deflection calculations. Therefore, the laboratory test data have been analysed in relation to this method. Values of the two of the principal variables that are the least well defined (E' and D_L) have been determined as described below.

6.2.1.1 Estimation of the Modulus of Soil Reaction, E'

The modulus of soil reaction E' has been calculated with reference to the static pressure phases in the laboratory tests. The recorded deflection data were substituted into the Iowa formula (Eq 2.6), which was then solved for E' . The load per unit length of pipe due to the fill in the box was calculated using Eq 2.2. The load per unit length due to the static pressure in the water bag was calculated using Eq 2.4. The effect of the trench walls perpendicular to the pipe axis were also accounted for.

The results are given in Table 6.2, 6.3 and 6.4 for each surround type. E' was evaluated in four ways, using data from different loading patterns, in order to determine the effect of the stress history on soil stiffness. The four values are quoted for each pipe in each type of surround, and are defined thus:

$E'(1)$ = value obtained using the deflection recorded at the end of the 70kPa static pressure phase,

$E'(2)$ = value obtained using the increment of deflection change recorded during the 70kPa static pressure phase,

$E'(3)$ = value obtained using the cumulative deflection recorded at the end of the 140kPa static pressure phase, and

$E'(4)$ = value obtained using the increment of deflection change recorded during the 140kPa static pressure phase.

$E'(1)$, $E'(2)$ and $E'(3)$ show reasonable agreement for the lightly compacted sand and gravel surround cases, although those for pipe D are higher than the others. The rounded mean values of E' using these three calculation methods are 17MPa for the lightly compacted sand case and, 33MPa for the gravel case.

However, $E'(4)$ is appreciably higher, with a mean value of 94MPa for the lightly compacted sand surround. The reason for this extremely high value is that the earlier loading phases compacted the surround material. This was noticed for some of the tests on removal of the box lid. The compaction allowed passive resistance in the soil to be mobilised at smaller strains (or pipe deflections) in the last pressure phase. This point is well illustrated by the similarity of $E'(4)$ for lightly compacted sand to $E'(3)$ for heavily compacted sand, with respective mean values of 94MPa and 81MPa, and confirms that the compaction of the former by the applied pressures caused it to become similar in stiffness to the latter (see 6.1.6).

The mean value of 148MPa obtained for gravel during the 140kPa static pressure phase must be treated with caution because it may have been influenced by the presence of the test box walls to a larger degree than the other surround types. The application of large static pressure

to the nominally single-sized surround would be expected to have caused a stiff matrix to form as the gravel particles impinged on each other and bore onto the box walls. In the field, it may be more likely that individual gravel particles would be able to penetrate the trench walls, leading to larger pipe deflections and a consequent reduction in back-calculated values of E' .

The values of E' obtained for the heavily compacted sand surround case represent the likely maximum in ideal conditions. The mean value of 74MPa (Table 6.4) may be appropriate as a conservative design value for this surround case because it is not influenced by some of the very large values that were obtained using extremely small measured deflections.

The values of E' recorded in the tables are considerably higher than those currently used (cf. Table 2.1, in which values of E' range from 0 to 20.57MPa). This may be partly due to the laboratory conditions (especially in the case of the gravel surround). Another reason is that the materials in Table 2.1 do not accurately reflect the materials and conditions used in the UK. Nevertheless, there appears to be a consistent underestimation of the stiffness of the soil surrounding a buried plastic pipe and a consequent overdesigning of the pipe, its surround and its installation environment. Recommended design values for UK applications, obtained from those used for the design of drainage installations (DoT, 1990) are 2MPa for sandy surrounds and 5MPa for granular surrounds.

Since the range of values of E' calculated in this research are much higher than those currently used, a reappraisal of soil stiffness data would be in order. The adoption of a factor of safety would be appropriate, and is usual in all other branches of civil engineering design. The factor of safety for imposed loading that is used in structural calculations is 1.6, and when this is applied to the mean values of E' from Tables 6.1, 6.2 and 6.3, the rounded values obtained are:

- (i) $E' = 10\text{MPa}$ for lightly compacted sand,
- (ii) $E' = 40\text{MPa}$ for heavily compacted sand, and
- (iii) $E' = 20\text{MPa}$ for gravel.

These remain somewhat higher than current values. There is clearly a case for the confirmation of these values by field observation. A suitable method would be a series of incremental plate-loading tests carried out on buried pipes that contained deflection measurement equipment.

6.2.1.2 Estimation of the Deflection Lag Factor, D_L

It has been demonstrated that the application of a static pressure to a buried pipe initially produced a rapid increase in pipe deflection. When the static pressure had stabilised the rate of deflection slowed markedly, by a degree dependent on the type of pipe surround. The rate of increase of VDS was largest for the lightly compacted sand case, smaller for the gravel case

and very small for the heavily compacted sand case. This phenomenon was termed the “deflection lag” by Spangler (1941), and a factor of 1.5 was found empirically (for the case of large steel culverts) which related the initial deflection to that which may be expected 50 years into the future.

The laboratory data have been analysed to estimate values of the deflection lag factor (D_L) for two surround conditions. The 70kPa static pressure phase was used for this exercise in preference to the 140kPa static phase, this was because the deflections measured in the latter may have been affected by the earlier cyclic pressure phase. The lightly compacted sand and the gravel cases were considered. The heavily compacted sand case was not considered because of the extremely small deflection lag recorded, which in some cases were negative or close to the accuracy of the measurement equipment.

The deflections recorded between one hour after load application and the end of the test phase were analysed. This portion of the curve was found to be a gradual slope for all tests. An EXCEL spreadsheet-based least-squares method of curve fitting was used to determine the best-fitting trend line to each test data series. It was found that a power curve of the form:

$$VDS = At^B \quad \text{Eq 6.3}$$

(where t is time and A and B are constants) provided the best fit.

The justification of extrapolation of deflection data to large degrees was discussed in 2.2.1.3. The same arguments apply to this exercise, and the results will be subject to a margin of error. The degree of fit of the test data to the trend curves, is therefore important, and this is considered in the calculations.

The range of the correlation coefficient R^2 was 0.892 to 0.977 for the lightly compacted sand case (neglecting an anomalous value of 0.70) and 0.836 to 0.995 for the gravel case. The tests relating to the highest value of R^2 for each surround case (pipe D in both cases) were used for forward prediction of the pipe deflection.

These were related to the initial (one hour) deflections as a ratio, which defined the deflection lag factor. Table 6.5 and 6.6 show the values determined for each of the two surround types for a range of time periods.

The predicted value of D_L of 1.59 for the lightly compacted sand case after fifty years of burial is slightly higher than that found by Spangler. Because of the poor installation condition that this represents it may be regarded as an upper limit. The lower value of D_L for the gravel case (1.28) shows that this surround is more able to resist gradual pipe deflection, although this would be affected in the laboratory by the trench walls. The relatively small variation of D_L at longer times shows that the pipe-soil system becomes stable if not acted upon by external forces, and provided also that the mode of deflection of the pipe does not change,

- which is unlikely at small deflections. The effects of creep of the pipe material may affect the long-term deflection of the pipe, and these have been discussed in 2.2.6.1 and 5.1.3.4. In the static pressure phases, the circumferential wall strain (and hence stress) continued in general to rise over the 24 hour test period, which would be larger in magnitude than the effects of creep over this time. However, the long term performance of a buried plastic pipe (as the deflection under loading decelerates) may be more significant and would require long-term testing to quantify.

6.2.1.3 Estimation of Trafficking Factors

The VDS data obtained from the laboratory tests (Figures 5.5 to 5.21) show that the test pipes deflected by different amounts as they were subjected to the cyclic pressure. This has been ascribed primarily to installation conditions. However, the trend of the increase in VDS was of a similar pattern for each pipe, namely a rapid increase at first followed by a more gradual increase. There may therefore be a general relation between the number of loading cycles and the deflection, and such a relationship would be useful for the estimation of the pipe deflection after a large number of loading cycles.

The graphs of VDS against the number of loading cycles are of the general shape of a power curve. The test data have been analysed using the EXCEL curve fitting facility. The general equation of the power curve is:

$$\text{VDS} = aN^b \quad \text{Eq 6.4}$$

where a and b are constants and N is the number of loading cycles.

The heavily compacted sand cases produced less accurately defined curves because of the small deflections recorded, which in some cases were at the limit of accuracy of the measurement equipment, and the correlation coefficients were relatively poor (0.923 and 0.951 for the two tests that could be analysed). These tests were not analysed in detail.

The range of correlation coefficients for the power curves was 0.970 to 0.990 for the lightly compacted sand and gravel cases. The test data were used to produce equations that related the VDS to the number of cycles. These were then used to predict the VDS at 1 000 000 loading cycles. This value was then related to the VDS measured at 1, 10, 100 and 1000 loading cycles in terms of multipliers which are now termed “trafficking factors”. The results are given in Table 6.7 and 6.8.

The trends for the lightly compacted sand case were:

- (i) the deflection at 1 000 000 cycles is between 2.4 and 3.8 (with a mean of 3.2) times the deflection at 1000 cycles,

- (ii) the deflection at 1 000 000 cycles is between 3.1 and 5.9 (with a mean of 4.7) times the deflection at 100 cycles,
- (iii) the deflection at 1 000 000 cycles is between 4.2 and 11.9 (with a mean of 9.2) times the deflection at 10 cycles, and
- (iv) the deflection at 1 000 000 cycles is between 5.8 and 32.8 (with a mean of 25.3) times the deflection at 1 cycle.

For the gravel case, the trends were:

- (i) the deflection at 1 000 000 cycles is between 2.1 and 2.6 (with a mean of 2.4) times the deflection at 1000 cycles,
- (ii) the deflection at 1 000 000 cycles is between 2.8 and 3.5 (with a mean of 3.1) times the deflection at 100 cycles,
- (iii) the deflection at 1 000 000 cycles is between 4.3 and 6.2 (with a mean of 5.2) times the deflection at 10 cycles, and
- (iii) the deflection at 1 000 000 cycles is between 5.9 and 11.5 (with a mean of 9.8) times the deflection at 1 cycle.

The ratios relating to the first pressure cycle display the greater scatter because of the small deflections measured at the first cycle. As the number of cycles (and the magnitude of the pipe deflections) increased, the scatter of results decreased and the ranges of the extrapolated results decreased. This may also be due to the stiffening and conditioning of the surround by the repeated loading, which results in a more uniform soil. The mean values of the trafficking factors were greater for lightly compacted sand than for gravel. This confirms that the deflection accumulated less rapidly in the case of the lightly compacted sand as a result of the greater amount of soil strain required to mobilise the passive resistance of the surround to pipe deflection. The trafficking factors for the lightly compacted sand surround also possessed a greater degree of scatter which is indicative of the less uniform stiffness that was achieved in this material. The relatively gradual decrease of the trafficking factors as the number of cycles increases (in both surround cases) shows that the rate of increase in pipe deflection decreases significantly with repeated loading.

6.2.2 Estimation of Trafficking Factors from Field Test Data

The method of analysis adopted in 6.1.11.3 was applied to the field data. Again the power curve gave the best fit, with correlation coefficients ranging from 0.960 to 0.993. The correlation coefficients were generally slightly lower than those for the laboratory data, indicating

that the field results were prone to greater scatter. This would most likely have been due to the more practical nature of installation practices on site, in which case the data now presented would be more representative of realistic pipe installations.

The appropriate field VDS measurements, predicted VDS at 1 000 000 loading cycles and computed trafficking factors are presented in Table 6.9 and 6.10 for the sand and gravel surround cases respectively. Pipes B and C in sand and pipe B in gravel were not included because extrapolation of the VDS gave values at 1 000 000 cycles exceeding 20%, which would not occur in practice because of the restraining nature of the surround material. Pipe D in sand was not included because of the inaccuracy of the potentiometer used to record its deflection.

For the sand cases, the results were:

- (i) the deflection at 1 000 000 cycles is between 6.1 and 9.1 (with a mean of 8.2) times the deflection at 1000 cycles,
- (ii) the deflection at 1 000 000 cycles is between 14.1 and 18.1 (with a mean of 15.5) times the deflection at 100 cycles,
- (iii) the deflection at 1 000 000 cycles is between 19.2 and 38.6 (with a mean of 26.3) times the deflection at 10 cycles and
- (iv) the deflection at 1 000 000 cycles is between 42.5 and 95.2 (with a mean of 63.0) times the deflection at 1 cycle.

For the gravel cases, the results were:

- (i) the deflection at 1 000 000 cycles is between 4.4 and 9.8 (with a mean of 7.3) times the deflection at 1000 cycles,
- (ii) the deflection at 1 000 000 cycles is between 12.3 and 19.9 (with a mean of 16.5) times the deflection at 100 cycles,
- (iii) the deflection at 1 000 000 cycles is between 16.2 and 36.4 (with a mean of 27.3) times the deflection at 10 cycles and
- (iv) the deflection at 1 000 000 cycles is between 39.8 and 92.3 (with a mean of 66.9) times the deflection at 1 cycle.

Factor (iv) again exhibits the greatest scatter in both surround cases because of the small deflections recorded during the first cycle. The mean values of each trafficking factor were greater for the field data than for the laboratory data. This would have been due partly to the greater degree of variability of site installation practice. The difference in boundary conditions in the field may also have influenced the pipe deflections.

The mean trafficking factors are remarkably similar for both surround types. This would suggest that in a practical installation factors such as installation procedures and trench conditions are more influential than the particular properties of the surround.

The trafficking factors may be used in various ways. The first loading cycle is important because the deflection can be calculated using, for instance, Marston's load theory (2.1.1) or by using soil mechanics techniques (e.g. Boussinesq's Theory). The deflection after several loading cycles may therefore be estimated in terms of this initial deflection. The first ten loading cycles may be easily carried out on site in a relatively short time in cases where the long-term integrity of a buried pipe needs to be assessed. This could be done with greater accuracy by carrying out 100 or 1000 loading cycles, but this may be uneconomical and time-consuming.

6.3 COMPARISON OF LABORATORY AND FIELD RESULTS

6.3.1 Introduction

The aim of this section is to compare critically the laboratory and field tests in order to ascertain whether the laboratory testing method is representative of field conditions. This is important because a representative laboratory test will be somewhat more economical to perform than full-scale field testing, and would therefore provide a useful and justifiable means by which to investigate pipe design, installation and loading specifications (see 2.5.2).

When comparing the results of the laboratory and field work, it is necessary to recognise the differences between the two sets of tests. These were due to both experimental and practical factors.

The installation and cyclic loading phases of the laboratory and field work involved similar processes and data for these phases may be compared. The static loading phases carried out in the laboratory had no equivalent in the field work. The results of this phase are therefore not considered in detail, although their effects are commented upon.

The relevant test data are summarised in Table 6.11. The test phases are represented thus:

SI - VDS at start of installation phase,

EI - VDS at end of installation phase,

E70CT - Total cumulative VDS at end of 70kPa cyclic pressure phase (i.e. including VDS accumulated during 70kPa static pressure phase.

E70CN - nett increase in VDS during cyclic pressure phase, and

E70CIT = EI+E70CN (i.e. VDS at end of installation plus nett increase in VDS during cyclic pressure phase).

The laboratory data for cyclic pressure phase is treated in three ways. The total VDS at the end of this stage is included for comparison with that obtained for the field test in order to determine whether the intermediate 70kPa static pressure phase had an effect on the pipe

deflection. The nett increase in VDS during the cyclic pressure phase is comparable between laboratory and field. The sum of the (nett) VDSs attained during the installation and cyclic loading phases in the laboratory is included since these phases are comparable to the complete field testing sequence (i.e. installation and trafficking).

6.3.2 Installation Phases

There were necessary differences in installation techniques between the laboratory and field tests. The laboratory test installation-procedures were designed for repeatability within the confined space of the test box. The field test reflected site practice and although the work was diligently executed by the site operatives, there would have been a degree of variability between individual installations. This was partly responsible for the degree of scatter observed in the field. The magnitudes of VDS during the installation phase were larger (by a factor of up to four) in the laboratory tests than the field tests in all cases except that of pipe B in gravel. The larger VDSs obtained in the field show that the installation practices (notably compaction of the trench fill) were more severe than those in the laboratory tests. This was due at least in part to the use of mechanical plant in the field, which would have generated larger transient stresses on the pipe than the manual methods used in the laboratory. In addition, because the trench walls on site are likely to be less stiff than the test box walls, the compaction plant may have allowed greater penetration of the trench walls by gravel particles, leading to larger displacements of the soil and the pipe. The anomalous result for pipe B in gravel shows that the site procedures were subject to a degree of variability.

Because the field trial used relatively severe compaction methods, the VDSs recorded may be considered to be near the upper limit typical "construction values". The maximum VDS recorded during the installation phase in the field (1%) should serve as the expected maximum for standard conditions. This would be useful in calculations of pipe deflections in design as an allowance for deflection during installation.

6.3.3 Cyclic Loading Phases

The cyclic loading waveform used in the laboratory testing (see 3.1.2) was designed to approximate to the shape of the vertical stress distribution in the region of a point load (see 2.2.5.2 and Figure 2.12). This would have resulted in soil stresses that varied in magnitude, but the principal plane of which did not change in orientation. The pipes under this type of loading

deformed largely symmetrically around the vertical pipe axis. The vehicular loading used in the field was different in nature in that its movement over the pipe would have led to rotation of the principal stresses at a point in a soil (near the pipe crown, for instance). This was seen to result in a different manner of deformation, in which a “wave” of deformation travelled over the pipe. (see 4.3.4). The detailed effects of these different soil stress states has not been considered, and the general similarity in the trends and orders of magnitudes between laboratory and field suggests that the effects may be of secondary significance in the context of this research.

The installation conditions in the laboratory and field would have caused differences in the proportion of the applied cyclic loading that was exerted on the buried pipes. In the laboratory, the surround material (sand or gravel) also served as the backfill material, resulting in a homogeneous body whose stress characteristics could be analysed using conventional soil mechanics techniques. The magnitudes of the applied cyclic pressures were different in the laboratory and field tests. In the laboratory work, the applied pressure of 70kPa must be reduced by approximately 15% to account for the frictional effects of the perpendicular trench box walls for a narrow trench case (see 6.1.5). Because of the frictional effects of the box walls were similar in magnitude to those of a conventional trench, the load on the pipe (computed from Marston Theory) was approximately 90% of the prism load, leading to a stress on the pipe crown of approximately 53kPa.

In the field, the surround material was overlaid by granular, well graded trench fill (Type 1 sub-base), a layer of geotextile and a haul road made from Type 1 sub-base. This would not form a homogeneous body and the stress characteristics of each layer would be different. Consideration of the soil as a homogeneous medium, and applying Boussinesq theory for point loads, resulted in a value of 26kPa for the stress at the depth of the pipe crown directly under the wheel. Consideration of the wheel imprint as a circular area yielded a value of 24kPa for the stress at the pipe crown. Newmark’s method yielded a value of 20kPa, although this last method was near its limits of application. These calculated values are upper limits because they do not take into account the frictional resistance offered by the trench walls or the “spreading” of the surface loading by the haul road, both of which would reduce the stress at the pipe crown by some degree.

The way in which the VDS increased under repeated loading differed between laboratory and field. In the laboratory, the deflection built up relatively rapidly (see Figures 5.15 to 5.17). In the field, the deflection built up at a slower rate (see Figures 5.26 and 5.27). The principal cause of this was the difference in the boundary conditions of the two test environments. The restrained steel walls of the laboratory testing box were unyielding to outward movement by the action of the surround material *en masse*. However, such outward movement that did occur, and the forces associated with them would not cause the steel to yield. The movement would be elastic

in nature and the wall would recover to its original position on release of the loading. In addition, its strength would not allow penetration of the walls by individual particles (of gravel) that caused high point loads. The trenches in the field were cut in a clay which, although stiff, would exhibit a larger propensity to plastic (i.e. non-recoverable) deformation under loading. In addition, the clay would be locally more likely to deform under the action of point loading by larger particles of surround or trench fill material. These additional soil movements would lead to a greater degree of soil deformation which had a larger non-recoverable element, thus increasing the magnitude and reducing the rate of accumulation of pipe deflection. The effects would however be slightly offset by the increase of the frictional resistance of the trench walls as a result of the particle penetration.

The magnitude of deflections recorded in the laboratory and field tests are compared in Table 6.11. For the sand surround case, the total VDS recorded in the field (E70CT) was generally comparable in magnitude to that recorded in the lightly compacted sand case in the laboratory, although there was no clear trend of one test environment resulting in consistently larger deflections and pipe E demonstrated an exceptionally small deflection in the field.

The increments (i.e. nett change) of VDS during cyclic loading (E70CN) recorded in the laboratory and field tests were similar for some pipes for the sand surround case (e.g. pipes A and C), but not in others. There was still a degree of variability in the lightly compacted sand surrounds in the laboratory after “conditioning” (i.e. stiffening) by the static pressure phase. This implies that the greatest degree of soil conditioning results from loading that is cyclic in nature as opposed to static. Nevertheless, the lightly compacted sand surround reduced the effect of the stiff box walls and as a result represented more accurately the boundary conditions and pipe-soil system of the moderately compacted sand case in the field.

The total and nett VDSs at the end of the cyclic pressure phase were in all cases greater in the field than in the heavily compacted sand cases in the laboratory. The heavily compacted sand case was therefore not wholly representative of normal compaction in the field. Additionally, if a heavily compacted sand was used in the field, the less stiff boundary conditions there may allow for greater surround movement with a consequent (small) increase in pipe deflection. Therefore, the heavily compacted sand case achieved in the laboratory represents the upper limit of surround soil stiffness.

Comparison of the sum of the VDSs recorded during installation and cyclic loading (E70CIT) shows that (with the exception of pipe E in sand) the deformations recorded in the field were greater than those in the laboratory (by a factor of 1.5 to 3 in general), regardless of surround type. These data are comparable because they relate to similar test phases (i.e. installation and cyclic loading). The larger deflections experienced in the field may be due in part to the lack of

conditioning by a static pressure phase, but the less stiff boundary conditions would also have led to larger deflections in the field.

For the gravel surround case, the total VDSs at the end of the cyclic loading phase (E70CT) were broadly similar. The VDS increments during installation and cyclic loading (E70CIT) were also similar in magnitude, but in all cases these quantities were larger for the field testing. These observations indicate that the installation and cyclic loading phases in a gravel surround in the laboratory were comparable and that the effect of the intermediate static loading phase was small. The larger overall deflections suggest that the frictional and boundary effects had an effect on pipe performance for this surround type.

It can be seen that the rate of accumulation of VDS was more uniform throughout the tests carried out in the field compared to those carried out in the laboratory. The less uniform rate observed in the laboratory (in which the rate was initially high and reduced as the test progressed) may have been due to the presence of the stiff and unyielding test box walls. During the early loading cycles, the material surrounding the pipe springers would move outwards by a degree that depended on the type of surround. The steel box walls would act as an artificially strong boundary that effectively limited the zone of these soil movements. The result of these would be to increase the stiffness of the pipe surround material (by compaction) and thereby lead to a progressive reduction in the measured pipe deflection. In the field, the trench walls would be more susceptible to local yielding, and the less restrained (including in the longitudinal pipe direction) surround material would have a greater facility for movement during sustained cyclic loading. The rate of accumulation of VDS would reduce as the soil movements reduced (again by compaction), but it would be expected that this would occur after a greater number of loading cycles in the field.

The frictional effects of the two sets of boundary conditions would have differed slightly. The frictional effects of the steel walls of the laboratory testing box (see 6.1.9) were ameliorated by their relative remoteness from the pipe, and this was calculated to reduce their effects to normal magnitudes. In the field testing, the trenches were certainly representative of normal practice, but the penetration of particles of fill (and possibly surround) material as a result of the compaction process may have increased the frictional properties. However, these effects could not be measured in the field. An important point in this area is that of the effect of water on the trench walls. If the clay is wet, it will soften and be more easily penetrated. This will have the greatest effect when the surround and fill materials are compacted.

The larger deflections in the field must also be considered in terms of the smaller (by about 50%) soil stresses at the pipe crown in these tests. The generally larger deflections (in terms of the quantity E70CIT) observed in the field which suggests that the laboratory test conditions are conservative in relation to the conditions in the field. This has already been ascribed to differences

in boundary conditions such as the proximity and frictional characteristics of the test box walls. The larger deflections recorded in the field under the action of smaller stresses suggests that the combined frictional and restraining effects of the test box walls are somewhat larger than “normal” site installation environments. There are, however, factors that may be considered to reduce the disparity between the tests. Firstly, the lack of a pavement structure (comprising a deeper layer of sub-base and a macadam or concrete surfacing) led to higher stresses at the pipe crown in the field trial than would occur in pipes buried under highways. The presence of these layers would lead to smaller pipe deflections in the field. Clearly, if the load “spreading” effects of pavement layers and depths of installation were calculated, it would be feasible to adjust the magnitude of the applied pressures in the laboratory test to reflect particular installations.

6.3.4 Trafficking Factors

There were differences in both the magnitudes and ranges of the trafficking factors calculated in 6.1.11.3 and 6.2.3 (see Tables 6.7 to 6.10). The field tests produced larger trafficking factors than the laboratory, which indicates that the deflections in the field after a very large number (e.g. 1 000 000) cycles are likely to be higher. This is consistent with the effect of the boundary conditions discussed in 6.3.3.

The factors calculated for both cases showed the greatest divergence between laboratory and field for the initial loading cycles, where the small deflections and differences in installation conditions had the greatest effect on the pipe deflection. As the number of loading cycles increased the movements of the pipes and surrounds would cause the surround to stiffen in the general manner shown in Figure 2.5 which would have reduced (to an extent) the differences in the surround conditions between laboratory and field. The trafficking factors the show closest agreement, and least scatter, at 1000 cycles, suggesting that in the very long term the rates of accumulation (and by implication the surround conditions) become more similar. This may be expected following sustained cyclic loading which has formed surrounds of reasonably similar particle packings that are both stiff and stable. Nevertheless, in the medium term it would be the case that the field condition would lead to larger deflections for the reasons described in 6.3.3.

In the field tests, the trafficking factors showed less difference between the sand and gravel surround cases than in the laboratory tests. This was partly due to the greater compactive effort applied to the sand surround in the field. However, the overall similarity in field conditions suggests that the two types of pipe-soil systems behaved similarly under cyclic loading. It is therefore possible that the absence of rigid boundaries and the greater facility for surround particle

movement in the field would offset any difference in the behaviour of these surrounds in the long term, with a consequent equalising effect on pipe deflection.

It is possible to establish a "rule of thumb" for the quick estimation of the long term pipe deflection based on field data. The maximum values obtained for each factor (regardless of pipe or surround type) may be rounded up to give approximate, conservative trafficking factors. The values so obtained estimate the deflection at 1 000 000 cycles to be (approximately) 10 times the deflection at 1000 cycles, 20 times the deflection at 100 cycles, 30 times the deflection at 10 cycles and 70 times the deflection at 1 cycle.

6.3.5 Concluding Discussion

The above discussion has shown that there were differences in the surround types, boundary conditions and applied soil stresses of the laboratory and field tests.

The sand surround cases in the laboratory and field test are not directly comparable because of the different states of compaction adopted. Nevertheless, certain trends can be identified. The field data correspond more closely to the lightly compacted sand case than the well compacted case, for which the VDSs were extremely low. It is probable that the heavily compacted sand in the laboratory test was well constrained by the box walls, which produced a very stiff system. The sand used in the field work was not so heavily compacted and, in combination with slightly less stiff trench walls, caused larger VDSs to occur. This means that the larger VDSs recorded in the field may be due to a combination of the state of compaction of the soil and the soil in which the trench was constructed, rather than the state of compaction alone. Therefore, the pipe-soil-trench *system* on site was more accurately represented by the lightly compacted sand case in the laboratory.

The use of a gravel surround in a rigid test box would have led to smaller pipe deflections because the relatively large and uniform particle size would facilitate the more rapid formation of inter-particle point forces that eventually be influenced by the stiff box walls. This would not occur in the field. In this surround type, the laboratory environment would tend to give rise to conservative pipe deflections.

The boundary conditions in the laboratory were assessed and found to be more frictional than those expected in field conditions. Nevertheless the deflections recorded in the laboratory were smaller, despite the larger calculated surface stresses. This important point may be resolved by experimental means (such as the use of pressure cells) or by the calculation of pipe crown stresses in the field and the subsequent adjustment of the applied cyclic pressure in the laboratory. Once the laboratory test equipment had been so "calibrated", the applied pressure

Table 6.1. Experimental Repeatability as Determined by Two Tests on Pipe B in Heavily Compacted Sand Surround.

PHASE	VDS(%) TEST 1	VDS (%) TEST 2
SI	0.00	0.00
EI	-0.35	-0.38
E70L	-0.27	-0.18
E70C	-0.25	-0.29
E70U	-0.29	-0.38
E70R	-0.29	-0.29
E140L	-0.07	-0.22
E140C	-0.04	-0.19
E140U	-0.15	-0.32
E140R	-0.17	-0.32

SI - start of installation

EI - end of installation

E70L - start of 70kPa static pressure application

E70C - end of 24 hours of 70kPa static pressure application

E70U - release of 70kPa static pressure

E140R - end of recovery period following release of 140kPa static pressure

E140L - start of 140kPa static pressure application

E140C - end of 24 hours of 140kPa static pressure application

E140U - release of 140kPa static pressure

E140R - end of recovery period following release of 140kPa static pressure

Table 6.2. Estimation of E' for Lightly Compacted Sand from Laboratory Test Data.

PIPE	E'1(MPa)	E'2(MPa)	E'3(MPa)	E'4(MPa)	MEAN E'1, E'2, E'3
A	12.5	15.3	11.1	95.5	
B	13.8	17.6	10.1	74.1	
C	16.2	16.6	10.8	81.5	
D	26.5	32.4	19.1	110.0	
E	19.8	19.8	12.3	110.0	
MEAN	17.8	20.3	12.7	94.2	16.9 MPa

Table 6.3. Estimation of E' for Heavily Compacted Sand from Laboratory Test Data.

PIPE	E'1(MPa)	E'2(MPa)	E'3(MPa)	E'4(MPa)	MEAN E'1, E'2, E'3
A	61.7	154.0	85.6		
B					
C	52.4	106.0	48.9	68.2	
D	86.9		111.0		
E					
MEAN	67.1	130	81.8	68.2	74.5 MPa (exc E'2)

Data have been omitted in cases where negative VDSs were measured or the VDSs were extremely small and resulted in extremely high values of E'.

Table 6.4. Estimation of E' for Gravel from Laboratory Test Data.

PIPE	E'1(MPa)	E'2(MPa)	E'3(MPa)	E'4(MPa)	MEAN E'1, E'2, E'3
A	28.4	41.8	29.2	157.0	
B	23.5	33.8	23.5	114.0	
C	35.2	50.1	30.4	137.0	
D	27.8	40.1	27.6	155.0	
E	28.9	45.6	28.3	178.0	
MEAN	28.8	42.3	27.8	148.2	32.9 MPa

E'(1) = value obtained using the deflection recorded at the end of the 70kPa static pressure phase,

E'(2) = value obtained using the increment of deflection change recorded during the 70kPa static pressure phase

E'(3) = value obtained using the cumulative deflection recorded at the end of the 140kPa static pressure phase

E'(4) = value obtained using the increment of deflection change recorded during the 140kPa static pressure phase.

Table 6.5. Estimation of Deflection Lag Factor for Pipes in Lightly Compacted Sand from Laboratory Test Data.

TIME (years)	VDS (%)	DL
0	0.00	-
0.00011	0.70	1.00
0.00274	0.78	1.12
0.083	0.88	1.26
1	0.96	1.38
2	0.99	1.41
5	1.02	1.46
10	1.05	1.50
25	1.08	1.55
50	1.11	1.59

Table 6.6. Estimation of Deflection Lag Factor for Pipes in Gravel from Laboratory Test Data.

TIME (years)	VDS (%)	DL
0	0.00	-
0.00011	0.59	1.00
0.00274	0.62	1.05
0.083	0.67	1.13
1	0.70	1.18
2	0.71	1.20
5	0.72	1.22
10	0.73	1.24
25	0.74	1.26
50	0.75	1.28

DL = deflection lag factor (Eq. 2.6)

VDS is calculated from best fit power curve

0.00011 years = 1 hour

0.00274 years = 1 day

0.083 years = 1 month

Table 6.7. Estimation of Trafficking Factor for Pipes in Lightly Compacted Sand from Laboratory Test Data.

PIPE	D1 M	D10M	D100 M	D1000 M	D10 ⁶	R ²	D10 ⁶ /D1	D10 ⁶ /D10	D10 ⁶ /100	D10 ⁶ /D1000
AL	0.12	0.47	1.02	1.43	3.93	0.983	32.8	8.4	3.9	2.7
BL	0.21	0.56	1.13	1.79	6.69	0.982	31.9	11.9	5.9	3.7
CL	0.23	0.6	1.33	1.91	7.17	0.974	31.2	12.0	5.4	3.8
DL	0.16	0.42	0.76	1.16	3.96	0.990	24.8	9.4	5.2	3.4
EL	0.86	1.21	1.63	2.11	5.03	0.976	5.8	4.2	3.1	2.4
MEAN							25.3	9.2	4.7	3.2

Table 6.8. Estimation of Trafficking Factor for Pipes in Gravel from Laboratory Test Data.

PIPE	D1 M	D10M	D100 M	D1000 M	D10 ⁶	R ²	D10 ⁶ /D1	D10 ⁶ /D10	D10 ⁶ /100	D10 ⁶ /D1000
AG	0.1	0.23	0.35	0.45	1.08	0.977	10.8	4.7	3.1	2.4
BG	0.11	0.26	0.41	0.53	1.11	0.990	10.1	4.3	2.7	2.1
CG	0.12	0.21	0.37	0.49	1.29	0.986	10.8	6.1	3.5	2.6
DG	0.21	0.27	0.44	0.57	1.24	0.987	5.9	4.6	2.8	2.2
EG	0.13	0.24	0.42	0.58	1.49	0.970	11.5	6.2	3.5	2.6
MEAN							9.8	5.2	3.1	2.4

A, B, C, D, E - pipe types

G - gravel surround

L - lightly compacted sand surround

D1M - measured VDS (in %) for 1st loading cycle

D10M - measured VDS (in %) for 10th loading cycle

D100M - measured VDS (in %) for 100th loading cycle

D1000M - measured VDS (in %) for 1000th loading cycle

D10⁶C - calculated VDS (in %) for 1 000 000th loading cycle

R² - correlation coefficient of fitted power curve

D10⁶/D1 - ratio of VDS at 1 000 000th loading cycle to VDS at 1st loading cycle

D10⁶/D10 - ratio of VDS at 1 000 000th loading cycle to VDS at 10th loading cycle

D10⁶/D100 - ratio of VDS at 1 000 000th loading cycle to VDS at 100th loading cycle

D10⁶/D1000 - ratio of VDS at 1 000 000th loading cycle to VDS at 1000th loading cycle

Table 6.9. Estimation of Trafficking Factor for Pipes in Sand from Field Test Data.

PIPE	D1 M	D10 M	D100 M	D1000 M	D106 C	R ²	D106/D1	D106/D10	D106/D100	D106/D1000
AS	0.116	0.286	0.609	1.223	11.040	0.980	95.2	38.6	18.1	9.1
ES	0.102	0.205	0.307	0.463	4.340	0.984	42.5	21.2	14.1	9.4
FS	0.192	0.513	0.697	1.603	9.830	0.981	51.2	19.2	14.1	6.1
MEAN							63.0	26.3	15.5	8.2

Table 6.10. Estimation of Trafficking Factor for Pipes in Gravel from Field Test Data.

PIPE	D1 M	D10 M	D100 M	D1000 M	D106 C	R ²	D106/D1	D106/D10	D106/D100	D106/D1000
AG	0.107	0.215	0.393	1.770	7.820	0.993	73.1	36.4	19.9	4.4
CG	0.126	0.270	0.440	1.034	7.400	0.978	58.7	27.4	16.8	7.2
DG	0.081	0.233	0.431	0.762	7.480	0.960	92.3	32.1	17.4	9.8
EG	0.113	0.184	0.277	0.563	4.500	0.969	39.8	24.5	16.2	8.0
FG	0.147	0.642	0.843	1.494	10.400	0.973	70.7	16.2	12.3	7.0
MEAN							66.9	27.3	16.5	7.3

A, C, D, E, F - pipe types

G - gravel surround

S - sand surround

D1M - measured VDS (in %) for 1st loading cycle

D10M - measured VDS (in %) for 10th loading cycle

D100M - measured VDS (in %) for 100th loading cycle

D1000M - measured VDS (in %) for 1000th loading cycle

D106C - calculated VDS (in %) for 1 000 000th loading cycle

R² - correlation coefficient of fitted power curve

D106/D1 - ratio of VDS at 1 000 000th loading cycle to VDS at 1st loading cycle

D106/D10 - ratio of VDS at 1 000 000th loading cycle to VDS at 10th loading cycle

D106/D100 - ratio of VDS at 1 000 000th loading cycle to VDS at 100th loading cycle

D106/D1000 - ratio of VDS at 1 000 000th loading cycle to VDS at 1000th loading cycle

Table 6.11. Summary Table of VDS (in %) for Comparable Test Phases in Laboratory and Field.

PIPE	PHASE	VDS(LL)	VDS(LH)	VDS(FS)	VDS(LG)	VDS(FG)
A	SI	0.00	0.00	0.00	0.00	0.00
A	EI	0.27	0.23	1.01	0.23	0.70
A	E70CT	2.83	0.31	2.11	1.02	1.36
A	E70CN	1.25	0.32	1.10	0.39	0.66
A	E70CIT	1.58	-0.01	-	0.63	-
B	SI	0.00	0.00	0.00	0.00	0.00
B	EI	0.16	-0.35	0.92	0.28	0.10
B	E70CT	3.09	-0.22	3.18	1.23	1.08
B	E70CN	1.23	0.05	2.26	0.53	0.98
B	E70CIT	1.86	0.27		0.70	
C	SI	0.00	0.00	0.00	0.00	0.00
C	EI	0.03	0.22	0.73	0.19	0.65
C	E70CT*	3.00	0.54	2.36	1.02	1.56
C	E70CN*	1.52	0.11	1.63	0.35	0.91
C	E70CIT*	1.55	0.33	-	0.52	-
D	SI	0.00	0.00	0.00	0.00	0.00
D	EI	0.16	0.20	0.66	0.26	0.36
D	E70CT	1.72	0.30	2.20	1.20	1.03
D	E70CN	0.57	0.05	1.54	0.98	0.67
D	E70CIT	1.15	0.25	-	0.22	-
E	SI	0.00	0.00	0.00	0.00	0.00
E	EI	-0.11	0.00	0.48	0.31	0.91
E	E70CT	3.08	-0.03	0.85	1.25	1.36
E	E70CN	1.27	0.00	0.37	0.57	0.45
E	E70CIT	1.81	-0.03	-	0.58	-

A, B, C, D, E - pipe types
LL - laboratory test with lightly compacted sand surround
LW - laboratory test with heavily compacted sand surround
FS - field test with sand surround
LG - laboratory test with gravel surround
FG - field test with gravel surround

SI - total VDS at start of installation phase
EI - total VDS at end of installation phase
E70CT - total VDS at end of 70kPa cyclic loading phase
E70CN - increment in VDS during 70kPa cyclic loading phase
E70CIT - increment in VDS during installation + increment in VDS during 70kPa cyclic loading phase

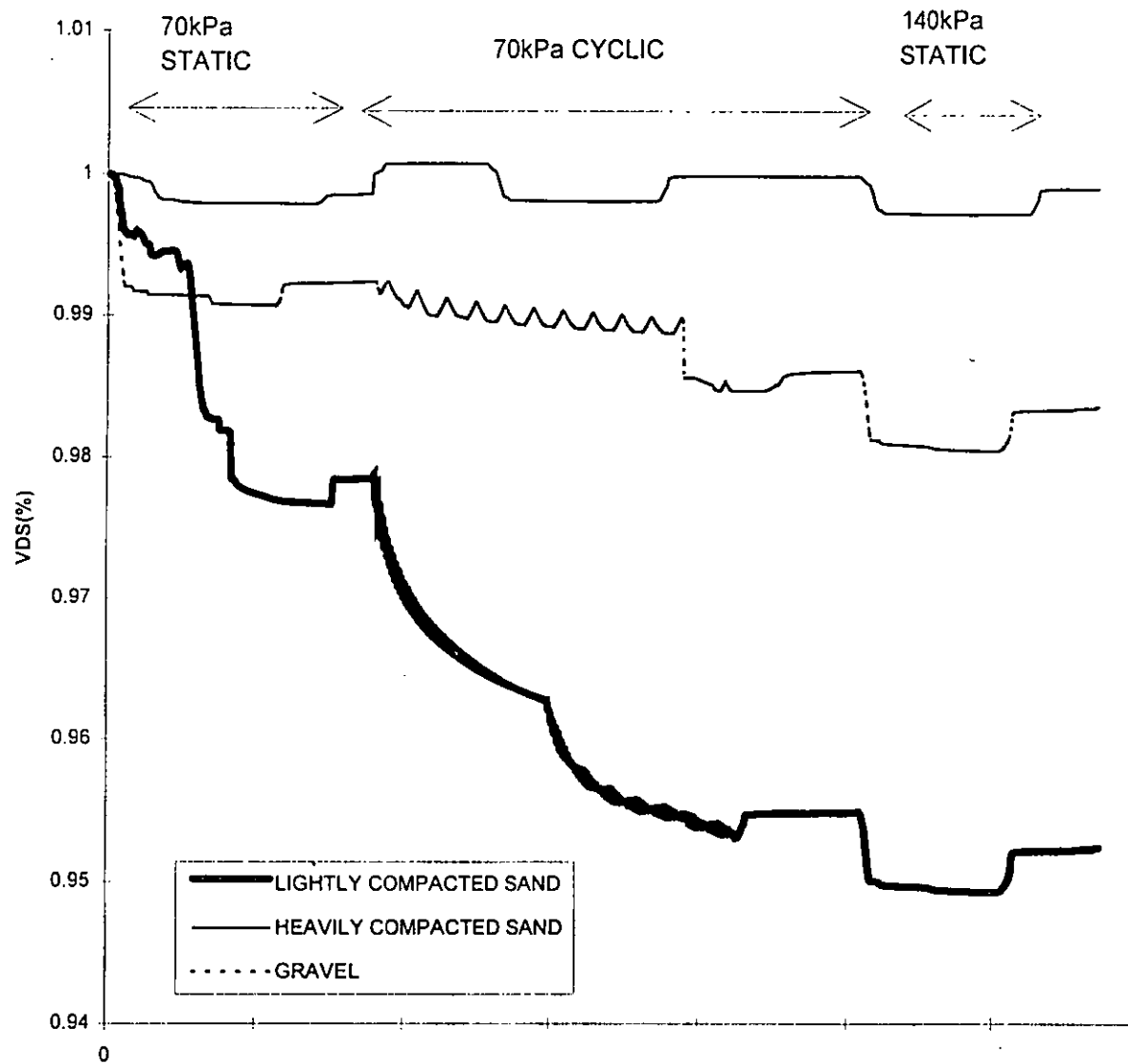


Figure 6.1. Ratio of Vertical Diameter to Horizontal Diameter for Laboratory Test Loading Phases for Pipe A.

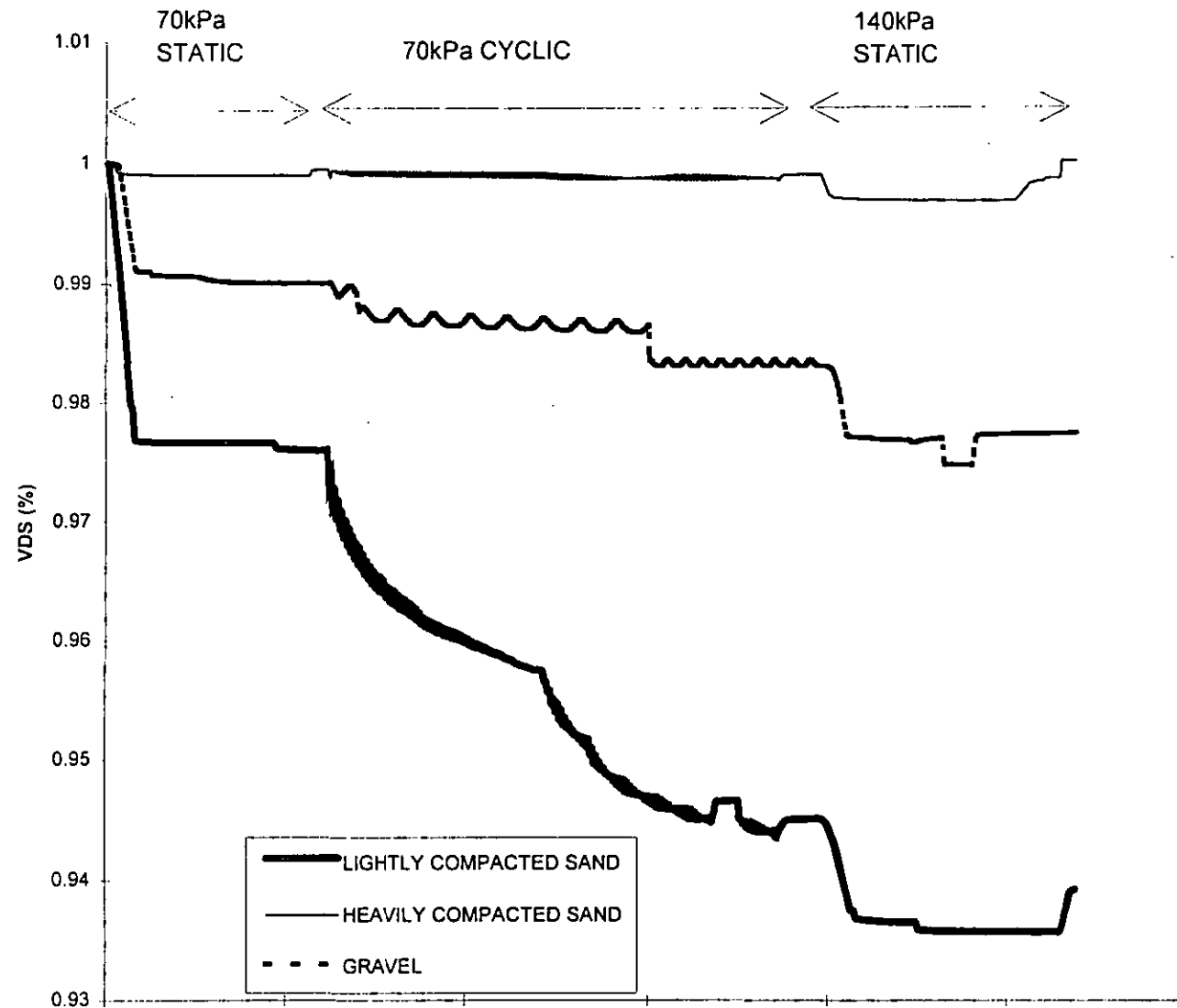


Figure 6.2. Ratio of Vertical Diameter to Horizontal Diameter for Laboratory Test Loading Phases for Pipe B.

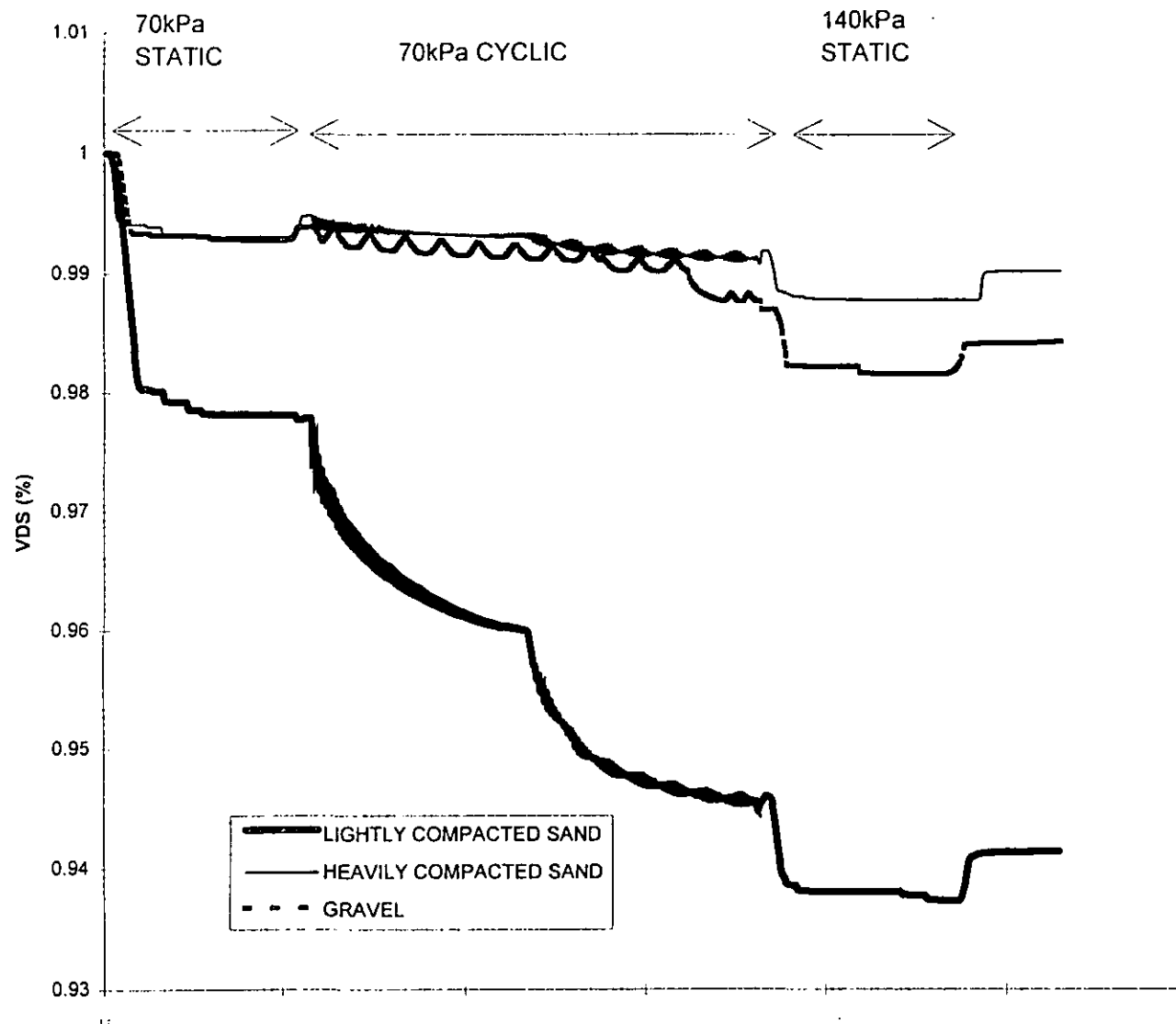


Figure 6.3. Ratio of Vertical Diameter to Horizontal Diameter for Laboratory Test Loading Phases for Pipe C.

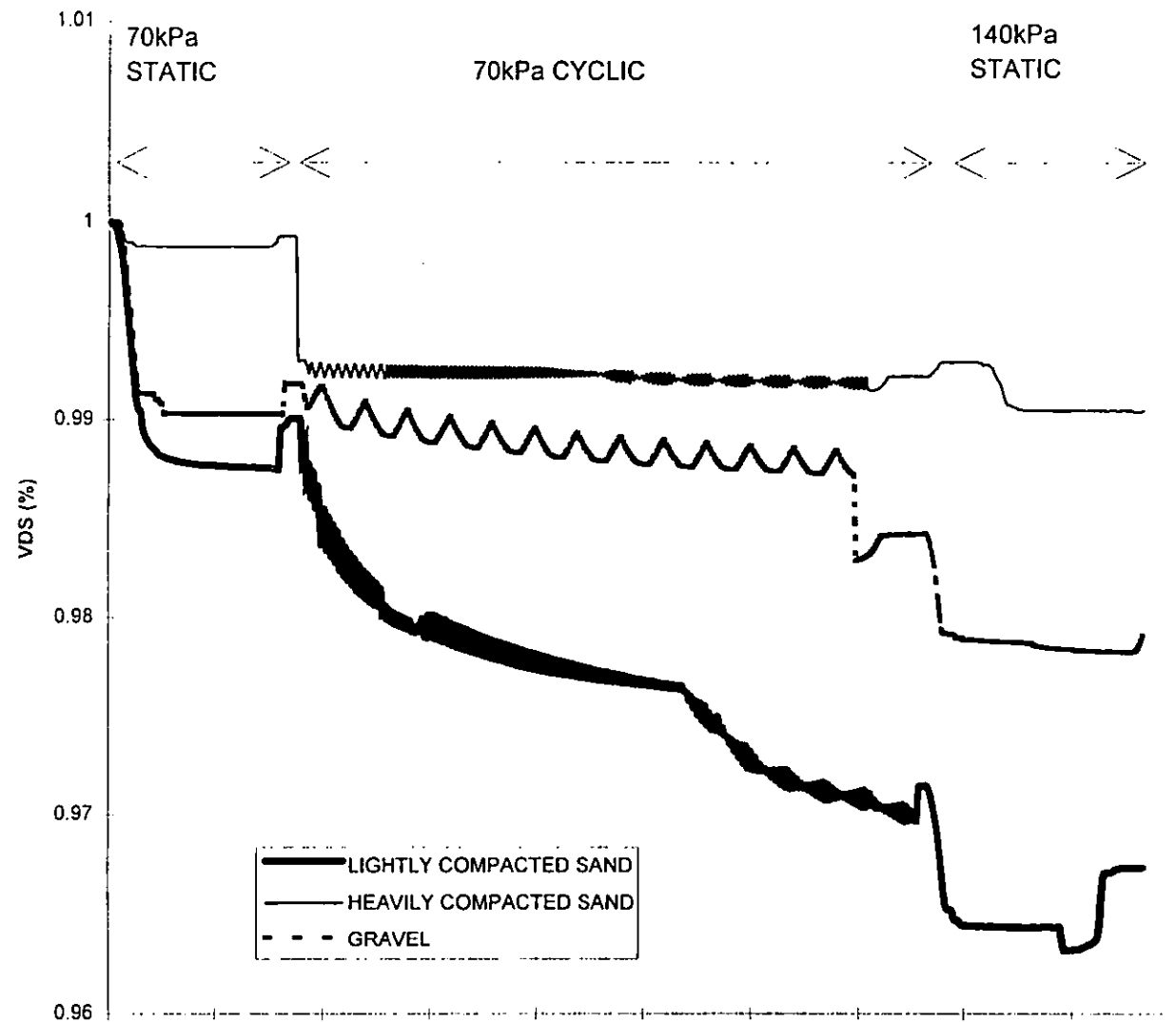


Figure 6.4. Ratio of Vertical Diameter to Horizontal Diameter for Laboratory Test Loading Phases for Pipe D.

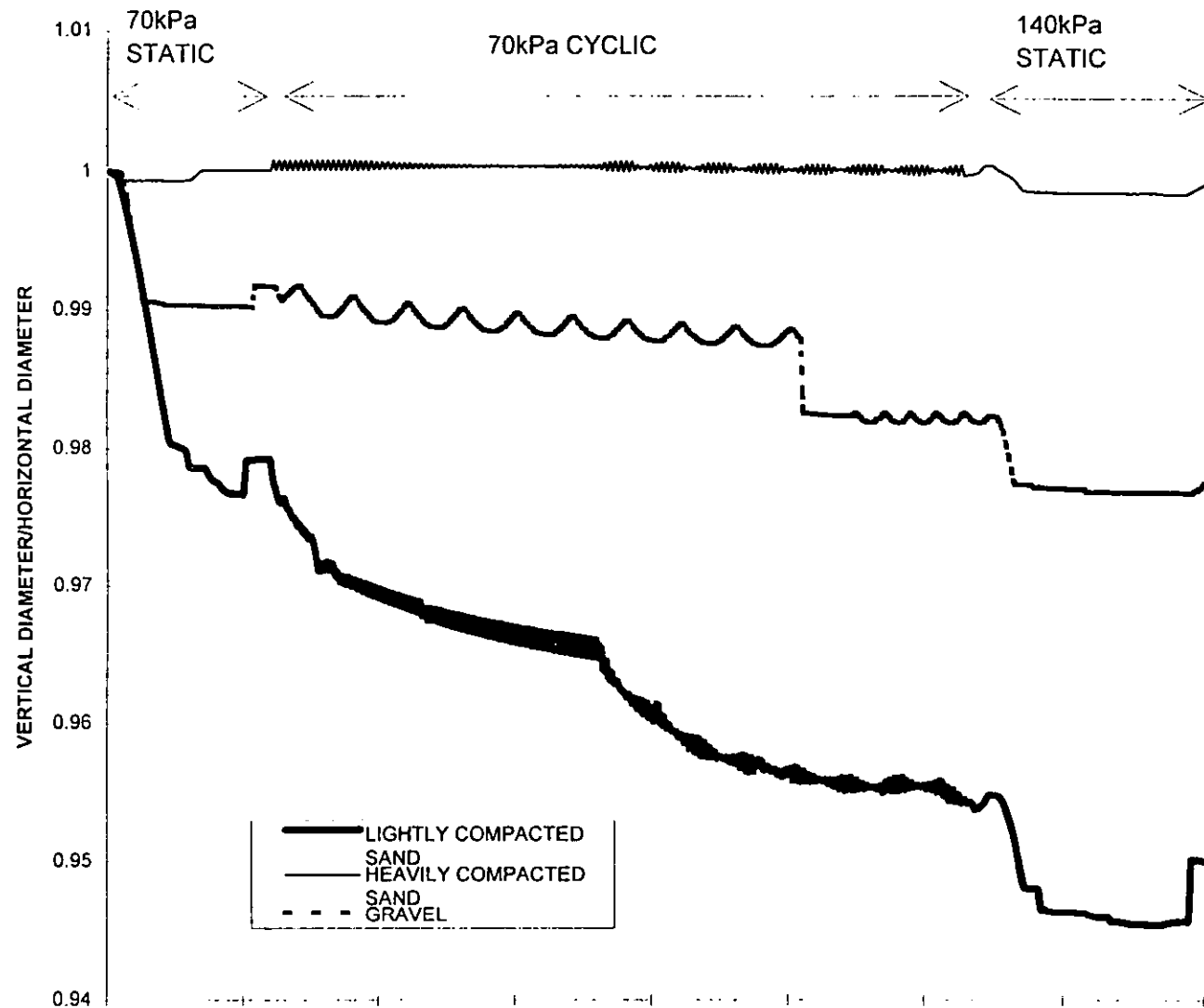


Figure 6.5. Ratio of Vertical Diameter to Horizontal Diameter for Laboratory Test Loading Phases for Pipe E.

7 CONCLUSIONS AND RECOMMENDATIONS FOR FURTHER WORK

7.1 CONCLUSIONS

A practical study of the structural performance of thermoplastic drainage pipes of the larger diameters currently in use has been presented. The initial development of the theory of pipe deflection by Marston and Spangler has been described. From this, the many factors that influence the deflection of a buried flexible pipe were identified and discussed. The most influential factor was found to be the soil that surrounded the pipe, in particular both its type and state of compaction. Because the compacted state is dependent to a large degree on the practices adopted during installation, the amount of deflection is likely to vary between individual installations. Nevertheless, some degree of consistency was found from the range of tests conducted, which showed that the VDS of the pipe during installation did not exceed 1%, and this value may serve as an upper limit of the deflection expected during installation.

The effect of applied loading on a buried pipe was discussed. In general, these are static and/or cyclic in nature. In general, the former case represents the application of overburden to a buried pipe, and the latter represents the passage of vehicles over a buried pipe. In the case of flexible pipes, these types of loading have been found to produce deflections that change as time passes. This is of considerable importance since the "lifetime" of a buried flexible pipe will be dependent on the possibility of the deflection increasing to such a level that the pipe is rendered unfit for use due to excessive deformation, collapse or leaking.

A review of some of the many methods by which the deflections of buried pipes may be calculated has also been carried out. These comprised semi-empirical and theoretical methods, including those based on the representation of the pipe-soil system by finite element meshes. Each method has its advantages and disadvantages depending on the nature of the pipe installation. For general use, simple methods such as the Iowa formula, the USBR equation and the ATV method are acceptable. For non-standard installations where loads, cover depths or soil properties may be extreme, more accurate (and more involved methods such) as those of Greenwood and Lang, Gumbel, Gerbault, and Chua and Lytton may be appropriate. The use of finite element methods to determine the stresses within a corrugated pipe was also described. This method (developed by Moore) is of particular interest because twin-wall pipes have become more common in use and the method, once calibrated with data from realistic installation conditions, will be invaluable for the efficient structural design of these types of pipes.

The review of the literature identified five major areas of interest that defined the philosophy of this research. The first of these was the change of deflection of a buried pipe with time, as a result of both the weight of the soil overlying the pipe and the passage of vehicles over the pipe trench. The former had previously been quantified by estimation of the deflection (or VDS) 50 years after installation, by multiplying the "immediate" value by a deflection lag factor of 1.5. Extrapolation of the laboratory test data yielded multipliers of 1.3 and 1.6 for gravel and lightly compacted sand surrounds respectively. The latter, which would equate to extremely poor installation practice, is likely to be an upper limit for the lag factor.

The effect of repeated loading was investigated. The experimental trends in the laboratory and field tests showed that the pipe deflection increased under repeated loading, but that the rate of increase slowed as the number of loading cycles increased. This was due to particle rearrangement and packing (densification) of the pipe surround material by the repeated stress application. This occurred in all surround types, but the effect was most marked in the lightly compacted sand surround, for which the densification was greatest. The gravel surround experienced a smaller degree of compaction and the heavily compacted sand experienced the smallest degree. The pipe deflections under a greater number of loading cycles was estimated by the extrapolation of laboratory and field test data to produce trafficking factors. The deflection at one million loading cycles has been estimated, from the more realistic field test data, to be approximately 70 times the deflection recorded during the first loading cycle, 30 times that recorded at the 10th loading cycle, 20 times that recorded at the hundredth loading cycle and 10 times that recorded at the thousandth loading cycle. These values are conservative approximations of the calculated values and may be used for sand or gravel surrounds, there being no significant difference between the trafficking factors for these surround types in the field. For the purposes of design, the factor relating the deflection to the first loading cycle is the most relevant, since the stresses generated can be determined theoretically. However, the deflection during the first cycle is likely to be small and therefore relatively inaccurate. The factor relating to the tenth cycle is of practical use since ten cycles of loading could be quickly and economically be performed on site. Additional loading cycles would increase the accuracy of the extrapolated deflection (as the range of the calculated values decreases), but the increased accuracy would have to be weighed against cost and time considerations.

The second objective was the development of a reproducible laboratory test that could represent, or be related to, field conditions. This has been achieved by the use of constant boundary conditions whose properties (notably interface friction) were taken into account in the analysis of pipe deflection data. The deflections measured in the laboratory were less than those that would be expected in the field under similar loading, based on the recorded field data.

Nevertheless the pipes that performed well in the laboratory also performed well under the relatively severe site conditions. Therefore the laboratory test would be a good “proof” test for plastic pipes if the magnitudes of loading therein were modified to be similar to the soil stresses at the depth of the pipe crown in the field. The expected stresses may be obtained from standard tables (e.g. Young et al, 1986), and corrected for box wall friction effects as described in 6.1.5.1. However, it would also be desirable to measure the soil stresses in the laboratory to ensure that field conditions were being replicated in terms of stress (and hence loading) on the buried pipe.

The third objective concerned the properties of the soil surrounding a buried pipe. These have been investigated in the laboratory and found to differ considerably from commonly used values. The modulus of soil reaction for the soils used in the laboratory were much higher than expected, with mean values (incorporating a factor of safety of 1.6) of 10MPa for lightly compacted sand, 20MPa for gravel and 40MPa for heavily compacted sand. These values were influenced by the boundary conditions that pertained in the laboratory, but despite this there appears to be a systematic underestimation of the amount of support that even a poor surround offers a buried pipe. The values of the modulus of soil reaction obtained for the two types of sand surround (10MPa and 40MPa) show the marked effect of compaction on soil stiffness and hence the reductions in pile deflections that may be obtained by adopting thorough, uniform compaction. The gravel case lies between the two sand cases in terms of stiffness, and it is considered that the stiffness of a gravel surround is developed in the field at a similar rate (in relation to strain) as that of a sand surround. This is because the relatively rapid mobilisation of passive resistance in this surround (due to the large and uniform particle size) is offset by high point stresses at the trench wall which cause the particles to penetrate it.

The fourth objective related to the problem of leakage of joints in pipes that have suffered large (i.e. VDS in excess of the 5% limit) deflections. Such deflections (and subsequent leakage) have been encountered in practice. The laboratory work carried out has shown that reductions of approximately 8% of the initial vertical diameter did not cause the test joint to leak. As well as establishing confidence in the joint, this result also allows the 5% limit of deflection currently used to be reviewed.

The fifth objective concerned the use of alternative surround materials and the results obtained using sharp particles (crushed flint) and a surround containing larger particles (Type 1 granular sub-base) showed that the pipes performed well, especially in the context of the very low cover depths and very high surface loads used. The acceptable deflections (i.e. under 5% VDS) recorded under these circumstances suggest that current installation specifications (that are less onerous than those achieved in this test programme) may be suitable for re-appraisal.

The laboratory research demonstrated the effect of the surrounding soil conditions on the shape, and hence mechanism, of pipe deformation. The worst case was that of lightly compacted sand, in which pipes exhibited the greatest change in shape under applied loading. It was observed that the deformed shape was not of the “pure” elliptical shape (i.e. that which would be observed in a parallel-plate test) assumed by Spangler in the development of his pipe deflection theory. Even under severe loading in this poor surround this shape was not achieved and the pipe exhibited a smaller component of horizontal diametral elongation than assumed by Spangler. The stiff, heavily compacted sand surround led to the creation of a very stable system in which the pipe received virtually uniform support around its circumference and as a result deviated little from its initial shape under applied loading. The lack of deformation prevented local yielding which in extreme cases would lead to the formation of plastic hinges (usually at the springers) and cause the collapse of the upper part of the pipe. When the pipe is restrained in this way, the mode of collapse would be by buckling of the pipe wall, and this takes place at applied stresses that are many times those expected even in severe circumstances. The gravel surround gave rise to deformed shapes that lay between these extremes, which confirmed that this surround type combines ease of placement with good levels of pipe support.

The good pipe performance observed in the practical work would justify a review of pipe stiffness, surround stiffness, installation and loading specifications. These subjects relate generally to the research objectives reported on above. It is apparent that, when designed and installed to current specifications, pipes do not exhibit excessive deflection under onerous loading. There is therefore a case for determining whether these specifications may be altered to reflect the findings of the research. However, any such work must be supported by appropriate laboratory (and ideally field) testing that can establish the effect of a change in specification on the long-term behaviour of the pipe. In addition, and of great importance, the limits of performance of the pipes (in terms of installation specifications, loading specifications and deflection), when identified must be subject to appropriate (that is sensible but not excessive) factors of safety, as is the case in all other types of civil engineering design work.

7.2 RECOMMENDATIONS FOR FURTHER WORK

Having established the need for further work, the means will be based to an extent on the work described above. It is apparent that the integrity of plastic pipes of the types tested must be preserved for the time that the pipe is in use. This may be several decades, and because of their relatively recent introduction they are at a disadvantage to clay and concrete pipes in this respect. It

would be of considerable interest to monitor the behaviour of plastic pipes for some years after their installation. Both the static and cyclic stress cases should be investigated. Given the experience gained from the field testing described in Chapter Four, it is evident that the instrumentation used must be sufficiently robust to withstand the effects of the outdoor environment. It would be feasible to adopt wholly manual means, such as measuring between permanent studs on the pipe wall using a vernier device. This would give sufficiently accurate measurements of the physical deflection of the pipe, which is the primary aim. The use of several measurement points would allow the shape of the deflected pipe to be established. This would be in lieu of using strain gauges which have been found to be susceptible to damage by atmospheric moisture and groundwater, both of which prejudice their accuracy in the long term.

A particular use for strain gauges would be to determine the strain (and hence stress) distributions at specific points in a multi-walled corrugated pipe. Some work has been carried out in this field (see 2.3.7), but the inclusion of a wider range of more practical installation conditions would be useful. This could be utilised in finite element modelling of the pipe profile. However, it would also be necessary to determine more accurately the effects of the presence of a strain gauge on the stress field of thin plastic sections. This matter was briefly discussed but was not of particular concern since the above research used strain gauge data qualitatively to determine the deflected shapes of the pipes. Data intended for finite element applications would require the reinforcing effects of the strain gauges to be quantified.

It would be advantageous to determine whether alternative surround materials such as “as-dug” general fills may be used without leading to large pipe deflections. This is especially relevant to the lowest 300mm of fill material, which the Department of Transport stipulates must be selected fill, the provision and preparation of which has time and cost implications. It may be possible in some cases to dispense with the granular surround medium entirely, which would have considerable benefits with regard to the costs of pipe installation.

The values of the modulus of soil reaction were calculated using data from the static pressure phases of the laboratory testing. These phases had no equivalent in the field testing, and the relatively small magnitudes and large degree of scatter of the pipe deflections observed in the field installation phase precluded accurate calculation using these data. It would therefore be of considerable benefit if static loading could be applied to pipes in field installations and their deflection observed. This could be done simply by recording pipe deflections after installation in various surround media and at different cover depths. Alternatively, incremental plate loading tests could be carried out on buried pipes, which would be more controllable and more accurate. Both of these approaches would take into account site boundary conditions and the effects (and variation with time) of the frictional trench walls.

The issue of specifications and testing methods may be reconsidered in the light of the relatively good performance of the pipes tested. The use of extrapolated parallel-plate test data has been questioned. There are strong practical considerations for using such a test, therefore there may be a case for maintaining the general test procedures but altering the pass criteria or relating the deflection trends to those experienced in the static pressure phases of the laboratory tests.

The deflection limits currently used (5%) may be relaxed somewhat, but this would require knowledge of the deflection at which the pipe becomes unfit for use. This has not been achieved in the above research, but is of self-evident importance in terms of establishing a safe (necessarily long-term) deflection limit.

REFERENCES

Abwassertechnische Vereinigung eV. Standards for the static calculation of drainage sewers and pipelines A127, second edition. ATV, St Augustin, Germany, 1988.

American National Standards Institute (ANSI). ANSI/AWWA Standard for fiberglass pressure pipe C950-88, ANSI, Washington DC, USA, 1988.

American Society of Civil Engineers. Development and use of the Modpares device. Journal of the Pipeline Division, American Society of Civil Engineers, New York, USA, 1964.

American Society for Testing and Materials. Standard test method for determination of external loading characteristics of plastic pipe by parallel-plate loading D2412-87. ASTM, Philadelphia, Pennsylvania, 1987.

Bauer DE. 15 year old polyvinylchloride (PVC) sewer pipe; a durability and performance review. Buried plastic pipe technology STP 1093, ASTM, Philadelphia, Pennsylvania, 1990.

Bishop, RR. Time dependent performance of buried PVC pipe. Proceedings of the ASCE International conference on underground plastic pipe, New Orleans, Louisiana, USA, 1981.

Boden JB, Farrar DM and Young OC. Standards of site practice-implications for innovation in the design and construction of flexible pipelines. Pipes and Pipelines International, London, England, 1978.

Bowles, JE. Foundation analysis and design. 4th Edition, McGraw-Hill, New York, USA, 1988.

Brandrup J and Immergut EM. Polymer Handbook. Wiley, New York, USA, 1989.

British Standards Institution. BS 2782, Methods of testing plastics, Part 3. London, England, 1978.

British Standards Institution. BS5400, steel, concrete and composite bridges-Part 2-specification for loads. London, England, 1978.

British Standards Institution. BS 5955, Installation of uPVC pipework for gravity drains and sewers. London, England, 1980.

British Standards Institution. BS 4962, Specification for pressure pipes and fittings for use as sub-soil field drains. London, England, 1989.

British Standards Institution. BS 1377, Methods of tests for soils for civil engineering purposes London, England, 1990.

British Standards Institution. DD200, Draft for development. Specification for plastic non-rigid conduits and fittings for direct burial underground. London, England, 1991.

British Standards Institution. BS 882, Specification for aggregates from natural sources for concrete. London, England, 1992.

British Standards Institution. BS EN 50086-2-4, Specification for conduit systems for electrical installations, particular requirements for conduit systems buried underground. London, England, 1994.

Brown, SF. Soil mechanics in pavement engineering. (The 1996 Rankine Lecture). Geotechnique, Volume 46 No.3, Institution of Civil Engineers, London, England, 1996.

Chua KM. Time dependent interaction of soil and flexible pipe. PhD thesis, Texas A&M University, Texas, USA, 1986.

Chua, KM and Lytton, RL. Visco-elastic approach to modeling performance of buried pipes. Vol. 115, Journal of the Transportation Engineering Division, American Society of Civil Engineers, Washington DC, USA, 1989.

Chua KM and Lytton RL. New method of time-dependent analysis for interaction of soil and large diameter flexible pipe. Transport Research Record 1315, Transportation Research Board, Washington DC, USA, 1991

Crabb GI and Carder DR. Loading tests on buried flexible pipe to validate a new design model. Research Report 28, Transport and Road Research Laboratory, Crowthorne, Berkshire, England, 1985.

Department of Transport. Highway Advice Note HA40/89, Determination of pipe and bedding combinations for drainage works. Her Majesty's Stationery Office, London, England, 1990.

Department of Transport. Manual of Contract Documents for Highway Works Volume 1, Specification for Highway Works. Her Majesty's Stationery Office, London, England, 1993.

Department of Transport. Manual of Contract Documents for Highway Works Volume 2, Highway Construction Details. Her Majesty's Stationery Office, London, England, 1993.

Engesser, F. Zu Theorie der Baugrundes. (The theory of site foundations). Zentralsblatt der Bauverwaltung, Germany, 1893.

Evans GA, Loeppky MWJ and Rogers CDF. A Critical Review of the Creep Stiffness Tests for Structured Wall Pipes. Proceedings of the 9th International Conference on Plastic Pipes, Edinburgh, Scotland, 1995.

Gehrels, JF and Elzink, WJ. Experience of Long Term Behaviour of uPVC Gravity Sewers. Proceedings of the 4th International Plastics Pipes Conference, University of Sussex, Brighton, Sussex, England, 1979.

Gemperline, MC. Construction-induced dynamic pressure and corresponding impact factors for pipelines. Proceedings of the ASCE International conference on advances in underground pipeline engineering, Madison, Wisconsin, USA, 1985.

Gerbault, M. A soil-structure interactive model Proceedings of the 2nd ASCE International Conference on advances in underground pipeline engineering, Seattle, Washington, USA, 1995

Greenwood ME and Lang C. Vertical deflection of buried flexible pipes. Specialist Technical Publication STP1093, American Society for Testing and Materials, Philadelphia, Pennsylvania, USA, 1990.

Gumbel JE, O'Reilly MP, Lake LM and Carder DR. The development of a new design method for buried flexible pipe. Europipe 82 conference, Basel, Switzerland, 1982

Handy RL. The arch in soil arching. Journal of the Geotechnical Engineering Division, Volume 111, ASCE, Washington DC, USA, 1985.

Hartley, JD and Duncan, JM. "E' and its variation with depth." Journal of the transportation engineering division, Volume 113, ASCE, Washington DC, USA, 1987

Howard AK. Modulus of Soil Reaction values for buried flexible pipe. Journal of the Geotechnical Engineering Division, Volume 103, ASCE, Washington DC, USA, 1977.

Howard, AK. The USBR equation for predicting flexible pipe deflection. Proceedings of the International conference on underground plastic pipe, New Orleans, Louisiana, USA, 1981.

International Standards Organisation. ISO 9967, Thermoplastic pipes, determination of creep ratio, British Standards Institution, London, England, 1994.

Janson, L-E. Short term versus long term pipe ring stiffness in the design of buried plastic sewer pipes. Proceedings of the ASCE International conference on pipeline design and installation, Las Vegas, Nevada, USA, 1990.

Janson, L-E. Stress relaxation in constantly deflected polyethylene pipes. Proceedings of the 2nd International ASCE conference on advances in underground pipeline engineering, Seattle, Washington, USA, 1995..

Joekes D and Elzink WJ. Deflection of PVC pipe and a new method for measuring and specifying stiffness of plastics pipes. Proceedings of Plastics pipes VI conference, 1985..

Katona, MG. CANDE: A modern approach for the structural design and analysis of buried culverts. US Naval Civil Engineering Laboratory, Point Hueneme, California, USA, 1976.

Krizek, RJ. Structural analysis and design of pipe culverts." Report No. 116, Highway Research Board, Washington DC, USA, 1972.)

Lawrence GJL. Trench wall jack: an apparatus to measure the equivalent elastic modulus of soil. Supplementary Report 347, Transport and Road Research Laboratory, Crowthorne, Berkshire, England, 1977.

Leonard DR, Grainger JW and Eyre R. Loads and vibrations caused by eight commercial vehicles with gross weights exceeding 32 tons. TRRL Laboratory Report LR582, Transport and Road Research Laboratory, Crowthorne, Berkshire, England, 1974.

Leonardt G. Die Erdlasten bei Überschüttungen Durchlässen. Die Bautechnik, Volume 56 No 11, Germany, 1979

Loeppky MWJ. BEng dissertation, Loughborough University of Technology, Loughborough, Leicestershire, England, 1992.

MacGregor P. Prediction of HDPE pipe response. BSc dissertation, University of Western Ontario, London, Ontario, Canada, 1995.

Marston A. Theory of Loads on Pipes in Ditches. Iowa Engineering Experiment Station, Ames, Iowa, USA, 1913.

McDowell JR, Reid D, Fairfield CA and Sibbald A. The performance of pipes in trench reinstatements. Highways and Transportation, London, England, 1994.

Moore ID and Hu F. Response of profiled high-density polyethylene pipe in hoop compression. Transportation Research Record 1514, Transportation Research Board, National Research Council, Washington DC, USA, 1995.

Neilson, FD. Modulus of soil reaction as determined from triaxial shear test. Highway Research Record 185, Highway Research Board, National Research Council, Washington DC, USA, 1967.

Neilson FD Experimental studies in soil-structure interaction. Highway Research Record 413, Highway Research Board, National Research Council, Washington DC, USA, 1972.

Page J. Impact tests on pipes buried under roads. Laboratory Report 35, Road Research Laboratory, Crowthorne, Berkshire, England, 1966.

Petroff, LJ.(a) Review of the relationship between soil shear resistance and arching in plastic pipe behaviour. Buried Plastic Pipe Technology ASTM STP 1093, American Society for Testing and Materials, Philadelphia, Pennsylvania, USA, 1990.

Petroff LJ (b). Stress relaxation characteristics of the HDPE pipe-soil system. Proceedings of the ASCE International conference on pipeline engineering, Las Vegas, Nevada, USA, 1990.

Petroff LJ Installation technique and field performance of HDPE profile pipe. Proceedings of the 2nd international ASCE conference on advances in underground pipeline engineering, Seattle, Washington, USA, 1995

Rogers CDF. The response of buried uPVC pipes to surface loading. PhD thesis, University of Nottingham, England, 1985.

Rogers CDF, Fleming PR, Loeppky MWJ and Faragher E. Buried plastic pipe - performance versus prediction. Proceedings of the 2nd ASCE International conference on advances in underground pipeline engineering, Seattle, USA, 1995.

Rogers CDF, Fleming PR and Talby R. Use of visual methods to investigate the influence of the installation procedure upon pipe/soil interaction, 75th Transportation Research Board annual meeting, Washington DC, USA, 1996.

Rogers CDF and Loeppky MWJ. The performance of B&H Ridgidrain pipe. Loughborough Consultants Ltd., Loughborough, Leicestershire, England, 1992 (unpublished).

Rogers, CDF, Loeppky, MWJ, and Faragher, E. The structural performance of profile-wall drainage pipes in relation to UK specifications. Proceedings of the 4th International Conference on pipeline engineering and construction, Hamburg, Germany, 1994.

Salisbury JV and Fleming PR. Pipe Research at Old Dalby - Ground Conditions. Loughborough University Internal Research Report, Loughborough; Leicestershire, England, 1993 (unpublished).

Sargand SM, Hazen GA, Liu X, Masada T and Hurd JO. Structural performance of buried polyvinylchloride pipes under large distributed load. Transportation Research Record 1514, Transportation Research Board, Washington DC, USA, 1995.

Selig, ET. Soil properties for plastic pipe installation. Buried plastic pipe technology, STP 1093, American Society for Testing and Materials, Philadelphia, Pennsylvania, USA, 1990.

Selig, ET, DiFrancesco LC and McGrath TJ. laboratory test of buried pipe in hoop compression. Buried plastic pipe technology ASTM STP1222, American Society for Testing and Materials, Philadelphia, Pennsylvania, USA, 1994

Spangler MG. The Structural design of Flexible Pipe Culverts. Iowa Engineering Experiment Station, Ames, Iowa, USA, 1941.

Terzaghi K. Theoretical soil mechanics. Wiley, New York, USA, 1943.

Terzaghi K. Evaluation of coefficients of subgrade reaction. Geotechnique, Vol 5, Institution of Civil Engineers, London, England, 1955.

Trott JJ and Gaunt J. Experimental performance of pipelines under a major road: performance during and after road construction. Laboratory Report 692, Transport and Road Research Laboratory, Crowthorne, Berkshire, England, 1976.

Vesic AS. Bending of Beams resting on isotropic elastic solid. Journal of the Engineering Mechanics Division, ASCE, Vol 87, 1961.

Walton J. The structural design of the cross-section of vitrified clay pipelines. Clay Pipe Development Association, London, England, 1970.

Water Research Centre. Guide to the Water Industry for the Structural Design of Underground Pipelines, ER201E. Water Research Centre, Swindon, Wiltshire, England, 1986.

Watkins RK. Plastic pipes under high landfills. Buried Plastic Pipe Technology ASTM STP 1093, American Society for Testing and Materials, Philadelphia, Pennsylvania, USA, 1990.

Watkins RK, Dwiggins JM and Altermatt WE. Structural design of buried corrugated polyethylene pipe. Transportation Research Record 1129, National Research Council, Washington DC, USA, 1993.

Watkins RK, Trench widths for buried pipes. Proceedings of the 2nd International ASCE conference on advances in underground pipeline engineering, Seattle, Washington, USA, 1995.

Watkins RK and Spangler MG. Some characteristics of the modulus of passive resistance of soil: a study in similitude. Volume 37, Proceedings of the Highway Research Board, Washington DC, USA, 1958

Wu TH and Leonards GA. Characterization of soil arching above buried conduits. Proceedings of the 1st International conference on advances in underground pipeline engineering, Madison, Wisconsin, USA, 1985.

Yapa KAS and Lytton RL. An analysis of soil-box tests on HDPE pipes, Research Report, Texas A&M University, Texas, USA, 1989.

Young OC, Brennan G and O'Reilly MP. Simplified tables of external loads on buried pipelines. Transport and Road Research Laboratory, Department of Transport, Her Majesty's Stationery Office, London, UK, 1986.

Zorn NF and van den Berg P. The effect of compaction on buried flexible pipes. Proceedings of the ASCE conference on buried pipes, 1990.

Appendix A.

Analogy of Beam on Elastic Foundation

The pipe springer may be considered as a vertical pile bearing against a soil, movement of which causes passive resistance in the soil. The soil properties in this instance are often depth-dependent and difficult to measure directly.

An approximation of the relationship between soil stiffness and depth was first put forward by Engesser (1893):

$$k = a + \frac{b}{B} \quad \text{Eq A1}$$

where:

k = soil stiffness coefficient

B = width of a beam through which the vertical load is exerted, and

a, b = empirical constants.

The value of k has been shown to depend on the size of the loaded area

Terzaghi (1955) introduced the coefficient of subgrade reaction, k_s , defined as

$$k_s = p/y \quad \text{Eq A2}$$

where:

p = pressure applied to an area of subgrade, and

y = deflection of the subgrade under pressure p .

The initial application of this expression was to vertical (e.g. wheel) loads on flexible road surfaces. Later work on the deflection of piles under lateral (horizontal) loads gave rise to the coefficient of horizontal subgrade reaction, k_h , which is defined also by Eq.A2. The theory is applicable to flexible pipes because the region of the pipe springer resembles a pile that is being pushed into adjacent soil at a particular depth. In cohesionless materials such as sand and gravel (typical pipe surround media), the pressure required to produce a deflection

increases proportionately with the depth (z) to the area of interest, and in these cases k_h is defined by:

$$k_h = p / y = m_h z \quad \text{Eq A3}$$

The constant of proportionality m_h is a function of the relative density of the sand and the area acted upon by the subgrade reaction. The latter point is significant as it demonstrates further that the soil property in question, which resembles the modulus of passive resistance, e_s , propounded by Spangler (1941), is dependent on both the properties and the geometry of the region of the structure undergoing displacement. Spangler overcame this complication by defining the modulus of soil reaction, E' .

Vesic (1961) derived the following relationship between the modulus of subgrade reaction k_s (or its horizontal counterpart k_h) and the elastic secant modulus of the soil (E_s) for a footing:

$$k_s = \left(\frac{E_s}{1 - \nu^2} \right) \left(\frac{0.65}{B} \right) \left(\frac{E_s B^4}{E_f I_f} \right)^{\frac{1}{12}} \quad \text{Eq A4}$$

where:

I_f = second moment of area of footing,

B = width of footing, and

E_f = elastic modulus of footing.

Vesic simplified Eq A4 by assuming that the twelfth root of any realistic combination of E_s , B , E_f and I_f in the third term of the product in Eq 2.27, when multiplied by 0.65, would be near unity. This gave:

$$k_s = \frac{E_s}{B(1 - \nu^2)} \quad \text{Eq A5}$$

This will be seen to be an important result in the context of later theoretical developments of flexible pipe deflection theories (see 2.3.2, for example). The right-hand side of Eq A5 is similar to the plane strain modulus of a soil, E_s' , defined as:

$$E_s' = \frac{E_s}{(1 - \nu^2)} \quad \text{Eq A6}$$

save that the term $1/B$ is included to modify the modulus to that of a unit width of foundation. Thus,

$$k_s = E'_s / B \quad \text{EqA7}$$

The plane strain modulus is used widely in theoretical studies of pipe deflection.

If Eq A7 and elastic theory are used to define the settlement a base of width B (Bowles, 1988), then k_s may be defined thus:

$$k_s = \frac{1}{BE'_s I_s I_f} \quad \text{Eq A8}$$

where:

I_s = settlement factor of a flexible foundation, and

I_f = second moment of area of footing.

Thus, k_s and E'_s can be related in terms of the geometry of the bearing area (B and I_f) and the settlement factor I_s , which is a function of Poisson's ratio of the soil, the depth of burial and the geometry of the footing. Values of k_s have been determined for a range of soils (Bowles, 1988) and are given in Table A1. The quantities k_s and k_h are interchangeable, so provided the directions of the applied stresses are in the same relative directions. k_h can be determined in the same way as k_s .

Table A1. Modulus of Subgrade Reaction for Various Soils (after Bowles, 1988).

soil	range of k_s , MPa/m
loose sand	5 - 16
medium sand	9 - 78
dense sand	63 - 126
clayey sand (medium)	31 - 78
silty sand (medium)	24 - 47
clayey soil (s_u in kPa):	
$s_u < 50$	0 - 15
$50 < s_u < 100$	15 - 30
$100 < s_u < 200$	30 - 62
$s_u > 200$	> 62

s_u = undrained shear strength

